UNDERSTANDING THE EFFECT OF CHANGING LAND USE ON FLOODS AND SOIL EROSION IN THE CAGAYAN DE ORO CATCHMENT

BY

RUBIANCA ANGELICA HONRADO BENAVIDEZ

A thesis

submitted to the Victoria University of Wellington

in fulfilment of the requirements for the degree of

Doctor of Philosophy

Victoria University of Wellington

2018

Ad majorem Dei gloriam

Table of Contents

Table of Contents 4

Thesis Abstract 7

Acknowledgements 9

Acronyms and Abbreviations 11

Units 12

Disclaimer 13

1 Introduction 14

1.1 Background and context 14

1.2 Watershed management 18

1.3 Ecosystem services 21

1.4 The Land Utilisation and Capability Indicator (LUCI) framework 26

1.5 Extreme events 29

1.6 Climate change 33

1.7 Background of Cagayan de Oro (CDO) 35

1.8 Aims and objectives 37

1.9 Thesis Structure 39

2 Overview of methodology and data sources 43

2.1 Data sources 43

2.2 Soil parameterisation 52

2.3 Land cover parameterisation 62

2.4 Correlation to New Zealand databases 73

2.5 Ecosystem services modelling 76

2.6 Extreme events and inundation 78

2.7 Summary of methodology 79

3 Application of the LUCI framework to the CDO catchment for flood mitigation and other ecosystem services 81

3.1 Introduction 81

3.2 Methodology 82

3.3 Results and discussion 87

3.4 Future work 114

3.5 Summary and conclusion 115

4 A review of the (Revised) Universal Soil Loss Equation (R/USLE): with a view to increasing its global applicability and improving soil loss estimates 118

4.1 Introduction 118
4.2 Universal Soil Loss Equation (USLE) 121
4.3 Limitations of R/USLE 144
4.4 Future directions 146
4.5 Summary and conclusion 150
5 Estimating soil erosion losses in the Cagayan de Oro catchment (Philippines) using the RUSLE under different land cover scenarios 152
5.1 Introduction 152
5.2 Aim and objectives 155
5.3 Methodology 156
5.4 Results & Discussion 164
5.5 Limitations and future work 179
5.6 Summary and conclusion 180
6 Improving the estimation of soil loss using a combination of the Revised Universal Soil Loss Equation (RUSLE) and the Compound Topographic Index (CTI) in the Mangatarere watershed 182
6.1 Introduction 182
6.2 Aim and objectives 185
6.3 Methodology 185
6.4 Results and discussion 193
6.5 Limitations and future work 212
6.6 Summary and conclusion 213
7 Incorporating and extending a flatwater inundation model for the Land Utilisation and Capability Indicator (LUCI) Framework 214
7.1 Introduction 214
7.2 The LUCI Floodplain Inundation Model 223
7.3 Application: Lower Hutt, New Zealand 228
7.4 Summary, conclusion, and future work 242
8 Extreme events modelling in the Cagayan de Oro catchment 244
8.1 Introduction 244
8.2 Methodology 247
8.3 Results and Discussion 253
8.4 Future work 260
8.5 Summary and conclusions 261

9 Synthesis of understanding the effect of changing land use on floods and soil erosion in the Cagayan de Oro catchment 263
9.1 Summary of the rationale and aims 263
9.2 Ecosystem services and extreme events 264
9.3 Model development 268
9.4 Limitations and future work 270
9.5 Implications 271
9.6 Summary and conclusion 273
Appendix 1. Summary of previous studies that have applied the USLE and RUSLE 276
References 279

Thesis Abstract

The destructive capability of typhoons affects lives and infrastructure around the world. Spatial analysis of historical typhoon records reveal an area of intense storm activity within the Southeast Asian (SEA) region. Within SEA is the Philippines, an archipelagic tropical country regularly struck by storms that often cause severe landslides, erosion and floods. Annually, ~20 cyclones enter the Philippine Area of Responsibility, with about nine making landfall, causing high winds and intense rainfall. Thus, significant research in the Philippines has focused on increasing the resilience of ecosystems and communities through real-time disaster forecasting, structural protections, and programmes for sustainable watershed management (e.g. rehabilitation and conservation agriculture). This dissertation focused on the third aspect through computer modelling and scenario analysis.

The study area is the Cagayan de Oro (CDO) catchment (~1400km^2) located in the Southern Philippines. The catchment experienced heavy flooding in 2012 from Typhoon Bopha and has major erosion problems due to mountainous slopes and heavy rainfall. Communities derive ecosystem services (ES) including agricultural production, water supply, recreation, mining resources, flood mitigation, etc. Since changes to the supply or distribution of these ES affects livelihoods and the hydrological response of the catchment to typhoon events, this research used the Land Utilisation and Capability Indicator (LUCI) model to understand the baseline ES and potential changes associated with basin management plans.

This was the first detailed tropical application of LUCI, including parameterising it for Philippine soil and land cover datasets in CDO and extending its capability to be applied in future tropical areas. Aside from applying LUCI in a new geoclimatic region, this research contributed to the general development of LUCI through testing and improving its sediment delivery and inundation modelling. The sediment delivery was enhanced using the Revised Universal Soil Loss Equation (RUSLE) model that allows LUCI for the first time to account for impacts of specific land management such as agroforestry and contour cropping on erosion and sediment delivery. Progress was made in updating a flatwater inundation model for use with LUCI, including converting

it to Python but this requires further development and testing before it is suitable for application in the Philippines.

The development and rehabilitation scenarios showed improved flood mitigation, lower surficial soil erosion rates, and lower loads of nutrients compared to the baseline scenario. Additionally, ES mapping under different land cover scenarios has not been previously accomplished in CDO, and this research provides useful information to guide local decision-making and management planning.

The rainfall-runoff model of LUCI was tested against the Hydrologic Engineering Center's Hydrological Modelling System (HEC-HMS), showing good agreement with observed flow. Since the rainfall-runoff model of LUCI has been minimally utilised in past applications, this CDO application elucidated directions for future work around further testing under extreme rainfall events and climate change.

Overall, this novel application of LUCI creates a framework to assist decision-making around land cover changes in the CDO, provides guidance around data requirements and parameterisation procedures to guide future international applications, and has significantly contributed to development and improvement of the LUCI framework to extend its modelling capabilities in the future.

Acknowledgements

This thesis would not have been possible without the support of many people, groups, and organisations. My heart is grateful for all their help, whether it be for their scientific input, their generosity and time, their love and friendship, their prayers, or just for being in my life.

I thank God for putting these people in my life, for His love and guidance, and for the trials through which He has carried me. He has given me a mind to think, a heart to empathise, and a voice to speak up. May I use these parts of me for His glory and to serve others, and not for my own glory.

My unending thanks to my parents who always supported and encouraged me but have never pressured me. They have always set an example for me, using their abilities and resources to help others achieve their goals and dreams. Thank you, Mum and Dad, for loving me and teaching me about serving others.

Thank you to my supervisors Bethanna Jackson, Deborah Maxwell, and Enrico Paringit, for their guidance throughout this thesis. Dr. Jackson and Dr. Maxwell have been with me since the beginning with continuing support and encouragement, sitting with me during coding sessions, and taking a red pen to my drafts to spin gold from straw. I thank Dr. Paringit for connecting me with my study site of Cagayan de Oro (CDO), introducing me to his research team, and for advising me on the potential research areas and directions for scientific study in the Philippines.

I also thank the Victoria University of Wellington for giving me the VUW Doctoral Scholarship that made it possible for me to focus on my research and the Doctoral Submission Scholarship for finishing off my dissertation.

My support system is loving and vast. My family always welcomed me home for Christmas and gave me much needed fun times over the holidays. I must thank my brother the computer whiz, and my supportive sister-in-law, for teaching me how to use our Windows 98 computer and setting me on a course towards coding and now modelling. *Mi corazon* Abel for his love, words of encouragement, and listening ears. The support of my *Ang Bahay* family all these years, especially *Ate* Rose for her faithfulness during my medical emergency and the times I could barely do anything for

myself. Thank you to my "other parents" here in New Zealand: *muchas gracias* to my *Tita* Agnes and *Tito* Ricardo, and *maraming salamat* to my *Tita* Marivic and *Tito* Larry. Thank you for supporting and loving me just like my parents would have, and for keeping an eye on me while my parents are back home in the Philippines!

All my friends with whom I do life, I thank you for laughing with me during the good times and praying with me during the bad times. Special shoutout to my friends, Coco Canseco and Sarah Chan, who let me drag them all way to CDO for fieldwork and for sending me silly things they found on the internet to make me laugh. My church families of Abundant Life Church and Word Community Church, I thank you for all your prayers and continual lessons on service, patience, and outreach. Thank you for keeping me focused and grounded on the truly important things in life.

I thank my colleagues here in New Zealand for allowing me to pick their scientific brains, to run to them with coding or modelling problems, and to chat about research. The VUW Hydrogroup, every officemate I have had, every single person who has given me a modicum of their time to listen to me go on about ecosystem services, I thank you. My gratitude goes out to my colleagues in the Philippines; especially the team led by Dr. Paringit who graciously led me use their computer models, come to their office, access their databases, and join them on their research trip. To the Disaster Risk and Exposure Assessment for Mitigation team, the Phil-LIDAR team, and especially to Ms. Sylvia Sueño and her team of young Filipino scientists for sharing their knowledge.

Lastly, I thank all the local government units, organisations, and people in CDO and Region X for providing their data and management plans, accommodating us in terms of board and time, and giving us the time to speak with their teams. Thank you to Director Dacanay and the National Economic and Development Authority (NEDA-X), to Director Tan and Region X branch of the Department of Public Works and Highways (DPWH), to the officials of the CDO City Hall and Engineer Borja of the City Planning and Development Office, and to the officials of the Talakag Municipal Hall. Thank you also to Kuya Teddy for guidance around the catchment and local knowledge of its nature.

Acronyms and Abbreviations

Acronym or Abbreviation	Meaning
ASTER GDEM	Advanced Spaceborne Thermal Emission and Reflection Radiometer Global Digital Elevation Model
AZ	Accumulation Zone
BSWM	Bureau of Soils and Water Management
CDO	Cagayan de Oro
CESM	Center for Environmental Studies and Management
CliFlo	National Climate Database (for New Zealand)
CTI	Compound Topographic Index
DEM	Digital Elevation Model
DREAM	Disaster Risk and Exposure Assessment for Mitigation Programme
ES	Ecosystem Services
ET	Evapotranspiration
FAC	Flow accumulation
FIM	Flood Inundation Model
Global-PET	Global Potential Evapotranspiration
GWRC	Greater Wellington Regional Council
HEC	Hydrologic Engineering Center
HEC-HMS	Hydrologic Engineering Center - Hydrological Modelling System
HEC-RAS	Hydrologic Engineering Center - River Analysis System
HydTopo	Hydrology and Topography tool in LUCI
HYPRES	Hydraulic Properties of European Soils
IGBP	International Geosphere-Biosphere Programme
IGBP-PTF	IGBP-DIS Soil dataset for Pedotransfer Function Development
IPCC	Intergovernmental Panel on Climate Change
IZ	Impact Zone
JICA	Japan International Cooperation Agency
LCDB	New Zealand Land Cover Database
LiDAR	Light Detection and Ranging
LUCI	Land Utilisation and Capability Indicator
MODIS	Moderate Resolution Imaging Spectroradiometer
MUSLE	Modified Universal Soil Loss Equation
NAMRIA	National Mapping and Resource Information Authority
NASA	National Aeronautics and Space Administration
NCSS	National Cooperative Soil Survey
NDRRMC	National Disaster Risk Reduction and Management Council
NDVI	Normalized Difference Vegetation Index
NIWA	National Institute of Water and Atmospheric Research
NOAH	Nationwide Operational Assessment of Hazards
NRCS	National Resources Conservation Service
NZ	New Zealand
OM	Organic Matter

PAW	Plant Available Water
PES	Payments of Ecosystem Services
PET	Potential Evapotranspiration
PH	Philippines
PHP	Philippine Pesos
PREDICT	Philippine Real-Time Environment Data Acquisition and Interpretation for Climate-Related Tragedy Prevention and Mitigation
PTFs	Pedotransfer Functions
R/USLE	Used to refer to RUSLE and USLE in combination
RPAW	Readily Plant Available Water
RUSLE	Revised Universal Soil Loss Equation
SALT	Sloping Agricultural Land Technology
SCS CN	Soil Conservation Service Curve Number
SWAT	Soil and Water Assessment Tool
TPAW	Total Plant Available Water
USD	United States Dollars
USDA	United States Department of Agriculture
USLE	Universal Soil Loss Equation
WC	Water Content

Units

Unit	Meaning
ton ha^{-1} yr^{-1}	Metric tons per hectare per year
MJ mm ha^{-1} hr^{-1} yr^{-1}	Megajoules millimetre per hectare hour year
ton hr MJ^{-1} mm^{-1}	Metric tons hour per megajoules millimetre
t km^{-2} yr^{-1}	Metric tons per square kilometre per year
m	Metre
m^2	Square metre
km	Kilometre
km^2	Square kilometre
m^3/s	Cubic metres per second
cumecs	Cubic metres per second
masl	Metres above sea level

Disclaimer

Components of this thesis have been previously published as conference proceedings and submitted to a journal. The PhD candidate is the primary author for these citations, doing all analysis and primary writer of the manuscript contents, with the co-authors providing feedback on the manuscript content.

The results in the chapter "Extreme events modelling in the Cagayan de Oro catchment" were published under the following citation: Benavidez, R., Jackson, B., Maxwell, D., and Paringit, E.: Improving predictions of the effects of extreme events, land use, and climate change on the hydrology of watersheds in the Philippines, *Proc. IAHS*, 373, 147-151, https://doi.org/10.5194/piahs-373-147-2016, 2016. This conference proceeding underwent a peer-review process before being accepted for publication and oral presentation.

The chapter "A review of the (Revised) Universal Soil Loss Equation (R/USLE): with a view to increasing its global applicability and improving soil loss estimates" has been submitted to Hydrology and Earth System Sciences and was underwent peer-review through public interactive discussion from February 23 2018. The discussion paper can be found under the following citation: Benavidez, R., Jackson, B., Maxwell, D., and Norton, K.: A review of the (Revised) Universal Soil Loss Equation (R/USLE): with a view to increasing its global applicability and improving soil loss estimates, *Hydrol. Earth Syst. Sci. Discuss.*, https://doi.org/10.5194/hess-2018-68, in review, 2018. Since the submission of this thesis for examination, the PhD candidate has submitted comments to reviewers and approval from the journal is pending.

1 Introduction

1.1 Background and context

This introductory chapter provides the rationale and context of this research through presenting the vulnerabilities of the Philippines to extreme events and the need for proactive disaster risk mitigation programmes through watershed management. The concept of watershed management and ecosystem services to increase the resilience of the catchment and communities to disasters are explained through a review of the existing literature on such topics in the Philippines. The Land Utilisation and Capability Indicator (LUCI) model, which has never previously been applied to the Philippines, is presented in this chapter. The aims and objectives section outlines the goals for this thesis: mainly to parameterise and apply the LUCI model to a catchment in the Philippines, but also contribute to the development of the LUCI framework's related sub-models. LUCI is an ecosystem services model with particular strengths in hydrology and trade-off analysis; this thesis contributed to development of LUCI through parameterisation for soil and land cover in the Philippines (Chapter 2), floodplain inundation mapping (Chapter 7), erosion modelling (Chapter 4), and rainfall-runoff modelling (Chapter 8). Finally, this chapter concludes with a description of the thesis structure of this dissertation.

Tropical cyclones are defined as "intense cyclonic storms that form over the tropical oceans … the most destructive storms on Earth" (Bedient et al., 2013). These extreme events are concerning because of their damaging capabilities, affecting lives and infrastructure around the world. Since 1980, annual losses from weather and climate-related disasters (cyclones, hurricanes, typhoons) have ranged from a few billion US dollars up to 200 billion US dollars globally (IPCC, 2012). With the looming threat of climate change, the IPCC (2012) noted the following likely (>66% probability) changes:

> *"It is likely that the frequency of heavy precipitation or the proportion of total rainfall from heavy rainfalls will increase in the 21st century over many areas of the globe. This is particularly the case in the high latitudes and tropical regions, and in winter in the northern mid-latitudes. Heavy rainfalls associated with tropical cyclones*

are likely to increase with continued warming induced by enhanced greenhouse gas concentrations." (pg. 113)

An analysis of global disasters that occurred in 2012 revealed the most devastating disasters were hydrological (flooding and associated landslides) and meteorological (storms), compared to other disasters such as droughts, earthquakes, or volcanoes (Guha-sapir et al., 2013). Within Asia, most of the recorded 2012 disasters were hydrological in nature (49%) followed by meteorological disasters (27%) (Guha-sapir et al., 2013). Global mapping of historical tropical storm records reveals areas of intense tropical storms, with a large concentration of severe storms in the West Pacific region or Southeast/East Asia region (Figure 1).

The Philippines is located within this area of intense tropical storm activity (Figure 1), and is regularly struck by tropical cyclones that can cause severe landslides and floods (Yusuf & Francisco, 2009). On average, 20 cyclones enter the Philippine Area of Responsibility each year (Figure 2), with about nine making landfall, causing strong winds and intense rainfall with the possibility of causing destructive floods (Lasco et al., 2009). These cyclones have the capability to endanger lives and communities, cause major damage to infrastructure, and result in a costly rebuild effort.

Cyclones in previous years have already had these destructive impacts. In 2009, Tropical Storm Ketsana caused major flooding in the capital of Metropolitan Manila, resulting in 464 casualties and PHP 11 billion (~USD 234 million in 2009) in damage (NDRRMC, 2009). In 2011, Tropical Storm Washi caused heavy flooding and destruction in the southern Philippines, causing 1,268 casualties and PHP 2 billion (~USD 46 million in 2011) in damage (NDRRMC, 2012a). In 2013, Typhoon Haiyan hit central Philippines and caused 6,300 casualties and almost PHP 90 billion (~USD 2 billion in 2013) in damage (NDRRMC, 2014b). Haiyan was reported as the strongest tropical cyclone to make landfall in recorded history, based on record-breaking sustained wind speeds of more than 310 kilometres per hour (Schiermeier, 2013).

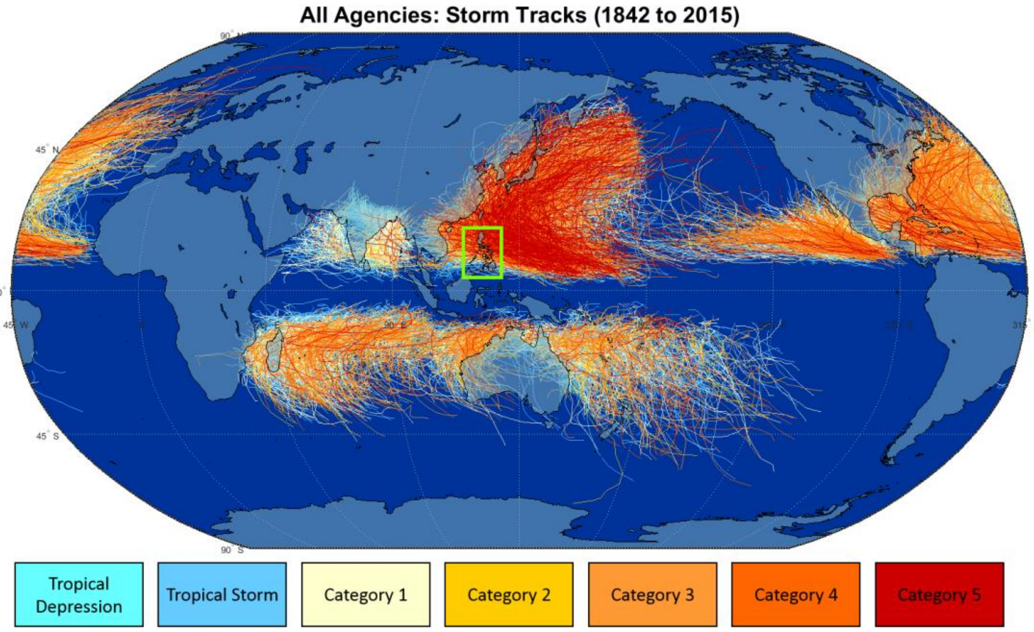

Figure 1. Map of the world showing the Philippines (green box) and storm tracks from 1842 to 2015, using data from all the agencies contributing to the International Best Track Archive for Climate Stewardship (IBTrACS) (Knapp et al., 2010).

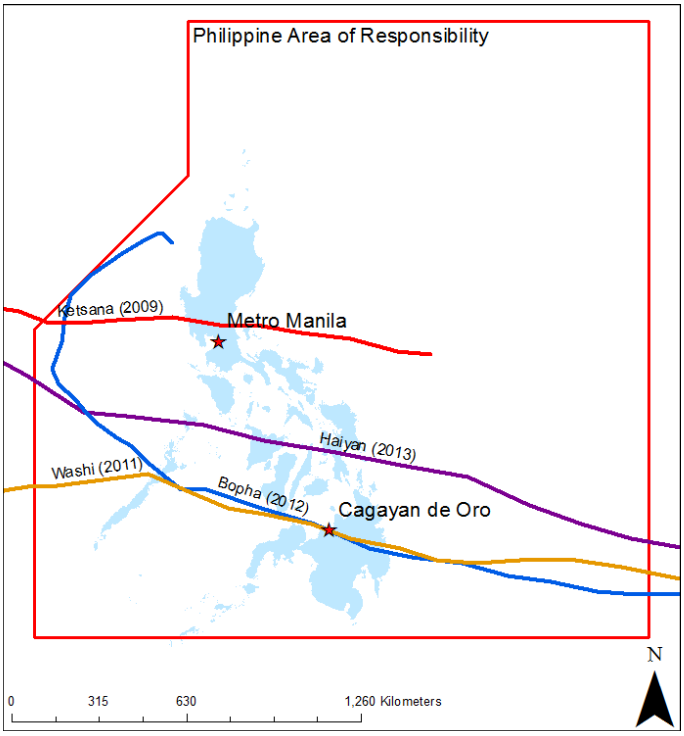

Figure 2. Map of the Philippines and PAR showing the study site Cagayan de Oro (CDO) watershed, the capital of Metro Manila, and tracks of the four extreme events of Ketsana, Washi, Bopha, and Haiyan (Knapp et al., 2010; World Meteorological Organization, 2016).

Given these problems relating to tropical cyclones and their disastrous effects, the field of disaster management and risk reduction is important to the Philippines. The nationwide disaster risk programme is Project NOAH[1] (Nationwide Operational Assessment of Hazards), a multi-disciplinary and multi-agency project aimed at real-time flood forecasting, mapping hazards, and empowering local government and communities through early warning systems (Figure 3 and Figure 4) (Lagmay et al., 2017). The multi-disciplinary approach is important because of the complex interactions between the climate, landscape, and communities, which need to be understood for effective disaster risk mitigation (DeFries & Eshleman, 2004). Through the work done by Project NOAH, at least 18 major river basins in the Philippines have the data and infrastructure capacity for real-time flood forecasting and have been given flood hazard maps at different return periods for the benefit of the local community (Lagmay et al., 2017). This system uses information sent from automated gauges (rainfall, water level, etc.) to forecast the possible water level for the next 48 hours to inform the disaster mitigation operations of the local government (Santillan et al., 2013). With an additional 200+ smaller river basins being studied by Project NOAH, more flood hazard maps will be distributed to aid in sustainable development planning (Lagmay et al., 2017).

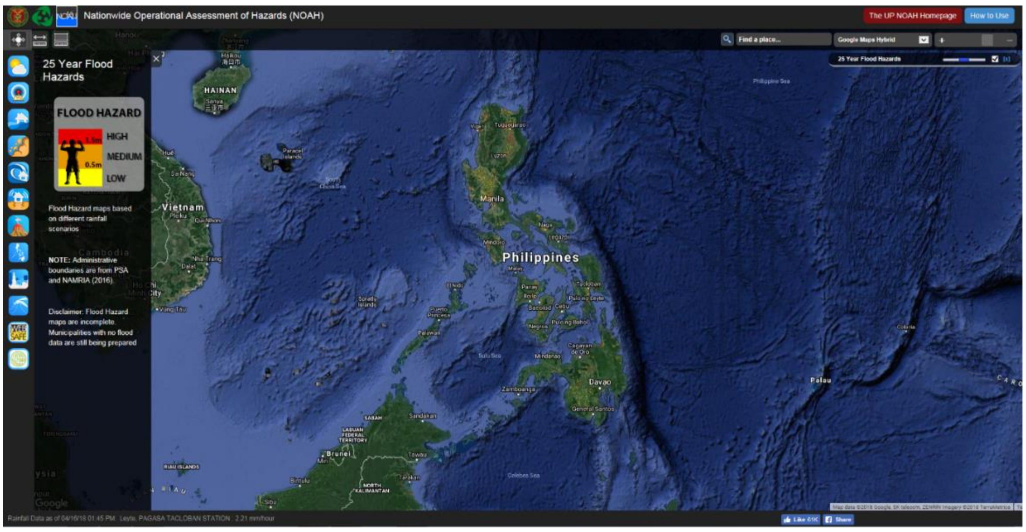

Figure 3. Screenshot of the Project NOAH website (as of 04/05/2018) showing the Philippines and different hazard maps available.

[1]http://noah.up.edu.ph/#/

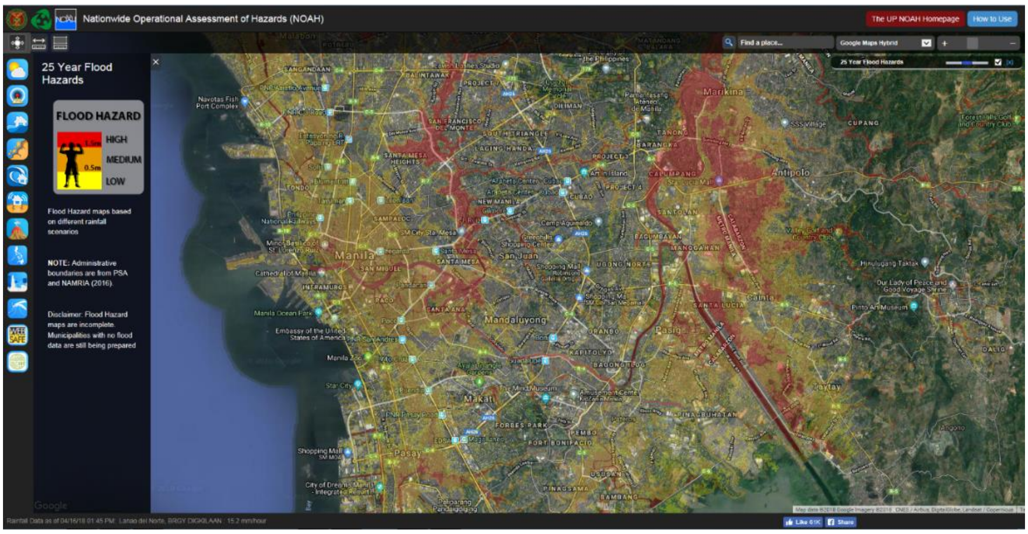

Figure 4. Screenshot of the 25-year flood hazard map for the city of Manila (as of 04/05/2018).

Aside from hazard mapping, disaster risk mitigation includes the following components: real-time forecasting, structural protections, and non-structural measures. Non-structural measures include watershed management, which aims to utilise catchment resources sustainably while not sacrificing the landscape's resilience. Watershed management is the focus of this research as it aims to use spatial data and ecosystem services (ES) modelling to understand the distribution of ES in a catchment, how land use change affects ES and hydrological response, and which areas can be managed to improve ES.

1.2 Watershed management

Sustainable watershed management is the process of planning the land management and resource use within a watershed to balance the production of goods and services with the land's ecological integrity (Cruz, 1999). Essentially, it is a way of sustainably using and managing the watershed without adversely affecting or degrading the landscape. The process of watershed management involves informed decision-making that accounts for the physical, biological, political, and socio-economic characteristics of a watershed (Voinov & Costanza, 1999). The goal is to ensure the continued provision of goods and services (e.g. water supply, agricultural productivity) while also minimising the impacts that anthropogenic activities have on the natural ecosystem (Wagner et al., 2002).

In the Philippines, watersheds are affected by soil erosion, depletion of water resources, and land degradation due to anthropogenic activity, thus requiring strategies to minimise or reverse these effects to ensure future provision of resources (Cruz, 1999). Since watersheds are delineated primarily through physical instead of political boundaries, management must consider the needs and plans of different administrative levels and communities (Voinov & Costanza, 1999). This is especially true for those communities located in the upland areas of the watershed, whose resource usage must be balanced with that of the downstream communities, and thus requires their participation (Fuentes & Concepcion, 2007). Due to this complexity, decision-making processes should be equitable and participatory, and the tools for decision-making should facilitate communication between different stakeholders, promote understanding of management impacts and recommend suitable management strategies (Miller et al., 2004).

Within the framework of watershed management, Cruz (1999) has three examples of management strategies that represent different ways to manage the catchment's existing resources. "Protection" ensures the safety of the current resources, measures such as forest reserves and natural parks with strict logging bans. "Conservation" promotes the sustainable use of these resources and involve programmes such as forest and timber management. Lastly, "Development" is geared towards the rehabilitation and improvement of the watershed and utilises revegetation of denuded slopes and other soil conservation efforts (Cruz, 1999).

Rehabilitation or the replanting of trees and vegetation on cleared areas is one of the methods used in watershed management to enhance the resilience of the watershed to hydrological events. Vegetation also assists in the mitigation of soil erosion, which involves soil particles being transported and deposited from one location to another. This phenomenon occurs naturally, but is exacerbated by anthropogenic activities such as deforestation (Adornado et al., 2009). In the Philippines, it is estimated that a third of the country's land area has been degraded due to excessive soil erosion (David, 1988). However, one of the problems of rehabilitation is that reforestation activities commonly occur in easily-accessible areas where the benefit to ES improvement may be marginal compared to rehabilitation in more critical areas (CESM, 2014). Therefore, it is important to guide rehabilitation efforts to areas that have the most potential to benefit from management interventions.

This spatial aspect of watershed management is important to consider within comprehensive land use planning (Jose & Cruz, 1999). Such planning requires an analysis of different scenarios and situations to identify which ones are suitable for the environment, promote societal well-being, and are economically viable (Reddy, 2000). Land use planning should be able to delineate the areas of protection and production within a watershed, and to examine the impacts of different potential land uses in order to decide which plans align with the goal of sustainable watershed management (Cruz, 1999). Through spatial visualisation (e.g. maps), the nature of the different land use scenarios and their impacts on the watershed can be better communicated to the different stakeholders and communities. The success of watershed management is dependent on those who are directly involved in its use and protection, thus underscoring the importance the participation of these stakeholders in the planning and implementation process (Cruz, 1999).

To summarise the requirements of sustainable watershed management, the process should:

1. Balance the needs of the community with ensuring the sustainable use and future development of the landscape
2. Consider the requirements of managing the watershed at different administrative levels
3. Analyse different scenarios of land use to assess the potential impacts on the landscape
4. Communicate these impacts to the different stakeholders to allow them to make decisions informed by science
5. Put appropriate protocols and resources in place to carry out these decisions and assess their effectiveness

This research primarily focuses on improving our ability to deliver on the third aspect through modelling different land cover scenarios and analysing the distribution of ecosystem services and how these services are affected by changes in land use. Given the benefits of ecosystem services, any changes in their supply and distribution has the power to enhance or degrade the resilience of a catchment. The process of watershed management inherently requires the participation of stakeholders and communities; hence, consultations and meetings are important to achieving the first and second aspects. To improve the fourth aspect, the modelling results should be communicated clearly to those same stakeholders and communities in a manner that can be easily understood and outlines the main conclusions of the modelling work. These results aid in helping stakeholders make decisions that are better informed by scientific research. The fifth aspect requires a multi-disciplinary approach through combining the results of scientific study of the catchment with economic valuation to determine the most cost-effective strategies for watershed management, and to consult with decision-making and policy implementation bodies such as local government. Overall, the physical science behind the decision-making process is part of a larger body of work that requires input from the social and economic spheres of research.

1.3 Ecosystem services

Ecosystem services (ES) are defined as the benefits, whether tangible or intangible, that humans receive from ecosystems (MEA, 2005). It is important to manage ecosystems sustainably for the purposes of their conservation and the continued delivery of ecosystem services for human well-being. Ecosystem services are generally classified into four categories: provisioning (e.g. agricultural production and water supply), regulating (e.g. flood mitigation, soil conservation), supporting (e.g. soil formation), and cultural services (recreation, spiritual, etc.) (MEA, 2005).

Understanding ES and their sensitivity to land cover change is important because of the risk posed by land degradation, such as decreases in agricultural production or increased flood risks (MEA, 2005). Aside from understanding what potential services are supplied by a catchment, it is important to identify which specific areas of that catchment can supply these services. Hence, the spatially explicit mapping of ES is useful for stakeholders to understand their priority areas for conservation and rehabilitation, or to understand the consequences of potential changes in land use and cover (Burkhard et al., 2015).

Given the complex interactions within ecosystems and their services, it is important to consider the trade-offs between ES (MEA, 2005). These services are not just limited to terrestrial ecosystems, as the marine ecosystem provides food supply for coastal communities, and the liminal ecosystem such as tidal swamps and mangroves are valued for their carbon sequestration and supporting fisheries (Castillo et al., 2017; Thompson et al., 2017). Approaches that address ecosystems holistically, such as one that focuses on both the terrestrial and marine ecosystems from mountain to coast, are more useful and highly valued compared to efforts that focus on terrestrial or marine ecosystems separately (Ureta et al., 2016).

In the Philippines, ecosystem services research has been done all over the country, covering all three of the major island groups (Figure 5). The country has a high environmental footprint (i.e. usage of resources and detrimental impacts on the environment) due to several anthropogenic activities such as deforestation, habitat conversion, water pollution, and carbon emissions (Bradshaw et al., 2010). Due to the degrading effects these activities have on ES, research involving mapping, valuing, and the sustainable management of landscapes is important for the country. Previous research on ES in the Philippines has been done in areas with high agricultural value, and in the context of understanding how local communities view and value ecosystem services. The involvement of the local community in ES research is important to understand how they value and perceive different services, to raise awareness of resource conservation, and to encourage community-based strategies to protect ecosystems (Macandog, 2016).

In terms of mapping, Burkhard et al. (2015) used interviews with local experts and land use/cover maps to assess local perceptions of ES in agricultural areas in Northern Philippines. Forests were recognised for their high capability to supply multiple services, which aids in supporting reforestation effects with the potential to increase ES supply (Burkhard et al., 2015). A similar study in Central Philippines of stakeholder perceptions also valued forests for their regulatory abilities (e.g. flood mitigation), as food and income sources, and the ability of trees to increase the landscape's resilience to climate change (Lasco et al., 2016). Spatial mapping of soil carbon stock in Palawan showed the capability of mangroves to sequester more carbon compared to other non-forest land uses, stressing the importance of knowing the location of services and the importance of maintaining beneficial land uses

(Castillo et al., 2017). Through ES maps, the critical areas that provide multiple services that require protection and areas that can be modified to increase service provision are identified.

One of the ES incentives in the Philippines is the Payments of Ecosystem Services (PES) scheme that incentivises stakeholders and local government to implement management strategies that conserve or even enhance ES supply (Thompson et al., 2017). Within the PES framework, those who receive the ecosystem services have a responsibility to support the communities that have the capability to maintain the ES supply through protection and rehabilitation efforts (Ureta et al., 2016). The aim of PES and PES-like programmes is to encourage the adoption of land use practices that are socially desirable or environmental, but were previously not profitable (Macandog, 2016). For example, a PES scheme was established in Southern Philippines involving the local indigenous communities for forest rehabilitation/protection and ES selling (ILC, 2013). In all these PES and similar schemes, inclusive and transparent decision-making was important to engage the local communities, and to encourage the continuation of these schemes.

Other studies have used economic models to understand the potential value of ES, and how climate change and changes in land use can affect their value (Estoque & Murayama, 2016; Langerwisch et al., 2018). A case study involving cost-benefit analysis and total economic valuation in Southern Philippines found that preservation and rehabilitation of the basin could provide USD 2 to 3 million in annual ecosystem services, with additional economic benefits from tourism activities (Baig et al., 2015). Although there are complexities in putting financial value on natural resources, valuation studies are useful for doing cost-benefit analysis, testing different possible scenarios, and for projects that require an economic component.

Aside from spatial mapping and economic valuation of existing ES, scenario analysis is another important aspect of ecosystem services research. Changes in the land use, land cover, and climate of a landscape have the capacity to affect the spatial distribution of ES, the supply of ES, and the value of ES (Kubiszewski et al., 2016). Scenario analysis is useful for testing possible land management plans and futures against the baseline, which can provide feedback and lead to the iterative improvement of these plans. A large-scale regional study of ES in Southeast Asia has predicted a decrease in ES value in all the countries in the study unless steps are taken for policy and land management to focus more on environmental and social well-being (Kubiszewski et al., 2016). In rice-producing ecosystems, research by Langerwisch et al. (2018) predicted a considerable decrease in ES due to climate change, while the effect of land use was dependent on the type of land use changes within the scenario. Trade-offs were also assessed, with adverse effects of climate change leading to potential increase of rice production through converting natural vegetation to rice-growing land, which causes a loss of habitat and biodiversity (Langerwisch et al., 2018).

The extent of all these studies (Figure 5) is indicative of the interest of scientists, government, and communities in ecosystem services and their sustainable use. The methods and types of research were also summarised to reflect the scope of previous ES studies in the Philippines (Table 1). Almost all the studies incorporated local knowledge as a formal part of their methodology, usually through surveys and focus group discussions with key stakeholders. Valuation and willingness-to-pay studies included the PES schemes and other monetary incentives for the protection and conservation of ecosystems. The mapping and scenario analysis studies assessed the spatial distribution of existing ES provision and possible changes to that distribution/quantity in the future.

Table 1. Summary of ecosystem services papers and reports reviewed for this chapter, with those located in or near the CDO catchment shaded.

Author	**Location**	**Local Knowledge**	**Mapping**	**Valuation**	**Scenario analysis**	**Willingness to pay**
Baig et al. (2013)	Calapan City, CDO watershed	X		X		X
Battista et al. (2017)	Cantilan	X				
Bulayong et al. (2015)	Sogod Bay, Southern Leyte	X		X	X	
Burkhard et al. (2015)	Laguna, Nueva Ecija, Ifugao	X	X			
Carandang et al. (2013)	Bohol and Palawan	X		X		
Castillo et al. (2017)	Honda Bay, Palawan		X			
Castonguay et al. (2016)	Banaue (Ifugao)	X				
Cremaschi et al. (2012)	Bakun WS, Maasin WS, Sibuyan WS, Baticulan WS	X				X
Duncan et al. (2016)	Panay Island		X			
Estoque and Murayama (2016)	Baguio			X	X	
Floresca et al. (2009)	Echague	X				

Table 1. Summary of ecosystem services papers and reports reviewed for this chapter, with those located in or near the CDO catchment shaded. (continued)

Author	Location	Local Knowledge	Mapping	Valuation	Scenario analysis	Willingness to pay
Garcia et al. (2009)	Coconut ecosystems *			X		
ILC (2013)	Cagayan de Oro	X				X
Juarez-Lucas et al. (2016)	Candaba floodplain	X		X		
Kubiszewski et al. (2016)	Southeast Asia and Pacific *		X	X	X	
Langerwisch et al. (2018)	Laguna, Nueva Ecija, Ifugao				X	
Lasco et al. (2016)	Bohol	X				
Macandog (2016)	National level *					X
Paelmo et al. (2015)	Makiling Forest Reserve	X				
Palao et al. (2013)	Layawan watershed		X		X	
Spangenberg et al. (2014)	Ifugao	X				
Tamayo et al. (2018)	National level *	X		X		X
Tekken et al. (2017)	Laguna, Nueva Ecija, Ifugao	X				
Thompson et al. (2017)	Panay Island	X				X
Tilliger et al. (2015)	Ifugao	X				
Ureta et al. (2016)	Layawan watershed	X				X

Figure 5. Map of ecosystem services research in the Philippines reviewed for this chapter, with the approximate location of the CDO catchment marked by the red star.

Through this review of ecosystem services research in the Philippines, there is a clear interest in evaluating and mapping services, assessing their economic value, and encouraging the national and local communities to be involved with sustainable land management. It is also clear that the process of ecosystem services research and creation of sustainable development plans is complex, multi-disciplinary, and must be inclusive. Through increasing the health of an ecosystem, this ecosystem also becomes more resilient and can provide continued benefits to the community (Baig et al., 2015). This work fits into the broader framework of ecosystem service modelling and watershed management in the Philippines through helping local government understand the distribution of ecosystem services such as flood mitigation and soil erosion across the study catchment. Using visualisation and scenario analysis, a greater understanding is gained of the potential impacts of land use change and management. Flooding associated with extreme events is a rapid disaster, bringing devastating effects in a short amount of time. On the other hand, soil erosion is a more prolonged problem, increasing loads of sediment passing through river systems and changing flood risk over longer time scales due to changes in river bathymetry. These two ecosystem services of flood mitigation and soil conservation are therefore two services that are very important to protect communities, and this application of an ecosystem services modelling and mapping can be used to provide feedback to stakeholders about their plans for land management.

1.4 The Land Utilisation and Capability Indicator (LUCI) framework

The LUCI framework is a GIS-based model that uses a digital elevation model (DEM), land cover data, and soil data to produce spatially-explicit maps of ecosystem services and trade-offs over a landscape that can range from the field scale to national scale (Jackson et al., 2013). These services are outlined in Table 2, but this research has a specific focus on the flooding, erosion, and flooding inundation risk components. Additional modelling was done for the agricultural productivity and water quality tools, and future work will require more detailed parameterisation for all these services. LUCI produces maps showing locations where land managers can place interventions to improve the ecosystem services and locations where any change in the land cover or land management may degrade the ecosystem services. The trade-off tool allows for several services to be analysed at once and produces maps that show the locations where changes may enhance or degrade multiple services.

Table 2. List of ecosystem services modelled by LUCI (Jackson et al., 2013).

Service	**Method**
Agricultural production	Based on slope, fertility, drainage, aspect, climate
C stock/emissions	IPCC Tier 1 compatible – based on soil & vegetation
CH_4/N_2O emissions	IPCC Tier 1 compatible – soils, veg, stocking rate, fertiliser
Water supply and floods/droughts	Topographical routing of water accounting for storage and infiltration capacity as function of soil & land use.
Erosion	Slope, curvature, contributing area, land use, soil type
Sediment delivery	Erosion combined with detailed topographical routing
Water quality	Export coefficients (land cover, farm type, regional fertiliser, stocking rate) combined with water and sediment delivery models
Habitat Approaches	Cost-distance approach: dispersal, fragmentation, connectivity. Identification of priority habitat by biophysical requirements e.g. wet grassland Measures of habitat richness, evenness, patch size etc.
Coast/floodplain inundation risk	Based on topography and input height of storm surge/long term rise etc: surface and groundwater impacts estimated
Trade-offs/synergy identification	Various layering options with categorised service maps; e.g. Boolean, conservative, weighted arithmetic, distribution plots

The LUCI framework has been applied to several different locations: the United Kingdom, New Zealand, Ghana, Greece, Bulgaria, and Vanuatu (Bagstad et al., 2013). However, it has not yet been applied to the Philippines, making this research the first detailed application of LUCI to this tropical country. By default, the LUCI framework uses a red-yellow-green colour scheme for its output maps with green areas providing good supply of ecosystem services and red areas being areas that could be managed to enhance ES (Figure 6). These yellow/red areas are therefore possible areas to place flood mitigation, soil conservation, or sediment trapping measures such as riparian planting or wetland creation.

LUCI was chosen for this research because the model is more spatially explicit compared to other ecosystem service models by accounting for physical configuration of land cover and soils affect ecosystem services (Jackson et al., 2013). The results are not only influenced by the type of land cover and soils, but also by the placement of these elements within the landscape and their interconnectedness. LUCI was also designed with stakeholder engagement in mind, with output maps that are relatively simple to interpret, and the capability of producing trade-off maps to show synergies within land cover scenarios (Bagstad et al., 2013).

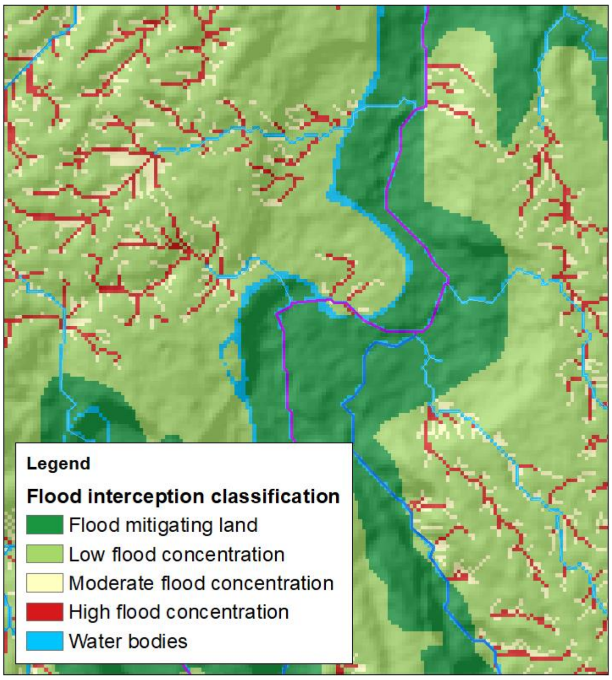

Figure 6. Sample flood interception classification output map from LUCI.

This is the first detailed application of LUCI on a tropical catchment in the Philippines, the Cagayan de Oro (CDO) catchment (Section 1.7). Since LUCI has never been applied to the Philippines, this novel application allowed testing and parameterisation of how LUCI represents hydrological and geomorphological processes in a different climate. This application extended the range of datasets that LUCI can support since the Philippines uses the United States soil classification system, which LUCI did not previously support. The information gathered from this application can be used to aid stakeholders in making better decisions regarding land management, such as where interventions can be placed. This is another novel aspect of this research because this type of ecosystem service modelling and mapping has not been previously accomplished in the CDO watershed.

This study also assessed how LUCI fits into the current management framework in the watershed. Currently, an automated real-time flood-forecasting framework exists within the catchment to provide hazard maps and warnings for local communities and government. This framework is run by the Disaster Risk and Exposure Assessment for Mitigation (DREAM) Program and uses two models from the United States Hydrologic Engineering Center (HEC): Hydrological Modelling System (HMS) for rainfall-runoff modelling and River Analysis System (RAS) for mapping floodplain inundation (Disaster Risk and Exposure Assessment for Mitigation Program, 2015). Figure 7 shows how LUCI complements the existing modelling framework in the study area. The CDO watershed already has an automated flood forecasting system that uses HEC-HMS and HEC-RAS, and plans for rehabilitation and development (CESM, 2015; Paringit et al., 2015). Therefore, LUCI's role is to elucidate how changes in land cover affect ES supply and distribution, return feedback to stakeholders about their management plans, and contribute to the iterative development of such plans.

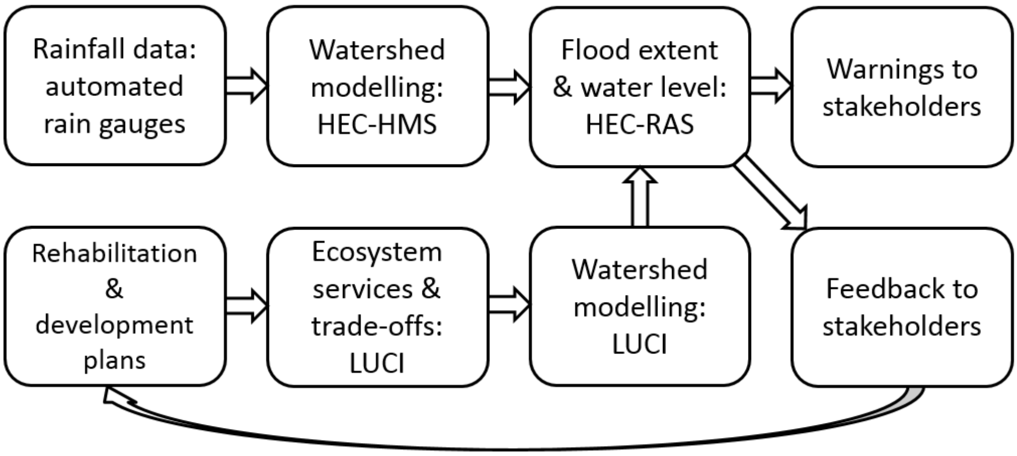

Figure 7. An illustration of how the LUCI model fits into the current disaster-risk management framework in the CDO watershed.

1.5 Extreme events

With the increasingly rapid development and land use change in Southeast Asia, the sustainability of these activities must be considered (Valentin et al., 2008). In particular, the influence of urbanisation and increased upland activity on the land cover and its potential consequences on runoff and flooding is an important area of research all over the Philippines (Figure 8) (Du et al., 2012). There are three strategies outlined by the Government of the Philippines to address flood mitigation: construction of structural measures in high-risk areas, include climate change adaptation in the design of these structural measures, and to also promote the usage of non-structural measures such as watershed management (JICA, 2014). Extreme events and flood modelling research has underscored the importance of restoration, real-time flood forecasting, and hazard mapping (Pati et al., 2014). Aside from the work done by Project NOAH, other researchers have used different watershed models and floodplain inundation models to elucidate the effect of changing land cover, extreme events, and a combination of both (Table 3).

Scenario analysis of different rainfall events helps management to understand the potential peak flows and floodplain inundation from events of different return periods or past typhoons. Modelling events of different return periods create flood hazard maps to help guide future urbanisation and land zoning development. Knowing the potential flow and inundation associated with rainfall events of different return periods is important to predict future runoff events (Abon et al., 2011; Bien & Plopenio, 2017). Although HEC-HMS and HEC-RAS are commonly used in the Philippines, other techniques such as Artificial Neutral Networks are also used to relate long records of rainfall and water level and are used for prediction (Malaguit et al., 2017).

Extreme events modelling also guides the design of different structural measures as structures such as dams are ideally designed for 25-year to 100-year events (Ternate et al., 2017). The construction and implementation of structural measures may be limited by logistical factors (e.g. funding), hence the design must balance the capability of the structure to protect infrastructure and communities and the ability to implement the flood mitigation project. Within the CDO catchment, the project by JICA (2014) used extreme event modelling under different return periods and the Washi/Sendong event to guide the design of the retaining wall to protect the CDO floodplain. Aside from the construction of structural measures, extreme events modelling can guide the operation of weirs and dams (Badilla, 2008).

Following hazard mapping of the floodplain, the social dimension of flooding can be understood through relating the spatial distribution of the flood to the population that may be potentially affected. By accounting for both hydrological factors and social vulnerability, the high-risk areas are delineated, and management efforts can be focused on those communities. These vulnerability indicators are dependent on population demographics, socio-economic factors, the dependence of the community on natural resources, and the accessibility of public infrastructure such as roads and hospitals (Pati et al., 2014). Adding even more complexity, the economic consequences of these hazards can be understood through depth-damage functions that relate flood depth with potential damage to calculate the potential loss from damaged infrastructure or losses in agricultural yield (Shrestha et al., 2016). This multi-disciplinary approach of hydrology, social factors, and economics is important for an integrated disaster risk management plan and for participatory decision-making.

Scenario analysis is used in flood modelling to understand the consequences associated with past land use change, or the potential consequences of future land use change. Using the Soil and Water Assessment Tool (SWAT)[2], the potential conversion of pasture and grassland to typical agricultural conditions in the Manupali catchment is predicted to increase runoff volume and sediment yield (Alibuyog et al., 2009). Another SWAT study in the Palico catchment, predicted increases in surface runoff associated with a reduction of forest cover and rangelands (Briones et al., 2016). The HEC-HMS model was used in the Taguibo catchment to model rehabilitation scenarios, predicting a likely reduction of runoff due to the rehabilitation of barren and deforested areas (Santillan et al., 2011). A long-term monitoring study of several catchments in Southeast Asia showed that conservation efforts such as contour tillage, bamboo-planting on slopes, and riparian planting reduced runoff and sediment yield (Valentin et al., 2008).

Modelling work was done in varying land cover scenarios and the rainfall events to elucidate the potential combined effect of these two factors. SWAT modelling in the Calumpang catchment showed increased streamflow during the monsoon season for sub-catchments with more built-up areas and reduced vegetation (Boongaling et al., 2018). Understanding how the hydrological response of a catchment varies with land cover and seasonal rainfall is important for understanding the possible effect on water security and sustainability (Briones et al., 2016).

[2] SWAT is a programme used to model runoff, water resources, sediment yield, and nonpoint-sources of pollution at different spatial scales under different environmental conditions (Alibuyog et al., 2009; Gassman et al., 2007).

Table 3. Extreme events modelling studies in the Philippines, with those in or near the CDO catchment shaded.

Author	**Study site**	**Model**	**Land use and land cover**	**Runoff and flow modelling**	**Inundation**
Abon et al. (2011)	Marikina	HEC-HMS		X	
Alibuyog et al. (2009)	Manupali	SWAT	X	X	
Badilla (2008)	Marikina	HBV and DUFLOW		X	
Bien & Plopenio (2017)	Albay	HEC-HMS		X	X
Boongaling et al. (2018)	Calumpang, Marikina	SWAT	X	X	
Briones et al. (2016)	Palico	SWAT	X	X	
JICA (2014)	Cagayan de Oro	Own model		X	X
Mabao & Cabahug (2014)	Cagayan de Oro	HEC-HMS and HEC-RAS		X	X
Malaguit et al. (2017)	Pampanga	ANN		X	
Otieno (2004)	Lower Bicol floodplain	Delft-FLS			X
Paringit et al. (2015)	Cagayan de Oro	HEC-HMS and HEC-RAS		X	X
Pati et al. (2014)	Laguna	HEC-HMS and HEC-RAS		X	X
Ross et al. (2015)	Compostela Valley	FLO-2D			X
Santillan et al. (2011)	Taguibo WS	HEC-HMS	X		
Santillan et al. (2013)	Marikina	HEC-HMS and HEC-RAS		X	X
Shrestha et al. (2016)	Pampanga	Own model		X	X
Ternate et al. (2017)	Malaking-Ilog, Batangas	HEC-HMS and HEC-RAS		X	X
Valentin et al. (2008)	Bukidnon	Monitoring	X	X (monitoring)	

Figure 8. Map of some extreme events studies in the Philippines.

1.6 Climate change

In Southeast Asia, there are strong regional variations in the IPCC projections due to terrain. Overall, warming is very likely and there is a medium confidence in the increase in rainfall (Christensen et al., 2013). Under the Representative Concentration Pathway (RCP) 4.5, a mean temperature increase of 0.5 to 2°C is projected for the period of 2081-2100 (IPCC, 2013). RCP4.5 represents a scenario where radiative forcing is stabilised at 4.5W m^{-2} by 2100 through policies aimed at limiting emissions (Thomson et al., 2011). Since warming will likely affect future water resources, understanding how climate change affects the hydrological cycle is critical for more efficient resource management (Ty et al., 2012). The hydrological cycle will also be affected by the likely changes in precipitation. Under RCP4.5, the 20-year mean rainfall in Southeast Asia is expected to increase, with significant increases in the 75th percentile by 2081 that deviate from natural variability (IPCC, 2013). This increase in rainfall is likely to lead to increases in water supply and runoff during the rainy season, but to increased water stress during the dry season (Ty et al., 2012). To summarise, dry seasons are predicted to be drier and hotter while wet seasons are predicted to have more intense rainfall.

The Philippines is vulnerable to climate change due to its dependence on water resources, for which demand is predicted to rise with projected population growth (Amadore et al., 1996). Additionally, the country's exposure to tropical cyclones makes it more vulnerable to increases in rainfall associated with extreme events. An analysis of the historical typhoon record shows no significant trends in the total number of typhoons making landfall in the Philippines, but increases in the intensity of typhoons and associated increases in economic damage (Cinco et al., 2016). Previous research around climate change modelling in the Philippines has centred around downscaling projections from Global Circulation Models (GCMs) for streamflow predictions, crop yield modelling, and water balance modelling. Generally, the increases in precipitation are projected to lead to increases in streamflow that provide more water for agriculture but with higher risks of flooding and soil erosion (Tolentino et al., 2016). However, these hydrological fluctuations are not consistent across all the different catchments within the Philippines. In the Mount Makiling watershed in Northern Philippines, water balance modelling predicted high evaporation losses and decrease in streamflow under climate change (Combalicer et al., 2010). Similarly, the Angat reservoir (Northern Philippines) and Lake Lanao (Southern Philippines) will be affected by changes in temperature and rainfall leading to decreases in runoff and a deficit in the water availability for future demand (Jose & Cruz, 1999). In various areas of the Philippines, crop modelling for rice and corn showed potential decrease in yields due to shorter maturity periods and increases in potential evapotranspiration from warmer temperatures (Buan et al., 1996).

A national-scale report has been previously published that reviews the potential physical impacts of climate change on the temperature, seasonal rainfall, precipitation extremes, and tropical cyclones that affect the Philippines (Villarin et al., 2016). Rainfall during the northeast monsoon (December to February) is expected to increase, while rainfall during the southwest monsoon (June to August) is expected to increase in Northern and Central Philippines with potential decreases for Southern Philippines (Hilario et al., 2011). A related report reviews the social impacts of climate change, the vulnerability of communities, and their potential adaptive capacity (Cruz et al., 2017). Given the strong regional variability in the potential effects of climate change, more work at the regional and catchment-level is essential to elucidate its local effects. Discussion about how climate change may potentially affect the study area of this thesis is detailed in the extreme events chapter (Chapter 8).

1.7 Background of Cagayan de Oro (CDO)

This study focuses on the Cagayan de Oro watershed, located in Northern Mindanao (Figure 9). The river passes through the city of the same name, which has a population of 600,000 as of May 1st 2010 (NSO, 2010). This watershed is an important source of drinking and irrigation water, area for agricultural production, mining, adventure tourism, and home of different indigenous communities (CESM, 2014). The watershed is approximately 1400km^2, with over 70% of its area devoted to agriculture (CESM, 2014; Mabao & Cabahug, 2014). The dominant soil series *Kidapawan* (subgroup: *Typic Paleudults*) which is characterised by good to excessive external drainage, and good internal drainage (Carating et al., 2014). However, unsustainable land management in the CDO catchment has led to erosion, loss of forest and habitat, decreases in water quality and supply, and flooding (CESM, 2014). Thus, sustainable land use management, zoning, and rehabilitation within the CDO catchment are important tools for catchment management.

The vulnerability of CDO to flooding, its problems associated with soil erosion, and heavy agricultural use of the catchment make it a good study site for ecosystem services modelling. LUCI produces spatially-explicit maps that show the distribution and supply of different services such as flood mitigation, agricultural productivity, and nutrient delivery. The site was also chosen because of the availability of detailed watershed reports that explained the land management options that local government is planning to carry out, which were used as input to the LUCI model to investigate how these land cover scenarios would affect ecosystem services and soil erosion. Given that real-time flood forecasting and structural measures against floods already exist in CDO, this research focused on the non-structural aspect of disaster risk management: promoting the sustainable land management within the catchment.

After Typhoon Washi affected the Cagayan de Oro (CDO) city and catchment in 2011, there has been more public interest in the rehabilitation of the CDO catchment through reforestation and tree-planting activities (CESM, 2014). Within the CDO river and floodplain, structural measures such as a flood wall and a retention basin have been planned and are being implemented (JICA, 2014).

Within the CDO catchment and floodplain, the real-time flood forecasting system by Project NOAH is operational and is key to providing adequate warning to local government and communities (Paringit et al., 2015). Similarly, hazard maps were produced under different rainfall events to show that the city of CDO is vulnerable to flooding under storms of 2-year and 5-year return periods (Mabao & Cabahug, 2014). The work by JICA (2014) on modelling extreme events and structural design has led to the construction of a retaining wall to protect riparian communities living on the floodplain. In terms of land cover and management, work by Valentin et al. (2008) in the nearby Mapawa catchment showed reductions in runoff and sediment yield through contour tillage and riparian planting. Aside from using ecosystem services modelling to understand the effect of land cover on different ecosystem services (Chapter 3) and soil erosion (Chapter 5), this research also did preliminary evaluation of the hydrologic response of the CDO catchment to extreme events (Chapter 8).

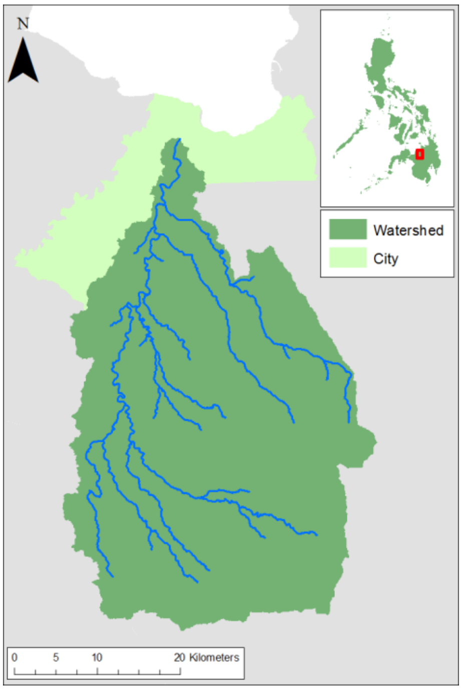

Figure 9. Map of the CDO watershed, river, and city, and their location relative to the rest of the Philippines.

1.8 Aims and objectives

This research contributes to the body of knowledge regarding ecosystem services modelling and watershed modelling in the Philippines. The overall aim of this study is to understand the changes to ecosystem services and hydrological responses of the CDO catchment associated with changes in land cover from the baseline scenario to plans involving catchment development and rehabilitation. The specific objectives are outlined below:

To apply LUCI to the CDO catchment to understand the spatial aspect of its ecosystem services and help identify priority areas for land management

Prior to this research, the LUCI framework has never been applied in the Philippines, and the local datasets for the CDO watershed utilise land cover and soil classification systems that are different from those already integrated into the LUCI framework. Through parameterisation of these datasets, this research tested the applicability and coverage of LUCI, allowing it to identify areas in the catchment that are providing different ecosystem services (i.e. flood mitigation, agricultural productivity, nitrogen and phosphorus delivery).

To assess how development and rehabilitation plans will affect the ecosystem services and soil erosion within the watershed

The development master plan for the CDO outlined the plans for basin rehabilitation and development, with the objectives of sustainable utilisation and decision-making supported by scientific research (CESM, 2014). This plan's scenario of management zoning and the rehabilitation scenario was run through LUCI to assess their potential effects on the spatial distribution of areas providing flood mitigation and other ES, and areas vulnerable to soil erosion (CESM, 2014; CESM, 2015).

To contribute to future development of LUCI through developing and testing new components of the LUCI framework (i.e. sheet/rill erosion modelling, floodplain inundation, and rainfall-runoff modelling)

First applications of the LUCI framework generally apply spatially explicit but temporally lumped GIS-based ES models but includes more detailed but less-applied models for rainfall-runoff modelling and floodplain inundation, both of which are required for floodplain hazard mapping. This thesis presented preliminary work in parameterising the LUCI model for rainfall-runoff modelling in CDO and comparing it to the results from HEC-HMS (Chapter 8), and to updating and implementing the previous LUCI inundation model into ArcMap (Chapter 7). Future work will involve understanding how changes in land use will affect how the CDO watershed will respond to extreme events based on the resulting flow hydrograph and floodplain inundation.

The existing sediment delivery model in LUCI uses the Compound Topographic Index (CTI) that predicts areas vulnerable to gully erosion but no other types of erosion such as sheet or rill erosion. Testing and applying the RUSLE (Chapters 4 to 6) allowed for inclusion of more erosion modelling into the LUCI framework and eventual implementation into the supported LUCI software.

Broadly, this pilot application of LUCI to the Philippines lays the groundwork for improving the applicability of LUCI in tropical areas through parameterisation of the soil and land cover specific to the Philippines, which were not previously supported in LUCI. Although the CDO application is starting with flood mitigation and soil erosion, preliminary runs for agricultural productivity and nutrient delivery were done. Future work revolves around better representing local conditions in CDO through more detailed parameterisation. The soil erosion component of this thesis contributes through LUCI development by implementing the Revised Universal Soil Loss Equation

(RUSLE). The implementation of the RUSLE within LUCI required testing the different components of the RUSLE, which resulted in a novel review of the different RUSLE sub-models and how they were used at varying spatial scales and sites of data availability around the world. The floodplain inundation model was also updated for this thesis and implemented as a Python script that will be integrated into future versions of LUCI.

1.9 Thesis Structure

This introductory chapter presented the background and rationale of the study, outlining the work previously done in the Philippines around watershed management, ecosystem services, and extreme events. The pilot site in the Philippines, the CDO catchment, was presented along with the LUCI model to provide context of why ES modelling is important in the area. Finally, the chapter outlines the aims and objectives of this thesis before concluding with a structure of the manuscript.

Chapter 2 is the methodology chapter that presents the data and respective sources used for this thesis. One of the main objectives of this thesis is to understand the effect of changing land cover on ecosystem services; hence, the chapter presents three different land cover scenarios (baseline, development, and rehabilitation) that were used in the various modelling components of this thesis. This chapter details the steps taken to parameterise the model for the kinds of soil and land cover present in the CDO catchment based on literature and fieldwork for Philippines-based data and characteristics. This parameterisation lays the groundwork for further applications of LUCI in the Philippines, further development of the LUCI model with tropical data, and serves as guidance for other applications of LUCI in new areas. Another component of the parameterisation was to link the soil and land cover to the New Zealand soil and land cover since the NZ classification is most supported in the LUCI framework. The purpose of correlating PH and NZ classifications was to test the effectiveness of linking soil and land cover from a different climate regime to the NZ parameterisation, as it can be used by future applications in data-scarce regions to be able to run LUCI. The methodology chapter also presents the two main ecosystem services focused on for this thesis: flood mitigation and soil erosion, and what models have been used to elucidate the distribution and effect of land cover on these services. Following this is detail about the preliminary work done on extreme events modelling including modelling the peak flows of LUCI and HEC-HMS under one extreme event, and mapping the potential inundation on the CDO floodplain. The methodology then concludes with a summary of the different components of this thesis and how they fit into the broader aim of this research.

The next section of this thesis focuses on the application of the LUCI model to CDO to run its ecosystem services modelling under different land cover scenarios (Chapter 3). The main focus of this work was flood mitigation and how its distribution and supply would be expected to change under the land cover scenarios. This was accomplished through gathering and incorporating soil and land cover characteristics specific to the Philippines, which is the PH-based parameterisation previously not supported by LUCI. Another component of this chapter is testing the NZ-based parameterisation outlined in the methodology by comparing the results of the flood mitigation maps with the PH-based parameterisation. The NZ-based parameterisation also enabled LUCI to produce indicative maps of agricultural productivity and water quality (nitrogen and phosphorus). Testing these parameterisations against each other is important due to the varying levels of data available in different study sites. In sites where soil and land cover characteristics are known, the parameterisation procedures outlined in Chapter 2 guides the user to set up LUCI for their study sites. In areas with scarcer data, the NZ-based parameterisation can be used to simplify the set up of LUCI.

With the LUCI model parameterised and applied to the CDO catchment, the next sections of the thesis focus on the contributions of this research to LUCI development through improvements in sediment delivery, inundation mapping, and rainfall-runoff modelling. The ES of soil conservation was analysed through soil erosion modelling using the Revised Universal Soil Loss Equation (RUSLE) over three chapters: a review of RUSLE in Chapter 4, the resulting applications of RUSLE in CDO (Chapter 5), and a case study of RUSLE in New Zealand due the availability of high-resolution datasets (Chapter 6). The purpose of the review chapter was to explain the RUSLE model and its various sub-equations account for rainfall, topography, etc. and to outline some of its limitations and the potential future directions to improve RUSLE estimates and incorporate the model into the LUCI framework. The CDO application is important in understanding the spatial aspect of soil erosion through delineating vulnerable areas as potential targets for soil conservation measures and the potential effects that changing land cover can have on these areas and soil erosion rates. The RUSLE was applied to the Mangatarere catchment in New Zealand to test the sensitivity of the model and its sub-equations, including the effect of different digital elevation model (DEM) resolutions. Since the only DEMs available for the CDO catchment had a minimum resolution of 30m, the NZ application was needed to elucidate the effect of finer DEM resolutions (15m and 5m) on soil erosion estimates.

Although the scope of this research is mainly modelling and mapping ecosystem services under different land cover scenarios, work was also done and presented that detailed the capability of the LUCI model to perform rainfall-runoff modelling and produce a flow hydrograph comparable to results from the widely-applied HEC-HMS (Benavidez et al., 2016). The extreme events chapter (Chapter 8) presented those results again but with more detail on the differences between HEC-HMS and LUCI, information about other extreme events that have impacted CDO, infilling and processing rainfall data, and directions for future work around event modelling. This chapter also includes a section discussing the potential impact of climate change on the extreme events that produce devastating floods and the possible changes to ecosystem services under climate change. The inundation chapter reviews the different methods of estimating and modelling floodplain inundation, presents the existing LUCI inundation model, and the potential improvements that will be incorporated into LUCI in future work (Chapter 7). These two chapters lay the groundwork for future comparisons of the LUCI framework to the more widely-applied models of HEC-HMS and HEC-RAS, contributing to improvements to future development of the LUCI model.

Lastly, this dissertation concludes with a synthesis chapter about how the different land cover scenarios affect flood mitigation and soil erosion. This chapter discusses the overarching themes that stemmed from the literature analysis, model development, and modelling results of this thesis. Additionally, this chapter outlines the key issues and limitations of this research and suggests future work that can be accomplished to overcome these issues. The chapter concludes with a discussion of the implications of this research for the CDO catchment, the Philippines, and the broader scale of global ecosystem services modelling. Overall, this thesis presents novel work regarding ecosystem services and disaster risk management in the Philippines through scenario analysis. It contributes to LUCI development by improving its applicability to tropical areas, testing a model for the soil erosion component, and updating its floodplain inundation modelling code.

2 Overview of methodology and data sources

2.1 Introduction

This chapter provides an overview of the methodology of this research and the different components of this thesis: Land Utilisation and Capability Indicator (LUCI) parameterisation (soil and land cover), ecosystem services modelling (soil erosion and flood mitigation) and extreme events modelling. Collecting information for the soil and land cover parameterisation was accomplished through a combination of using national/local GIS datasets, information from external databases, and fieldwork. Three different land cover scenarios were assessed for changes in ecosystem services (Chapter 3) and areas vulnerable to soil erosion (Chapter 5): baseline, development, and rehabilitation, all of which differ in the distribution of land cover types and management strategies. Extreme events modelling was achieved for Typhoon Bopha under the baseline scenario to test the rainfall-runoff modelling capabilities of LUCI against HEC-HMS (Chapter 8).

2.2 Data sources

This section summarises the data used for this thesis, which is mainly spatial data that was used in ArcMap 10.4.1 (Table 4). At the minimum, the LUCI framework needs three input files: a digital elevation model (DEM), land cover shapefile, and soil shapefile. The HEC-HMS and HEC-RAS models parameterised for the Cagayan de Oro (CDO) catchment were kindly provided by the DREAM programme (Disaster Risk and Exposure Assessment for Mitigation Program, 2015).

Table 4. Summary of the data used for this thesis, the source, and the purpose.

Data	Source	Purpose
Digital Elevation Model	ASTER GDEM v2 (NASA JPL, 2011)	• Flood mitigation modelling in LUCI • Soil erosion modelling in RUSLE • Extreme events modelling in LUCI

Table 4. Summary of the data used for this thesis, the source, and the purpose. (continued)

Data	**Source**	**Purpose**
Land cover scenarios	• Baseline (DREAM, 2015) • Development (CESM, 2014) Rehabilitation (CESM, 2015)	• Flood mitigation modelling in LUCI • Soil erosion modelling in RUSLE Extreme events modelling in LUCI and HEC-HMS
Soil physical and textural characteristics	• IGBP-PTF database (Tempel et al., 1996) • NCSS database (Reinsch & West, 2010)	• Flood mitigation modelling in LUCI • Soil erosion modelling in RUSLE • Extreme events modelling in LUCI and HEC-HMS
Stream network	DREAM (2015)	• Flood mitigation modelling in LUCI • Extreme events modelling in LUCI
Gridded rainfall data at annual scale	WorldClim (Hijmans et al., 2005)	• Flood mitigation modelling in LUCI • Soil erosion modelling in RUSLE
Monthly rainfall data as time-series	• WorldClim (Hijmans et al., 2005) • CESM (2014)	• Soil erosion modelling in RUSLE
Event-based rainfall data as time-series	• DREAM (2015) • PREDICT framework	• Extreme events modelling in LUCI and HEC-HMS
LiDAR-derived DEM for floodplain	• DREAM (2015)	• Inundation mapping in LUCI and HEC-RAS

The DEM was extracted from the Advanced Spaceborne Thermal Emission and Reflection Radiometer (ASTER) Global Digital Elevation Model Version 2 (GDEM V2) and clipped to the study area (NASA JPL, 2011). The resolution of this dataset is ~30m and it is the highest resolution DEM available that covers the entire catchment (Figure 10). Steeper slopes occur in the upland areas in the south and southeastern portion of the catchment where the peaks of Mount Kalatungan (2,824 masl) and Mount Kitanglad (2,899 masl) are located (CESM, 2014). Although LiDAR-derived products exist for this region, the LiDAR only covers the floodplain area at the outlet of the catchment and is commonly used for floodplain inundation modelling (DREAM, 2015). This DEM was used as input to the soil erosion and the flood mitigation models. The DEM represents the topography of the catchment, giving information about slope and allowing the models to simulate the susceptibility of areas to soil erosion or the routing of surface flow through the landscape.

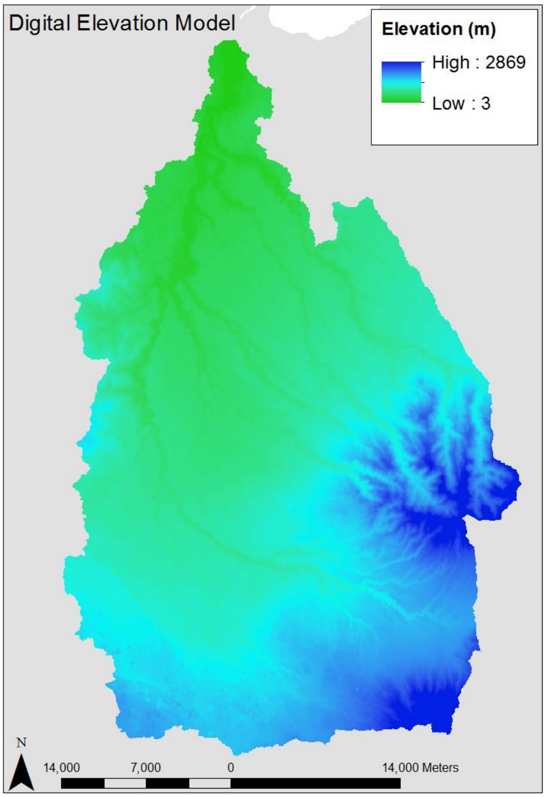

Figure 10. Digital elevation model of the CDO catchment.

The baseline land cover scenario was taken from the national land cover map produced by the National Mapping and Resource Information Authority (NAMRIA), the centralised institution for mapping, storage and distribution of maps (DREAM, 2014). The HEC-HMS parameterisation with CDO uses the baseline scenario for the flood forecasting model (DREAM, 2015). The development scenario was created using information from existing land cover, mapped restricted areas such as forest reserves, delineated areas of different ownership (public and private), and topographic information such as slope (CESM, 2014). The rehabilitation scenario was based on the development scenario, but with additional recommendations for rehabilitation strategies such as reforestation, natural regeneration, agroforestry and sustainable farming (CESM, 2015). Three main land use scenarios for the CDO basin were the land cover input for the ecosystem service and soil erosion models (Figure 11).

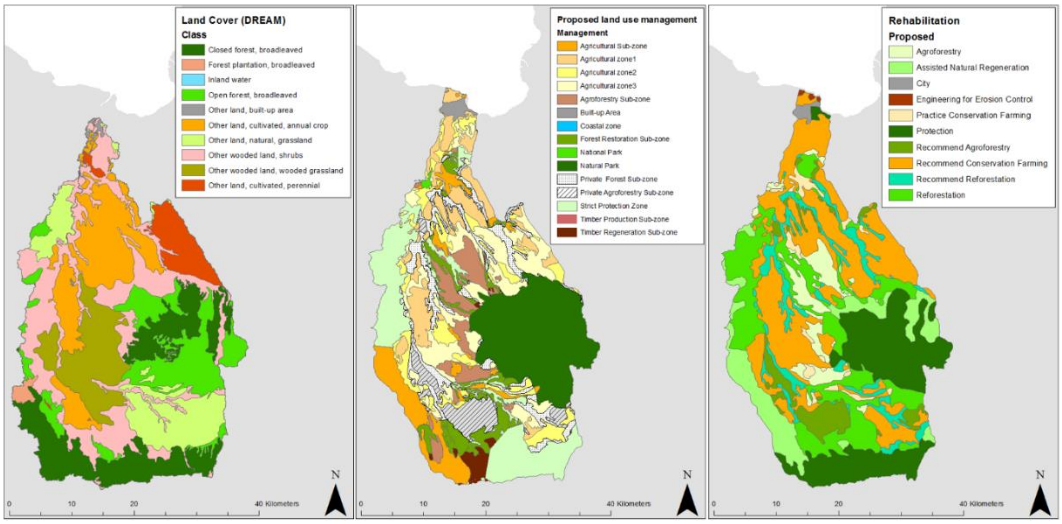

Figure 11. Maps of the different land use scenarios.

Figure 11 shows the different land cover scenarios as taken from the original sources (NAMRIA, CESM, etc.) For consistency, preprocessing was carried out to align the spatial coverage of the development and rehabilitation scenario to the coverage of the baseline scenario (Figure 12). The development and rehabilitation scenarios were made consistent with the baseline scenario and the land cover classes were generalised for easier visual comparison. Since development and rehabilitation plans have specific land management techniques recommended for different zones, the land cover parameterisation uses this further level of detail instead of the generalised land cover classes shown in Figure 12. For example, the agricultural areas in the development scenario have recommendations for contour farming and agroforestry while the rehabilitation plans have similar recommendations for conservation farming. More detail on the specific management strategies and land cover parameterisation is found in Section 2.4.

Table 5. Land use percentages for each of the land cover scenarios.

Land Use	Baseline (%)	Management (%)	Rehabilitation (%)
Agriculture	16.1671	40.3862	28.7510
Brushland	34.0080		
Built-up	0.3414		0.0001
Forest	31.9112	46.5895	60.0879
Grassland	11.6624		
Tree Plantation	5.9099	13.0242	11.1609

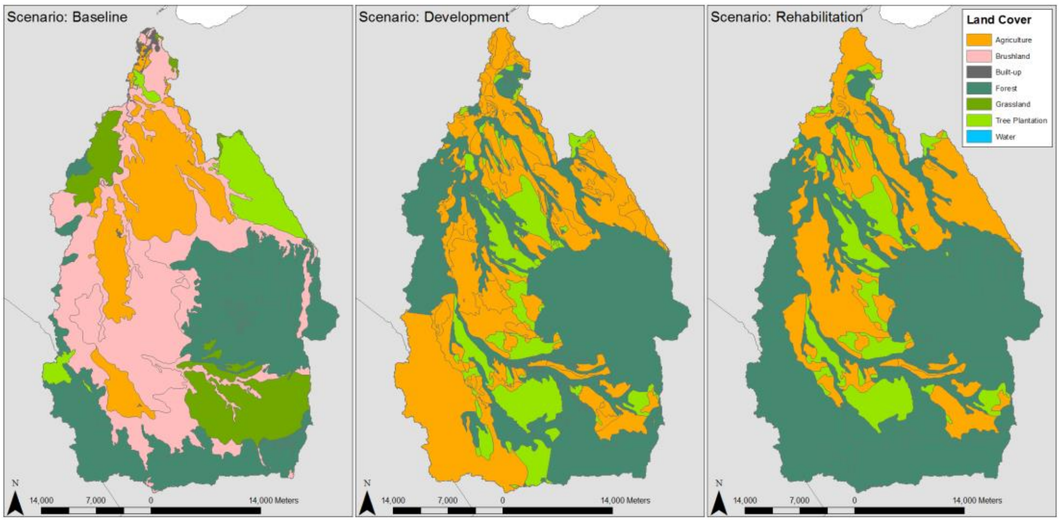

Figure 12. Land cover scenarios aggregated to more general land cover classes.

Brushland and grassland are not classified in the development and rehabilitation scenarios, as both scenarios divide the areas originally classified as brush/grassland into either forest or agriculture. In the CESM (2014) report, the areas classified in the baseline scenario are a mix of brush/grassland and agricultural activities. This mix of brush/grassland with agricultural activity would be more accurate due to the CDO catchment being heavily utilised for agriculture, with reports identifying 70% of its land area devoted to agricultural activity (CESM, 2014).

The soil shapefile was provided by DREAM (2015) but was originally produced by the Bureau of Soils and Water Management (BSWM, 2013). The soil map is classified at the local names of soil series level (Figure 13) but these local names have already been correlated to the USDA subgroup level (Carating et al., 2014). More detail on the soil parameterisation is found in Section 2.3.

Other data used to inform the hydrology of the catchment are a stream network, rainfall data, and evapotranspiration data. The stream network was created by DREAM (2015) through digitising river centre lines through Google Earth (Paringit et al., 2015). The stream network is used to recondition the DEM to more accurately simulate the flow of water through the landscape (Chapter 3) that may be hindered by errors or artefacts in the DEM.

For rainfall data, several types were used for this thesis: gridded rainfall data (raster layers), monthly rainfall data (time-series), and event rainfall (time-series). Gridded rainfall data was taken from WorldClim, a database of climate surfaces at 30-

arc second resolution (~1km) that used weather station data from other databases to produce gridded datasets of bioclimatic variables (precipitation, temperature, etc.) at the global scale (Hijmans et al., 2005). The annual rainfall data from WorldClim ranges from 1,700 mm yr^{-1} to 3,214 mm yr^{-1}, with a mean of 2,550 mm yr^{-1} for CDO. The WorldClim estimate of mean rainfall is higher compared to the historical annual precipitation of Cagayan de Oro, which is approximately 2,376 mm yr^{-1} (CESM, 2014). The gridded annual rainfall for the CDO catchment (Figure 15) is an input to the LUCI framework for its hydrological calculations.

The evapotranspiration data was extracted from the Global Potential Evapo-Transpiration (Global-PET) Geospatial Dataset, which uses the WorldClim climate data and the Penman-Monteith equation to create a global evapotranspiration dataset (CGIAR-CSI, 2005; Zomer et al., 2008). The evapotranspiration values from Zomer et al. (2008) ranged from 1,148 mm yr^{-1} to 1,673 mm yr^{-1} with a mean of 1,517 mm yr^{-1}. Previous water balance work in CDO estimated an annual evapotranspiration of 1,679 mm yr^{-1} using an input rainfall value of 2,855 mm yr^{-1} (CESM, 2014). This evapotranspiration data was used as input to the LUCI framework for its hydrological modelling and calculation of the water balance, which influences the resulting flood mitigation and risk maps.

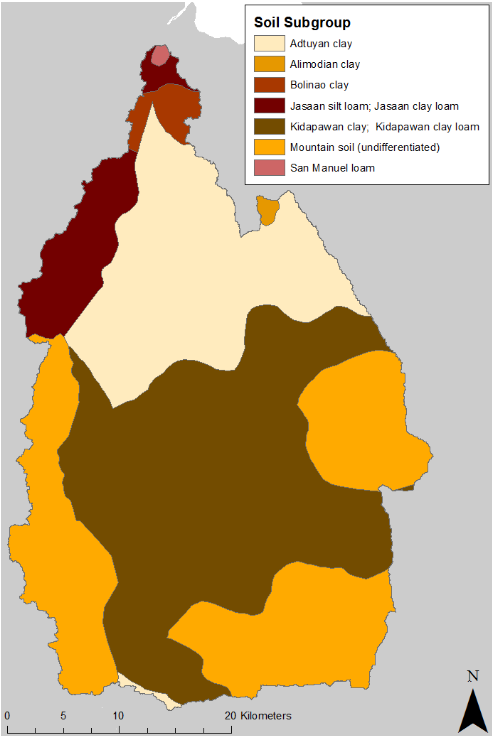

Figure 13. Soil map within the CDO catchment at the soil series classification level.

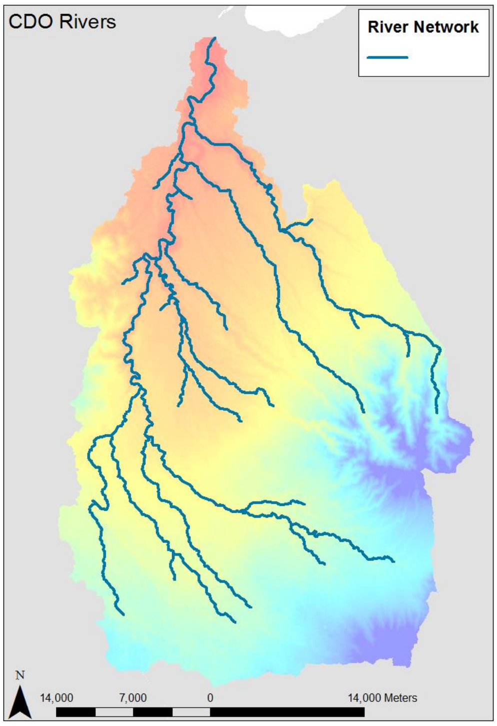

Figure 14. Stream network within the CDO catchment derived by DREAM (2015).

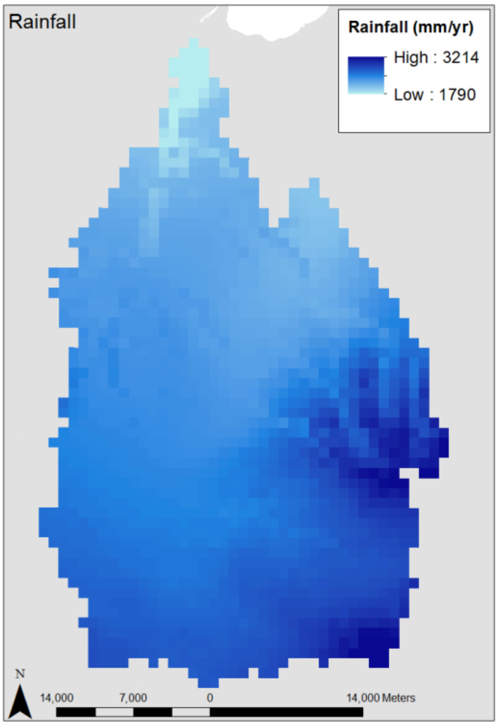

Figure 15. Gridded annual rainfall over the CDO catchment from WorldClim.

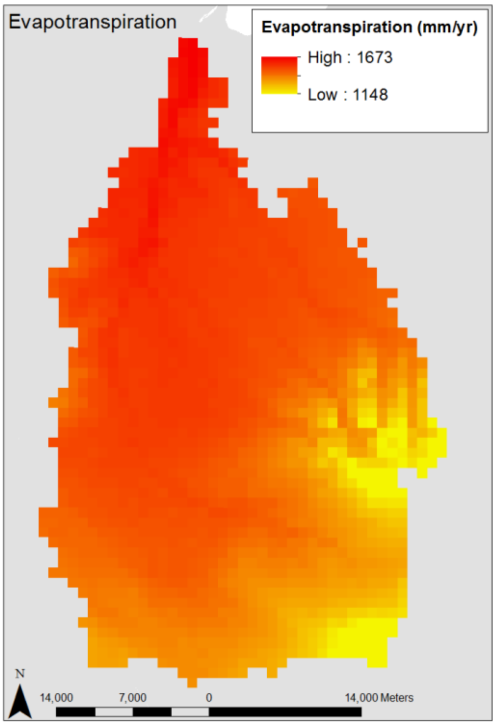

Figure 16. Gridded evapotranspiration over the CDO catchment from Zomer et al. (2008).

The rainfall data for WorldClim was also compared to the monthly average rainfall reported by CESM (2014) for the CDO catchment (Figure 17). These monthly rainfall values were used to estimate monthly soil erosion estimates in CDO to observe which months and seasons were most prone to soil loss (Chapter 5). When comparing WorldClim to the CESM data, the monthly rainfall values were similar, with the rainiest months being from June to October for the monsoon season (Figure 17).

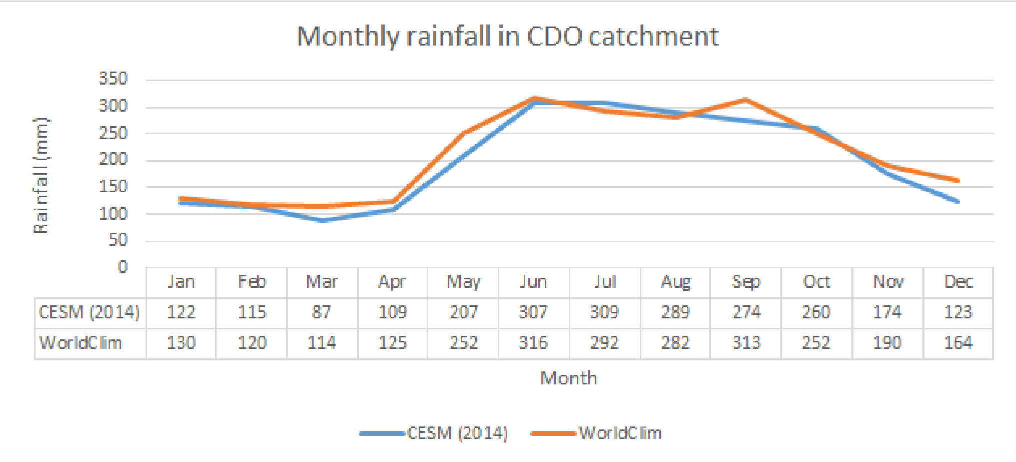

	Jan	Feb	Mar	Apr	May	Jun	Jul	Aug	Sep	Oct	Nov	Dec
CESM (2014)	122	115	87	109	207	307	309	289	274	260	174	123
WorldClim	130	120	114	125	252	316	292	282	313	252	190	164

Figure 17. Monthly rainfall in the CDO catchment from CESM (2014) and the WorldClim database.

The extreme events rainfall data was taken from the network of automated rainfall gauges operated by the Department of Science and Technology[3] through the Philippine Real-Time Environment Data Acquisition and Interpretation for Climate-Related Tragedy Prevention and Mitigation (PREDICT) interface. The event-based rainfall data for Typhoon Bopha (Pablo) was provided by DREAM (2015) and shows a peak rainfall of 32 mm in 15 minutes for the Bubunawan rain gauge (Figure 18). This rainfall data and the baseline scenario were modelled to compare the capability of LUCI's rainfall-runoff model with HEC-HMS and the results of both to the observed flow data (Chapter 8).

[3] http://fmon.asti.dost.gov.ph/

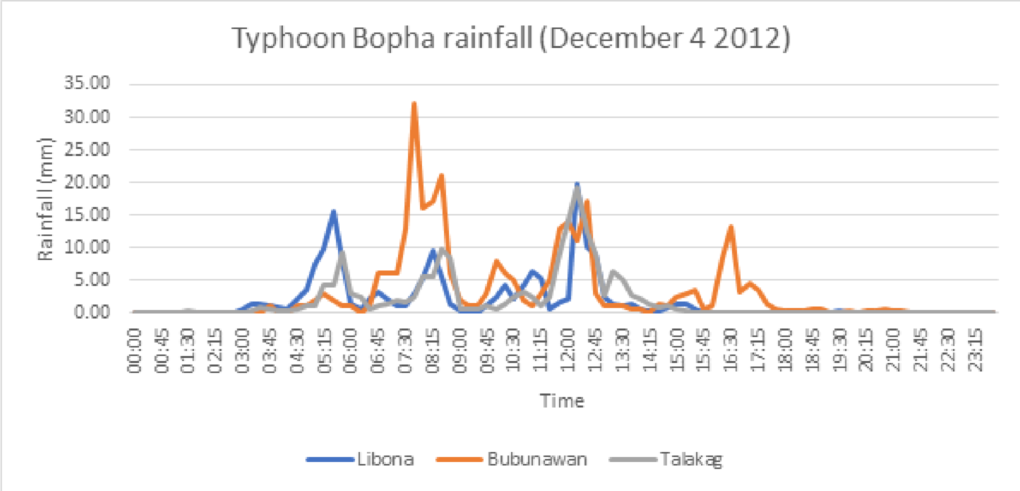

Figure 18. Time-series for the rainfall of Typhoon Bopha.

Two other extreme events were also considered for this research: Jangmi (Seniang) from 2014 and Tembin (Vinta) from 2017. The rainfall data for Jangmi and Tembin were taken directly from PREDICT and underwent data infilling to account for gauges that stopped recording over the course of the event. Future work on extreme events modelling includes running both LUCI and HEC-HMS for the land cover scenarios under Bopha, Jangmi, and Tembin to assess the potential changes in flooding events for the CDO catchment.

The floodplain LiDAR was also provided by DREAM (2015) and is used for their floodplain inundation mapping, with the river bathymetry burned into the LiDAR-derived DEM through river surveys (Paringit et al., 2015) (Figure 19). The LUCI model's capability to do rainfall-runoff modelling was tested against the DREAM (2015) parameterisation of HEC-HMS, and the flow hydrographs from both LUCI and HEC-HMS were used for inundation mapping in HEC-RAS. The HEC-HMS and HEC-RAS parameterisation for the CDO catchment was done by DREAM (2015) and was provided for use within this thesis.

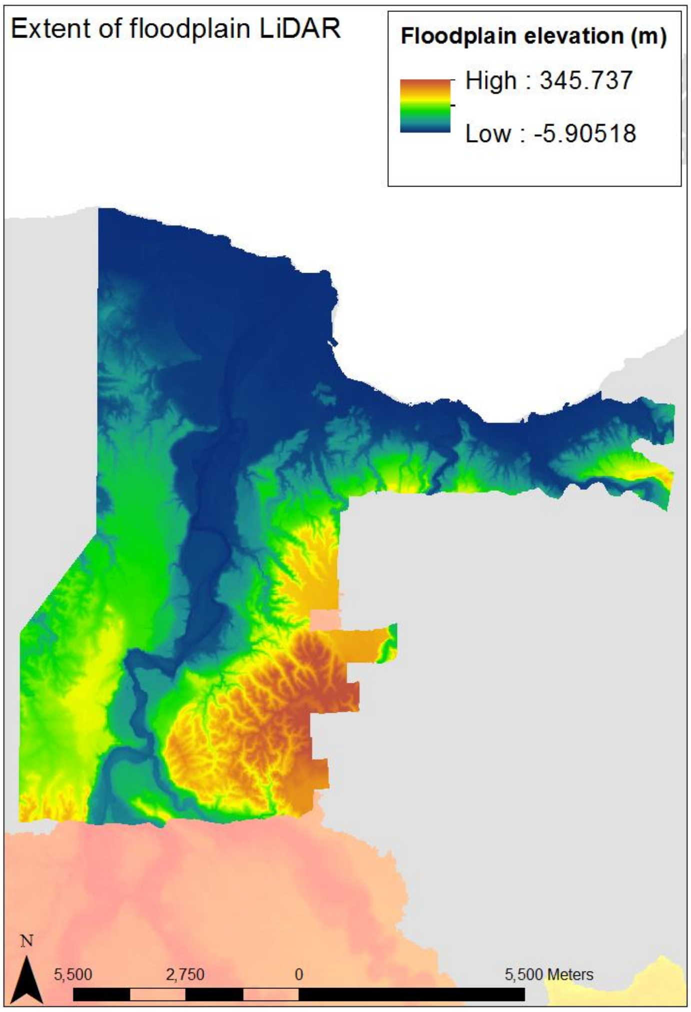

Figure 19. Extent of floodplain LiDAR provided by DREAM (2015) from the outlet to the coast of the catchment.

2.3 Soil parameterisation

Within LUCI, the soil and land cover classes supported by the model are primarily based on data from New Zealand and the United Kingdom (Jackson et al., 2013). Hence, applying LUCI to a novel study area requires parameterisation of the soil and land cover characteristics to ensure the successful modelling of ES. The soil classification used in the CDO catchment is at the soil series level or the local name, which was correlated to the USDA subgroup level by Carating et al. (2014). The USDA soil classification was not initially supported by LUCI, hence the need for soil parameterisation before it was applied to the CDO catchment. The LUCI model requires soil information about soil water holding capacity and hydraulic conductivity (Jackson et al., 2013). Soil hydraulic characteristics are important for models to simulate how water and chemicals move through the soil (Wösten et al., 2001). LUCI uses a modified form of soil moisture accounting (SMA) taking into account the permeability of elements within the landscape at the sub-field scale (Jackson et al., 2013). In order to run its modelling algorithms, it requires several soil hydraulic properties that are needed by models to simulate how water and chemicals move through different soils. Within the model, water moves through the soil matrix in response to gravity and water pressure depending on soil moisture content and hydraulic conductivity, while also accounting for plant transpiration (Jackson et al., 2008). This is similar to the SMA technique of simulating water flow through different storage reservoirs (e.g. soil profile, groundwater storage) using rates of infiltration and drainage (Feldman, 2000).

Soil hydraulic parameters are also important for determining the available soil water at different pressures: saturation, field capacity, and wilting point (Wösten et al., 2001). Any water content above field capacity is drained by gravity. At wilting point, the plants are unable to extract water from the soil (Bedient et al., 2013). To use the analogy of soil being like a bucket, saturation point would be when the bucket is "full" and any additional water becomes surface runoff (N. Romano et al., 2011). LUCI requires the following soil hydraulic parameters:

- Total water content (WC): WC between field capacity and saturation (%)
- Total plant available water (TPAW): WC between field capacity and wilting point (%)
- Readily plant available water (RPAW): WC between stomata closure or plant stress and field capacity, which can be assumed as half of TPAW (%)
- Depth to root impeding zone (mm)
- Depth to less permeable layer (mm)
- Max soil infiltration rate or saturated hydraulic conductivity (mm day^{-1})
- Max drainage rate or sat hydraulic conductivity at bottom of soil profile (mm day^{-1})

The most direct method for determining soil hydraulic properties is through conducting field and laboratory tests on soil samples, but this is heavy on time and resources (Schaap et al., 2001). Pedotransfer functions (PTFs) are used to relate hydraulic properties to soil properties that are more easily measured, such as textural information and organic matter (Wösten et al., 2001).

Computer models have been developed to facilitate the usage of pedotransfer functions. One example of this is the ROSETTA programme which was developed by the United States Salinity Laboratory, and uses several PTFs depending on the detail of the input soil data (Schaap et al., 2001). The SOILPAR 2.00 programme uses textural information, organic carbon, and bulk density with a range of PTFs to estimate hydraulic characteristics (Acutis & Donatelli, 2003). The Soil Water Characteristics (SWC) model developed PTFs that utilise textural information and organic matter to return soil moisture content at different pressures and hydraulic conductivity (Saxton & Rawls, 2006).

PTFs were used with databases to derive the spatial distribution of hydraulic properties. The Hydraulic Properties of European Soils (HYPRES) database utilised textural information, organic matter, and bulk density of soil samples from 20 institutions from 12 European countries with the Mualem-van Genuchten model to map hydraulic properties at a European scale (Wösten et al., 1999). One important note about PTFs is their regional specificity, where PTFs developed in one region may not necessarily apply to soils located in a different climate region (Wösten et al., 1999).

The Philippines does not have a national quantitative database of soil physical and textural characteristics, but soil surveys were previously accomplished to create soil maps (Figure 20) and record soil qualitative characteristics. The soil map compiled by the Bureau of Soils and Water Management (BSWM) uses the Philippine classification system at the soil series level, which has been correlated to the United States Department of Agriculture (USDA) taxonomy at the subgroup level (Carating et al., 2014). The undifferentiated mountain soil may be dominated by the Kidapawan soil series or the Typic Paleudults subgroup.

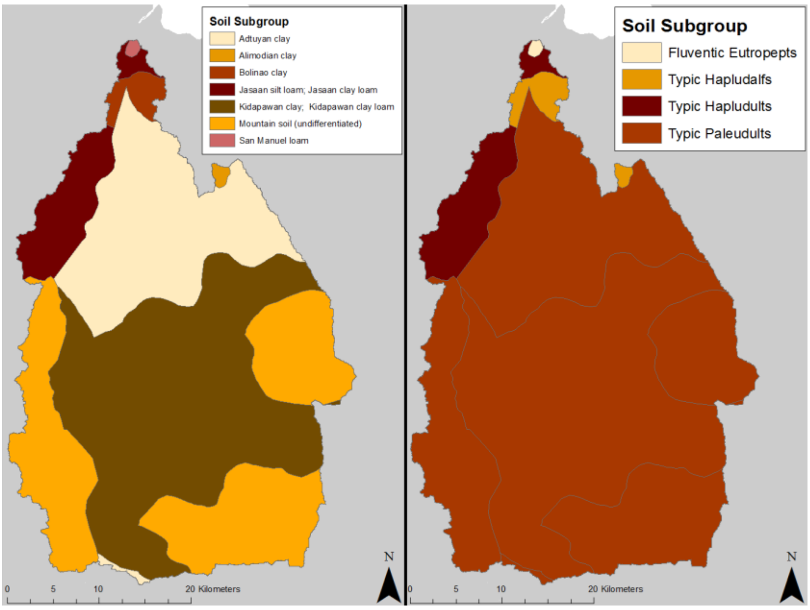

Figure 20. Map of the soils with the Cagayan de Oro catchment using two classifications: Philippine local names at the series level, and the USDA subgroup level.

Given the lack of quantitative data, the soil characteristics information was sourced from two databases: National Cooperative Soil Survey (NCSS) Soil Characterization Database and the IGBP-DIS Soil dataset for Pedotransfer Function Development (IGBP-PTF). Soil records of each subgroup were extracted from these databases and used as input to the Soil Water Characteristics model for parameterisation into the LUCI framework (Figure 21).

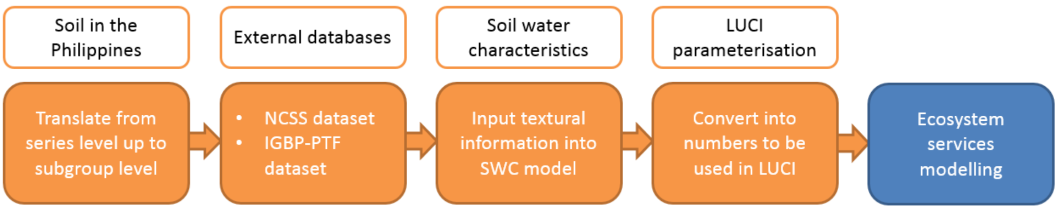

Figure 21. Flowchart for soil parameterisation.

2.3.1 Soil Water Characteristics (SWC) model

The SWC contains a range of PTFs that were used to estimate soil hydraulic properties from the information in the NCSS and IGBP-PTF datasets. SWC was developed by Saxton and Rawls (2006) using the USDA-NRSC National Soil Characterization Database by correlating soil water retention data with sand and clay textural information, bulk density, and organic matter. These soil water characteristics equations accessible through an Excel spreadsheet (Saxton & Rawls, 2006). The soil equations were recreated in MATLAB R2015a (8.5.0.197613) to batch-process the large amount of soil records. The following inputs are needed by the SWC model: sand fraction, clay fraction, organic matter, density factor, and gravel content. In the records where the organic matter, density factor, and gravel content were not available, the model default values were used: 2.5% (OM), 1.00 (DF), and 0.00 % weight (gravel). The output parameters from SWC that were used for LUCI parameterisation were water content at: wilting point (% volume), field capacity (% volume), and saturation (% volume).

2.3.2 National Cooperative Soil Survey (NCSS) Soil Characterisation Database

This database is a compilation of soil survey data from institutions such as the USDA National Resources Conservation Service (NRCS) Soil Survey Laboratory and university laboratories (Reinsch & West, 2010). This database is accessible online through the NCSS Laboratory Data Mart[4]. Table 6 summarises the number of records for each subgroup found in the Cagayan de Oro catchment. The following parameters were extracted from the database for input into the model:

- Total Clay (%)
- Total Sand (%)
- Depth to the top and bottom of the sample (cm)

The model uses the PTFs formulated by Saxton and Rawls (2006) which requires textural information, organic matter, density factor, and gravel. Even though the NCSS database contains estimated organic matter, many of the records are missing this variable. For example, out of 574 records of Typic Paleudults, only three records have information about organic matter. Similarly, this database does not contain information for density factor and gravel content. Thus, these parameters were held at the model's default values (organic matter: 2.5%, density factor: 1.00, gravel content: 0.00% weight).

2.3.3 IGBP-DIS Soil dataset for Pedotransfer Function Development (IGBP-PTF)

This database was compiled by the International Soil Reference and Information Centre (ISRIC) to facilitate developing PTFs and includes ISRIC's Soil Information System and the CD-ROM of the National Resources Conservation Service (Tempel et al., 1996). Although the original dataset is no longer accessible online, ISRIC has a

[4] http://ncsslabdatamart.sc.egov.usda.gov/

repository of global soil data available[5]. The following parameters were extracted from the IGBP-PTF database:

- Clay (% weight)
- Sand (% weight)
- Organic carbon (% weight) (Was converted to organic carbon by multiplying by 1.72 as per Walkley and Black method (Adornado et al., 2009))
- Depth to the top and bottom of the sample (cm)

Table 6. Number of soil records for subgroups present in the CDO river basin.

Subgroup	NCSS Soil Characterization Database	IGBP-DIS Soil dataset for Pedotransfer Function Development
Fluventic Eutropepts	2	10
Typic Hapludalfs	902	1039
Typic Hapludults	574	583
Typic Paleudults	206	395

2.3.4 Field measurements

During fieldwork in the Cagayan de Oro watershed during November 2016 and January 2017, soil water content and matric potential measurements were taken with a Hydrosense and an Infields Tensiometer respectively. Two probe lengths were used with the Hydrosense: 12cm and 20cm probes to measure water content at different depths. For both probe lengths and the tensiometer, a maximum of three readings were taken at each site. The GPS locations were recorded with the Garmin Etrex 10 and are shown on the map in Figure 22. The soil measurements were taken in the southern section of the watershed because of the site's accessibility by road and presence of road cuts where profile observations could be taken. All the measured soil hydraulic data were taken for only one soil subgroup: Typic Paleudults, which is the most ubiquitous soil group in the CDO watershed. Profile observations of depth, colour, texture, structure, and presence of stones or roots were recording, with the aim to build a database of soil physical and hydraulic characteristics for future implementation into the LUCI framework.

[5] http://www.isric.org/index.php/explore

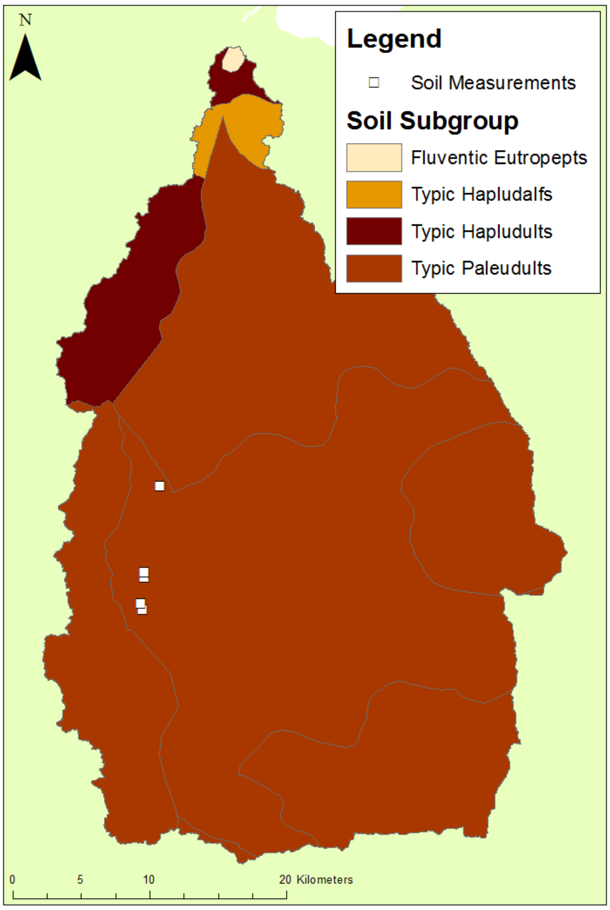

Figure 22. Map of where the soil water content and matric potential measurements (white squares) were taken.

2.3.5 Converting to LUCI Parameterisation

The volumetric water content was estimated through differences in the water content at different pressures:

$$WC_{Total} = WC_{Sat} - WC_{FC}$$

$$WC_{TPAW} = WC_{FC} - WC_{WP}$$

$$WC_{RPAW} = \frac{WC_{TPAW}}{2}$$

Where:

WC_{Sat}	Water content at saturation
WC_{FC}	Water content at field capacity
WC_{TPAW}	Total plant available water
WC_{WP}	Water content at wilting point
WC_{RPAW}	Readily plant available water

The relationship between WC_{TPAW} and WC_{RPAW} is an assumption of this parameterisation, not a true relationship. The ability of a plant to take up water is dependent on its rooting depth and on the hydraulic properties of the soil, especially the water content at different pressures (L. Zhang et al., 2001). WC_{RPAW} is a fraction of WC_{TPAW} defined as the water available to plants between field capacity and the point where the plants experience water stress and varies between soil types. Hence, future improvements to the CDO parameterisation in LUCI include analysing moisture retention curves to determine a more accurate relationship between WC_{TPAW} and WC_{RPAW}.

The depths from the NCSS and IGBP-PTF datasets were the depth from the top of the sample and depth to the bottom of the sample:

$$Depth = (D_{bottom} - D_{top}) \times 10$$

To get the daily saturated hydraulic conductivity (mm day^{-1}), the hourly saturated hydraulic conductivity (mm hr^{-1}) obtained from the SWC model was simply multiplied by 24. The drainage rate was estimated to be the minimum daily saturated hydraulic conductivity value for that soil subgroup.

Using the estimates of hydraulic properties, the soil subgroups were classified as either very permeable soils or soils that were not as permeable. The very permeable soils are those with high daily saturated hydraulic conductivity or infiltration rates, and high drainage rates. The less permeable soils had low infiltration rates and low drainage rates. As LUCI is continually developed, the permeability classification system will be phased out in favour of using the actual values of hydraulic properties to determine soil hydrology.

2.3.6 Soil parameterisation results

In terms of differences between results from the two databases, the plant available water values (total and readily) and depth values were consistently higher for the records extracted from the NCSS database compared to the IGBP-PTF database (Figure 23, Figure 24 and Figure 25). The NCSS results had a larger variation in the plant available water values compared to the results from the IGBP-PTF database, with Fluventic Eutropepts having the highest values while Typic Hapludalfs had the lowest. In terms of infiltration rates, Typic Hapludults had the highest daily rates while Fluventic Eutropepts had the lowest. The differences between the two databases for water content were within a few percent, and the patterns of which soil subgroups had the highest or lowest water contents were the same.

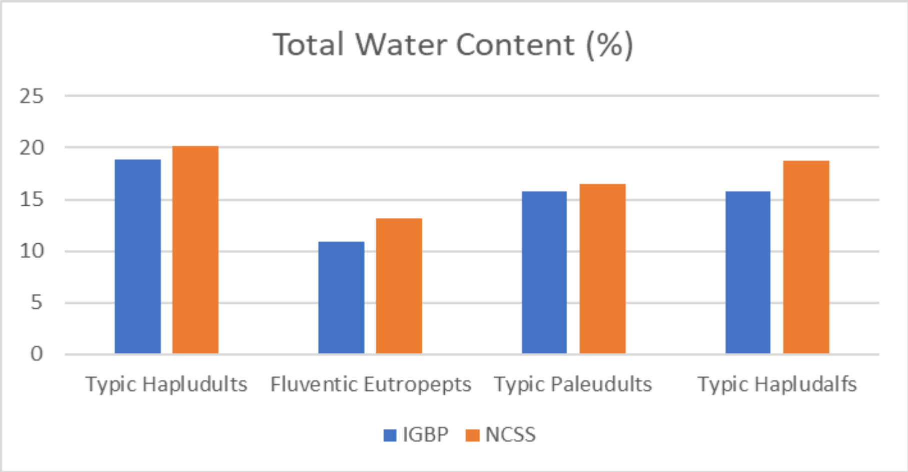

Figure 23. Total water content (%) for all soil subgroups in the CDO catchment from the IGBP and NCSS databases.

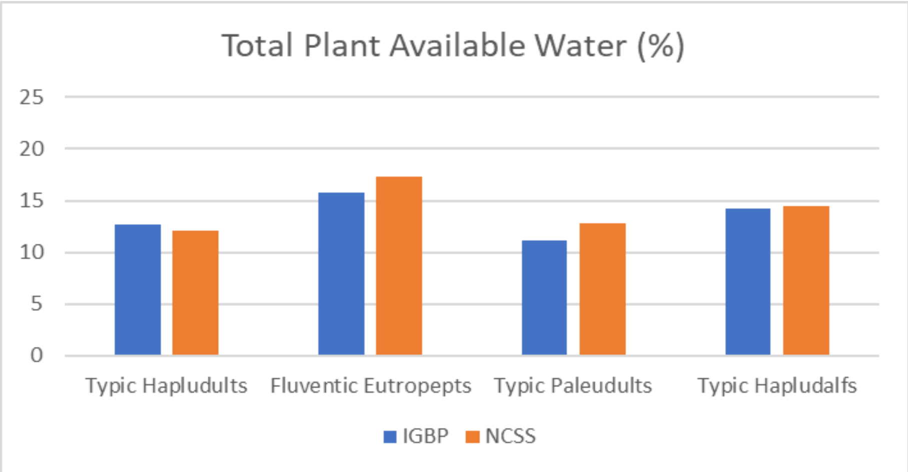

Figure 24. Total plant available water (%) for all soil subgroups in the CDO catchment from the IGBP and NCSS databases.

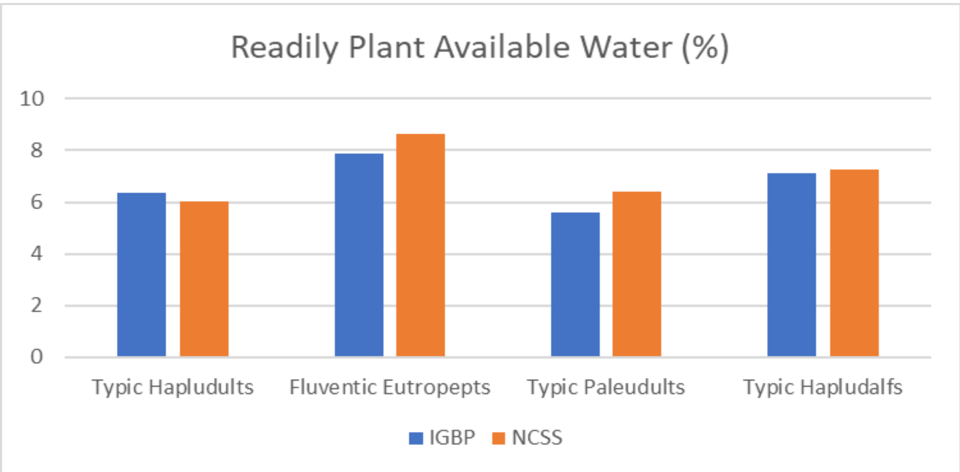

Figure 25. Readily plant available water (%) for all soil subgroups in the CDO catchment from the IGBP and NCSS databases.

The estimated values of infiltration rates and drainage rates for the different USDA subgroups were not an exact match but were similar in terms of which subgroups had the highest and lowest daily infiltration and drainage (Table 7).

According to Carating et al. (2014), Jasaan soil series (Typic Hapludults) has an external drainage of good to excessive while the internal drainage is fair (Carating et al., 2014). This subgroup has the highest estimated daily infiltration rate for all the subgroups present in the CDO watershed. Generally, all the soils present in the CDO catchment are classified as having good drainage (Carating et al., 2014) but the actual variation of hydraulic properties between soils has not been published.

For implementation into the LUCI framework, the Typic Hapludults, Fluventic Eutropepts, and Typic Hapludalfs were classified as more permeable soils compared to the Typic Paleudults subgroups. As LUCI is further developed, this existing database of hydraulic characteristics within the CDO watershed will have more influence on the hydrological operations of the model.

Table 7. Infiltration and drainage rate estimates for the different subgroups for both databases.

USDA Subgroup	**Max infiltration rate (mm day^{-1})**		**Max drainage rate (mm day^{-1})**	
	IGBP	**NCSS**	**IGBP**	**NCSS**
Typic Hapludults	1605.71	1046.97	2.06	0.31
Fluventic Eutropepts	80.42	145.14	20.88	144.63
Typic Paleudults	435.58	441.86	1.47	4.08
Typic Hapludalfs	951.06	614.31	4.55	7.7

Due to the similarity of the water content information and hydraulic data for the soil subgroups obtained from the two different databases, both sets of values were used to inform the permeability of the soil, and the values from the IGBP-PTF database were coded into the LUCI framework. The NCSS database contains information mostly from the United States, while the IGBP-PTF database contains more global data and has more records for all the soil subgroups (Table 6).

Since the soil water content and matric potential values obtained during fieldwork were only obtained for one soil subgroup and within one small region of the catchment, these values were not coded into LUCI at this stage. However, the observational data was used to understand the physical characteristics of the soils present in the CDO watershed, with rooting information that will be useful in later versions of LUCI where rooting depth will be used. Future fieldwork can be done to obtain soil hydraulic characteristics over more soil subgroups and locations within CDO to compare the values to the ones obtained from the databases and water content model. Within the LUCI framework, the *Generate Scenario User Specified Land Use* tool is used with the soil linking code "SOILCODE" and input data source as 32. These two parameters are used by LUCI to link the information in the soil shapefile with the tabular information present within LUCI.

In future applications of LUCI, a soil map may be available to an area of interest but have limited information about the soil textural and hydraulic characteristics. Testing the hydraulic characteristics derived from external databases will help extend the application of LUCI to similarly data-sparse regions. The hydraulic characteristics needed by LUCI include information about soil water content, soil water available to vegetation, and rates of infiltration and drainage. At this current stage, the LUCI framework uses classifications of permeability for data-sparse regions, but future development of LUCI will phase out this classification-based system in favour of using the actual values for hydraulic characteristics that were compiled during this research.

2.4 Land cover parameterisation

Although LUCI already supports many land cover types, this research tested two methods of incorporating Philippines-specific land cover into LUCI: correlation and custom coding and then running it through the ecosystem service models (Figure 26). Correlation involves cross-referencing the existing LUCI database of supported land cover types and matching them with the land cover present in the CDO catchment. This is a straightforward way to parameterise LUCI for a new study site, allowing applications where information about the specific land cover characteristics is scarce or not practically possible to obtain. Custom coding involves collecting data about more specific characteristics of the land cover in the CDO catchment to classify the land cover's ability to perform certain ecosystem services. This is more time-consuming but can account for site-specific characteristics, such as types of agriculture (e.g. rice paddies) or types of forests not included in previous versions of LUCI.

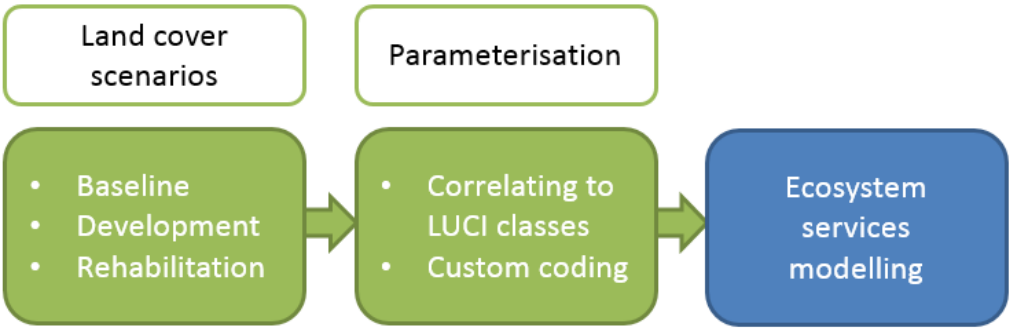

Figure 26. Flowchart for land cover parameterisation experiments.

As noted in Section 2.2, for comparison the shapefiles for the development and rehabilitation scenarios were modified to match the shape of the baseline scenario. For visual comparison, the land cover types were aggregated into more general land cover classes (Figure 12). The development and rehabilitation scenario are very similar, but with the rehabilitation scenario focusing on tree re-planting in the southern part of the watershed where the development scenario proposes agricultural and tree plantation use. Additional information from CESM (2014) classifies brush/grassland areas in the baseline scenario as a mixture of brush/grass and arable land.

Although the land cover classes have been aggregated for visualisation purposes, the LUCI land cover parameterisation was based on the original land cover classification proposed by the different scenarios (Table 8). This is due to the fact that the management practices suggested by the development and rehabilitation scenario are more detailed (e.g. agricultural zones being recommended to use contour farming and other soil conservation techniques (CESM, 2014)).

Table 8. Aggregated and individual land cover classes for the different scenarios.

Aggregated	**Baseline**	**Development**	**Rehabilitation**
Agriculture	Other land, cultivated, annual crop Other land, cultivated, perennial	Agriculture Sub-zone Agricultural zone1 Agricultural zone2 Agricultural zone3	Practice Conservation Farming Recommend Conservation Farming
Brushland	Other wooded land, shrubs	None	None

Table 8. Aggregated and individual land cover classes for the different scenarios. (continued)

Aggregated	Baseline	Development	Rehabilitation
Forest	Closed forest, broadleaved Open forest, broadleaved	Forest Restoration Sub-zone National Park Natural Park Private Forest Sub-zone Strict Protection Zone	Assisted Natural Regeneration Protection Recommend Reforestation Reforestation
Grassland	Other land, natural, grassland Other wooded land, wooded grassland	None	None
Tree Plantation	Forest plantation, broadleaved	Agroforesty Sub-zone Private Agroforestry Sub-zone Timber Production Sub-zone Timber Regeneration Sub-zone	Agroforestry Recommend Agroforestry
Water	Inland water	Coastal zone	Engineering for Erosion Control

For the correlation method, each of the land cover classes in the proposed scenarios were compared to the master list of LUCI land cover classes that were already supported. For all the land cover classes present in the CDO catchment and potential scenarios, there were similar land cover classes already supported in the LUCI framework. The descriptions of all the land cover classes in CDO were compared to the descriptions of the classes in LUCI and were matched based on their similarity (Table 9). This type of parameterisation is a good initial method of setting up LUCI to support a new site because the relatively low data requirements. However, it excludes information about the types of land cover management that could potentially occur in later land management plans, such as the use of soil conservation practices (e.g. contour farming). Within the LUCI framework, the *Generate Scenario User Specified Land Use* tool uses the “myLCid” field in the scenario shapefile and compares it to the land cover classes already supported within LUCI. This comparison is done through a user-defined land cover linking table that matches the "myLCid" field to a matching "LUCIid" field.

Table 9. Correlation of the original land cover scenarios for CDO with the LUCI master land cover classes.

Original LC ID	Original LC Description	LUCI ID	LUCI Description
Baseline Scenario			
Sh	Other wooded land, shrubs	201	Scrub/shrub generic
GL	Other land, natural, grassland	401	Improved grassland not fertilised
AC	Other land, cultivated, annual crop	301	Annual generic
PC	other land, cultivated, perennial	391	Tree plantation and perennial crops (tropical)
BUA	Other land, built-up area	801	Urban generic
PINE	Pineapple plantation	322	Pineapples
NF4F	Closed forest, broadleaved	101	Broadleaved, deciduous
NF2B	Open forest, broadleaved	101	Broadleaved, deciduous
IW	Inland water	906	Water river
FPB	Forest plantation, broadleaved	391	Tree plantation and perennial crops (tropical)
WGL	Other wooded land, wooded grassland	391	Tree plantation and perennial crops (tropical)
Development Scenario			
Ag	Agricultural Sub-zone	301	Arable generic
Ag1	Agricultural Zone 1	301	Arable generic
Ag2	Agricultural Zone 2	391	Tree plantation and perennial crops (tropical)
Ag3	Agricultural Zone 3	391	Tree plantation and perennial crops (tropical)
AgFor	Agroforestry Sub-zone	391	Tree plantation and perennial crops (tropical)
AgForPriv	Private Agroforestry Sub-zone	391	Tree plantation and perennial crops (tropical)
ForPriv	Private Forest Sub-zone	105	Mixed forest
ForRest	Forest Restoration Sub-zone	101	Broadleaved, deciduous
NatioPark	National Park	101	Broadleaved, deciduous
NatuPark	Natural Park	101	Broadleaved, deciduous
Prot	Strict Protection Zone	101	Broadleaved, deciduous
TimProd	Timber Production Sub-zone	106	Plantation forest generic
TimReg	Timber Regeneration Sub-zone	106	Plantation forest generic

Table 9. Correlation of the original land cover scenarios for CDO with the LUCI master land cover classes. (continued)

Rehabilitation Scenario			
Bu	City	801	Urban generic
AgFor	Agroforestry	391	Tree plantation and perennial crops (tropical)
Ref	Reforestation	105	Mixed forest
RecAgFor	Recommend Agroforestry	391	Tree plantation and perennial crops (tropical)
RecRef	Recommend Reforestation	101	Broadleaved, deciduous
AgCons	Practice Conservation Farming	301	Arable generic
Prot	Protection	102	Broadleaved evergreen
NatReg	Assisted Natural Regeneration	105	Mixed forest
RecAgCons	Recommend Conservation Farming	301	Arable generic

For the custom coding approach, the types of crops and trees present in the watershed were based on fieldwork observations (Table 10). The growth stages, rooting depth, and water needs for these crops and trees were sourced from literature and agriculture models. One such model is CROPWAT, a decision support tool used to calculate crop water requirements under particular of climate and growth conditions (FAO, 2018). Based on fieldwork observations, the crops that had the largest fields were pineapple, mango, rubber trees, banana, and papaya.

Table 10. Crops and trees observed in the CDO watershed through fieldwork.

Common name	Frequency	Scientific name
Acacia	4	*Acacia crassicarpa*
Alim	1	*Melanolepis multiglandulosa*
Bamboo	14	*Dendrocalamus asper*
Banana	19	*Musa acuminata*
Cacao	1	*Theobroma cacao*
Camote	1	*Ipomoea batatas*
Cassava	8	*Manihot esculenta*
Coconut	16	*Cocos nucifera*
Corn	10	*Zea mays*
Fire trees	1	*Delonix regia*
Fruit trees	1	*Unidentified fruit trees*
Fortune plant	1	*Dracaena fragrans*
Gemelina	9	*Gmelina arborea*
Hanabdong	1	
Ipil-ipil	7	*Leucaena glauca*
Jackfruit	3	*Artocarpus heterophyllus*

Table 10. Crops and trees observed in the CDO watershed through fieldwork. (continued)

Common name	Frequency	Scientific name
Mahogany	3	*Toona calantas*
Makahiya	4	*Mimosa pudica*
Malunggay	1	*Moringa oleifera*
Mango	9	*Mangifera indica*
Narra	1	*Pterocarpus indicus*
Palcata	5	*Acacia falcata*
Papaya	5	*Carica papaya*
Pine	2	*Pinus kesiya*
Pineapple	5	*Ananas comosus*
Rice	2	*Oryza sativa*
Rubber	7	*Hevea brasiliensis*
Saluyot	1	*Corchorus olitorius*
Santol	2	*Sandoricum koetjape*
Star apple	3	*Chrysophyllum cainito*
Talahib (wild grass)	10	
Talisay	2	*Terminalia catappa*

To code custom land cover classes for LUCI and create a more detailed parameterisation, the physical characteristics (rooting depth) and water requirements for the different crops and trees must be compiled. These values influence the way the water balance of the catchment is calculated, which influences the way that the catchment can respond to rainfall events. The rooting depth of the crops in the CDO catchment ranged from 0.10m (rice) up to 6m (acacia) based on the values from literature (Table 11). In a global study of maximum rooting depths, tropical deciduous forests had a depth of 3.7m while tropical evergreen forests had a depth of 7.3m (Canadell et al., 1996). In terms of water needs, a study on tropical trees found maximum transpiration rates to range from 0.4 to 4.9 mm day^{-1} (Dierick et al., 2010). The CDO catchment receives almost 3000mm of rainfall annually, which can support the water needs of the crops and even trees with high water consumption such as acacia trees (CESM, 2014; Morris et al., 2011). Fieldwork showed the crops as commonly rainfed rather than irrigated. This information about crop water needs and changes in rooting depth is important to further parameterise the tropical soil hydraulic properties in LUCI to better represent different combinations of soil and land cover.

Through the literature review and fieldwork observations, the different land cover types were classified into several types of flood mitigation land: flood-generating, flood-mitigating, and water bodies. Flood-generating lands are those that have low permeability and low storage of water, while flood-mitigating lands have high permeability and can store more water. Water bodies included the river and any inland lakes or reservoirs. By compiling all the crop and tree information through literature review and fieldwork, the CDO catchment is ready for the next stage of LUCI development where these values will have a greater influence on the hydrological operations of LUCI. Like the soil parameterisation process, this classification-based land cover parameterisation approach will be phased out in future versions of LUCI in favour of utilising the specific land cover characteristics such as rooting depths and water needs to give more detailed hydrological information of any point in the landscape. Since these factors also change with crop growth, future work can include a crop model to handle dynamic rooting depth and water needs.

Table 11. Physical characteristics of the different crops and trees observed in the CDO catchment.

Crop name and scientific name	**Growth stages**	**Rooting depth**	**Rooting depth for LUCI**	**Water management needs**	**Source**
		Agricultural section			
Camote (*Ipomoea batatas*)	~ 150 days Planting to tubers: 40 to 60 days Tubers to maximum leaf development: 60 to 120 days Maximum leaf development to harvest: 45 to 90 days	~ 0.20 to 0.25m	0.25m	360 to 800mm for growing season Optimal rainfall of 750mm to 1,000mm annually	(Alvim & Kozlowski, 1977; Atu, 2013; Ramirez, 1992)
Cassava (*Manihot esculenta*)	Harvest at 12 months	Up to 2m	2m	Can tolerate ~600mm of annual precipitation Optimal rainfall of 1,000mm to 1,500mm annually	(Alvim & Kozlowski, 1977; El-Sharkawy, 2006)

Table 11. Physical characteristics of the different crops and trees observed in the CDO catchment. (continued)

Crop name and scientific name	**Growth stages**	**Rooting depth**	**Rooting depth for LUCI**	**Water management needs**	**Source**
Corn or maize (*Zea mays*)	~ 125 days Initial and development: 55 days Mid-season: 40 days Late season: 30 days	Initial and development: 0.3m Mid and late season: 1.00m	1.00m	500 to 800mm annually	CROPWAT
Pineapple (*Ananas comosus*)	~ 790 days	Up to 0.85m depth, lateral spread of 1 to 2m	0.85m	650 to 3,800mm annual precipitation (Ideally 1,000 to 1,500mm annually) Maximum ET: 700 to 1000mm year^{-1}	CROPWAT and Morton (1987)
Rice (*Oryza sativa*)	~ 150 days Nursery to transplant: 55 days Growth: 120 days	Transplant: 0.10m Mid/late growth: 0.60m	0.60m	In standing water, levels: Transplant: 0.10m Vegetative: 0.02 to 0.05m Mid-season: 0.10m Late: none	CROPWAT
		Agroforestry section			
Banana (*Musa acuminata*)	~ 330 days for 1st year Initial: 90 days Development: 165 Mid/late season: 75 days ~ 240 days for 2nd year Initial: 60 days Development: 60 days Mid/late season: 120 days	1st year: Initial and development: 0.3m Mid/late season: 0.90m	0.90m	Annual rainfall of at least 1,000mm (monthly rainfall of 200 to 300mm) ET: 1.5 to 9.8mm day^{-1}	CROPWAT
Cacao (*Theobroma cacao*)	Produces pods at ~ 4 years, maximum productivity at ~8 to 10 years	1.0m to 1.3m	1.3m	1,400mm to 2,000mm annual rainfall Affected when water content is below 60% to 70% of maximum available soil water capacity	(Alvim & Kozlowski, 1977; De Almeida & Valle, 2007)

Table 11. Physical characteristics of the different crops and trees observed in the CDO catchment. (continued)

Crop name and scientific name	**Growth stages**	**Rooting depth**	**Rooting depth for LUCI**	**Water management needs**	**Source**
Coconut (*Cocos nucifera*)	Rapid growth from 2 to 5 years, flowering at 4 to 5 years	Adventitious root system, 2000 to 4000 fibrous roots that can go down to 5m but mostly found within 1.5m of surface	1.5m	1,500 to 2,500mm annual rainfall	(Chan & Elevitch, 2006)
Jackfruit (*Artocarpus heterophyllus*)	Fruiting between 4 to 14 years	0.3 to 0.9m	0.6m	Sensitive to drought, similar to kamansi/breadfruit	(Jamaludheen et al., 1997; Morton, 1987)
Kamansi /breadfruit (*Artocarpus altilis*)	Fruiting at ~5 years, productive for up to 50 years	0.3 to 0.9m	0.6m	~ 2,500mm annual rainfall	(Jamaludheen et al., 1997; Morton, 1987)
Malunggay (*Moringa oleifera*)	Bearing pods at 6 to 8 months, regular bearing after 2 years	Tough fibrous roots		480 to 4,000 mm annual rainfall	(Duke, 1998)
Mango (*Mangifera indica*)	Fruiting at 6 years, maximum productivity at 15 years Initial and development: 180 days Mid/late season: 185 days	Usually 2m, can be up to 6m; finer roots found at the 0.25 to 0.5m depth	2m	~750 to 2,500mm annual rainfall	(Alvim & Kozlowski, 1977; Morton, 1987)
Papaya (*Carica papaya*)	Up to 20 years	Up to 2m, but usually found in within 0.5m of surface with 0.25m depth having most concentration of roots	2m	Stress occurs when readily available water goes below 75%	(Campostrini & Glenn, 2007; DAFF, 2009)

Table 11. Physical characteristics of the different crops and trees observed in the CDO catchment. (continued)

Crop name and scientific name	**Growth stages**	**Rooting depth**	**Rooting depth for LUCI**	**Water management needs**	**Source**
Rubber (*Hevea brasiliensis*)	~ 5 to 6 years to maturity	2 to 5m after 3 years, up to 10m	5m	Rainfall best between 1800 to 2500mm	(Verheye, 2010)
Santol (*Sandoricum koetjape*)				Can flourish in dry and wet areas	(Morton, 1987) Fruit tree, ornamental evergreen
Star apple (*Chrysophyllum cainito*)	Fruiting at 5 to 10 years			Tropical	(Morton, 1987)
			Forest		
Acacia (*Acacia crassicarpa*)	Deep roots after 4 years, can be ~20 years	~6m after 4 years, can be up to 16m	6m	500 to 3000mm rainfall	(Eyles et al., 2015; Morris et al., 2011)
Alim (*Melanolepis multiglandulosa*)					
Bamboo (*Dendrocalamus asper*)	Harvest after 3 years	Usually down to 0.4m, most roots found near surface	0.4m	Frequent rainfall; grows continuously in humid and tropical environments	(Kittur, 2011)
Fire trees (*Delonix regia*)	5 years to maturity			High tolerance for drought, needs well-drained soil	(Barwick, 2004)
Fortune plant (*Dracaena fragrans*)	Ornamental, observed infrequently				
Gemelina (*Gmelina arborea*)	10 to 12 years to harvest	Taproot system; Most roots within 0.4m of soil profile with lateral root spread	0.4m	750 to 4,500mm annual precipitation	(Mayavel et al., 2014; Swamy et al., 2003)
Ipil-ipil (*Leucaena glauca*) or wild tamarind (*Leucaena leucocephala*)	20 to 40 years	Taproot system; 2m depth at 1 year and over 5m depth at 5 years	2.5m	High tolerance for drought, needs well-drained soil; annual rainfall of 500mm to 3,500mm	Nitrogen-fixing plant (Barwick, 2004; Global Invasive Species Database, 2010a)

Table 11. Physical characteristics of the different crops and trees observed in the CDO catchment. (continued)

Crop name and scientific name	Growth stages	Rooting depth	Rooting depth for LUCI	Water management needs	Source
Philippine mahogany (*Toona calantas*)	30 to 40 years before harvest	0.20m to 0.7m (mean of ~0.5m) with lateral spread of the roots (buttressing)	0.5m	Possibly like narra, another Philippine hardwood	Wang et al. (2002) but their study was about redcedar, which is another name for the *Toona* genus
Narra (*Pterocarpus indicus*)	30 to 40-year rotations	Near surface lateral rooting; 80% of root matrix found within 0.6m of surface	0.6m	1300 to 1400mm annual rainfall	(Saifuddin & Normaniza, 2016; Thomson, 2006)
Palcata (*Acacia falcata*) which is the same family as the acacia	Deep roots after 4 years, can be ~20 years	~6m after 4 years, can be up to 16m	6m	500 to 3000mm rainfall	(Eyles et al., 2015; Morris et al., 2011)
Pine (*Pinus kesiya*)	Cone-bearing at 12-18 years	Tap root system 1 to 1.5 years: Up to 2.75m 3 years: almost equal to height of tree	2.75m	~1,300mm annual rainfall ET: 1 mm day^{-1} for seedings	(Armitage & Burley, 1980)
Talisay (*Terminalia catappa*)	Fast-growing perennial, agroforestry rotations at 10 to 15 years	Lateral root system, buttressed roots		1,500mm to 3,400mm annual rainfall	(FAO, 2007)
		Grassland and brushland			
Makahiya (*Mimosa pudica*)	Seedling stage of 2 to 3 months; live up to 1 to 2 years	Creeping plant/weed		Annual rainfall of 1,000mm to 2,000mm	(Global Invasive Species Database, 2010b)

Table 11. Physical characteristics of the different crops and trees observed in the CDO catchment. (continued)

Crop name and scientific name	Growth stages	Rooting depth	Rooting depth for LUCI	Water management needs	Source
Grassland and brushland					
Talahib and other wild grasses (Pasture grass from CROPWAT)	Initial and development: 200 days Mid/late season: 165 days	0.80m, can go down to 1.6m depth	0.80m	At least 150mm to 250mm available water capacity	CROPWAT for pasture grass information; Australian wild tropical pasture grasses (Murphy, 2010)
Saluyot (*Corchorus olitorius*)	~ 120 days	0.15 to 0.20m, can be up to 0.60m	0.20m	Rain-fed, sensitive to water stress	(Mahapatra et al., 2009)

2.5 Correlation to New Zealand databases

The LUCI framework has been applied to several sites within New Zealand: including the Wairarapa, Rotorua, and Canterbury at various spatial scales (Easton, 2015; Marapara, 2016). The parameterisation information for New Zealand soils and land cover types is therefore the most supported and detailed within LUCI. The Philippine soils and land cover types were correlated to the New Zealand Soil Classification (NZSC) at the order level (Hewitt, 2010) and the New Zealand Land Cover Database[6] respectively, and then re-run within LUCI to test the relatively general Philippine parameterisation against the more detailed NZ-based parameterisation. In addition to correlating to the NZ databases, information about the stocking rates and fertiliser applications were taken from CountryStat so that LUCI was able to apply the nitrogen and phosphorus transport models to CDO (PSA, 2018). The purpose of testing the NZ-based parameterisation is to benefit future applications of LUCI in areas with limited information about specific soil and land cover characteristics.

The Philippine soils were correlated to the NZSC through comparing the general properties of the soil subgroups and their highest-level order classification to the highest level of the NZSC. The USDA subgroups were matched to the NZSC order level

[6] http://www.lcdb.scinfo.org.nz/

based on comparison between Hewitt et al. (2010), the work of Carating et al. (2014) on the Philippine soils, the USDA Keys to Soil Taxonomy (USDA, 2014), and to previously published correlation tables (NZ Soils, 2011). Most of the soils in the CDO catchment were classified as Ultic soils, with Pallic and Brown soils also present. The correlation between the subgroups of Typic Hapludults, Typic Paleudults, and Typic Hapludalfs was straightforward as there was a direct correlation between these subgroups and orders with the NZSC (NZ Soils, 2011). For the *Fluventic Eutropepts* (*San Manuel* series), the information from Carating et al. (2014) was compared to Hewitt et al. (2010) and the soil subgroup was matched to the Brown soils due to the similarities in typical colour properties. For actual use in the LUCI framework's *General Landcover Scenario* tool, the soil input data must have a field called "SOIORDER" as the linking code and the soil data source as 24.

Table 12. Correlation of the USDA subgroups present in the CDO catchment with the New Zealand Soil Classification at the order level.

USDA Subgroup	NZSC Order
Typic Hapludults	Ultic
Fluventic Eutropepts	Brown
Typic Paleudults	Ultic
Typic Hapludalfs	Pallic

The land cover types in the CDO catchment and potential scenarios were compared to the New Zealand Land Cover Database (NZLCDB) v4.0 through comparing the descriptions of the land cover classes present in the documentation. The shrubs, grassland, and forest plantations were classified as exotic vegetation classes in LCDB4 because they are types of plants common to the Philippines. The open forest was classified as deciduous hardwoods because of their tropical nature, while the closed forest and areas of protection were classified as indigenous forest because of their relatively good condition and presence of trees such as pines and other Philippine hardwoods. For use in the LUCI framework's *Generate Landcover Scenario* tool, the input data file must have the "LCBD4CLASS" field as its linking code and the land cover data source set to 24.

Table 13. Correlation of the original land cover scenarios for CDO with the New Zealand Land Cover Database version 4.0.

Original LC ID	Original LC Description	LCDB4 Class	LCDB4 Name
Baseline Scenario			
Sh	Other wooded land, shrubs	56	Mixed Exotic Shrubland
GL	Other land, natural, grassland	40	High Producing Exotic Grassland
AC	Other land, cultivated, annual crop	30	Short-rotation Cropland
PC	other land, cultivated, perennial	33	Orchards, Vineyards or Other Perennial Crops
BUA	Other land, built-up area	1	Built-up Area (settlement)
PINE	Pineapple plantation	33	Orchards, Vineyards or Other Perennial Crops
NF4F	Closed forest, broadleaved	69	Indigenous Forest
NF2B	Open forest, broadleaved	68	Deciduous Hardwoods
IW	Inland water	21	River
FPB	Forest plantation, broadleaved	71	Exotic Forest
WGL	Other wooded land, wooded grassland	54	Broadleaved Indigenous Hardwoods
Development Scenario			
Ag	Agricultural Sub-zone	30	Short-rotation Cropland
Ag1	Agricultural Zone 1	30	Short-rotation Cropland
Ag2	Agricultural Zone 2	33	Orchards, Vineyards or Other Perennial Crops
Ag3	Agricultural Zone 3	33	Orchards, Vineyards or Other Perennial Crops
AgFor	Agroforestry Sub-zone	33	Orchards, Vineyards or Other Perennial Crops
AgForPriv	Private Agroforestry Sub-zone	33	Orchards, Vineyards or Other Perennial Crops
ForPriv	Private Forest Sub-zone	71	Exotic Forest
ForRest	Forest Restoration Sub-zone	69	Indigenous Forest
NatioPark	National Park	69	Indigenous Forest
NatuPark	Natural Park	69	Indigenous Forest
Prot	Strict Protection Zone	69	Indigenous Forest
TimProd	Timber Production Sub-zone	71	Exotic Forest
TimReg	Timber Regeneration Sub-zone	71	Exotic Forest

Table 13. Correlation of the original land cover scenarios for CDO with the New Zealand Land Cover Database version 4.0. (continued)

Original LC ID	Original LC Description	LCDB4 Class	LCDB4 Name
Rehabilitation Scenario			
Bu	City	1	Built-up Area (settlement)
AgFor	Agroforestry	33	Orchards, Vineyards or Other Perennial Crops
Ref	Reforestation	71	Exotic Forest
RecAgFor	Recommend Agroforestry	33	Orchards, Vineyards or Other Perennial Crops
RecRef	Recommend Reforestation	71	Exotic Forest
AgCons	Practice Conservation Farming	30	Short-rotation Cropland
Prot	Protection	69	Indigenous Forest
NatReg	Assisted Natural Regeneration	69	Indigenous Forest
RecAgCon s	Recommend Conservation Farming	30	Short-rotation Cropland

2.6 Ecosystem services modelling

For this thesis, two ecosystem services were assessed through modelling and spatial analysis: soil conservation (ability to mitigate erosion) and flood mitigation. The soil erosion modelling was done using the RUSLE (Chapter 4) to identify the annual soil erosion rates and the areas of the catchment vulnerable to soil erosion under the three different land cover scenarios. The flood mitigation modelling was done in the LUCI framework to identify areas that are already providing mitigation and those that can be managed differently to improve mitigation services.

2.6.1 Flood mitigation

The flood mitigation module is already implemented in LUCI so the modelling for this ecosystem service was completed within the actual LUCI model in ArcMap. The aim is to answer the following questions:

- Which areas are providing the ecosystem service of flood mitigation?
- Which areas have the potential to be developed and provide flood mitigation?
- How will different land cover scenarios affect the hydrological response of the watershed?

Figure 27 shows the general flowchart of this ecosystem services modelling component. Since an NZ-based parameterisation was also set up for CDO, more ecosystem service models were run using that NZ-based parameterisation to produce initial ecosystem services maps for agricultural productivity, and transport of nitrogen and phosphorus.

By running the baseline, development, and rehabilitation scenarios through LUCI's flood mitigation module, it not only shows how much of the CDO watershed is critical to mitigating floods, but which areas can be targeted for future management interventions. The comparison of the PH-based parameterisation and the NZ-based parameterisation is also useful to test the effect of various levels of parameterisation detail on the ecosystem services results. In future applications of LUCI in new countries, the steps outlined in this research guide future users to more easily parameterise their site's land cover scenarios.

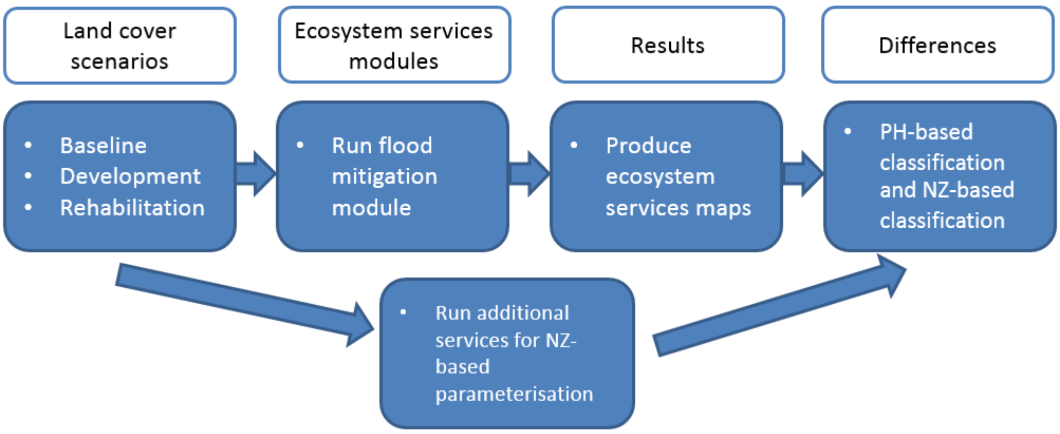

Figure 27. Flowchart for the LUCI ecosystem services runs.

2.6.2 Soil conservation

To understand soil conservation, soil erosion runs were done independently to the LUCI software to test the RUSLE before it will be fully implemented into LUCI in future work (Figure 28). The parameterisation data and equations were taken from an extensive literature review of RUSLE applications in tropical locations, specifically in Southeast Asia. Several equations were tested to assess their applicability to the CDO watershed because of the regional specificity of some sub-factors, making sensitivity analysis important in RUSLE applications. The different RUSLE layers were created as raster layers in ArcMap and run through different scenarios and combinations to assess how changes in components affect the final soil loss estimates. More detail about the RUSLE application the CDO is in Chapter 5, and the RUSLE model was also tested and applied in the Mangatarere catchment, New Zealand (Chapter 6).

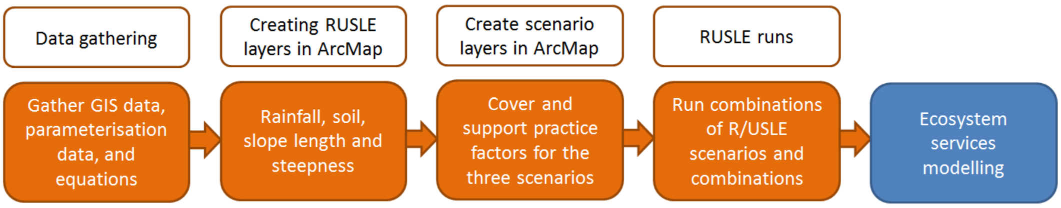

Figure 28. Methodology for soil erosion runs.

2.7 Extreme events and inundation

In December 2011, Typhoon Washi caused heavy flooding and destruction in the region. Typhoon Washi caused a total of 1,268 casualties, half of whom were located in CDO City, and damages amounting to PHP 2 billion (~USD 46 million in 2011) (NDRRMC, 2012a). In December 2012, Typhoon Bopha (local name: Pablo) caused a total of 1,067 casualties and estimated PHP 36 billion in damages (~USD 870 million in 2012) (NDRRMC, 2012b). In December 2014, Tropical Storm Jangmi (local name: Seniang) caused a total of 66 casualties and estimated PHP 1 billion in damages (~USD 28 million in 2014) (NDRRMC, 2014a). In December 2017, Typhoon Tembin (local name: Vinta) caused 1 confirmed death, 160+ missing or presumed dead, and estimated PHP 1.5 billion in damages (~USD 31 million in 2017) (NDRRMC, 2017).

Since flooding associated with extreme events is a major issue in CDO, this research also tested the rainfall-runoff modelling and inundation mapping capabilities of the LUCI framework (Figure 29). Both LUCI and HEC-HMS have the capability to perform watershed modelling but have different ways of modelling runoff. LUCI does this through a cascade of form of soil moisture accounting units, taking into account permeability of different elements in the landscape (Jackson et al., 2013). The current configuration of the HEC-HMS model used by DREAM (2015) utilises the Soil Conservation Service Curve Number method, which assigns a parameter to each sub-basin based on soil type, land use, hydrologic condition, and antecedent runoff conditions (USDA NRSC, 1986). More detail on the differences between the two rainfall-runoff models is found in the extreme events chapter (Chapter 8).

Under the baseline land cover scenario, the rainfall data from Typhoon Bopha was run through both LUCI and HEC-HMS to produce flood hydrographs. These hydrographs were then compared to the observed flow at the outlet of the catchment. To map inundation, the flood hydrographs were run through HEC-RAS.

Future work for extreme events modelling in CDO includes running the LUCI rainfall-runoff model for the other rainfall events under the different land cover scenarios to assess how land cover changes affect peak flows. Structural measures such as a new retaining wall are being implemented in the floodplain of the CDO watershed to protect the city (JICA, 2014). These structural measures are built to cope with a 25-year flood event (159.7mm in 1 day) having a peak discharge of 3,257 $m^3 s^{-1}$. The peak flow of the hydrographs was compared to this exceedance probability to check the possible effectiveness of the retaining wall.

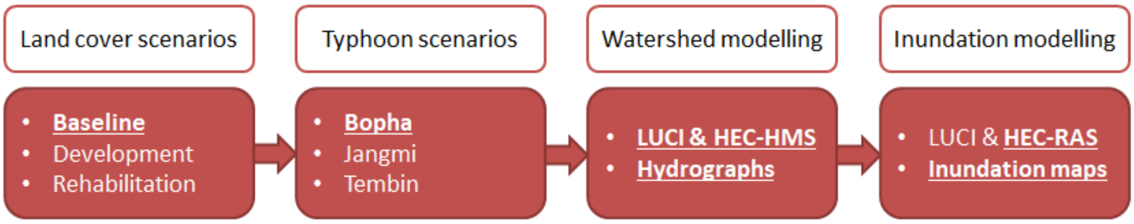

Figure 29. Flowchart for the extreme events modelling, items emphasised are presented in this thesis.

2.8 Summary of methodology

The overview of the different components of this research are shown in Figure 30. The land cover and soil parameterisation produce values that were tested by running the ecosystem services modelling capabilities within the LUCI framework. The ecosystem services runs had three main land cover scenarios: baseline, development, and rehabilitation. These scenarios were also run through the RUSLE to assess how land cover changes would affect soil erosion in CDO. The results from these ecosystem services and soil erosion modelling runs can help inform land management of the potential impact of changing land cover in the CDO catchment.

The extreme events component of this thesis tested the capability of the LUCI model to do rainfall-runoff modelling compared to HEC-HMS and to flow observations under one typhoon event. To include the effect of climate change, a brief review of climate change studies in the Philippines and the region where CDO is located was accomplished and included a commentary on the possible effects of changing climate on the ecosystem services and hydrological response of the catchment to extreme rainfall events.

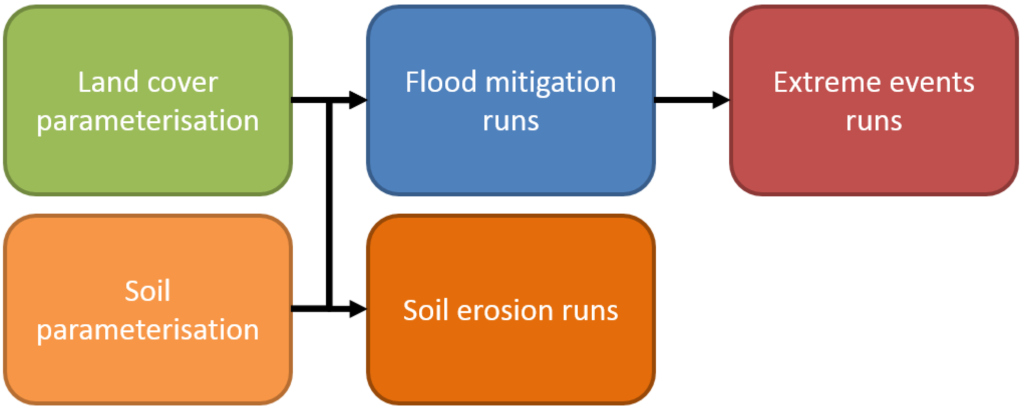

Figure 30. Simplified flowchart of the different modelling groups that composed this research.

The main outputs of this dissertation are as follows:

- LUCI parameters for the soil present in the Cagayan de Oro watershed, which in turn will guide how to parameterise for soils present in the rest of the Philippines
- LUCI parameters for the land cover present in the Cagayan de Oro watershed, which included crops commonly found in the Philippines, which can be used for future research in the country
- RUSLE soil erosion vulnerability maps for the different land use scenarios
- LUCI ecosystem services maps showing how ecosystem services are distributed under the different land use scenarios for flood mitigation, and where are the areas recommended for management interventions
- Hydrographs at the watershed outlet and inundation maps generated by LUCI, HEC-HMS and HEC-RAS for the baseline scenario under Typhoon Bopha

This research also contributed the following for LUCI development:

- Calculating weighted curve numbers for subwatersheds within the Cagayan de Oro watershed
- Estimating the soil loss using the Revised Universal Soil Loss Equation (RUSLE)
- Mapping inundation extent for LUCI's flatwater inundation module

3 Application of the LUCI framework to the CDO catchment for flood mitigation and other ecosystem services

3.1 Introduction

As detailed in Chapter 1, the vulnerability of the Philippines to tropical cyclones and climate change underscores the need for more proactive disaster risk management, which to date is carried out mainly through flood-forecasting and structural flood protection projects to protect communities and infrastructures. The official programme of disaster prevention and mitigation in the Philippines is Project NOAH (Nationwide Operational Assessment of Hazards). This programme mainly uses two hydrological models from the Hydrologic Engineering Center (HEC) to assist in flood forecasting and making flood hazard maps: the Hydrologic Modeling System (HMS) for watershed modelling, and the River Analysis System (RAS) for inundation modelling (Brunner, 2010b; Scharffenberg, 2013). These models have been calibrated to local conditions in order to generate flood extent maps using real-time rainfall data that can be viewed through a public website (Santillan et al., 2013). The current real-time flood-forecasting framework in the Philippines is shown in Figure 31. This framework is also present in the Cagayan de Oro (CDO) catchment to provide early warnings to communities and government to prompt evacuation efforts (Paringit et al., 2015). Aside from warning systems, flood prevention in CDO is also achieved through the use of structural measures such as retaining walls on the floodplain (JICA, 2014).

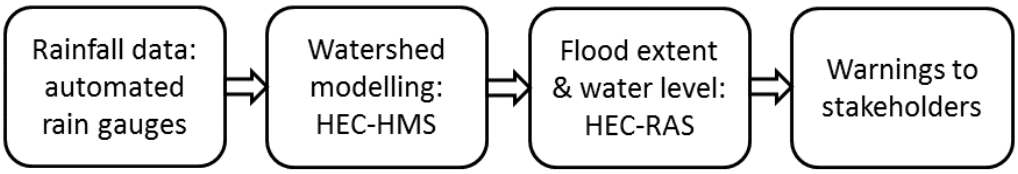

Figure 31. The current real-time flood-forecasting framework in the Philippines.

As also established in Chapter 1, watershed management through ecosystem services modelling is another option in the toolbox of disaster risk mitigation for more sustainable land management. Although ecosystem service studies have been done in CDO, these have focused on communicating with the local community to understand how they value ecosystem services and their willingness-to-pay for the maintenance and protection of these services (Baig et al., 2015; ILC, 2013). To date, there is no published scientific literature regarding the mapping of ecosystem services in the CDO catchment under different scenarios of land cover.

The aim of this chapter is the scientific evaluation and mapping of ecosystem services, particularly flood mitigation, in the CDO catchment. The specific objectives are as follows:

- Apply the Land Utilisation and Capability Indicator (LUCI) model to the CDO catchment to identify the areas that are already providing flood mitigating services, and the areas that can be targeted for management strategies;
- Run the three land cover scenarios (Chapter 2) to assess how future catchment management plans will affect flood mitigation; and
- Using the New Zealand-based parameterisation, run the three land cover scenarios to assess how future catchment management plans will affect agricultural productivity, nitrogen delivery, and phosphorus delivery.

In terms of soil erosion and its mitigation, the Revised Universal Soil Loss Equation (RUSLE) application was applied to CDO and detailed in Chapter 5. Further development of LUCI will incorporate the RUSLE in its framework and as an option for soil erosion modelling. Since the CDO soil and land cover datasets were also correlated to the New Zealand soils and land cover, three other ecosystem services were run in LUCI for the CDO catchment. These services are agricultural productivity, which is important for the CDO catchment since it is heavily-utilised for agriculture, and nitrogen and phosphorus transport to assess effects on water quality.

3.2 Methodology

The methodology chapter (Chapter 2) outlines the DEM, soil information, land cover information, rainfall, and evapotranspiration datasets that were used to run LUCI in the CDO catchment. The DEM influences the topographical routing of flow through the landscape, the rainfall and evapotranspiration influences the water balance of the catchment, and the soil and land cover give information about the permeability and flood mitigation capacity of different areas of the catchment.

This chapter utilises the LUCI model that was explained in the introduction of this thesis (Figure 32). The three main tools used are:

1. *Generate HydTopo Inputs*: to produce the hydrological information needed for ecosystem services runs;
2. *Generate Scenario User Specified Land Use*: to produce the land management and soil information needed for ecosystem services runs; and
3. *Flood Mitigation Tool*: to identify the areas providing flood mitigation services and those that can be modified to enhance that service.

Since this is the first application of LUCI to CDO, the model was parameterised for local soil and land cover. Two kinds of parameterisation were done to set up LUCI for the CDO catchment: a Philippine-based parameterisation and a New Zealand-based parameterisation. More detail about how this parameterisation was carried out is in the methodology (Chapter 2). The flood mitigation tool was run for both the PH-based and NZ-based parameterisation to test how differing levels of parameterisation detail changed the ecosystem services maps since the NZ classification system is more detailed within LUCI. This comparison illustrated the differences in output between the correlation to the default LUCI land cover classes and to the more detailed parameterisation information within LUCI for New Zealand soils and land cover. The NZ-based parameterisation also allowed the following tools to be run: agricultural productivity, nitrogen delivery, and phosphorous delivery.

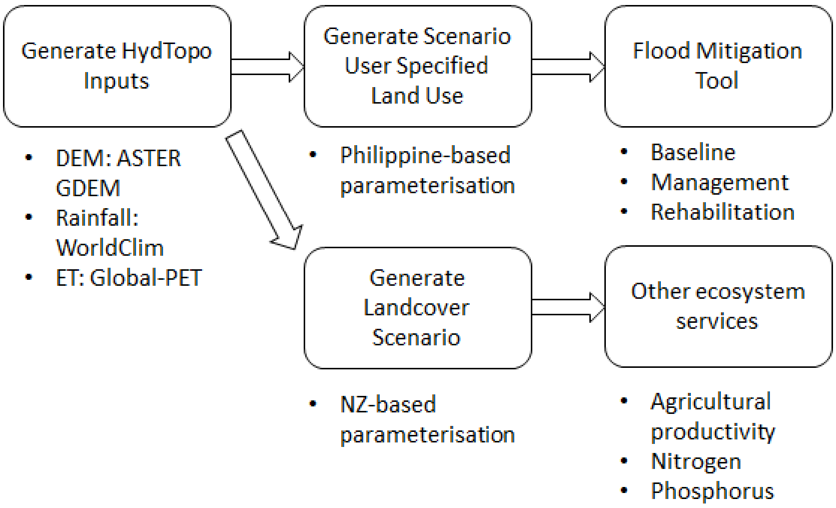

Figure 32. Overview of the methodology of this chapter with each of the LUCI tools used.

3.2.1 LUCI preprocessing

Before running any of the ecosystem services modules within LUCI, the preprocessing step of generating the hydrological and topographical information must first be done (Jackson et al., 2013). This step requires a digital elevation model (DEM) and climate information such as annual rainfall and annual evapotranspiration in mm day^{-1}. The raw DEM may contain depressions, flat areas, and artefacts that may hinder flow algorithms from accurately representing the stream network within the catchment, hence the need for DEM reconditioning (Lindsay, 2016).

The LUCI HydTopo tool fills sinks within the DEM and uses the AGREE reconditioning approach to "burn" river networks into the DEM. The AGREE approach adjusts the elevation information of a DEM based on the known stream network through decreasing the elevation of the raster cells in the stream network and "smoothing" the path where water flows downwards towards the streams (Hellweger, 1997). This approach reconciles the DEM information with the mapped stream network and, through subsequent flow algorithms and runoff modelling, directs the flow towards the stream network more effectively (Figure 33).

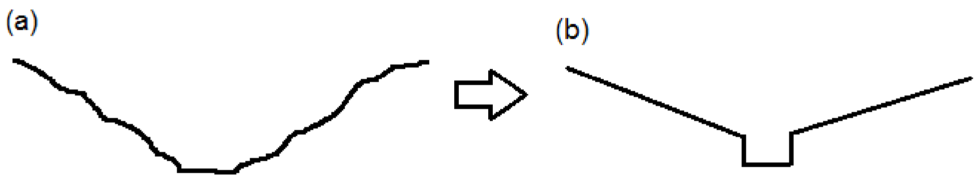

Figure 33. Sketch showing the effect of stream reconditioning on the raw DEM (a) and the subsequent reconditoned DEM (b).

Within LUCI, there are default values for the buffer distance (75m), stream drop (3m), and buffer drop (2m) (Figure 34). The values of these parameters will depend on the characteristics of DEM such as resolution and accuracy (Hellweger, 1997). Within this chapter, the different values of these parameters were used to test the accuracy of the stream network predicted from the reconditioned DEM with the mapped stream network.

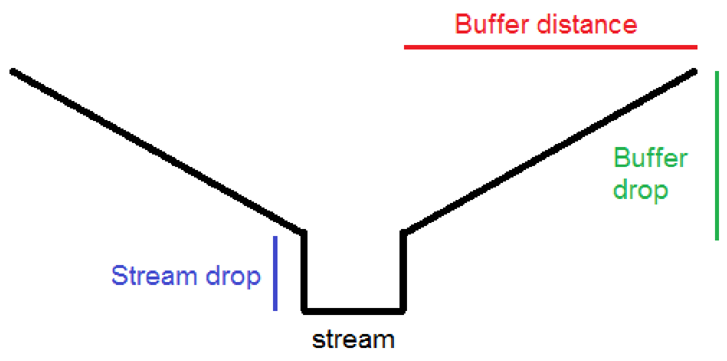

Figure 34. Sketch showing the stream and what the different AGREE reconditioning parameters represent.

3.2.2 Flood mitigation module

The LUCI flood mitigation module uses information about the topography generated from the previous step, soil and land cover to map the areas where water may accumulate and which areas are "mitigating features". Mitigating features are those with high storage and/or infiltration capacity that act as sinks for overland and near-surface flow, thus mitigating the flood risk (Jackson et al., 2013). Other studies that map flood mitigating areas use similar approaches that take into account the topography, soil, and land cover of a landscape to identify which areas have the capability to regulate flow (Bellu et al., 2016; Nedkov & Burkhard, 2012; Stürck et al., 2014). However, the LUCI model is more spatially explicit due to its capability to perform calculations at the sub-field scale compared to the coarser applications of modelling at the sub-catchment or catchment scale.

Sensitivity testing was also done for the flood mitigation tool to analyse possible changes in results. Within the flood mitigation tool, two parameters can be modified: lower threshold for flood mitigation opportunity and lower threshold for very high flood mitigation opportunity. These values relate to the amount of flow accumulating to any given cell to its potential to become a significant flow pathway to a stream or river network (Jackson et al., 2013). For example, Scenario 1 uses the values of 5 and 20 as the parameters (Table 14). With a value of 5, LUCI identifies the cells where accumulation exceeds five times their area of flow and has no significant mitigation potential (i.e. has low permeability and limited water storage capacity) and considers those areas targets for potential mitigation. If the upstream contributing area to a cell is sufficiently large and that cell is mitigating that flow, it comes a target for potential mitigation. The threshold parameter for very high flood mitigation opportunity uses similar operations to identify cells where accumulation exceeds twenty times their area of flow and are thus more critical target areas for mitigation.

Table 14. Mitigation threshold parameters for sensitivity testing.

Threshold	Lower threshold for:	
	Flood mitigation opportunity	**Very high flood mitigation opportunity**
1	5	20
2	2	10
3	10	40
4	15	60
5	20	80
6	25	100
7	30	120
8	35	140
9	40	160
10	45	180

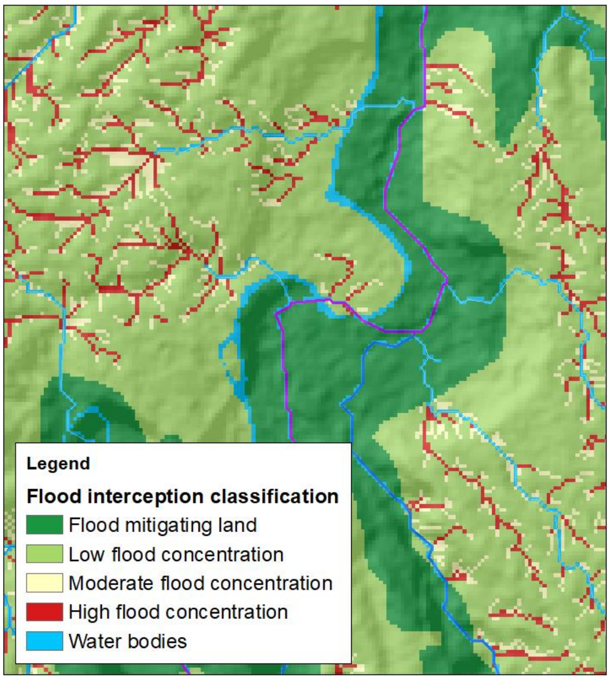

Figure 35. An example map of the output from the flood mitigation module.

3.3 Results and discussion

The main scope of this section is the flood mitigation mapping done through LUCI, but also presents some results from the preprocessing and stream burning steps in LUCI.

3.3.1 LUCI preprocessing

Within the HydTopo tool (Section 3.2.1), there are three parameters that influence the stream network generated from the DEM and three parameters that influence the stream burning operations. The upstream contributing area to a cell is based on the flow direction and flow accumulation, which is a digital representation of the amount of water flowing through the landscape and to that cell. If these accumulation thresholds are exceeded, those cells are identified as part of the stream network, whether small ephemeral streams, normal streams, or major rivers. These parameters, combined with the ones that influence stream burning, derive a stream network from the DEM. The derived stream network should be consistent with the actual stream network present in the catchment; parameter values require testing as they can differ between catchments. The resolution of the DEM is also important, as coarse-resolution DEMS may not be able to identify the smaller streams present in the catchment.

Table 15. LUCI HydTopo parameters that influence the stream network and stream burning.

Parameters that influence the stream network	
Accumulation threshold for stream initiation (ha)	Identifies a cell as part of the stream network
Accumulation threshold for major rivers (ha)	Identifies a cell as part of a major river
Accumulation threshold for ephemeral streams (ha)	Identifies a cell as part of an ephemeral stream
Parameters that influence stream burning	
Buffer distance (m)	Horizontal distance from stream that will be reconditioned
Stream drop (m)	Increase in vertical depth of the reconditioned stream
Buffer drop (m)	Vertical depth from top of the buffer distance to the top of the stream

Table 16. HydTopo input parameters tested.

HydTopo	Accumulation threshold (ha)			Stream burning (m)		
	Stream initiation	Major rivers	Ephemeral streams	Buffer distance	Stream drop	Buffer drop
Default (1)	10	200	5	75	3	2
2				60	3	2
3				90	3	2
4				120	30	20
5				150	30	20
6				180	30	20
7				210	30	20
8				240	30	20
9				270	30	20
10				300	30	20
11	20	400	10	300	30	20
12	200	7200 (based on FAC of headwaters)	100	300	30	20

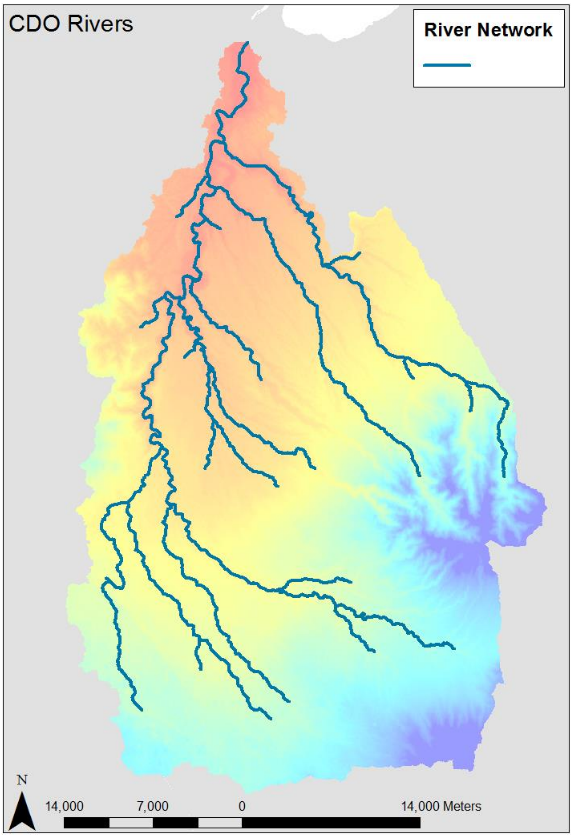

Figure 36. Stream network within the CDO catchment derived by DREAM (2015).

The different parameters for the HydTopo tool were tested with differing values, starting with the default LUCI values, then increasing the stream burning parameters and accumulation thresholds (Table 16). The DEM-derived stream network was then compared to the network derived by DREAM (2015) to check the efficacy of the reconditioning. For the default value (HydTopo 1), the generated stream network was inconsistent with the known stream network, especially at the outlet of the catchment (Figure 37). For a relatively coarse-resolution DEM (~30m), the default LUCI values for reconditioning were too low to direct the flow of water towards the outlet of the catchment.

In HydTopo 4, where the buffer distance was 120m, the stream drop was 30m, and the buffer drop was 20m, the generated stream network became more consistent with the actual stream network. The generated stream network had the river going towards the outlet of the catchment (Figure 38). This completes the main stem of the river, which is very important for later modelling of ecosystem services.

To test the effect of increasing buffer distance, this parameter was increased by 30m increments until the distance of 300m was reached. This accounts for ten pixels on either side of the stream pixel. When compared to the buffer distance of 120, there were minor differences in terms of smaller streams being different, but the main stream network was still consistent each other and with the reference network (Figure 39).

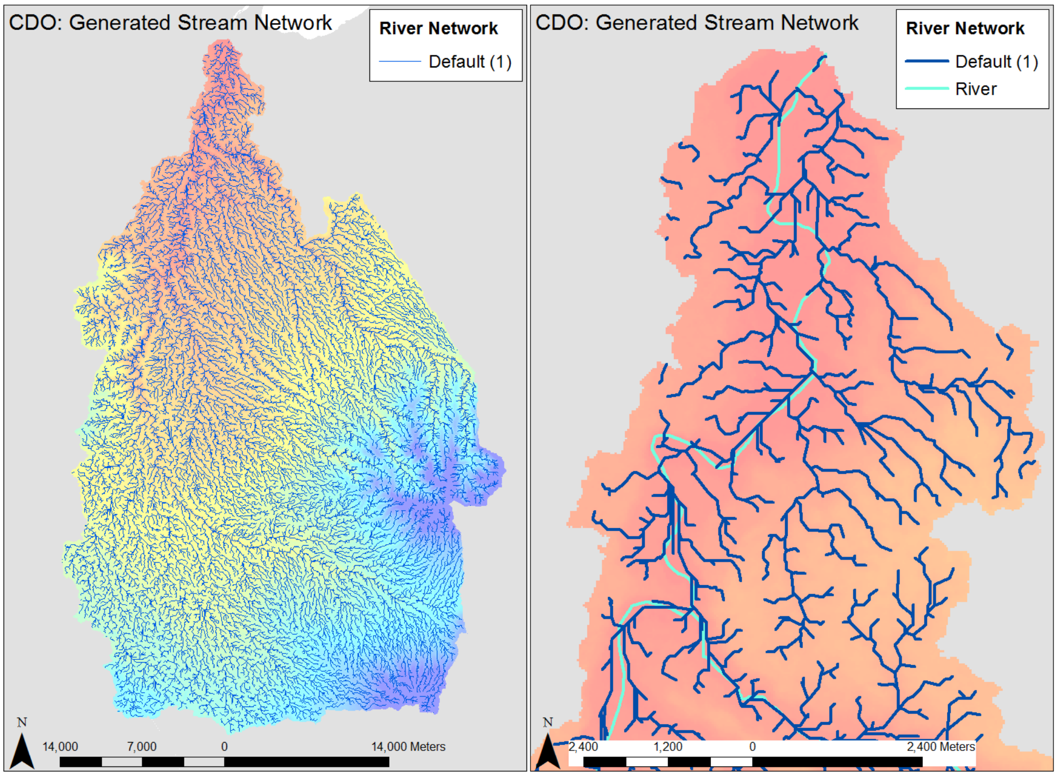

Figure 37. Stream network generated from default LUCI values (HydTopo1) at the catchment scale (left) and at the outlet (right).

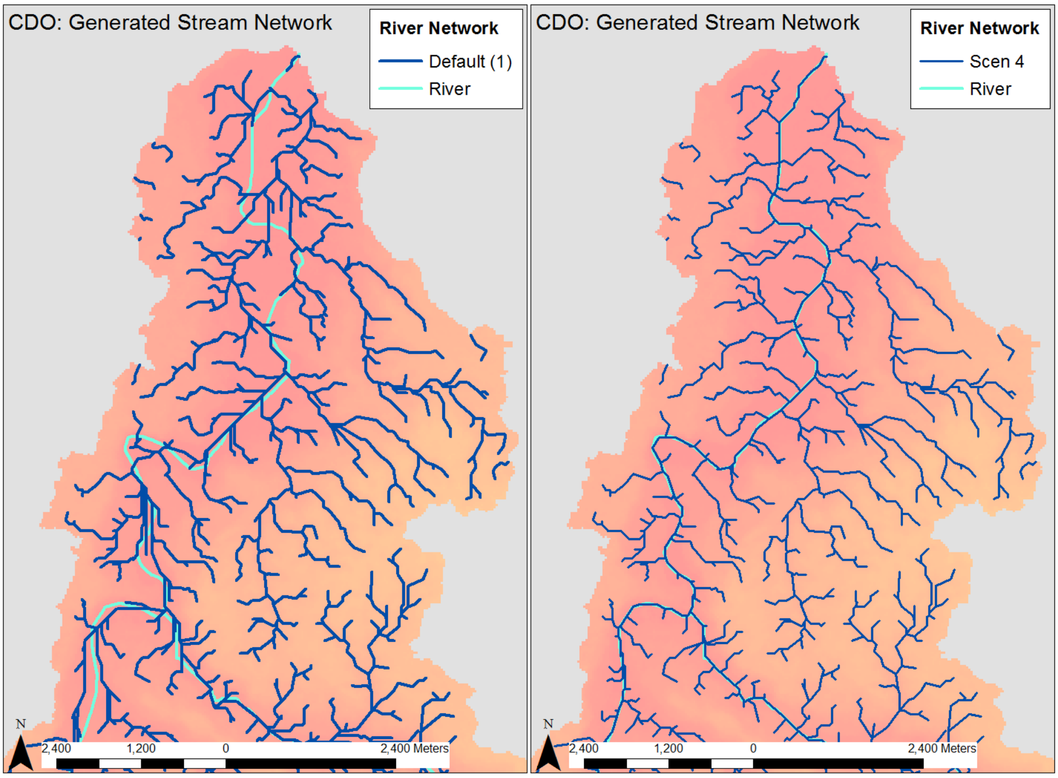

Figure 38. Comparison of the stream network at the outlet using the default HydTopo 1 (left) and HydTopo 4 (right).

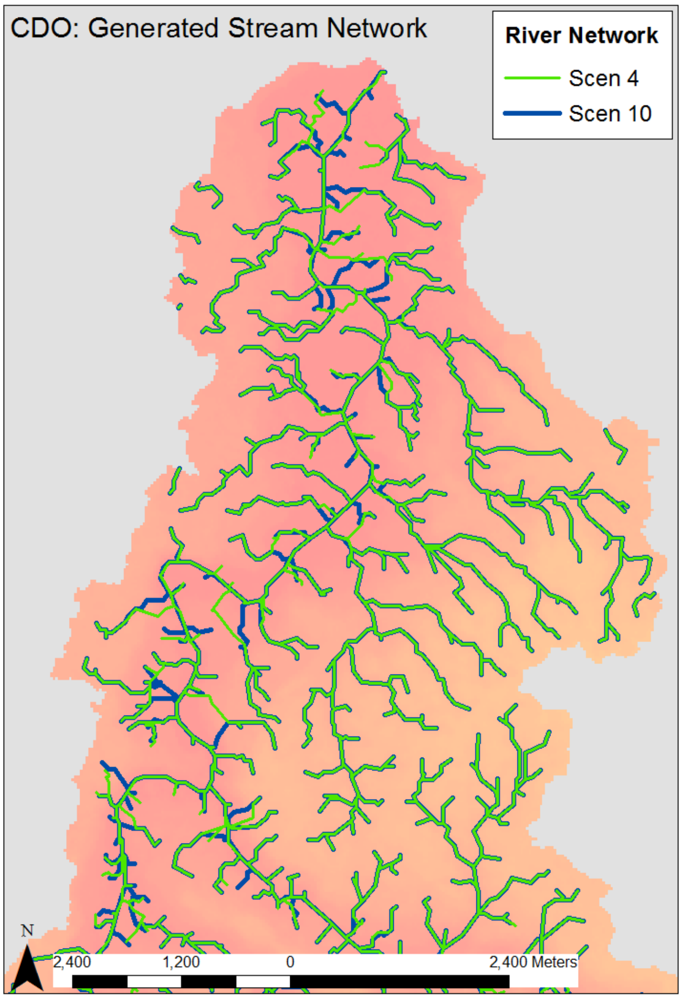

Figure 39. Comparison of HydTopo 4 and HydTopo 10 at the outlet of the catchment showing HydTopo 4 streams (green), HydTopo 10 streams (blue) and streams present in both HydTopo 4 and HydTopo 10 (green with blue outline).

Next, the accumulation thresholds were tested to check their effect on the derived stream network. With higher accumulation thresholds for stream initiation, the number of streams over the watershed decreased. HydTopo 10 used the default values for stream initiation, major rivers, and ephemeral streams. In HydTopo 11, those values were doubled and caused a decrease in the amount and density of streams in the generated stream network (Figure 40). Visual inspection at the outlet of the catchment confirms that the amount and density of streams decreased, but the major rivers in the generated stream network were still consistent with the known river network (Figure 41 and Figure 42).

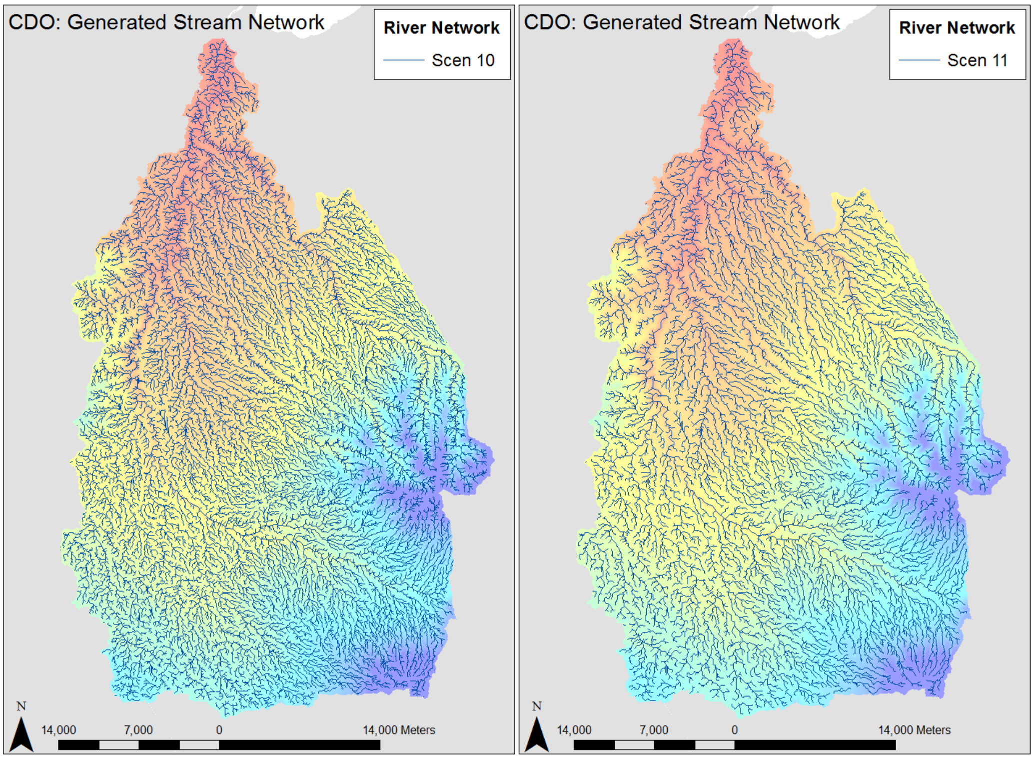

Figure 40. Comparison of HydTopo 10 (left) and HydTopo 11 (right) showing effect of increasing accumulation threshold.

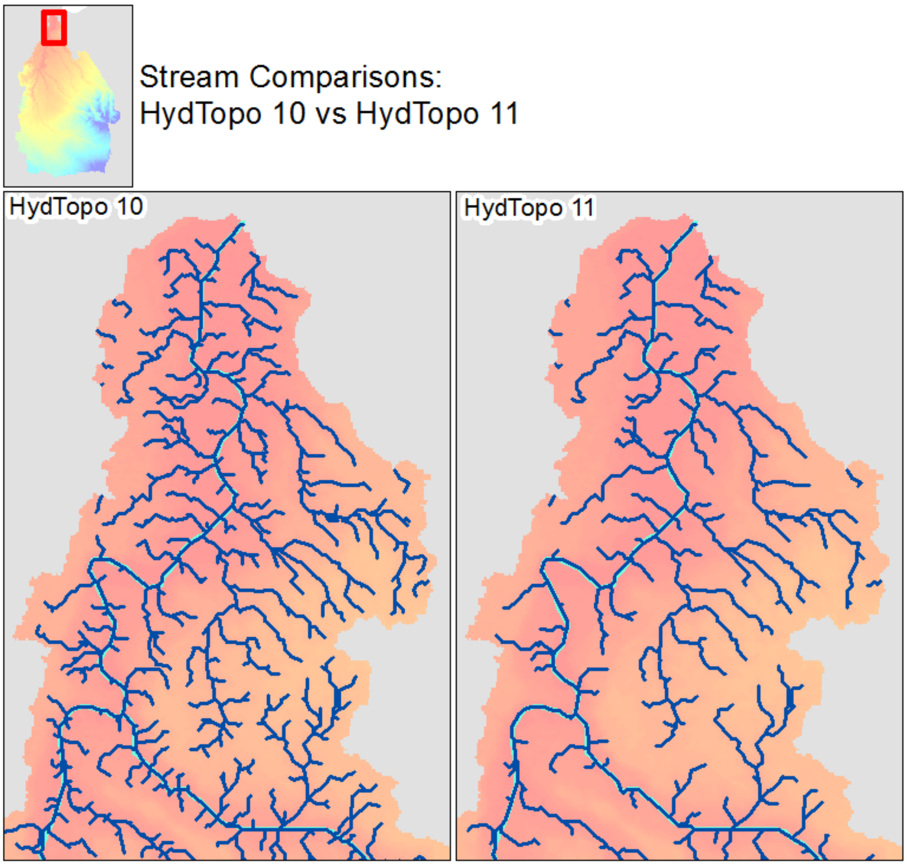

Figure 41. Comparison of HydTopo 10 (left) and HydTopo 11 (right) at the outlet to show the effect of increasing accumulation threshold.

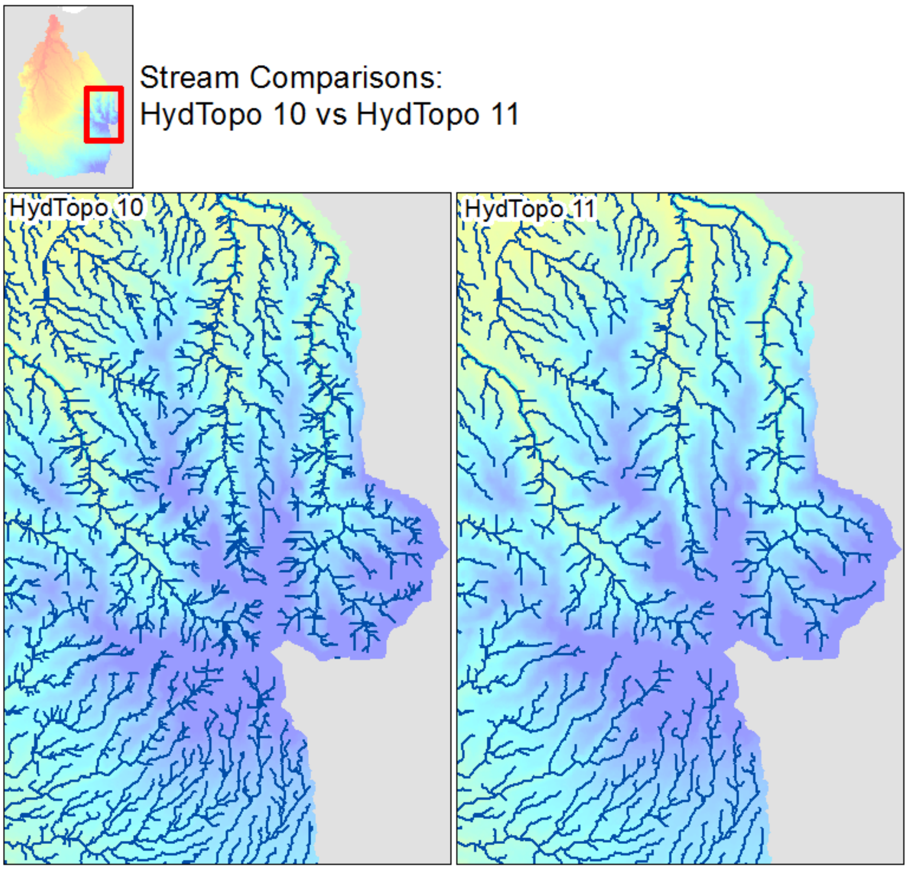

Figure 42. Comparison of HydTopo 10 (left) and HydTopo 11 (right) on the mountainous area on the eastern side of the catchment to show the effect of increasing accumulation threshold.

In HydTopo 12, the values for stream initiation and ephemeral streams were increased by 20 times from the default values to become 200 and 100 ha respectively. The accumulation threshold was determined through checking the flow accumulation at the channel heads of the derived river network. The average value of the flow accumulations at the channel heads was converted to hectares and used as the accumulation threshold for major rivers (7200 ha). The resulting river network had less streams compared to HydTopo 11, and like Figure 41, the major rivers in the generated network were consistent with those in the reference network at the outlet, mountainous areas, and flat areas (Figure 43 to Figure 46).

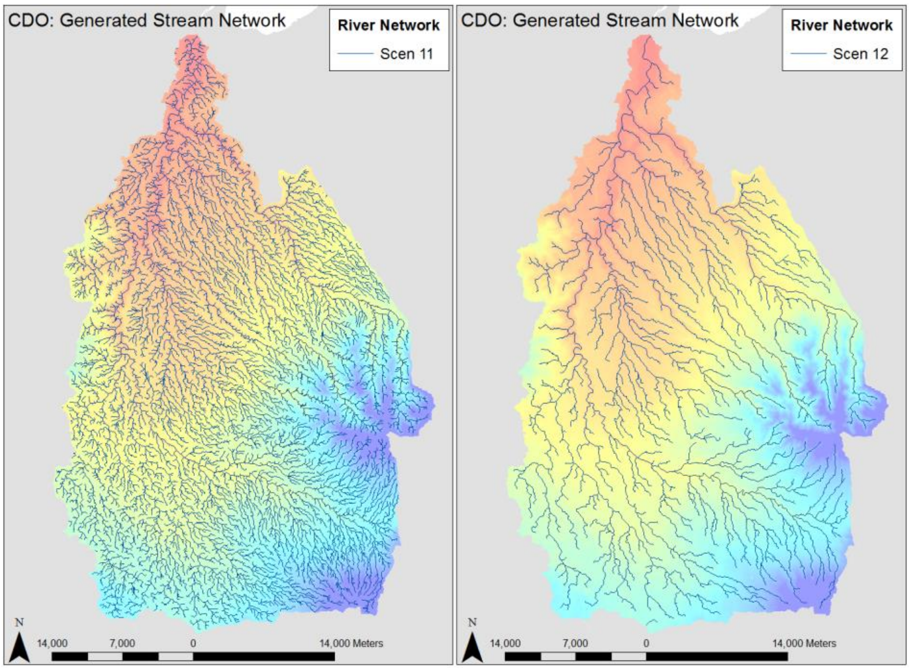

Figure 43. Comparison of HydTopo 11 (left) and HydTopo 12 (right) showing effect of increasing accumulation threshold.

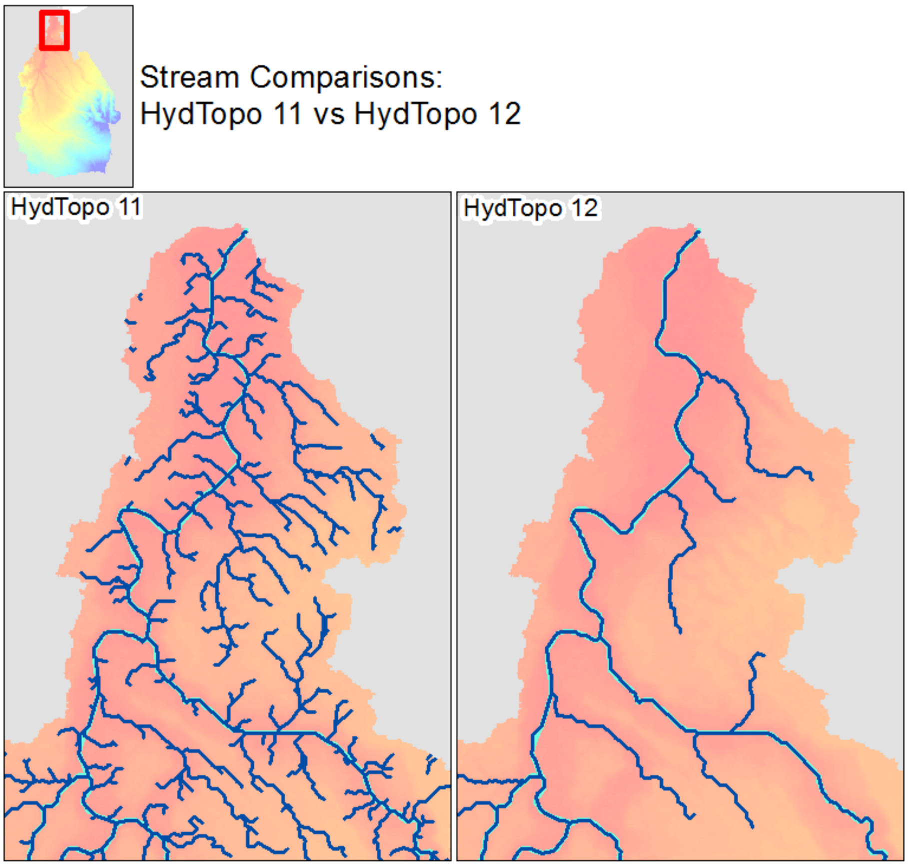

Figure 44. Comparison of HydTopo 11 (left) and HydTopo 12 (right) at the outlet to show the effect of increasing accumulation threshold.

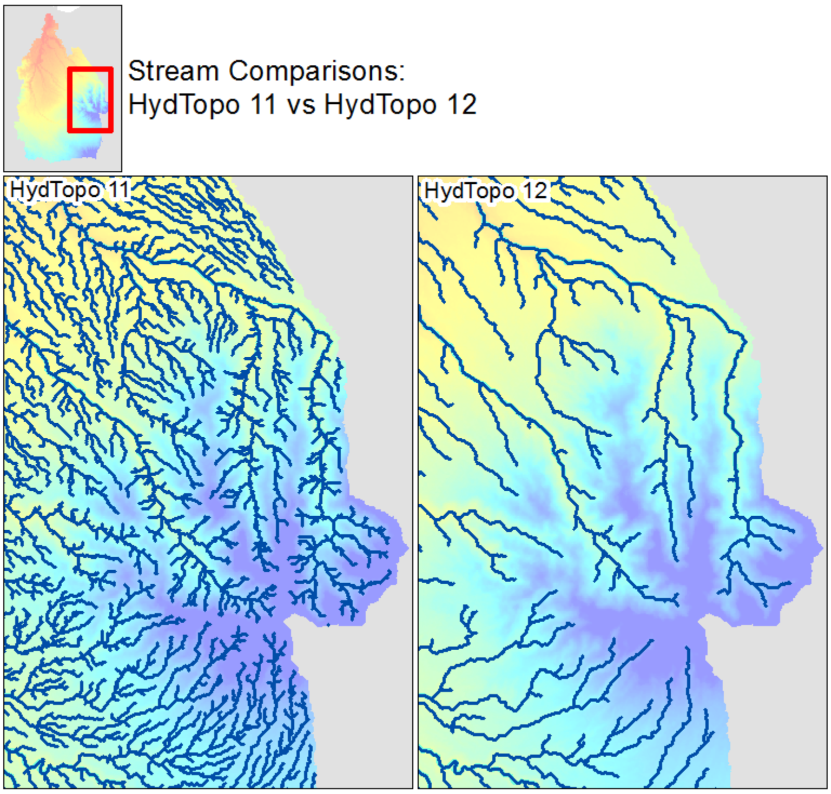

Figure 45. Comparison of HydTopo 11 (left) and HydTopo 12 (right) on the mountainous area on the eastern side of the catchment to show the effect of increasing accumulation threshold.

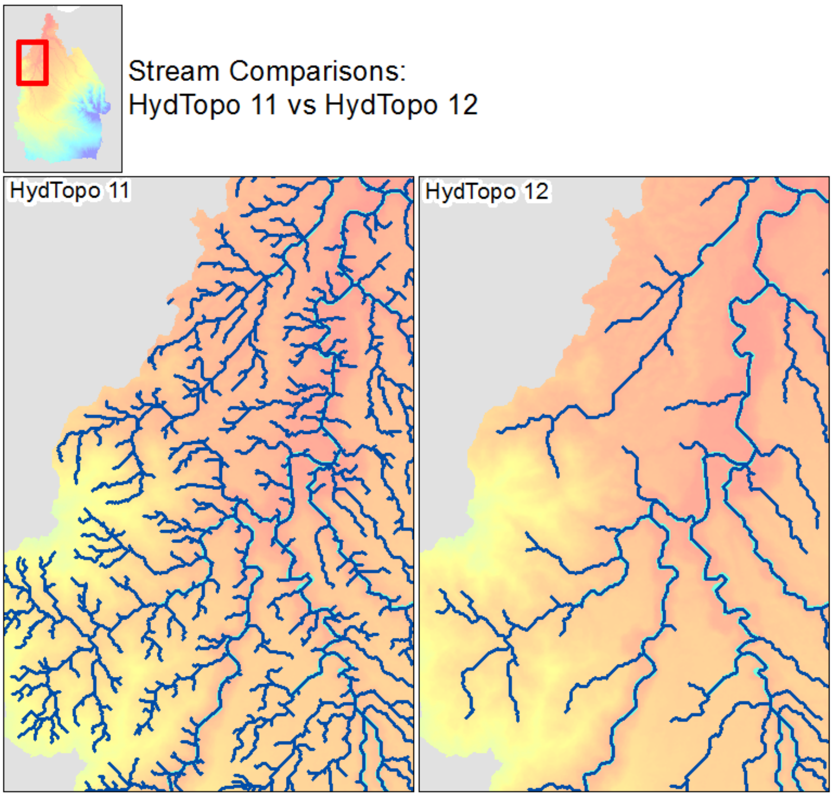

Figure 46. Comparison of HydTopo 11 (left) and HydTopo 12 (right) on the flat area on the western side of the catchment to show the effect of increasing accumulation threshold.

There are techniques for comparing the DEM-derived stream network with a reference network: comparing the drainage densities, lumped basin characteristics, delineated watersheds, prediction of channel heads, and visual inspection (Sousa & Paz, 2017). To compare the derived stream network with the reference network in CDO, the percentage within buffer (PWB) comparison was used: a buffer is added to the reference stream network and the percentage of DEM-derived stream cells that fall within that buffer is counted (Davies & Bell, 2009). The reference network was generated through digitising and primarily identifies the major rivers and streams within CDO but may exclude the smaller and ephemeral streams predicted by the DEM and LUCI. As the buffer distance for the stream burning increased, the PWB also increased by small amounts (Table 17). With the greater buffer distance for stream burning, more flow is being diverted towards the reference stream network, hence the increase in PWB. Once the buffer distance of 300m (~10 pixels on either side) was reached and the accumulation thresholds were changed raised, the PWB values further increased. Increased accumulation thresholds led to a decrease of the number of cells classified as streams because the smaller streams identified in the previous runs were excluded, leading to an increase in the PWB.

Table 17. Number of stream cells, cells within the buffer, and PWB values for the different DEM-derived networks compared to the reference network.

HydTopo	**Number of stream cells**	**Cells within buffer**	**Percentage of derived stream cells within the buffer (PWB)**
Reference Network	13,855	13,855	100
1	174,643	12,991	7.44
2	174,715	13,081	7.49
3	174,604	12,965	7.43
4	172,862	14,089	8.15
5	172,696	14,210	8.23
6	172,514	14,191	8.23
7	172,341	14,153	8.21
8	172,453	14,270	8.27
9	172,583	14,377	8.33
10	172,723	14,416	8.35
11	123,204	12,644	10.26
12	53,151	12,200	22.95

Finding the balance of stream burning parameters and accumulation thresholds is important to make the DEM-derived stream network become consistent with the reference network to simulate the actual flow of water through the landscape. Using the DEM to identify smaller streams not present in the reference network is also important for the same reason, to simulate the flow of water through the landscape through smaller pathways that may not be present in the major river network (Figure 47 and Figure 48). After running with the default LUCI parameters, the user must check the derived stream network to ensure that it is consistent with the reference stream network, and then against satellite observations due to possible uncertainties in how the reference network was derived. If the main stem of the derived stream network is significantly different compared to the observations, the user can increase the stream burning parameters to direct more flow towards the known streams. During each iteration, checking against the observed stream work and satellite imagery is important for the main stem and any smaller streams. The accumulation thresholds can be raised if the drainage density is high or there are too many small streams to optimise the computational efficiency of the model.

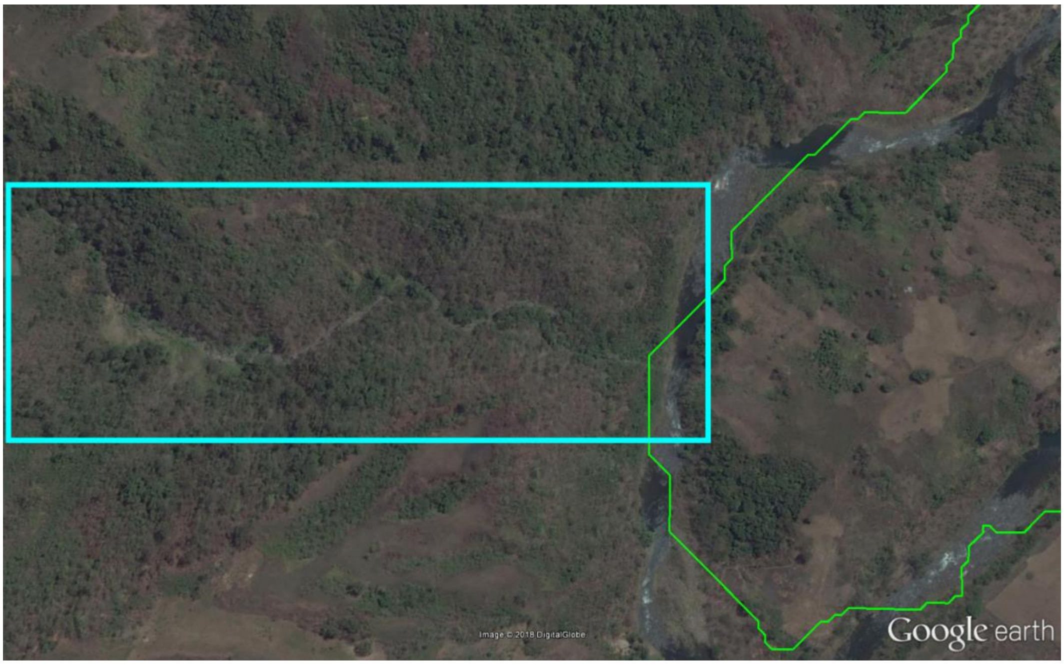

Figure 47. Reference network (green) showing the major stem of the CDO river and a possible smaller stream leading into it (blue box).

Figure 48. Comparison of the reference network (green) and the DEM-derived network for HydTopo 12 (blue) showing the identification of the smaller stream.

For this chapter, the DEM-derived stream network for HydTopo 12 was chosen as the HydTopo input for further modelling within LUCI. A component of future work with LUCI could be testing the sensitivity of the ecosystem services results to the different parameters used for stream reconditioning and network delineation.

3.3.2 Results of Philippine-based parameterisation

This section presents the results of the flood mitigation maps that used the Philippine-based land cover and soil parameterisation. The sensitivity testing results of the thresholds for flood mitigation opportunity under the baseline scenario are also presented. At the catchment level, the difference in the results generated from Threshold 01 (default parameters) and Threshold 10 (45 and 180 threshold values) are not immediately obvious (Table 14 and Figure 49). The same areas of land are identified as already providing flood mitigation services and those with low flood concentration. However, the differences become more obvious at the finer spatial scales (Figure 50). There are fewer cells identified as areas of moderate and high flood classification in Scenario 10 that used higher mitigation threshold values. At higher thresholds, only the very significant water pathways where the cells' accumulation exceeds at least 45 times their flow is considered target areas of mitigation. By lowering the mitigation threshold values, more areas for mitigation opportunities can be identified and this can be used as the initial broad identification of possible target areas. By raising the mitigation threshold values, only the most critical target areas are identified. This is useful for several types of planning situations, whether land management would need identification of all possible target areas or only the critical target areas. Logistical limitations such as funding make it necessary to reduce the number of targeted areas to those that are more critical/vulnerable, or those whose rehabilitation would provide the most benefit (EPA, 2013). In future work, testing these mitigation thresholds would be useful for cost-benefit analysis where applying management interventions must be done with logistical or monetary constraints as higher mitigation thresholds would only identify the most critical target areas.

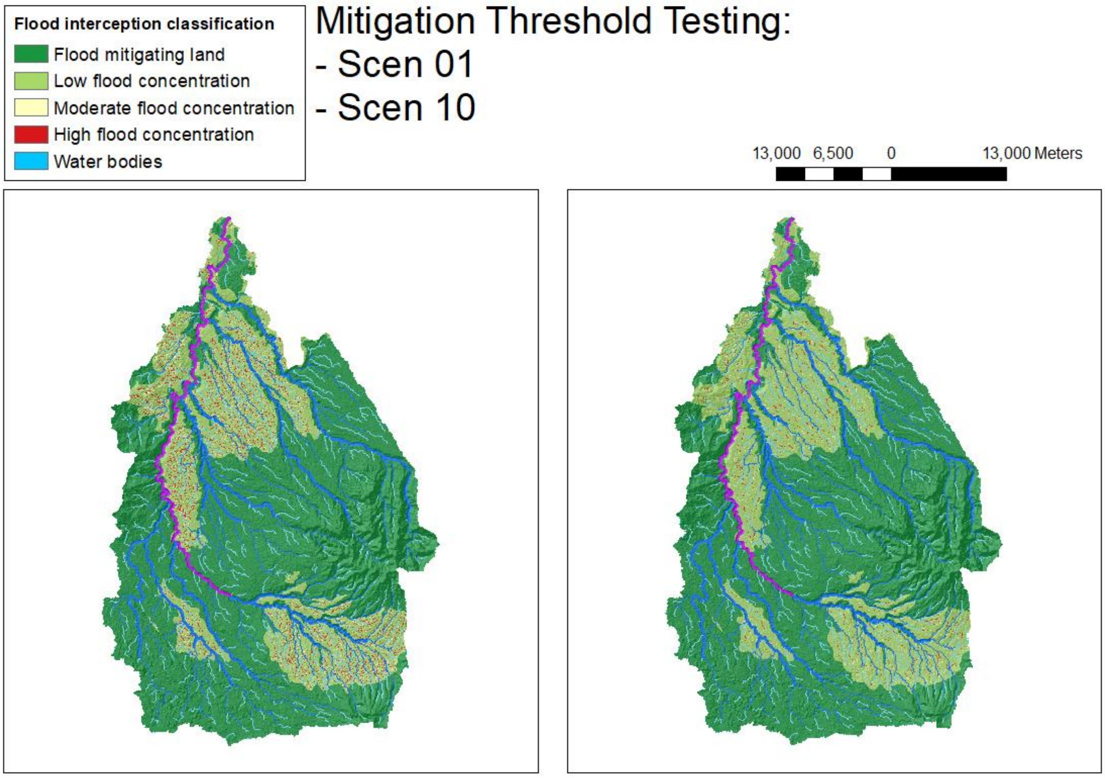

Figure 49. Catchment-scale comparison of mitigation threshold testing for Threshold 1 (5 and 20) and Threshold 10 (45 and 180).

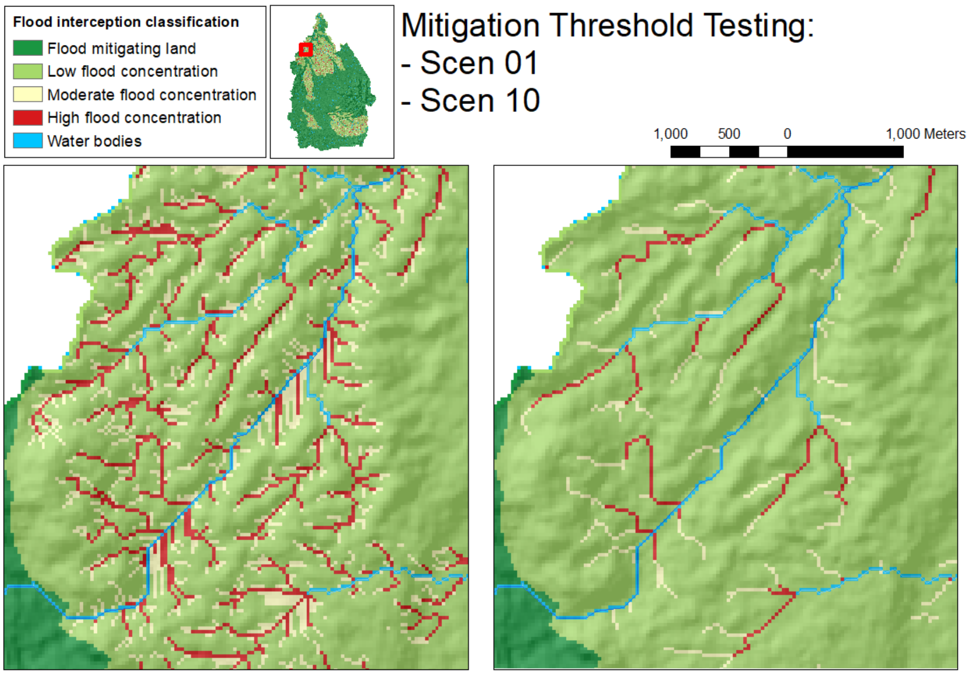

Figure 50. Zoomed-in comparison of mitigation threshold testing for Threshold 1 and Threshold 10.

Across all the three land cover scenarios, the areas of flood mitigating land were areas classified as forest: protected forest zones, national parks, areas marked as potential rehabilitation sites, and areas of agroforestry. Forests have the capacity to absorb and intercept rainfall, which reduces surface runoff and discharge to the stream network (Nedkov & Burkhard, 2012). LUCI's identification of forested, agroforestry, and rehabilitated areas as zones of flood mitigating fits with existing knowledge of ecosystem services. The areas not providing flood mitigation services were those classified as built-up areas, grassland, and agricultural areas. One of the main differences between the development and rehabilitation scenarios is in the southern area of the watershed (Figure 51) where the area planned for agriculture in the development scenario is classified an area of low flood concentration instead of possible flood mitigating land under forest (rehabilitation). In terms of flood interception classification, the development scenario has a lower proportion of the watershed classified as flood mitigating but higher proportions classified as having negligible, moderate, and high flood concentration (Table 18).

One of the limitations of the current parameterisation is that it does not account for the specific land management support practises outlined in the plans for development and rehabilitation. These practices are mostly soil conservation practices such as contour-cropping, inter-cropping, promotion of agroforestry, and adoption of Sloping Agricultural Land Technology (CESM, 2014; CESM, 2015). More information about these practices and their possible effect on soil erosion are found in the chapter about the RUSLE application in CDO (Chapter 5). The restoration practices such as stream rehabilitation can also mitigate soil erosion through streambank stabilisation, suggesting possible synergies between rehabilitation for flood mitigation and soil conservation measures (EPA, 2013). Therefore, potential future parameterisation work should involve options to delineate areas where specific support practices are planned and compare these to conventional agricultural techniques to improve future LUCI applications.

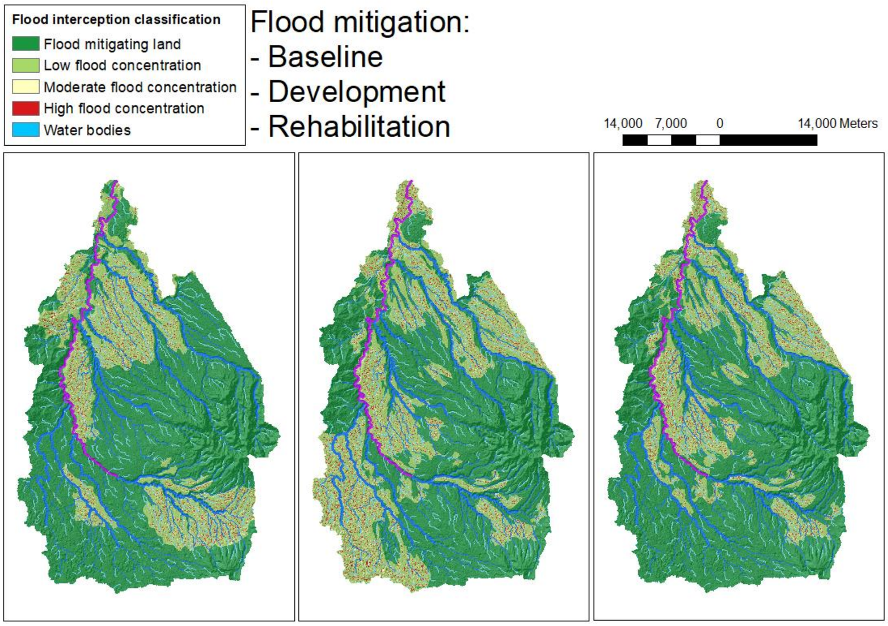

Figure 51. Flood mitigation maps at the catchment scale for baseline (left), development (centre), and rehabilitation (right) using the Philippine-based parameterisation.

Table 18. Flood interception classification percentages for the different scenarios for the Philippine-based parameterisation.

Description	Philippine-based Parameterisation		
	Baseline (%)	Development (%)	Rehabilitation (%)
Flood Mitigating Land	69	58	69
Negligible Flood Concentration	23	32	23
Moderate Flood Concentration	3	4	3
High Flood Concentration	2	3	2
Water Bodies	3	3	3

At the finer scale (Figure 52 and Figure 53), the areas classified as agriculture have areas of moderate and high flood concentration that are in very close proximity to streams. These results suggest the possible target areas for mitigation should be riverbanks or steep slopes that cause more water to be diverted towards the streams more quickly. In the plan for development, one of the recommendations is to use bamboo as stabilising vegetation for riverbanks and valley slopes, which agrees with the results suggested by LUCI. Such riparian planting has a reducing effect on the peak discharges of floods and subsequent inundation due to the capacity of that landscape to absorb and intercept water prior to entering the stream network (Barth & Döll, 2016). There is also a relatively large area of moderate and high flood concentration at the southern section of the current agricultural extent that could be targeted for flood mitigation (Figure 52).

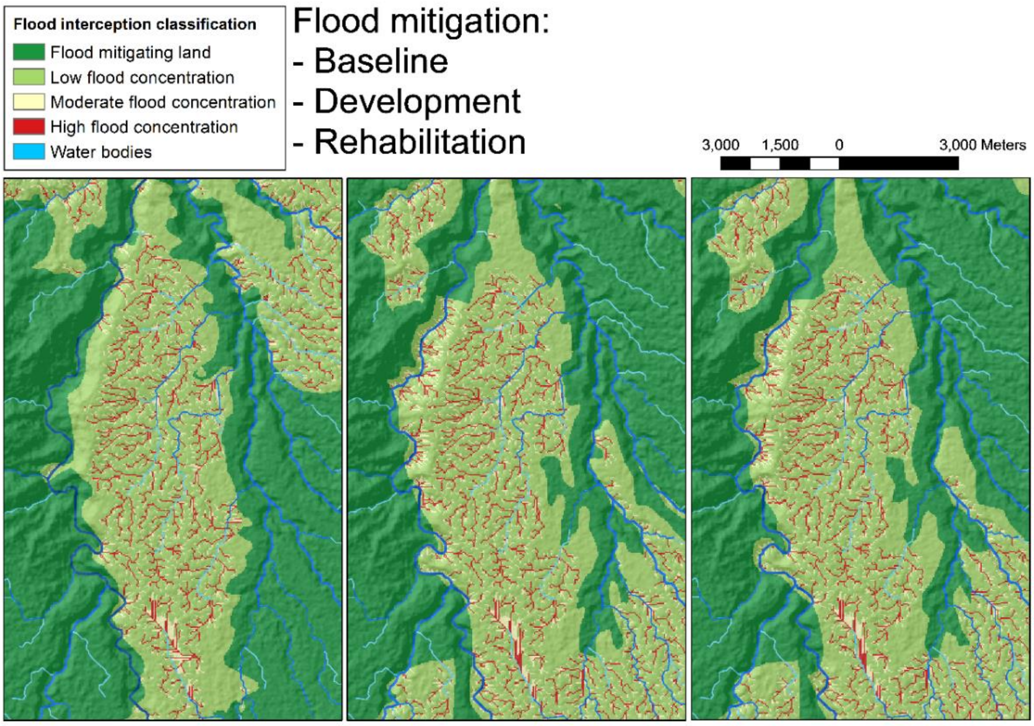

Figure 52. Zoomed-in map of area defined as agriculture for baseline (left), development (centre), and rehabilitation (right).

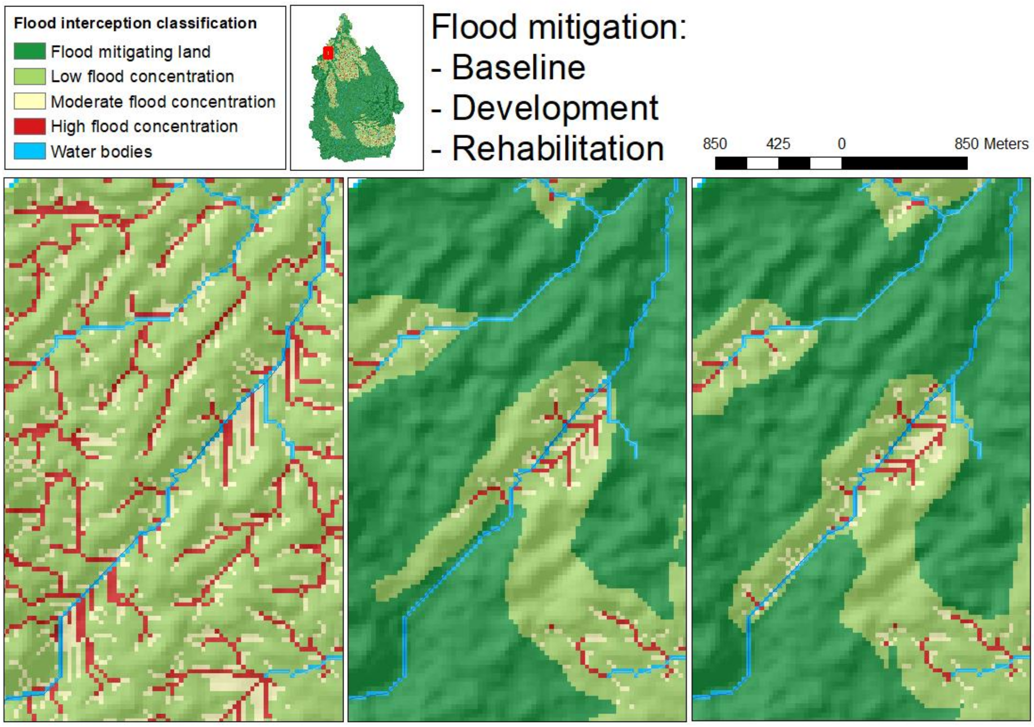

Figure 53. Zoomed-in map of areas classified as agriculture and in close proximity to streams for baseline (left), development (centre), and rehabilitation (right).

The results of the LUCI application to CDO have broadly identified the forested areas as flood mitigating land, requiring protection or monitoring to prevent degradation of that ecosystem service, and agricultural areas as having low flood concentration. Within the latter, mitigation efforts are directed towards areas near streams, suggesting riparian planting efforts or bank rehabilitation. This identification of areas to conserve or rehabilitate is important to the broader context of mapping ecosystem services in CDO and in the Philippines. Through ecosystem services mapping, large areas for protection can be identified. Another possible component of mapping is to map the demand for ecosystem services to understand how a service can change as it moves through the landscape and the demands of the end-user are being met (Bagstad et al., 2014). In terms of flood mitigation, the "demand" is either the reduction of flow during periods of extreme events or the maintenance of flow needed to support agricultural activities, anthropogenic usage, and biological needs. This thesis touched on the reduction of flow during extreme events, but future applications can also consider flow maintenance or water supply as a potential ecosystem service. The benefits of an ecosystem service is more clearly understood in terms of supply, demand, and their spatial interactions with the landscape (Stürck et al., 2014). This application of LUCI to CDO identified areas of flood mitigation (supply), areas that require flood mitigation (partial demand), and was spatially explicit in mapping the ES of flood mitigation. Under the baseline scenario, these maps are good indicators of areas with high existing ES provision and potential areas to improve that provision. Through running the development and rehabilitation scenarios, these maps can show the potential improvements or consequences before any large-scale management interventions are carried out.

3.3.3 Results of New Zealand-based parameterisation

The purpose of the New Zealand-based parameterisation was to test differences between the new Philippine-based parameterisation of LUCI (presented in this chapter) and the already existing New Zealand-based parameterisation that has been coded into the LUCI model. One thing to keep in mind is that the climate regimes and vegetation types differ between New Zealand and Philippines, thus future work requires more detailed parameterisation for the conditions specific to the Philippines and more broadly for tropical areas. This section summarises the results of the following tools: flood mitigation, agricultural productivity, nitrogen loading, and phosphorus loading.

At the catchment scale, the areas identified as low flood concentration are those classified as short-rotation cropland, built-up areas, and high-producing exotic grassland. The differences between the scenarios are clearer compared to the watershed scale, with the development scenario having more areas of flood mitigating land compared to the baseline and rehabilitation scenario (Figure 54). The tabular information confirms this, showing that the development scenario has the highest proportion of flood mitigating land among all the three scenarios, and the rehabilitation scenario having the lowest (Table 19). This is because some of the agricultural areas in the development scenario are recommended for agroforestry and classified in the NZ land cover as orchards and vineyards, thus contributing to their flood mitigating capacity. This shows that a more detailed parameterisation for the Philippines, to account for several types of land management practices, extends LUCI's utility and can make the differences in scenarios clearer. For example, management may choose to zone one area as forestry but has different potential plans of support practices (e.g. intercropping or contour cropping) and adding a support practice layer to LUCI's modelling can help in that decision-making. At a finer spatial scale (Figure 55), the areas identified as possible targets for mitigation are like the areas identified in the Philippine-based parameterisation. The areas that are near the streams are potential target areas, underscoring the importance of riparian planting and streambank restoration in flood mitigation strategies.

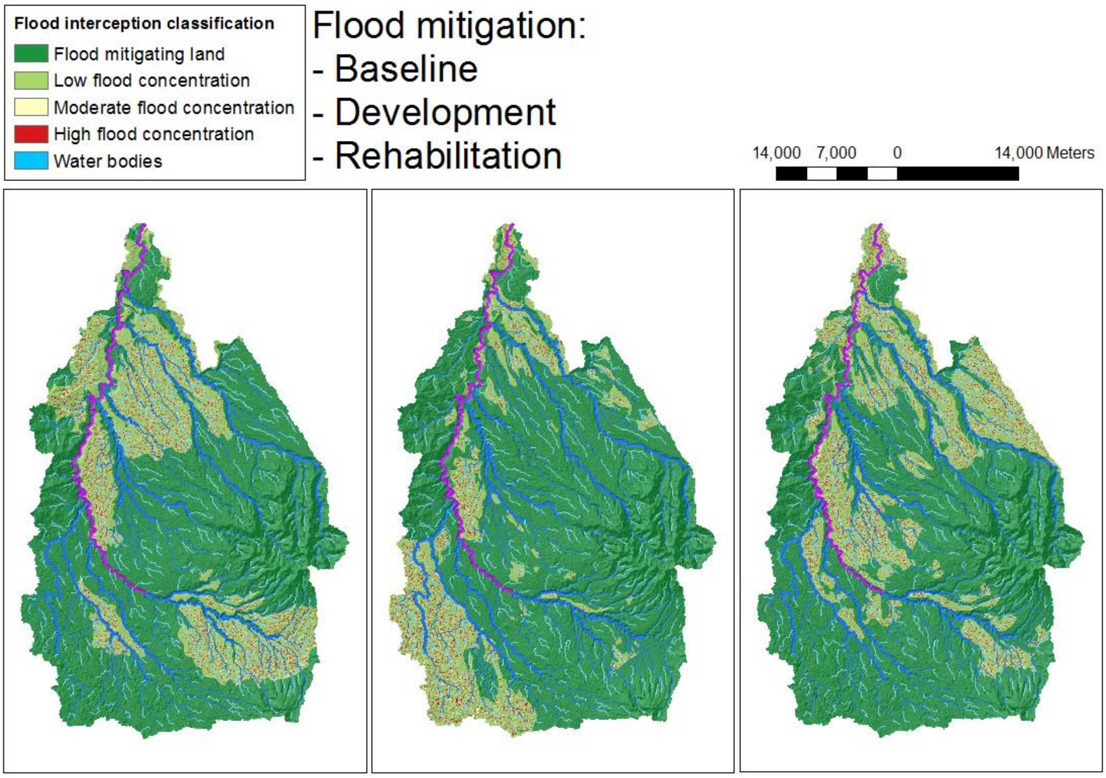

Figure 54. Flood mitigation maps at the catchment scale for baseline (left), development (centre), and rehabilitation (right) using the New Zealand-based parameterisation

Table 19. Flood interception classification percentages for the different scenarios for the New Zealand-based parameterisation.

Description	New Zealand-based Parameterisation		
	Baseline (%)	Development (%)	Rehabilitation (%)
Flood Mitigating Land	70	76	69
Negligible Flood Concentration	23	17	23
Moderate Flood Concentration	2	2	3
High Flood Concentration	2	2	2
Water Bodies	3	3	3

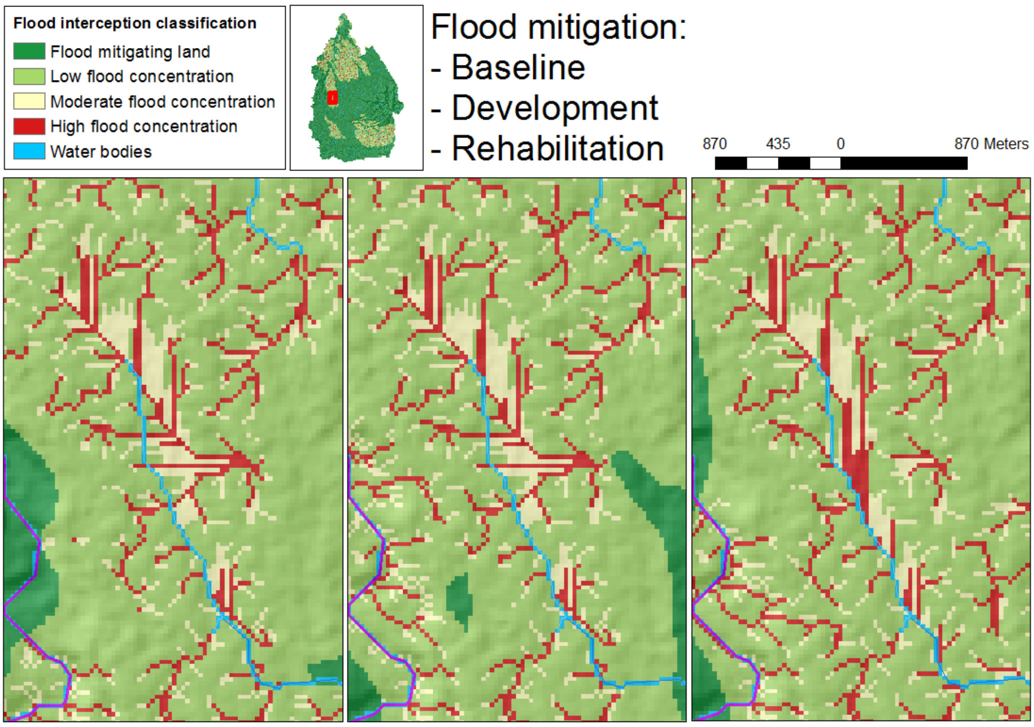

Figure 55. Zoomed in map showing the proximity of priority areas to streams for baseline (left), development (centre), and rehabilitation (right).

The agricultural productivity tool uses information about slope, aspect, hydrology (e.g. freely draining or waterlogged) and fertility to determine the agricultural value of the landscape (Jackson et al., 2013). Since the majority of the CDO catchment is utilised for agriculture, applying the agricultural productivity tool was useful to check the optimal usage between the three land cover scenarios. The rules around agricultural productivity were based on consultation with farmers and rural industries in temperate upland regions, and future work would include consultation with farmers located in tropical areas that may have different farming practices. The agricultural utilisation status delineates the areas receiving optimum and near-optimum utilisation that are being used appropriately while the non-optimum utilisation and production potential not realised are the areas that may require more management interventions before becoming more productive land (Jackson et al., 2013). Across all three scenarios, the red areas of production potential are the steeper areas associated with streams and river valleys (Figure 56). The development and rehabilitation scenarios differ mainly in the area at the southern area of the catchment, which was classified as agricultural land in the development scenario and as reforestation area in the rehabilitation scenario. According to LUCI, utilising this area for agriculture in the development scenario would require management interventions to achieve optimum utilisation compared to the rehabilitation scenario. Future work in the Philippines can include parameterisation for the management practices associated with steep slopes (e.g. terracing) that is common in the Philippines to test if this agricultural practice can potentially improve productivity.

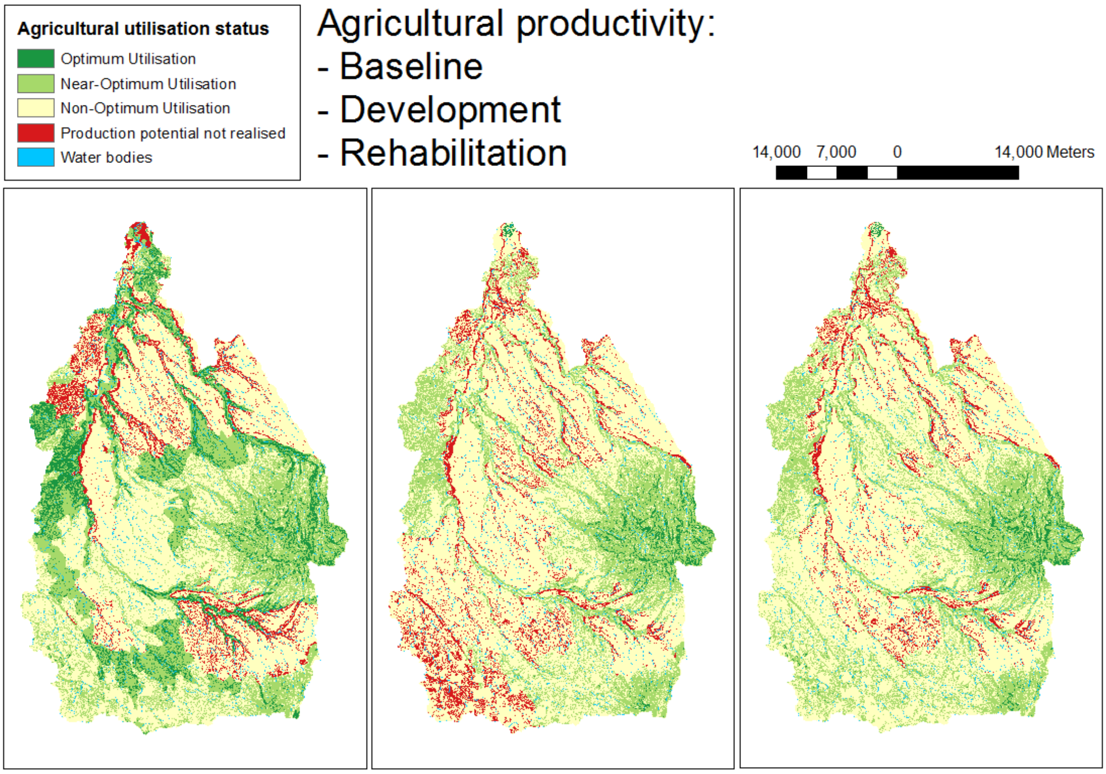

Figure 56. The agricultural utilisation status maps in the baseline (left), development (centre), and rehabilitation (right) scenarios.

Both the nitrogen and phosphorus tools utilise the export coefficient approach to predict the potential loads from different combinations of land use, fertiliser application, livestock, other nutrient inputs, soil type, and geology (Johnes, 1996). These export coefficients are reported in the literature based on reviews and field experiments and influence the potential nitrogen or phosphorus exported at each grid cell, and LUCI uses its hydrological routing functions to determine the flow from source cell to streams (Jackson et al., 2013). The export coefficients used for this modelling run were based on New Zealand, and future work around compiling export coefficients for the Philippines and tropical areas is crucial for broadening LUCI applicability. Nitrogen and phosphorus loads are affected by changes in fertiliser input (e.g. decreases for compliance to standards) or conversions of land cover (e.g.

agriculture to grassland) (Johnes, 1996). Through understanding which areas have the potential to produce the highest nitrogen and phosphorus loads, management interventions can be carried out in those areas to benefit the resulting water quality. Across all three scenarios, the areas with the highest potential nitrogen loads are those associated with grassland or agricultural activity while the lowest nitrogen loads are associated with forested areas (Figure 57). With standardised symbology (Figure 58), the differences in maximum potential nitrogen load between the baseline and the other two scenarios are clearer. The agricultural management interventions of agroforestry and forest restoration efforts led to lower nitrogen loads in areas that were formerly using standard agricultural practices and grassland.

In terms of statistics, the baseline scenario had the highest minimum, maximum, and mean nitrogen load of all the scenarios, while the development and rehabilitation scenarios had similar values of nitrogen load (Table 20). The average of nitrogen loads from tropical catchments is ~3.10 kg ha^{-1} yr^{-1} (Saunders & Lewis, 1988). The mean nitrogen load in the baseline exceeds this value, while the development and rehabilitation values are similar or lower compared to this value.

Table 20. Minimum, maximum, and mean values for nitrogen load (kg ha^{-1} yr^{-1}) for the three land cover scenarios.

Scenario	Nitrogen load (kg ha^{-1} yr^{-1})		
	Minimum	**Maximum**	**Mean**
Baseline	0.95	15.3	4.29
Development	0.82	7.41	3.32
Rehabilitation	0.76	7.41	2.89

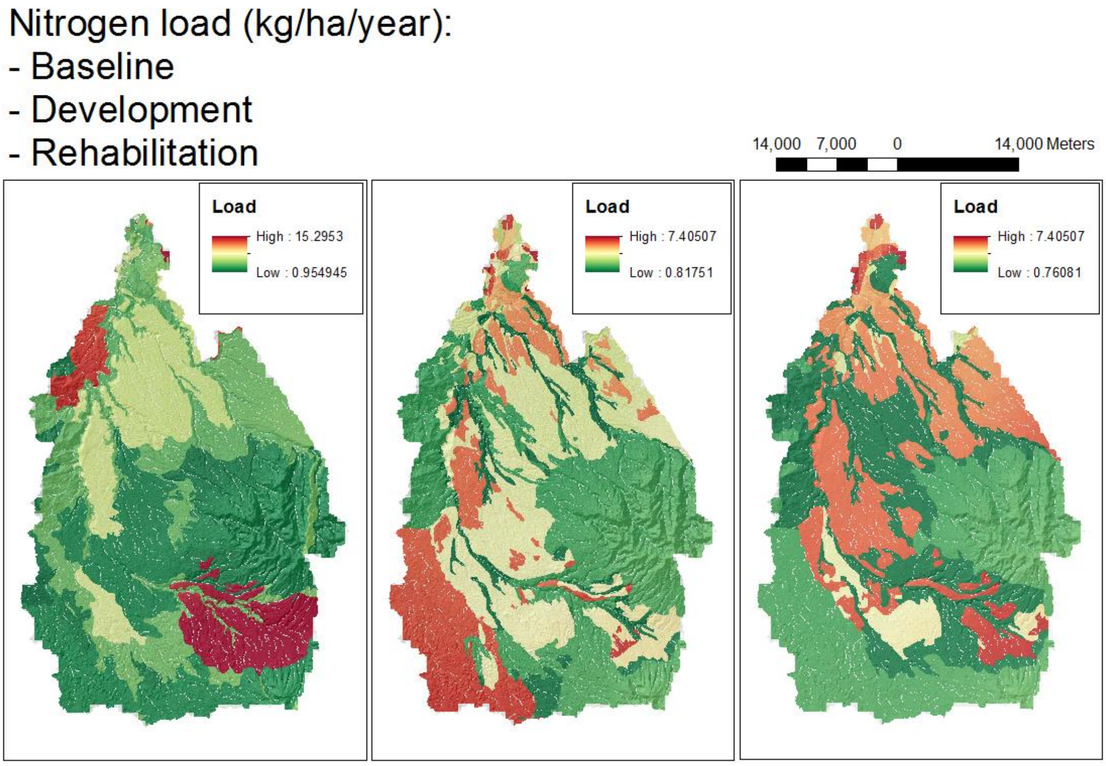

Figure 57. Nitrogen load (kg ha^{-1} yr^{-1}) for baseline (left), development (center), and rehabilitation (right) scenarios with individual symbology.

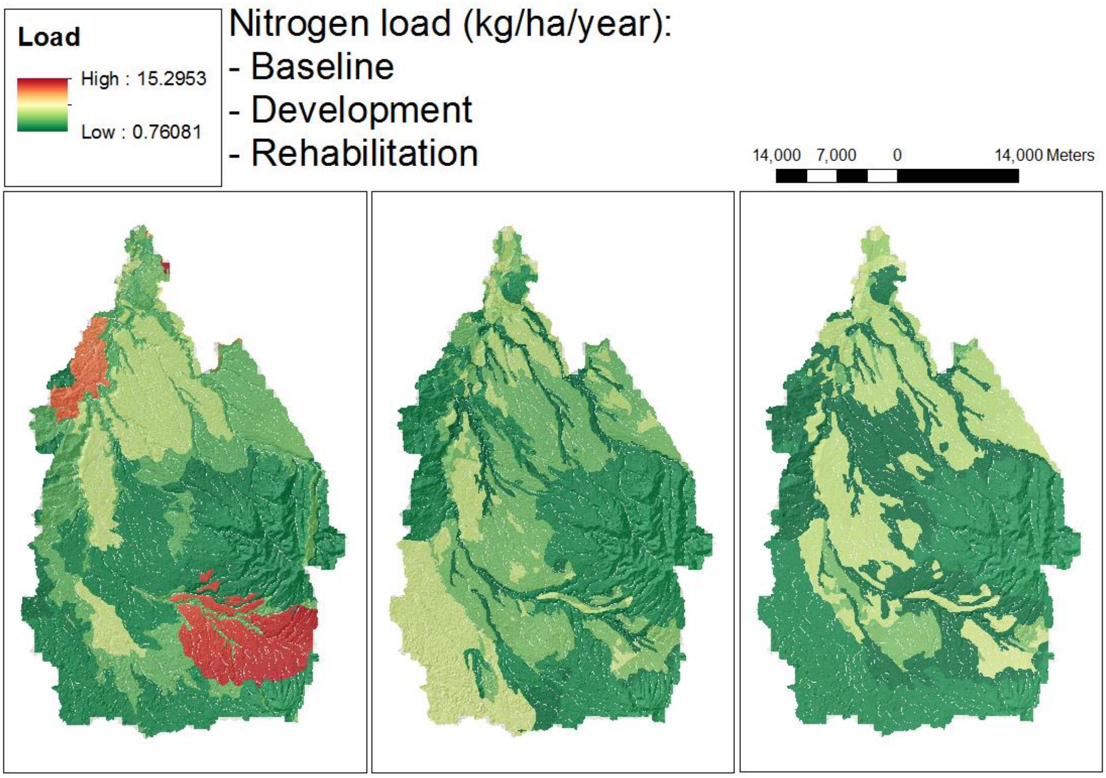

Figure 58. Nitrogen load (kg ha^{-1} yr^{-1}) for baseline (left), development (center), and rehabilitation (right) scenarios with symbology standardised across scenarios.

Some of the phosphorus tool results are similar to the nitrogen tool output, in that the baseline scenario produced the highest minimum, maximum, and mean phosphorus load values (Table 21). However, the development scenario had the lowest phosphorus loads while the rehabilitation scenario that had the lowest nitrogen loads, instead of one scenario having the lowest loads for both elements. This is due to the difference in the mechanisms of nitrogen and phosphorus transport. Although both are affected by landscape characteristics, nitrogen is more commonly associated with organic material and affected by runoff while phosphorus is more commonly associated with mineral material and is less mobile (Saunders & Lewis, 1988). The agroforestry interventions in the development scenario affected phosphorus loads more than the interventions in the rehabilitation scenario. One reason for this is the current parameterisation does not include detailed information about soil conservation measures recommended by CESM (2014) and future work around the Philippine-based parameterisation will include such measures to test their effectiveness in reducing nutrient loads. The average phosphorus loads from tropical catchments is reported as 1,850 g ha^{-1} yr^{-1} (Saunders & Lewis, 1988). The modelled phosphorus results fall below this average, but since phosphorus is associated with mineral materials, future work will include parameterisation for rock types in the Philippines to test the difference in results compared to this New Zealand-based parameterisation

Table 21. Minimum, maximum, and mean values for phosphorus load (g ha^{-1} yr^{-1}) for the three land cover scenarios.

Scenario	Phosphorus load (g ha^{-1} yr^{-1})		
	Minimum	**Maximum**	**Mean**
Baseline	19.38	959	386
Development	8.31	958	276
Rehabilitation	19.38	954	345

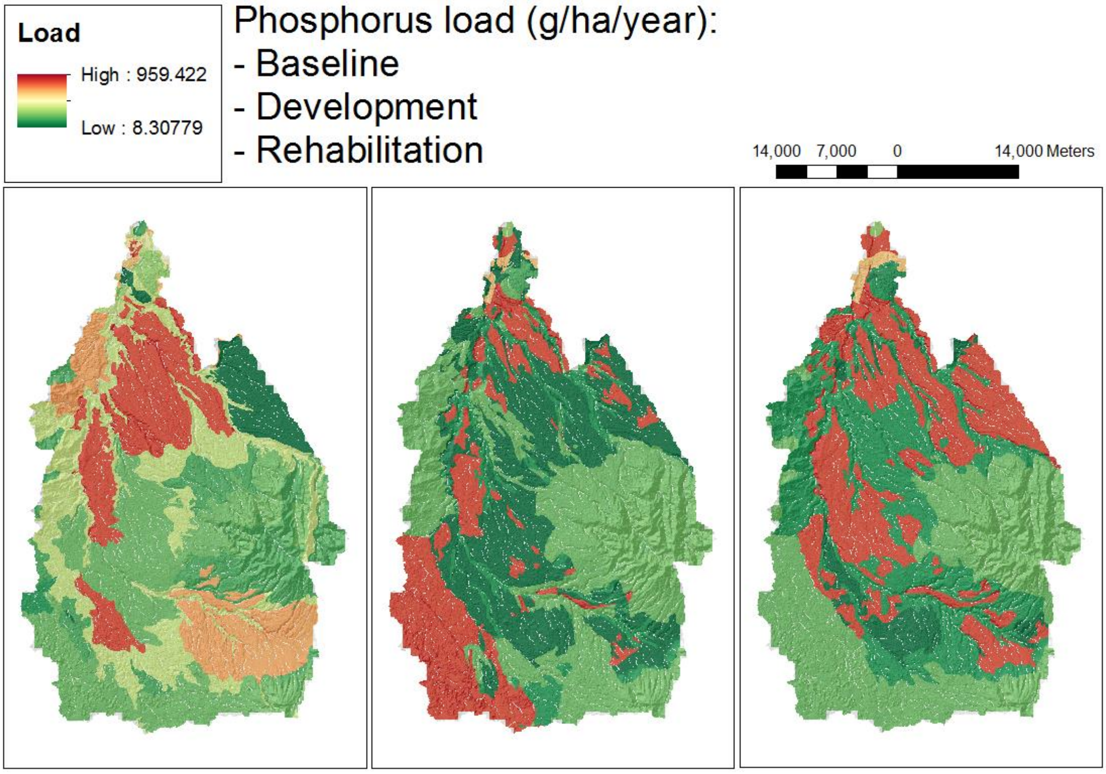

Figure 59. Phosphorus load (g ha^{-1} yr^{-1}) for baseline (left), development (center), and rehabilitation (right) scenarios with symbology standardised across scenarios.

3.3.4 Comparison of Philippine-based and New Zealand-based parameterisation

The differences between the Philippine-based and New Zealand-based parameterisation were briefly mentioned in the previous section but are discussed further here by comparing the flood mitigation maps by scenario. For the baseline scenario, the flood interception classification is almost the same, apart from one small area near the outlet of the catchment (Figure 60). In the Philippine-based parameterisation, that area is classified as an agricultural area with perennial crops, while the NZ-based parameterisation has included it in the “orchards, vineyards, or other perennial crops” land cover classification. This small difference can be seen in the catchment-scale flood interception classification where the values differ by 1% (Table 22). The development scenario is where the two parameterisation sets produce different results (Figure 61). The New Zealand-based parameterisation has a higher proportion of flood mitigating land, which was explained in Chapter 2, due to that area being classified as “orchards, vineyards, or other perennial crops”. In the original scenario, this area is zoned as “Agricultural Sub-zone 3” where orchards and agroforestry were recommended; the New Zealand-based parameterisation is unable to fully account for that difference in land management. In the rehabilitation scenario, the spatial results and the tabular results are the same (Figure 62). In the original rehabilitation scenario, the different zones have accompanying land management strategies. Accounting for these within LUCI would help capture some of the complex interactions between rainfall, soil, land use, and support practices.

Table 22. Flood interception classification for all scenarios for both parameterisation sets.

Description	Baseline (%)		Development (%)		Rehabilitation (%)	
	PH	NZ	PH	NZ	PH	NZ
Flood Mitigating Land	69	70	58	76	69	69
Negligible Flood Concentration	23	23	32	17	23	23
Moderate Flood Concentration	3	2	4	2	3	3
High Flood Concentration	2	2	3	2	2	2
Water Bodies	3	3	3	3	3	3

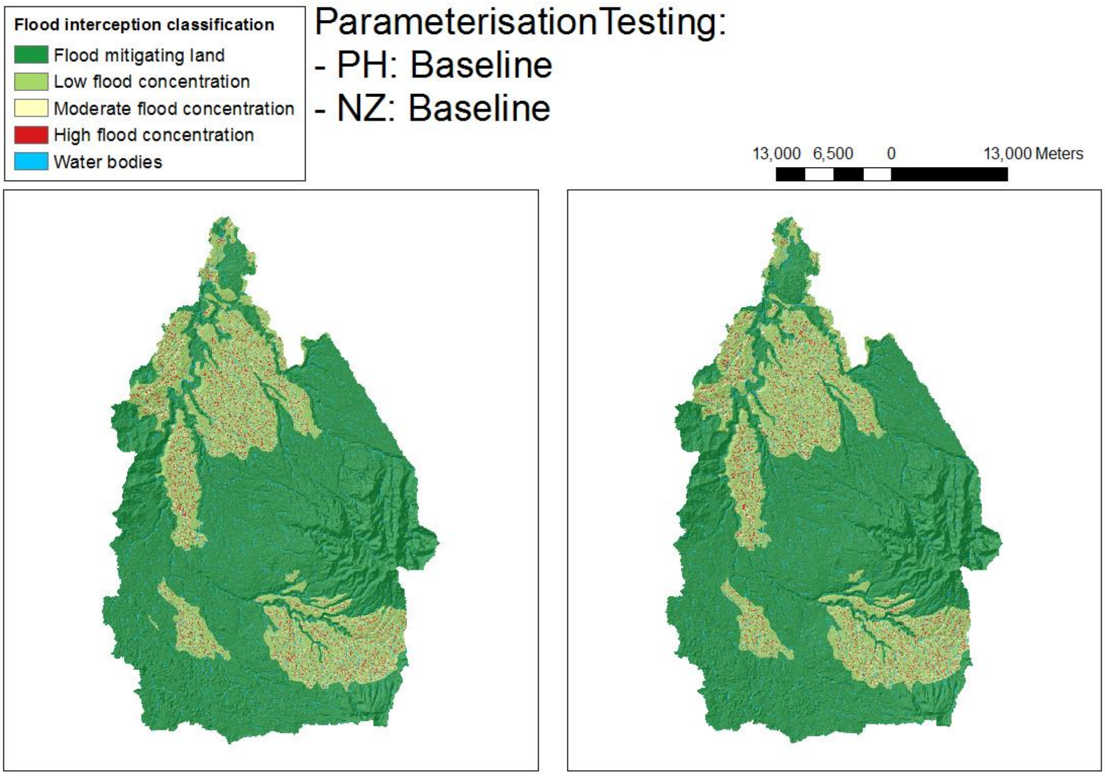

Figure 60. Flood mitigation maps at the catchment scale for the baseline scenario using the Philippine (left) and New Zealand (right) parameterisations.

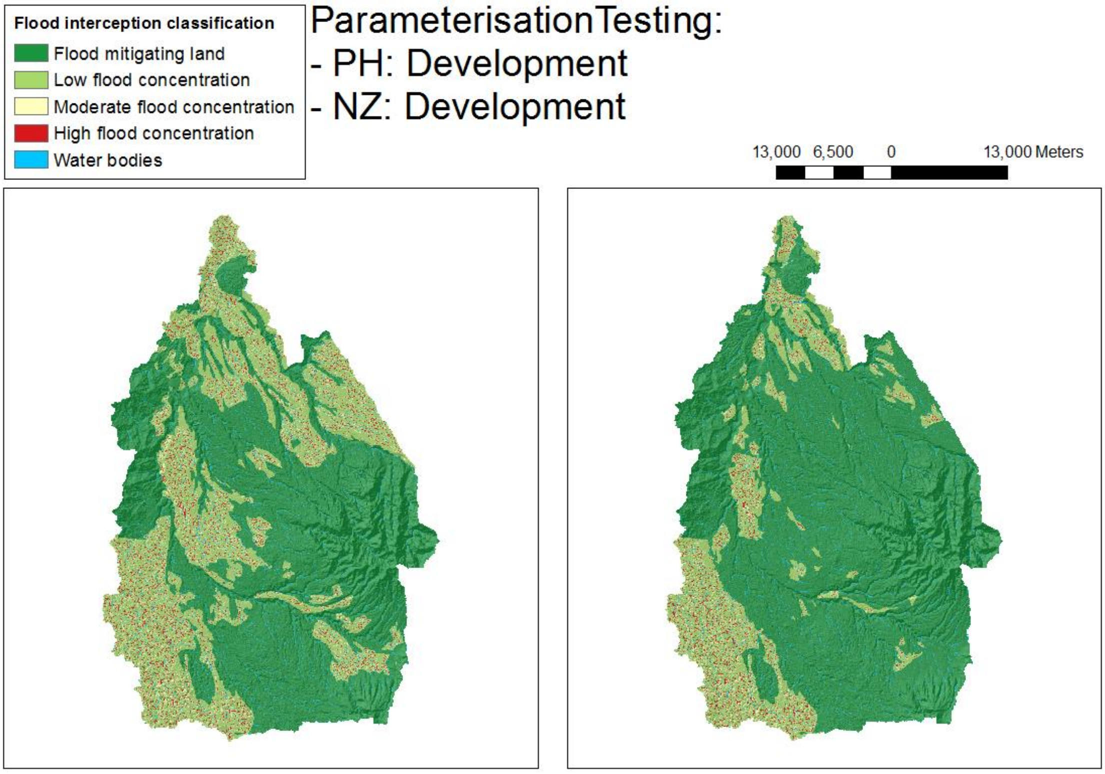

Figure 61. Flood mitigation maps at the catchment scale for the development scenario using the Philippine (left) and New Zealand (right) parameterisations.

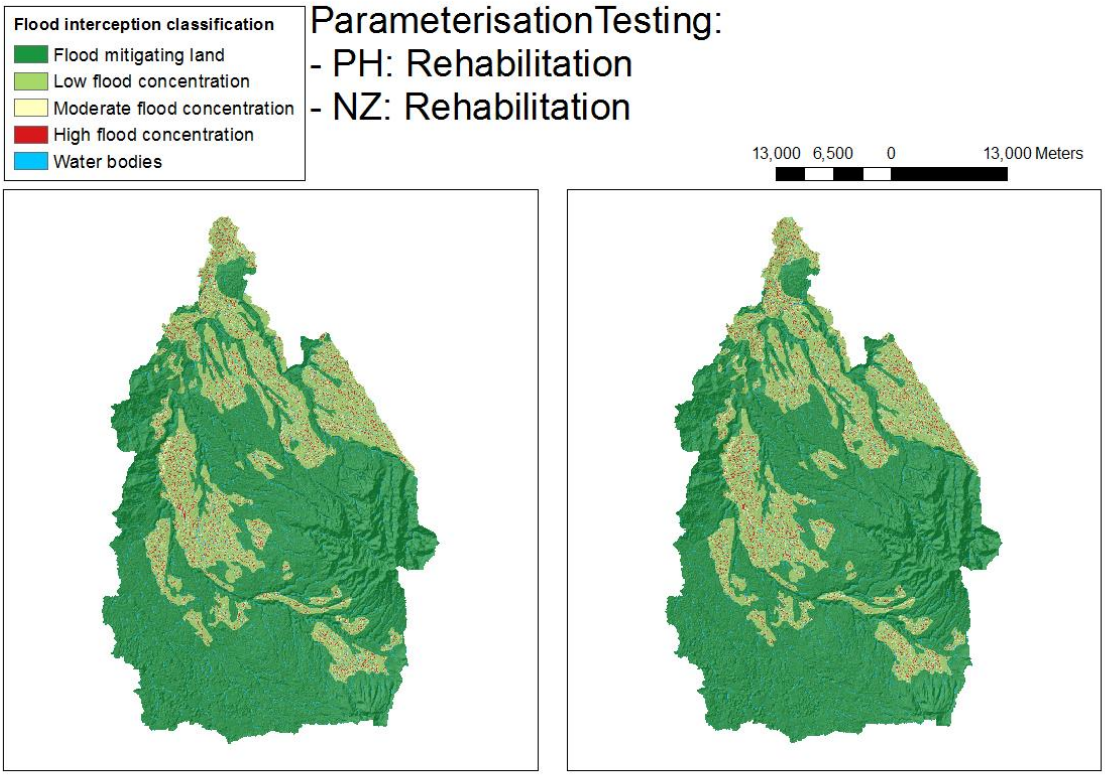

Figure 62. Flood mitigation maps at the catchment scale for the rehabilitation scenario using the Philippine (left) and New Zealand (right) parameterisations.

With more data relating to specific agricultural practices and fertiliser applications in the Philippines, the agricultural productivity, nitrogen delivery, and phosphorus delivery tools can be re-run for CDO and compared to the results of the New Zealand-based parameterisation. This will show how detailed parameterisation sets from different climatic regions can affect the modelled ecosystem services of the same study area. In other study areas where LUCI has not yet been applied, two options for parameterisation are presented. The user can utilise the correlation parameterisation, like the Philippine-based parameterisation undertaken in this study, with information about the types of agricultural practices, crops, and vegetation in the study area. In an area with less information about their agricultural practices and vegetation, but with general descriptions of the land cover classes, a technique like the New Zealand-based parameterisation can be applied.

3.4 Future work

The future work of flood mitigation in the CDO watershed include improvements in representing the vegetation and the different agricultural and management practices included in the current management plans. Work has already been achieved compiling the possible crops and trees present within CDO, their physical characteristics and water needs, which will be replacing the classification-based parameterisation in future versions of LUCI. This more detailed parameterisation can also represent changing characteristics with growth. In the rehabilitation scenario, areas are marked for reforestation and having a crop growth model would be useful to model changes in flood mitigation provision at distinct stages of restoration. Since different tree species have different characteristics and water use, an economic valuation component could be added that uses cost-benefit analysis to determine the suitable trees to be planted for a particular landscape (Camacho et al., 2007). Inclusion of planned management practices could refine the ecosystem services maps with broad classifications such as agroforestry or more specific classifications that include the type of stabilising vegetation that will be planted (e.g. bamboo on riverbanks). Parameterising for riparian planting in the Philippines is important as this has the potential to mitigate floods, erosion, and nutrient delivery. Aside from vegetation, assembling a database of export coefficients specific to tropical areas and the

Philippines improves the nitrogen and phosphorus tools' applicability in tropical catchments. Through creating a more robust parameterisation dataset for the CDO catchment, the LUCI framework is more applicable to other areas of the Philippines and to broader tropical areas.

This chapter included some sensitivity testing on the DEM reconditioning, but those parameters will vary between catchments and more extensive testing is needed to compare the generated stream network with the actual stream network. The sensitivity testing can also go further into the flood mitigation modelling to understand how much the flood mitigation results can vary between different parameters used for DEM reconditioning. Going further than mapping potential supply, it is important to quantify the demand or value of a particular ecosystem service (Bagstad et al., 2014). In terms of disaster risk reduction for urban systems, the "value" of flood mitigation can be estimated from the avoided costs of infrastructural damage under different extreme events and land cover scenarios (Pappalardo et al., 2017).

Lastly, it is important to do more engagement with the local stakeholders, such as government units and local indigenous communities. This social aspect of ecosystem services mapping helps elucidate how the community itself perceives ecosystem services to know which service to prioritise, to share knowledge gained from modelling and local expert knowledge, and feed into more participatory decision-making in the future.

3.5 Summary and conclusion

The main aims of this chapter were to apply the LUCI model to the CDO catchment to identify the areas that are already providing flood mitigating services and the areas that can be targeted for management strategies through different land cover scenarios. Both those aims were achieved through running the flood mitigation tool in LUCI for the CDO under the three different land cover scenarios, and more ecosystem services maps were also produced for agricultural productivity, nitrogen delivery, and phosphorus delivery. The areas providing flood mitigating services are the forested areas such as the national parks, agroforestry areas, and areas planned for restoration. This supports the efforts of protecting and monitoring these areas, as deforestation or illegal logging would lead to a degradation in the flood mitigating services provided by the landscape. The areas that are classified as possible targets for mitigation are those areas within the agricultural lands that were close to the streams, suggesting restoration measures such as riparian planting and streambank stabilisation, would be beneficial for flood mitigation. Based on the results, forested areas can provide the most flood mitigation benefits, underscoring the importance of rehabilitation activities within the CDO catchment.

The New Zealand-based parameterisation was useful in testing additional ecosystem services available in LUCI: agricultural productivity, nitrogen loads, and phosphorus loads. The agricultural productivity tool delineated areas that are being underutilised and can be targeted to improve agricultural yields. These areas were steep slopes associated with streams and future work that parameterises for upland agricultural practices in the Philippines is needed. The nitrogen and phosphorus tools showed a decrease in both nutrient loads under the development and rehabilitation scenario, suggesting that conservation farming (e.g. agroforestry) and reforestation has the potential to improve water quality in the CDO catchment. In future LUCI applications, specific land cover and soil characteristics may be unavailable and thus correlation to the detailed NZ classification is an option to set up LUCI for an area of interest.

Some of the key future directions of this research are: more detailed land cover parameterisation, ecosystem services modelling for other services within LUCI, adding an economic valuation component, and more engagement with local stakeholders. A database of detailed land cover and vegetation characteristics was compiled for this research that will be used in future versions of LUCI that can account for different stages of growth and water use characteristics. An extensive literature review of export coefficients in the Philippines and tropical catchments can be carried out to construct an export coefficient database for similar areas that will be used as input to the nitrogen and phosphorus tools. Through a more detailed parameterisation, the other ecosystem service models within LUCI can be run for the CDO catchment and compared with the New Zealand-based parameterisation. By running LUCI for multiple ecosystem services, trade-offs and synergies can be identified. These trade-offs aid the economic valuation in cost-benefit analysis and larger-scale planning where logistical limitations such as funding must be considered for management interventions. Through engaging the local community, LUCI can be used in more participatory decision-making.

This first application of LUCI for CDO lays the groundwork for future applications within the Philippines, especially as the database of Philippine-specific land cover and soil grows and is implemented into future LUCI versions. At the broader scale, this application can serve as a guide for future study areas in countries where LUCI has never been applied, especially in other tropical areas.

4 A review of the (Revised) Universal Soil Loss Equation (R/USLE): with a view to increasing its global applicability and improving soil loss estimates

4.1 Introduction

Soil erosion involves many processes but one effect is particles being transported and deposited from one location to another. Although it occurs naturally, it is often exacerbated by anthropogenic activities (Adornado et al., 2009). Soil erosion is affected by wind, rainfall and associated runoff processes, vulnerability of soil to erosion, and the characteristics of land cover and management (Aksoy & Kavvas, 2005; Bagherzadeh, 2014; Panagos et al., 2015c). Managing and understanding erosion and associated degradation is critical because of its possible effects: nutrient loss, river and reservoir siltation, water quality degradation, and decreases in soil productivity (Bagherzadeh, 2014). Pimentel et al. (1995) reported soil erosion rates for regions around the world: Asia, South America, and Africa with an average of 30 to 40 ton ha^{-1} yr^{-1} and an average of 17 ton ha^{-1} yr^{-1} for the United States of America and Europe. For comparison, the soil erosion rate for undisturbed forests was reported to range from 0.004 ton ha^{-1} yr^{-1} to 0.05 ton ha^{-1} yr^{-1} globally (Pimentel et al., 1995). Within a landscape, erosion due to water can be caused by unconcentrated flow (sheet), flow within small channels (rills), raindrop impact and overland flow (inter-rill), and larger channels of concentrated flow (gullies) (Aksoy & Kavvas, 2005; Morgan, 2005). Land management can be improved through understanding how these erosion processes occur and what areas are vulnerable to soil loss. Advances in technology such as the development of soil erosion models and increases in computing power for spatial analysis have assisted in making this process faster and more accurate.

Soil erosion models aid land management by helping understand sediment transport and its effects on a landscape. They range from relatively simple empirical models, and conceptual models, to more complicated physics-based models (Merritt et al., 2003). Extensive reviews of soil erosion models of varying complexity have been done before, but tend to focus on input requirements and applications (Aksoy & Kavvas, 2005; Merritt et al., 2003). A review by de Vente & Posen (2005) differs by focusing on semi-quantitative models that include several types of soil erosion to estimate basin sediment yield. Other reviews have focused on the use of several soil erosion models applied to one geographic area, such as Brazilian watersheds for de Mello et al. (2016).

One family of empirical soil loss models is the Universal Soil Loss Equation (USLE) models including the original USLE, the Revised Universal Soil Loss Equation (RUSLE), the Revised Universal Soil Loss Equation version 2 (RUSLE2), and the Modified Universal Soil Loss Equation (MUSLE). The USLE is an empirical model used to estimate the average rate of soil erosion (tons per unit area) for a given combination of crop system, management practice, soil type, rainfall pattern, and topography. It was originally developed at the plot-scale for agricultural plots in the United States of America (Wischmeier & Smith, 1978). An updated form of USLE (RUSLE) was published to include new rainfall erosivity maps for the United States of America and improvements to the method of calculating the different USLE factors (Renard et al., 1997). RUSLE accounted for changes in soil erodibility due to freeze-thaw and soil moisture, a method for calculating cover and management factors, changes to how the influence of topography is incorporated into the model, and updated values for conservation practices (Renard & Freimund, 1994). The RUSLE2 framework is a computer interface to handle more complex field situations, including an updated database of factors (Foster et al., 2003). These three variations of R/USLE measure soil loss per unit area at an annual time scale, but the MUSLE uses runoff and peak flow rate to estimate event-based soil loss (Sadeghi et al., 2014). These models have been used around the world due to their relative simplicity and seemingly low data requirements (Appendix 1).

This simplicity of the R/USLE has been integrated into more complex soil erosion models to help with management and decision-making, including the Agricultural Non-Point Source model (AGNPS), the Chemical Runoff and Erosion from Agricultural Management Systems model (CREAMS), and the Sediment River Network model (SedNet) (Aksoy & Kavvas, 2005; de Vente & Poesen, 2005; Merritt et al., 2003). The AGNPS estimates upland erosion using the USLE and then uses sediment transport algorithms to simulate runoff, sediment and nutrient transport within watersheds (Aksoy & Kavvas, 2005). The usage of RUSLE in large models is mainly for the purpose of assisting with decision-making, such as prioritising land use objectives in the Philippines (Bantayan & Bishop, 1998), scenario analysis for water quality in catchments in New Zealand (Rodda et al., 2001), or delineating unique soil landscapes in Australia (X. Yang et al., 2007).

This review addresses the complexity of the different factors, and the issues for researchers to consider before applying R/USLE to their study area. These issues range from equation choices, DEM resolution, granularity in land cover characteristics, scale, etc. The MUSLE is not included in this review because Sadeghi et al. (2014) have already done an extensive review of the model and event-scale estimates are beyond the scope of this paper. Annual estimates of soil loss are useful for understanding the baseline erosion in a catchment, but intra-annual and event-based soil loss estimates are useful to elucidate temporal variations in erosion. The seasonal estimation of soil loss is discussed in Section 4.4.2 and in the two case studies (Chapter 5 and 6). Performing event-based soil loss modelling is important for areas that frequently experience extreme events as these can cause large-scale sediment transport and mass wasting. Future work will include improvements to seasonal soil loss modelling and application of the MUSLE to CDO to understand the catchment's issues of event-based sedimentation.

The main aim of this chapter is to review the (Revised) Universal Soil Loss Equation through the following objectives:

- Review the USLE and RUSLE literature to compile equations for the different sub-factors within the R/USLE;
- Provide guidance as to which datasets and equations are appropriate over a range of geoclimatic regions with varying levels of data availability;
- Outline the limitations and caveats of the R/USLE that future users must consider; and
- Outline potential future directions to overcome these limitations and to improve R/USLE applications

This chapter discusses the influences on the subsequent applications in CDO (Chapter 5) and the Mangatarere catchment in New Zealand (Chapter 6). These chapters tested different equations for R/USLE subfactors and produced output maps showing the differences in soil loss estimates. Although this work is primarly concerned with increasing LUCI applicability in tropical environments, specifically the Philippines, the Mangatarere application was carried out due to the availability of high-resolution DEMs (15m and 5m) and daily rainfall data that allowed for further testing of RUSLE factor equations.

4.2 Universal Soil Loss Equation (USLE)

The principal equation for the USLE model family is below:

$$A = R \times K \times L \times S \times C \times P$$

Where:

A	Mean annual soil loss (metric tons hectare^{-1} year^{-1})
R	Rainfall and runoff factor or rainfall erosivity factor (megajoules millimetre hectare^{-1} hour^{-1} year^{-1})
K[7]	Soil erodibility factor (metric tons hour megajoules^{-1} millimetre^{-1})
L	Slope-length factor (unitless)
S	Slope-steepness factor (unitless)
C	Cover and management factor (unitless)
P	Support practice factor (unitless)

The USLE was originally developed at the farm-plot scale for agricultural land in the United States of America, but has seen use in many other countries, scales, and geoclimatic regions. In the original development of the model, this farm plot is called the "unit plot" and is defined as a plot that is 22.1m long, 1.83m wide, and has a slope of 9% (Wischmeier & Smith, 1978). Although the model accounts for rill and inter-rill erosion, it does not account for soil loss from gullies or mass wasting events such as landslides (Thorne et al., 1985). The appendix of this dissertation compiles a non-exhaustive list of studies that have applied the USLE and RUSLE models to watersheds around the world. The uncertainties in soil erosion modelling stem from the availability of long-term reliable data, which includes issues of temporal resolution (e.g. <30-minute resolution required for R/USLE) and the availability of spatial data over a catchment. This issue is not unique to R/USLE applications and is more pressing

[7] The RUSLE handbook by Renard et al. (1997) indicates that the K-factor metric units are metric tons hectare hour megajoules^{-1} hectare^{-1} millimetre^{-1}, but for mathematical correctness, the hectare units cancel out.

for more complex models that have a large amount of variables that require detailed data (de Vente & Poesen, 2005; Hernandez et al., 2012). Hence, the ubiquitous usage of the R/USLE can be attributed to its relatively low data requirements compared to more complex soil loss models, making it potentially easier to apply in areas with scarce data. Another limitation of the R/USLE and arguably many erosion model applications is the lack of validation data to verify model outputs, which is discussed further in Section 4.3.

Although the application of the R/USLE seems to be a simple linear equation at first glance, this review addresses the complex equations that go into calculating its factors, such as rainfall erosivity which requires detailed pluviographic data. Although alternative equations are presented, we also discuss questions of suitability that future users should consider before applying these equations to their study area.

4.2.1 Rainfall erosivity factor (R)

The R-factor represents the effect that rainfall has on soil erosion and was included after observing sediment deposits after an intense storm (Wischmeier & Smith, 1978). The annual R-factor is a function of the mean annual EI_{30} that is calculated from detailed and long-term records of storm kinetic energy (E) and maximum thirty-minute intensity (I_{30}) (Morgan, 2005; Renard et al., 1997). Due to the detailed data requirements for the standard R/USLE calculation of rainfall erosivity, studies in areas with less detailed data have used alternative equations depending on the temporal resolution and availability of the rainfall data. These compiled studies have used long-term datasets with at least daily temporal resolution to construct their R-factor equation. Extensive work by Naipal et al. (2015) attempted to apply the R/USLE at a coarse global scale (30 arcsecond) by using USA and European databases to derive rainfall erosivity equations. These equations use a combination of annual precipitation (mm), mean elevation (m), and simple precipitation intensity index (mm day^{-1}) to calculate the R-factor for different Köppen-Geiger climate classifications (Naipal et al., 2015). Loureiro and Coutinho (2001) used 27 years of daily rainfall data from Portugal and the R/USLE method of calculating EI_{30} to construct an equation that uses the number of days that received over 10.0 mm of rainfall and the amount of rainfall per month when the day's rainfall exceeded 10.0 mm. The Loureiro and

Coutinho (2001) equation was modified by Shamshad et al. (2008) using long-term rainfall data in Malaysia and used to construct a regression equation relating monthly rainfall and annual rainfall with the R-factor. The equation was modified because the original Loureiro and Coutinho (2001) equation was developed in Portugal, and the aim of Shamshad et al. (2008) was to modify it to suit the climatic conditions of tropical Malaysia. Similarly, Sholagberu et al. (2016) used 23 years of daily rainfall data to create a regression equation relating annual rainfall and the R-factor for the highlands of Malaysia. These equations that use monthly or annual rainfall are valuable in study areas that do not have long-term detailed rainfall data, but have a similar climate. The imperial units of erosivity are in hundreds of foot tonf inch acre^{-1} hour^{-1} year^{-1}, and multiplying by 17.02 will give the SI units of megajoule millimetre hectare^{-1} hour^{-1} year^{-1} (Renard et al., 1997).

With the body of work that has been done in rainfall erosivity, some studies have managed to construct rainfall erosivity maps over large countries and regions. Panagos et al. (2017) have used pluviographic data from 63 countries to calculate rainfall erosivity and spatially interpolated the results to construct a global rainfall erosivity map at 30 arcsecond resolution. Despite its coarse resolution, this global dataset can be used as a resource for rainfall erosivity in data-sparse regions. For the United States, Renard et al. (1997) details the procedure for obtaining rainfall erosivity values from their large national database. Renard et al. (1997) would be the recommended reference for study areas in the United States because of the extensive database that already exists for that country. For the European Union, Panagos et al. (2015a) constructed a rainfall erosivity map at 1km resolution and published descriptive statistics for R-values in each of the member countries. The interpolated map showed good agreement through cross-validation and to previous studies, but areas that had less rainfall stations and more diverse terrain caused higher prediction uncertainty (Panagos et al., 2015a). A review of rainfall erosivity in Brazil used a large rainfall dataset with R-factors from different locations to a spatially interpolated map of rainfall erosivity, and the observed trends in the map agreed with previous work on rainfall erosivity the country (da Silva, 2004).

In areas that only have annual precipitation available, several equations and their studies are used as a reference. In their global application, Naipal et al. (2015) published different R-factor equations depending on a study area's climate classification. One caveat is that the data for these equations had a large percentage of USA and European records, so resulting accuracy of R-factors might be better for those locations (Naipal et al., 2015). In tropical areas such as Southeast Asia, the R-factor by El-Swaify et al. (1987) as cited in Post & Hartcher (2006) was used extensively in Thailand, the Philippines, and Sri Lanka. However, the units for the R-factor in this equation are given as tons hectare^{-1} year^{-1}, which do not correspond to the original units used by R/USLE (Merritt et al., 2004). This lack of consistency regarding units is not uncommon in the reviewed literature, which sometimes fails to explicitly report the units used for the different factors. For example, Renard & Freimund (1994) report that the units of R-factor equations by Arnoldus (1977) were presumed to be in metric units. By being clear and consistent about units in R/USLE literature, future researchers can be more certain about the accuracy of their borrowed R-factor equations instead of presuming the units to be the same as the original R/USLE. Work by Bonilla & Vidal (2011) produced an R-factor equation for Chile and published erosivity values similar to those produced by work in areas of similar geography and geology. For New Zealand, Klik et al. (2015) proposed equations for calculating the annual R-factor and seasonal R-factor with coefficients that change depending on the study area's location within the country.

The usage of monthly precipitation data to determine the R-factor is due to monthly data being more readily available compared to detailed storm records (Renard & Freimund, 1994). Renard & Freimund (1994) used data from 155 stations with known R-factors based on the original USLE approach and related their R-factors to observed annual and monthly precipitation. These equations developed by Renard & Freimund (1994) in the west coast of USA were used in Ecuador (Ochoa-Cueva et al., 2015), and Honduras and El Salvador (Kim et al., 2005). Work by Arnoldus (1980) developed R-factor equations in West Africa that use monthly and annual precipitation. However, these equations present a problem in terms of consistent units, as reported by Renard & Freimund (1994) in their review of previous R-factor work. In Southeast Asia, Shamsad et al. (2008) developed an R-factor equation in Malaysia that was used in the Philippines by Delgado & Canters (2012). In New Zealand, the monthly precipitation can be aggregated to seasonal precipitation and used in the equation for seasonal R-factor derived by Klik et al. (2015)

Monthly or better precipitation records are very useful in R/USLE applications because of the option of estimating soil loss at a monthly or seasonal scale, which can be useful in countries with high temporal variation of rainfall throughout the year. Monthly and seasonal erosion has been estimated by varying the R-factor depending on the monthly precipitation while leaving all the other factors constant (Ferreira & Panagopoulos, 2014; Kavian et al., 2011). Klik et al. (2015) emphasised the need to understand the drivers of soil erosion, including whether rainfall intensity had a stronger effect compared to mean annual rainfall. In an assessment of spatial and temporal variations in rainfall erosivity over New Zealand, December and January were associated with higher erosivities while August was associated with lowest erosivity (Klik et al., 2015). Similar work by Diodato (2004) has cited the use of monthly erosivity data to be more useful with respect to managing crop growing cycles and tillage practices, especially during seasons where high rainfall erosivity is expected. In locations where there is a large temporal variation in rainfall throughout the year, the seasonal approach of estimating soil erosion is more important for sustainable land management (Ferreira & Panagopoulos, 2014).

As an example of how R-factor equations can give different estimates of rainfall erosivity, the equations by Klik et al. (2015) developed in New Zealand, Loureiro and Coutinho (2001) developed in Portugal, and Ferreira and Panagopolous (2014) also developed in Portugal were used to estimate annual and seasonal erosivity in the Mangatarere watershed (Table 23, Table 24, and Figure 63). For the same set of rainfall data, the three equations predicted different annual and seasonal values of erosivity. Regarding seasonal patterns of erosivity, Klik et al. (2015) predicted highest erosivity occurring during summer but lowest in winter and spring. This trend matches the national observations of the most erosive storms occur during summer, and the lowest occurring during winter (Klik et al., 2015). By contrast, both Loureiro & Coutinho (2001) and Ferreira & Panagopolous (2014) predicted highest erosivity during spring and lowest during summer. The soil loss results were affected by these differences in erosivity and more detail is found in the Mangatarere chapter (Chapter 6).

These differences highlight the importance of understanding the regional applicability of rainfall erosivity equations. In the reviewed R/USLE studies for this chapter, a common occurrence was using equations derived in different countries and regions without much justification why those equations were chosen with little consideration for their suitability. These studies also did not publish any testing of how different R-factors produce different erosivity values from the same input dataset. The purpose of testing the different R-factors is to illustrate this variation and encourages future users of R/USLE to do the same sensitivity testing in their area.

Table 23. Annual estimates of erosivity in the Mangatarere (MJ mm ha^{-1} h^{-1} yr^{-1}).

Equation Source	Klik et al. (2015)	Loureiro & Coutinho (2001)	Ferreira & Panagopolous (2014)
Annual erosivity	2607	1391	1715

Table 24. Seasonal rainfall and estimates of erosivity in the Mangatarere (MJ mm ha^{-1} h^{-1} yr^{-1}).

Season	Rainfall	Klik et al. (2015)	Loureiro & Coutinho (2001)	Ferreira & Panagopolous (2014)
Spring	322	317	656	733
Summer	553	1283	72	208
Autumn	386	611	288	360
Winter	541	288	375	494

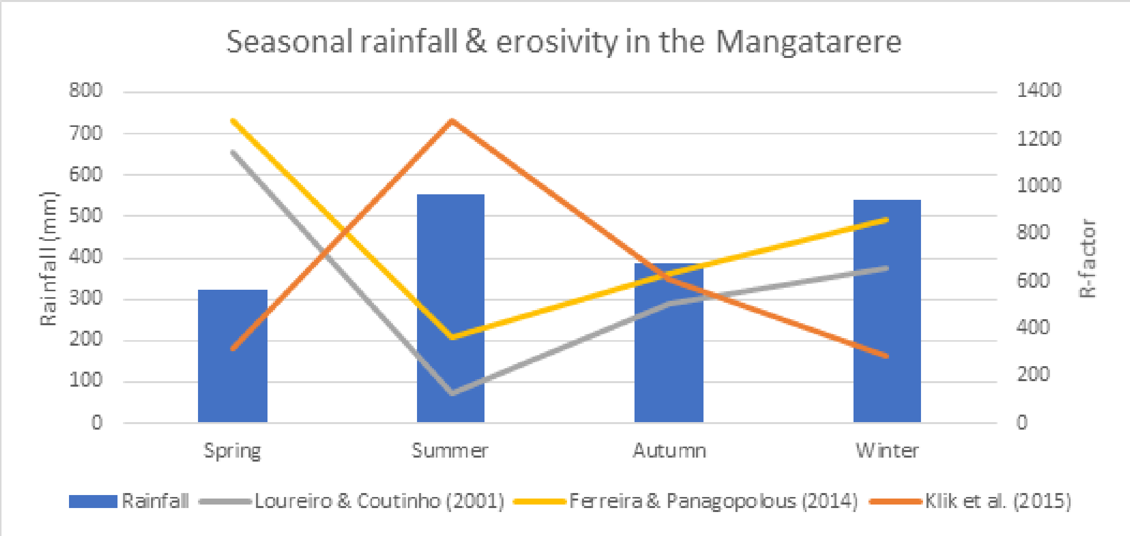

Figure 63. Graph of seasonal rainfall and estimates of erosivity in the Mangatarere.

In summary, there are many rainfall erosivity datasets and equations in the R/USLE literature that can be used by new researchers applying the RUSLE to their study area. The erosivity dataset produced by Panagos et al. (2017) is recommended for areas with no rainfall data or in ungauged catchments since this is a raster dataset with a global coverage (~30 arcsecond resolution) and is freely available. For areas in the European Union, work by Panagos et al. (2015a) and related papers has produced a rainfall erosivity map with regional coverage at ~1km resolution. These datasets can also be used to validate the erosivity factors calculated at the national or catchment scale. If annual precipitation and the study area's Köppen-Geiger classification are known, Naipal et al. (2015) has published rainfall erosivity equations and values for 17 different climate zones. Several studies have published erosivity equations for tropical areas: da Silva (2004) for Brazil, Shamshad et al. (2008) for Malaysia, and Jain & Das (2010) for India. For arid areas, Arnoldus (1980) as cited in Renard & Freimund has derived erosivity equations for Morocco and other locations in West Africa. Many other equations are found in Table 25, and choosing several for sensitivity testing is recommended for future R/USLE applications. It is also important to test against observed data or R-factors derived by previous applications in the same study area or in study areas with similar climatic regimes.

Table 25. Summary of different studies that developed rainfall erosivity equations, original locations, and other studies that used their equations.

#	Author	Original Location	Resolution	Equation and requirements	Other studies
1	Wischmeier and Smith (1978) and Renard et al. (1997)	United States of America	Sub-daily	$$R = \frac{\sum_{i=1}^{j}(EI_{30})_i}{N}$$ $$EI_{30} = E \times I_{30}$$ $$E = 916 + 331 \times log_{10}\, \mathrm{I}$$ I = intensity (in hr^{-1}) EI_{30i} = EI_{30} for storm i j = number of storms in an N-year period <u>Units</u> Imperial: Hundreds of foot • tonf • inch • $acre^{-1}$ • $hour^{-1}$ • year-1 Metric (multiply by 17.02): Megajoule •millimetre • $hectare^{-1}$ • $hour^{-1}$ • $year^{-1}$	Applied around USA
2	Mihara (1951) and Hudson (1971) as cited in David (1988)	USA	Daily	$$R = A \times \sum_{1}^{n} P_i^m$$ A = 0.002 M = 2 P_i = Precipitation total for day *i* when *P* exceeds 25mm Units: Not specified, likely to be original USLE imperial units	Watersheds around the Philippines (David, 1988)
3	Arnoldus (1980) as cited in Renard and Freimund (1994)	Morocco and other locations in West Africa	Monthly and annual	West Africa $$R = 4.79MFI - 142$$ $$R = 5.44MFI - 416$$ Eastern USA $$R = 6.86MFI - 420$$ Western USA $$R = 4.79MFI - 143$$ Northwest USA $$R = 0.66MFI - 3$$ $$MFI = \sum_{i=1}^{12} \frac{P_i^2}{P}$$ MFI = Modified Fournier's Index P_i = monthly precipitation P = annual precipitation Units: Ton-metre • centimetre • $hectare^{-1}$ • $hour^{-1}$ • $year^{-1}$ (Renard and Freimund, 1994)	Turkey (Demirci & Karaburun, 2012); Morocco (Raissouni et al., 2016)

Table 25. Summary of different studies that developed rainfall erosivity equations, original locations, and other studies that used their equations. (continued)

#	Author	Original Location	Resolution	Equation and requirements	Other studies
4	Renard and Freimund (1994)	West coast of USA	Monthly and annual	$R = 0.0483 \times P^{1.610}$ $R = 587.8 - 1.219P + 0.004105P^2$ Using MFI (Arnoldus, 1980): $R = 0.07397 \times MFI^{1.847}$ $R = 95.77 - 6.081MFI + 0.4770MFI^2$ P_i = monthly precipitation P = annual precipitation Units: Megajoule •millimetre • hectare^{-1} • hour^{-1} • year^{-1}	Central America (Kim et al., 2005); Iran (Zakerinejad & Maerker, 2015); Ecuador (Ochoa-Cueva et al., 2015)
5	Zhou et al. (1995) as cited in Li et al. (2014)	Southern China	Monthly	$R = \sum_{i=1}^{12} -1.15527 + 1.792P_i$ P_i = monthly precipitation Units: Megajoule •millimetre • hectare^{-1} • hour^{-1} • year^{-1}	China (L. Li et al., 2014)
6	Roose (1975) and Morgan (1974) as cited in Morgan (2005)	Peninsular Malaysia and Africa	Annual	Africa (Roose, 1975): $R = 0.5 \times P \times 17.3$ Peninsular Malaysia: $R = (9.28 \times P - 8838)\left(\frac{75}{1000}\right)$ P = mean annual precipitation (mm) Units: Megajoule •millimetre • hectare^{-1} • hour^{-1} • year^{-1}	Malaysia (Roslee et al., 2017); Vanuatu (Dumas & Fossey, 2009); Iran (Zakerinejad & Maerker, 2015)
7	El-Swaify et al. (1987) as cited in Post & Hartcher (2006)	Possibly Thailand	Annual	$R = 38.5 + 0.35P$ P = mean annual precipitation Units: Tons • hectare^{-1} • year^{-1} (All the other factors must have been developed to have no units so that the final soil loss is in tons/ha/year)	Thailand (Eiumnoh, 2000; Merritt et al., 2004); Philippines (Adornado et al., 2009; Adornado & Yoshida, 2010; Hernandez et al., 2012); Sri Lanka (Jayasinghe et al., 2010)
8	Land Development Department (2000), as cited in Nontananandh and Changnoi (2012)	Thailand	Annual	$R = 0.04669P - 12.1415$ P = mean annual rainfall Units: Megajoule •millimetre • hectare^{-1} • hour^{-1} • year^{-1}	Thailand (Nontananandh & Changnoi, 2012)

Table 25. Summary of different studies that developed rainfall erosivity equations, original locations, and other studies that used their equations. (continued)

#	Author	Original Location	Resolution	Equation and requirements	Other studies
9	Loureiro and Coutinho (2001)	Portugal	Daily	$R = \frac{1}{N}\sum_{i=1}^{N}\sum_{m=1}^{12} EI_{30(monthly)}$ $EI_{30\ (monthly)} = 7.05rain_{10} - 88.92days_{10}$ $Rain_{10}$ = monthly rainfall for days with $\geq$ 10.0mm of rain $Days_{10}$ = monthly number of days with rainfall $\geq$ 10.0mm of rain N = number of years Units: Megajoule •millimetre • hectare^{-1} • hour^{-1} • year^{-1}	Spain (López-Vicente et al., 2008)
10	Fernandez et al. (2003), originally developed by the USDA-ARS (2002)	USA	Annual	$R = -823.8 + 5.213P$ P = annual precipitation Units: Megajoule •millimetre • hectare^{-1} • hour^{-1} • year^{-1}	USA (C. Fernandez et al., 2003); Greece (Jahun et al., 2015)
11	Ram et al. (2004), as cited in Jain and Das (2010)	India	Annual	$R = 81.5 + 0.38P$ P = annual precipitation for areas where annual precipitation ranges between 340mm to 3500mm Units: Megajoule •millimetre • hectare^{-1} • hour^{-1} • year^{-1}	India (Jain & Das, 2010)
12	Shamshad et al. (2008)	Malaysia	Monthly and annual	Based on Loureiro and Coutinho (2001) but for Malaysia: $R = \sum_{i=1}^{12} 6.97rain_{10} - 11.23days_{10}$ $R = \sum_{i=1}^{12} 0.266 \times rain_{10}^{2.071} \times days_{10}^{-1.367}$ $R = \sum_{i=1}^{12} 227 \times \left(\frac{P_i^2}{P}\right)^{0.548}$ $Rain_{10}$ = monthly rainfall for days with $\geq$ 10.0mm of rain $Days_{10}$ = monthly number of days with rainfall $\geq$ 10.0mm of rain P_i = monthly precipitation P = annual precipitation Units: Megajoule •millimetre • hectare^{-1} • hour^{-1} • year^{-1}	Philippines (Delgado & Canters, 2012)
13	Irvem et al. (2007)	Turkey	Monthly and annual	$R = 0.1215 \times MFI^{2.2421}$ $MFI = \sum_{i=1}^{12} \frac{P_i^2}{P}$ P_i = monthly precipitation P = annual precipitation Units: Megajoule •millimetre • hectare^{-1} • hour^{-1} • year^{-1}	Turkey (Ozsoy et al., 2012)

Table 25. Summary of different studies that developed rainfall erosivity equations, original locations, and other studies that used their equations. (continued)

#	Author	Original Location	Resolution	Equation and requirements	Other studies
14	Ferreira and Panagopolous (2014), similar to Loureiro and Coutinho (2001)	Portugal	Daily	$$R = \sum_{i=1}^{12} 6.56 rain_{10} - 75.09 days_{10}$$ $Rain_{10}$ = monthly rainfall for days with ≥ 10.0mm of rain $Days_{10}$ = monthly number of days with rainfall ≥ 10.0mm of rain Units: Megajoule •millimetre • hectare^{-1} • hour^{-1} • year^{-1}	Portugal (Ferreira & Panagopoulos, 2014)
15	Nakil (2014) as cited in Nakil and Khire (2016)	India	Annual	$$R = 839.15 \times e^{0.0008P}$$ P = annual precipitation Units: Megajoule •millimetre • hectare^{-1} • hour^{-1} • year^{-1}	India (Nakil & Khire, 2016)
18	Naipal et al. (2015)	Global application, but original data from USA and Europe	Annual	Various equations depending on Köppen climate classification, including alternate equations if SDII is not available P = annual precipitation (mm) Z = mean elevation (m) SDII = simple precipitation intensity index (mm day^{-1})	
19	Klik et al. (2015)	New Zealand	Annual or seasonal	Annual or seasonal: $$R = aP^b$$ $$R = aP + b$$ P = annual precipitation (mm) or seasonal precipitation (mm) a & b = constants depending on region of New Zealand The equation used will depend on the region of New Zealand, and the season. Units: Megajoule •millimetre • hectare^{-1} • hour^{-1}	
20	Sholagberu et al. (2016)	Malaysia	Annual	$$R = 0.0003P^{1.771}$$ P = annual precipitation Units: Megajoule •millimetre • hectare^{-1} • hour^{-1} • year^{-1}	

4.2.2 Slope length (L) and steepness (S) factor

The LS-factor represents the effect that the slope's length and steepness affect sheet, rill, and inter-rill erosion by water, and is the ratio of expected soil loss from a field slope relative to the original USLE unit plot (Wischmeier & Smith, 1978). The USLE method of calculating the slope length and steepness factor was originally applied at the unit plot and field scale, and the RUSLE extended this to the one-dimensional hillslope scale, with different equations depending on whether the slope had a gradient of more than 9% (Renard et al., 1997; Wischmeier & Smith, 1978). Further research extends the LS-factor to topographically complex units using a method that incorporates contributing area and flow accumulation (Desmet & Govers, 1996). The USLE and RUSLE method of calculating the LS-factor uses slope length, angle, and a parameter that depends on the steepness of the slope in percent (Wischmeier & Smith, 1978).

However, one of the criticisms of the original USLE method of calculating LS-factor is its applicability to more complex topography. With advances in GIS technology, the method of determining the LS-factor as a function of upslope contributing area or flow accumulation and slope has risen in popularity (26). The use of digital elevation models (DEMs) to calculate upslope contributing area and the resulting LS-factor allows researchers to account for more topographically complex landscapes (Desmet & Govers, 1996; Moore & Burch, 1986). Desmet and Govers (1996) have also built on this method through showing its application in a GIS environment over topographically complex terrain when compared to the original method proposed by Wischmeier and Smith (1978). This method of using flow accumulation for slope length and steepness explicitly accounts for convergence and divergence of flow, which is important when considering soil erosion over a complex landscape (Wilson & Gallant, 2000). It is possible to use this method to calculate the LS-factor over a large extent, but a high-resolution DEM is needed for accurate representation of the topography. The resolution required depends on the study area's scale. Coarse DEMs (~30m) are less suited to field and sub-catchment scale studies where it may be important to capture effects of micro-topography. At DEMs larger than ~100m resolution, there is significant loss of detail regarding the flow network (Panagos et al., 2015b).

The original equations for LS-factor assume that slopes have uniform gradients and any irregular slopes would have to be divided into smaller segments of uniform gradients for the equations to be more accurate (Wischmeier & Smith, 1978). At the plot or small field scale, this manual measurement of slopes and dividing into segments may be manageable, but less useful at larger scales. In terms of practicality, Desmet & Govers (1996) have reported studies of this method applied at a watershed scale with the disadvantages of it being time-consuming. Studies in Iran and the Philippines have implemented the R/USLE methods within a GIS environment by calculating the LS-factor for each raster cell in a DEM, essentially treating each pixel as its own segment of uniform slope (Bagherzadeh, 2014; Schmitt, 2009). Applications using these methods must be mindful of the appropriate DEM resolution of their study area, as using DEMs that are too coarse can lead to loss of detail associated with flow patterns.

As explained above, the method of using flow accumulation, upslope contributing area, and slope in a GIS environment has gained popularity due to its ability to explicitly account for convergence and divergence of flow, thus capturing more complex topography (Wilson & Gallant, 2000). In the New Zealand application using high-resolution DEMs (~15m and 5m), this method is appropriate at the sub-catchment or field scale while the original RUSLE method can still be applied at the national, regional, or catchment scale if limited by computing resources. This flow accumulation method was applied at the scales of watersheds and regions (26) and has even been applied by Panagos et al. (2015b) at the scale of the European Union using a 25m DEM. The factors that limit users is the availability of high-resolution DEMs and the trade-off between processing time and accuracy. The original R/USLE methods require only slope angle and length, operates over a single cell in a DEM by treating it as a uniform slope, and would take less processing time compared to the method using flow accumulation. However, the user must remember that this cannot capture the convergence and divergence of flow and thus can sacrifice accuracy for time at the sub-catchment or field scale.

Table 26. Summary of methods of calculating LS-factor, original locations, and other studies that used these methods.

#	Author	Original Location	Data requirements	Equation	Other studies that utilised similar methods
1	Wischmeier and Smith (1978)	USA	Slope length and angle	$LS = \left(\frac{\lambda}{72.6}\right)^m \times [(65.41 \times \sin^2\theta) + (4.56 \times \sin\theta) + 0.065]$ λ = Slope length in feet Θ = Angle of slope m = Dependent on the slope • 0.5 if slope > 5% • 0.4 if slope is between 3.5% and 4.5% • 0.3 if slope is between 1% and 3% • 0.2 if slope is less than 1%	Thailand (Eiumnoh, 2000; Merritt et al., 2004); Vanuatu (Dumas & Fossey, 2009); Iran (Bagherzadeh, 2014)
2	Renard et al. (1997)	USA	Slope length and angle	$L = \left(\frac{\lambda}{72.6}\right)^m$ $m = \frac{\beta}{1+\beta}$ $\beta = \frac{(\frac{\sin\theta}{0.0896})}{[3.0 \times (\sin\theta)^{0.8} + 0.56]}$ If slope is less than 9%: $S = 10.8 \times \sin\theta + 0.03$ If slope is greater or equal to 9%: $S = 16.8 \times \sin\theta - 0.50$ But if the slope is shorter than 15 feet: $S = 3.0 \times (\sin\theta)^{0.8} + 0.56$ λ = Slope length in feet Θ = Angle of slope m = Dependent on the slope • 0.5 if slope > 5% • 0.4 if slope is between 3.5% and 4.5% • 0.3 if slope is between 1% and 3% • 0.2 if slope is less than 1%	Philippines (Schmitt, 2009); China (L. Li et al., 2014); Thailand (Nontananandh & Changnoi, 2012); Turkey (Ozsoy et al., 2012)

Table 26. Summary of methods of calculating LS-factor, original locations, and other studies that used these methods. (continued)

#	Author	Original Location	Data requirements	Equation	Other studies that utilised similar methods
3	David (1988), based on work by Madarcos (1985) and Smith & Whitt (1947)	Philippines, but based on work from the USA	Slope rise in percent	$LS = a + b \times S_L^{4/3}$ a = 0.1 b = 0.21 S_L = Slope in percent	Philippines (David, 1988)
4	Morgan (2005) but previously published in earlier editions	Britain	Slope length and gradient in percent	$LS = \left(\frac{l}{22}\right)^{0.5} \times (0.065 + 0.045s + 0.0065s^2)$ l = slope length (m) s = slope steepness (%)	India (Nakil & Khire, 2016; Sinha & Joshi, 2012); Greece (Rozos et al., 2013)
5	Moore & Burch (1986) as cited in Mitasova et al. (1996); Desmet & Govers (1996); Mitasova et al. (2013);	USA	Upslope contributing area per unit width, which can be approximated through flow accumulation, cell size, slope	$LS = (m+1)\left(\frac{U}{L_0}\right)^m \left(\frac{\sin\beta}{S_0}\right)^n$ U (m^2m^{-1}) = upslope contributing area per unit width as a proxy for discharge $U = Flow\ Accumulation \times Cell\ Size$ L_0 = length of the unit plot (22.1) S_0 = slope of unit plot (0.09) β = slope m (sheet) and n (rill) depend on the prevailing type of erosion (m= 0.4 to 0.6) and n (1.0 to 1.3)	Philippines (Adornado et al., 2009; Adornado & Yoshida, 2010); Sri Lanka (Jayasinghe et al., 2010); China (L. Chen et al., 2011); Iran (Zakerinejad & Maerker, 2015); Jordan (Farhan & Nawaiseh, 2015); Morocco (Raissouni et al., 2016); New Zealand (M. A. Fernandez & Daigneault, 2016) Similar methods from Moore & Burch (1986): India (Jain & Das, 2010); Portugal (Ferreira & Panagopoulos, 2014); Greece (Jahun et al., 2015); India (Nakil & Khire, 2016) Similar methods from Desmet & Govers (1996): USA (Boyle et al., 2011); Turkey (Demirci & Karaburun, 2012); Philippines (Delgado & Canters, 2012)

4.2.3 Soil erodibility factor (K)

The K-factor represents the influence of different soil properties on the slope's susceptibility to erosion (Renard et al., 1997). It is defined as the "mean annual soil loss per unit of rainfall erosivity for a standard condition of bare soil, recently tilled up-and-down slope with no conservation practice" (Morgan, 2005). The K-factor essentially represents the soil loss that would occur on the R/USLE unit plot, which is a plot that is 22.1m long, 1.83m wide, and has a slope of 9% (López-Vicente et al., 2008).

Higher K-factor values indicate the soil's higher susceptibility to soil erosion (Adornado et al., 2009). In the R/USLE, Wischmeier and Smith (1978) and Renard et al. (1997) use an equation that relates textural information, organic matter, information about the soil structure and profile-permeability with the K-factor or soil erodibility factor. However, other soil classifications might not include soil structure and profile-permeability information that matches the information required by R/USLE nomograph. Hence, alternative equations were developed that exclude the soil structure and profile-permeability (Table 27). The question of which equation to use depends on the availability of soil data. Where only the textural class and organic matter content is known, Stewart et al. (1975) have approximated K-factor values based on these inputs. Similar to the R-factor, the imperial units of soil erodibility are in ton acre hour hundreds of acre^{-1} foot^{-1} tonf^{-1} inch^{-1}, and multiplying by 0.1317 gives the erodibility in SI units of metric ton hectare hour hectare^{-1} megajoule^{-1} millimetre^{-1} (Renard et al., 1997).

Although seemingly relatively straightforward, the K-factor equation proposed by Wischmeier and Smith (1978) comes with a few limitations regarding soil type. This equation was developed using data from medium-textured surface soils in the Midwestern USA, with an upper silt fraction limit of 70% (Renard et al., 1997). An equation for volcanic soils in Hawaii was proposed by El-Swaify & Dangler (1976) as cited in Renard et al. (1997) but is only appropriate for soils similar to Hawaiian soils and not for all tropical soils. Despite these limitations, many studies outside the USA have used the original Wischmeier & Smith (1978) K-factor equation (Table 27). Being aware of the regional specificity of K-factor equations is important and using different

K-factor equations in one study area to find a range of soil erodibility could be a way of testing their applicability.

Similar to the sensitivity analysis of the R-factor equations, testing different K-factor equations to see the variation in erodibility values, and then comparing these K-factors with published values from similar soils would be a good way to test applicability. For the spatial coverage of European Union, a soil erodibility raster dataset (~500m resolution) is available for validation (Panagos et al., 2014). David (1988) and Dymond (2010) have published K-factor values for soils of different textural classes (e.g. clay, loam, etc.) that can be used if only soil texture is known. Like the R-factor, it is important to check the derived K-factor values for the site-specific soil against previously published K-factor values for comparable sites and soil types.

Table 27. Summary of different studies with soil erodibility equations, original locations, and other studies that used their equations. All of the equations in Table 27 use imperial units of soil erodibility: ton • acre • hour • hundreds of acre^{-1} • foot^{-1} • tonf^{-1} • inch^{-1}. Multiply by 0.1317 to give in SI units of metric ton • hectare • hour • hectare^{-1} • megajoule^{-1} • millimetre^{-1}.

#	Author	Original Location	Data requirements	Equation	Other studies
1	Wischmeier and Smith (1978) and Renard et al. (1997)	USA	Very fine sand (%), clay (%), silt (%), organic matter (%), soil structure, profile-permeability	$M = Silt \times (100 - Clay)$ $K = \frac{\left\{ \begin{matrix} [2.1 \times M^{1.14} \times (10^{-4}) \times (12 - a)] + \\ [3.25 \times (b - 2)] + \\ [2.5 \times (c - 3)] \end{matrix} \right\}}{100}$ M = Particle-size parameter Silt = Silt (%) but also includes the percentage of very fine said (0.1 to 0.05mm) Clay = Clay (%) a = Organic matter (%) b = Soil-structure code used in soil classification: • 1: Very fine granular • 2: Fine granular • 3: Medium or coarse granular • 4: Blocky, platy, or massive c = Profile-permeability class • 1: Rapid • 2: Moderate to rapid • 3: Moderate • 4: Slow to moderate • 5: Slow • 6: Very slow	Thailand (Eiumnoh, 2000); Vanuatu (Dumas & Fossey, 2009); Philippines (Schmitt, 2009); India (Jain & Das, 2010); Turkey (Ozsoy et al., 2012); Iran (Bagherzadeh, 2014); Portugal (Ferreira & Panagopoulos, 2014); China (L. Li et al., 2014); European Union (Panagos et al., 2014)

Table 27. Summary of different studies with soil erodibility equations, original locations, and other studies that used their equations. All of the equations in Table 27 use imperial units of soil erodibility: ton • acre • hour • hundreds of acre-1 • foot-1 • tonf-1 • inch-1. Multiply by 0.1317 to give in SI units of metric ton • hectare • hour • hectare-1 • megajoule-1 • millimetre-1. (continued)

#	Author	Original Location	Data requirements	Equation	Other studies
2	Williams and Renard (1983) as cited in Chen et al. (2011)	USA	Sand (%), silt (%), clay (%), organic carbon (%)	$K = 0.2 + 0.3\exp\left(0.0256 \times Sa \times \left(1 - \frac{Si}{100}\right)\right) \times \left(\frac{Si}{Cl + Si}\right)^{0.3} \times \left(1.0 - \frac{0.25 \times C}{C + \exp(3.72 - 2.95C)}\right) \times \left(1.0 - \frac{0.7 \times SN}{SN + \exp(-5.51 + 22.9SN)}\right)$ Sa = Sand % Si = Silt % Cl = Clay % SN = 1-(Sa/100) C = Organic Carbon	China (L. Chen et al., 2011)
3	David (1988), a simplified version of Wischmeier and Mannering (1969)	USA	Sand (%), clay (%), silt (%), organic matter (%), pH	$K = \begin{bmatrix} (0.043 \times pH) + \\ (0.62 \div OM) + \\ (0.0082 \times S) - (0.0062 \times C) \end{bmatrix} \times Si$ pH = pH of the soil OM = Organic matter in percent S = Sand content in percent C = Clay ratio = % clay / (% sand + % silt) Si = Silt content = % silt / 100	Philippines (David, 1988; Hernandez et al., 2012)
4	El-Swaify & Dangler (1976) as cited in Renard et al. (1997)	Hawaii, USA	Textural information, base saturation	$K = -0.03970 + 0.00311x_1 + 0.00043x_2 + 0.00185x_3 + 0.00258x_4 - 0.00823x_5$ x_1 = unstable aggregate size fraction (<0.250mm) (%) x_2 = modified silt (0.002 - 0.1mm) (%) * modified sand (0.1 - 2mm) (%) x_3 = % base saturation x_4 = silt fraction (0.002 - 0.050mm) (%) x_5 = modified sand fraction (0.1 - 2mm) (%)	

4.2.4 Cover and management factor (C)

The cover and management factor (C) is defined as the ratio of soil loss from a field with a particular cover and management compared to a field under “clean-tilled continuous fallow” (Wischmeier & Smith, 1978). The R/USLE uses a combination of sub-factors such as impacts of previous management, canopy cover, surface cover and roughness, and soil moisture on potential erosion to produce a value for soil loss ratio, which is used with R-factor to produce a value for C-factor (Renard et al., 1997). This method requires extensive knowledge of the study area’s cover characteristics including agricultural management and may be suitable at field or farm scale but monitoring all these characteristics at the watershed scale may not be feasible.

A simpler method of determining the C-factor is referencing studies that have reported values for similar land cover, or from studies done in the same area or region. Table 28 and Table 29 give a broad overview of C-factors for different cover types and common crops. Wischmeier & Smith (1987) also include the effect of percent ground cover, reporting C-factor values for the same cover type over a range of cover percentage and condition. Morgan (2005) and David (1988) have reported values for the different growth stages of the same types of trees. A simple method of creating a C-factor layer by using lookup tables to assign C-factor values to the land cover classes present in the study area. When using C-factors from literature, it is important to note the definition of land cover type between two countries may vary. For example, land classified as forest in one country may be different in terms of vegetation cover or type compared to forest in another country (e.g. differences in pine forests and tropical forests). Therefore, it is crucial to understand the differences between land cover classifications before applying C-factor values from literature. Van der Knijff et al. (2000) cites the large spatial and temporal variations in cover and crop over a large region such as the European Union as another reason why using the lookup table-based approach is inadequate and tedious.

To address this, another method of determining the C-factor is through the Normalized Difference Vegetation Index (NDVI) estimated from satellite imagery. Although there are NDVI layers available, these are limited by geographical coverage, date of acquisition, and resolution. The MODIS NDVI dataset made by Caroll et al. (2004) at 250m resolution covers the USA and South America[8]. NASA produced a global dataset of NDVI values at 1-degree resolution for the timespan of July 1983 to June 1984, making it suitable for studying historical soil erosion but not necessarily for the current state of land cover[9].

[8] http://glcf.umd.edu/data/ndvi/
[9] https://data.giss.nasa.gov/landuse/ndvi.html

In areas where ready-made NDVI products are unavailable, authors used satellite imagery to obtain NDVI such as AVHRR or Landsat ETM (de Asis & Omasa, 2007; van der Knijff et al., 2000). De Asis & Omasa (2007) related C-factor and NDVI through fieldwork and image classification; determining C-factor at several points within the study area using the R/USLE approach and relating it to the NDVI through regression correlation analysis. For larger study areas, this may not be feasible such as in the European Union where Van der Knijff et al. (2000) determined NDVI from satellite imagery, and since NDVI is positively correlated with green vegetation, they created this equation:

$$C = \exp\left[-\propto\left(\frac{NDVI}{\beta - NDVI}\right)\right]$$

Where α and β are parameters that determine the shape of the NDVI-C curve, and van der Knijff et al. (2000) used values of 2 and 1, respectively. This approach enabled them to create a C-factor map over the European Union. However, C-factors were unrealistically high in some areas such as woodland and grassland, so values for those areas were taken from literature to limit a maximum of 0.01 for woodland and 0.05 for grassland. This verification of C-factors is important to keep in mind when using satellite imagery and NDVI, and the resulting C-factor values should be tested against literature to check if they exceed the maximum values for land cover types. In China, Ma et al. (2001) as cited in Li et al. (2014) uses the following relationship between NDVI and C:

$$f_g = \frac{NDVI - NDVI_{min}}{NDVI_{max} - NDVI_{min}}$$

$$C = \begin{cases} 1 & f_g = 0 \\ 0.6508 - 0.343 \times \log(f_g) & 0 < f_g < 78.3\% \\ 0 & f_g \geq 78.3\% \end{cases}$$

An advantage of using is NDVI that researchers can determine sub-annual C-factors if there is satellite imagery available, which can lead to understanding the contribution of cover to seasonal soil erosion and identifying critical periods within the year were soil erosion is a risk (Ferreira & Panagopoulos, 2014). Similar methods have been applied in Brazil by Durigon et al. (2014), Greece by Alexandridis et al. (2015), and Kyrgyzstan by Kulikov et al. (2016). Determining C-factors at the seasonal scale is important because vegetation cover can change throughout the year due to agricultural and forestry practices. In study areas with a high temporal variation of rainfall throughout the year, seasonal vegetation can play a big part in exacerbating or mitigating soil erosion.

To summarise, the choice of which method to use depends on the scale of the study area, reported C-factors for similar cover, and availability of high-resolution imagery. For small-scale studies, it is more feasible to determine the C-factors through fieldwork. If previous R/USLE studies have reported C-factors for cover like the study area, those values can be used for the table-based approach. Lastly, high-resolution imagery can be used to determine the study area's NDVI. At small scales and with a good understanding of differences in land cover classifications, pulling values from literature may be the most efficient choice but at larger regional scales, this may become tedious. At larger scales, high-resolution satellite imagery may be available to determine NDVI but authors must be mindful of its acquisition date in relation to their study period, and requires pre-processing such as masking cloud cover and creating aggregates from these masked images (Kulikov et al., 2016; van der Knijff et al., 2000).

Table 28. C-factors for aggregated types of land cover compiled from various sources.

Cover	Dymond (2010) (New Zealand)	David (1988) (Philippines)	Morgan (2005) (Various)	Fernandez et al. (2003) (USA)	Dumas & Fossey (2009) (Vanuatu)	LDD (2002) as cited in Nontananandh & Changnoi (2012)
Bare ground	1	1	1			
Built-up areas		0.2		0.03	0	0
Crop				0.128	0.01	0.255 to 0.525
Forest	0.005	0.001 to 0.006	0.001	0.001	0.001	0.003 to 0.048
Pasture	0.01		0.1			
Scrub	0.005	0.007 to 0.9	0.01	0.003	0.16	0.01 to 0.1

Table 29. C-factors for general types of land cover compiled from various sources.

Cover	Panagos et al. (2015d) (Europe)	David (1988) (Philippines)	Morgan (2005) (Various)
Bananas		0.1 to 0.3	
Barley	0.21		
Chili			0.33
Cocoa			0.1 to 0.3
Coffee			0.1 to 0.3
Common wheat and spelt	0.2		0.1 to 0.4
Cotton seed	0.5	0.4 to 0.6	0.4 to 0.7
Dried pulses (legumes) and protein crop	0.32	0.3 to 0.5	0.04 to 0.7
Durum wheat	0.2		
Fallow land	0.5		
Grain maize-corn	0.38	0.3 to 0.6	0.02 to 0.9
Groundnuts			0.3 to 0.8
Linseed	0.25		0.1 to 0.2
Oilseeds	0.28		
Palm with cover crops		0.05 to 0.3	0.1 to 0.3
Pineapple		0.2 to 0.5	0.01 to 0.4
Potatoes	0.34		0.1 to 0.4
Rape and turnip rape	0.3		
Rice	0.15	0.1 to 0.2	0.1 to 0.2
Rye	0.2		
Soya	0.28		0.2 to 0.5
Sugar beet	0.34		
Sugarcane			0.13 to 0.4
Sunflower seed	0.32		
Tobacco	0.49	0.4 to 0.6	
Yams			0.4 to 0.5

4.2.5 Support practice factor (P)

The support practice factor (P) is defined as the ratio of soil loss under a specific soil conservation practice (e.g. contouring, terracing) compared to a field with upslope and downslope tillage (Renard et al., 1997). The P-factor accounts for management practices that affect soil erosion through modifying the flow pattern, such as contouring, strip-cropping, or terracing (Renard et al., 1997). The more effective the conservation practice is at mitigating soil erosion, the lower the P-factor (Bagherzadeh, 2014). Like the C-factor, values for P-factors can be taken from literature and if there are no support practices observed, the P-factor is 1.0 (Adornado et al., 2009). The P-factor can also be estimated using subfactors, but the difficulty of accurately mapping support practice factors or not observing support practices leads to many studies ignoring it by giving their P-factor a value of 1.0 as seen in Appendix 1 (Adornado et al., 2009; Renard et al., 1997; Schmitt, 2009).

Another likely reason why studies may ignore P-factor is due to the nature of their chosen C-factors. Some C-factors already account for the presence of a support factor such as intercropping or contouring. For example, Morgan (2005) and David (1988) give C-factors for one type of crop, but with distinct types of management.

Table 30. Examples of where C-factor accounts for crop management from Morgan (2005) and David (1988).

Crop	Management	C-factor
Maize, sorghum or millet	High productivity; conventional tillage	0.20 to 0.55
	Low productivity; conventional tillage	0.50 to 0.90
	High productivity; chisel ploughing into residue	0.12 to 0.20
	Low productivity; chisel ploughing into residue	0.30 to 0.45
	High productivity; no or minimum tillage	0.02 to 0.10
Coconuts	Tree intercrops	0.05 to 0.1
	Annual crops as intercrop	0.1 to 0.30

Despite the P-factor being commonly ignored, a few studies have reported possible P-factors for different kinds of tillage, terracing, contouring, and strip-cropping (Table 31). The P-factor has a significant impact on the estimation of soil loss. For example, a P-factor of 0.25 for zoned tillage reflects the potential for this management factor to reduce soil by 75% loss compared to conventional tillage (P-factor: 1.00). At suitably detailed scales and with enough knowledge of farming practices, using these P-factors may lead to a more accurate estimation of soil loss. Additionally, these P-factors can be used in scenario analysis to understand how changing farming practices may mitigate or exacerbate soil loss. In the CDO application

(Chapter 5), the P-factor was included, and it was seen that soil conservation strategies such as agroforestry and line-planting can lead to reductions in mean annual soil loss.

Table 31. P-factors for several types of agricultural management practices.

<table>
<tr><th colspan="5">David (1988)</th></tr>
<tr><th colspan="2">Tillage and Residue Management</th><th colspan="3">P-factor</th></tr>
<tr><td colspan="2">Conventional tillage</td><td colspan="3">1.00</td></tr>
<tr><td colspan="2">Zoned tillage</td><td colspan="3">0.25</td></tr>
<tr><td colspan="2">Mulch tillage</td><td colspan="3">0.26</td></tr>
<tr><td colspan="2">Minimum tillage</td><td colspan="3">0.52</td></tr>
<tr><th rowspan="2">Slope (%)</th><th colspan="2">Terracing</th><th rowspan="2">Contouring</th><th rowspan="2">Contour Strip Cropping</th></tr>
<tr><th>Bench</th><th>Broad-based</th></tr>
<tr><td>1 – 2</td><td>0.10</td><td>0.12</td><td>0.60</td><td>0.30</td></tr>
<tr><td>3 – 8</td><td>0.10</td><td>0.10</td><td>0.50</td><td>0.15</td></tr>
<tr><td>9 – 12</td><td>0.10</td><td>0.12</td><td>0.60</td><td>0.30</td></tr>
<tr><td>13 – 16</td><td>0.10</td><td>0.14</td><td>0.70</td><td>0.35</td></tr>
<tr><td>17 – 20</td><td>0.12</td><td>0.16</td><td>0.80</td><td>0.40</td></tr>
<tr><td>21 – 25</td><td>0.12</td><td>0.18</td><td>0.90</td><td>0.45</td></tr>
<tr><td>> 25</td><td>0.14</td><td>0.20</td><td>0.95</td><td>0.50</td></tr>
<tr><th colspan="5">Panagos et al. (2015e)</th></tr>
<tr><td colspan="2">Slope (%)</td><td colspan="3">Contouring P-factor</td></tr>
<tr><td colspan="2">9 – 12</td><td colspan="3">0.6</td></tr>
<tr><td colspan="2">13 – 16</td><td colspan="3">0.7</td></tr>
<tr><td colspan="2">17 – 20</td><td colspan="3">0.8</td></tr>
<tr><td colspan="2">21 – 25</td><td colspan="3">0.9</td></tr>
<tr><td colspan="2">> 25</td><td colspan="3">0.95</td></tr>
</table>

4.3 Limitations of R/USLE

The most commonly cited limitation of the R/USLE models is their applicability to regions outside of the United States of America (Aksoy & Kavvas, 2005; Naipal et al., 2015; Sadeghi et al., 2014). The original USLE was formulated based on soil erosion studies on agricultural land in the USA and when applied to different climate regimes and land cover conditions may lead to uncertainties associated with estimates of average annual soil loss (Kinnell, 2010). For example, the original equation for soil erodibility is less accurate for soils with high clay content, sandy loams, and soils with high organic matter (Stewart et al., 1975). Since the R/USLE parameters were developed based on studies of agricultural plots, there are uncertainties associated with using the original USLE at the catchment or regional scale (Nagle et al., 1999;

Naipal et al., 2015). Improvements and modifications to the R/USLE, especially to the LS-factor as detailed in the corresponding section, have made it applicable to larger scales, including a coarse resolution at the global scale (Naipal et al., 2015). The regional applicability is not the only issue of R/USLE, as the simplified empirical model does not capture the complexities associated with soil loss such as delivery to streams, streambank erosion, or mass wasting events.

The uncertainties from soil erosion modelling also stem from the low availability of long-term reliable data for modelling, which is a problem not unique to R/USLE applications and is more pressing for more complex models that have high data inputs (de Vente & Poesen, 2005; Hernandez et al., 2012). Its application in data-scarce regions leads to uncertainty in actual soil loss quantities, and such applications have reported erosion vulnerability as categories (low to extreme) rather than annual average amounts (Adornado et al., 2009; Schmitt, 2009). Even so, the R/USLE is seen as the preliminary attempt at estimating soil loss for a landscape due to its relative simplicity and less data requirements (Aksoy & Kavvas, 2005). Future work in soil erosion modelling could include assembling a comprehensive database of global, regional, and national soil erosion rates to allow comparison between soil erosion modelling methods, not just R/USLE results. Another proxy for understanding soil erosion is water quality data such as total suspended solids (TSS) that includes sediment delivery and organic sources (CESM, 2014). However, TSS usually excludes the larger and heavier bedload sediments that could be resulting from mass wasting events or erosion (Nagle et al., 1999). Related to this, assembling published estimates of R/USLE sub-factors from different climatic regions and soil types would help in sensitivity testing R/USLE equations, deciding the most appropriate equation to use, and verifying the derived R/USLE sub-factor values.

Another frequently-cited limitation is that the R/USLE estimates soil loss through sheet and rill erosion, but not from other types of erosion such as gully erosion, channel erosion, bank erosion, or from mass wasting events such as landslides (Nagle et al., 1999; Wischmeier & Smith, 1978). By excluding these types of erosion, the R/USLE may underestimate the actual soil loss (Thorne et al., 1985). The model also does not account for deposition, leading to overestimation, or sediment routing

(Desmet & Govers, 1996; Wischmeier & Smith, 1978). Since it does not predict the sediment pathways from hillslopes to water bodies, it is difficult to analyse possible effects on downstream areas, such as pollution or sedimentation (Jahun et al., 2015). One of the possible methods to link the R/USLE results to sediment delivery to streams is using the stream delivery ratio (SDR) defined as "the ratio of the sediment delivered at a location in the stream system to the gross erosion from the drainage area above that point" (Yoon et al., 2009). This parameter varies depending on the gradient, slope shape, and length and can also be influenced by land cover, roughness, etc. (Wu et al., 2005). Given that it is influenced by similar characteristics as the R/USLE, future work can include combining the R/USLE with the SDR to estimate sediment delivery to streams, but also avoiding possible double-counting. These two limitations of deposition and routing are linked to the model's representation of more topographically complex terrain, and previous studies have attempted to address it by improving on the LS-factor by incorporating upstream contributing area (Desmet & Govers, 1996; Moore et al., 1991).

Despite these drawbacks, the USLE family of models is still widely used because of is relative simplicity and low data requirements compared to more complex physically based models. Studies around the world continue to improve R/USLE parameterisation and application in different climate regimes and locations.

4.4 Future directions

Since the R/USLE and its family of models are used over different geographic locations and climate types, it is important for future research to build on them and improve their representation of real-world soil loss. Some of the future directions include incorporating soil loss from other types of erosion, estimating soil loss at seasonal or sub-annual temporal scales, and improving the consistency of formulae and units in the scientific literature.

4.4.1 Representing other types of erosion

The R/USLE accounts for rill and inter-rill erosion, but not for soil losses due to ephemeral gullies, which can lead to under-prediction of soil loss estimates (Thorne et al., 1985). In their research on improving the topographic factor in R/USLE, Desmet & Grovers (1996) recommended that delineation of ephemeral gullies combined with

R/USLE could improve the identification of vulnerable areas within a watershed. These ephemeral gullies are small channels that form due to the erosive action of overland flow during a rainfall event (Momm et al., 2012). One of the studies referenced by Desmet & Govers (1996) was work by Thorne et al. (1985) and the compound topographic index (CTI). This CTI is not to be confused with the CTI formulated by Beven and Kirkby (1979), which is used within TOPMODEL (a watershed model) to identify source areas for saturation overland flow and runoff that may cause soil erosion (Aksoy & Kavvas, 2005; Beven & Kirkby, 1979). Both indices utilise contributing area and slope, but the objective of Beven and Kirkby (1979) was to use topographic analysis to derive a relationship between basin storage and contributing area in order to predict basin response. On the other hand, the objective of Thorne et al. (1985) was to use topographic analysis to predict locations of ephemeral gullies based on upstream drainage area, slope, and the planform curvature.

Topography has a large influence on watershed hydrology due to its effects on soil moisture distribution and flow (Sørensen et al., 2006). In the USLE, the topography is accounted for in the LS-factor which is a function of slope length and steepness, which affects the rate of soil erosion due to water (Wischmeier & Mannering, 1968). Since the USLE was originally designed at the plot scale, its use causes issues when used at larger scales with more complex topography. R/USLE compensates for this by using a Geographic Information System (GIS) method of determining runoff contribution from upstream areas to downstream locations (de Mello et al., 2016). A common criticism of R/USLE is the exclusion of sediment yields from gully, streambank, and streambed erosion. Gully erosion can contribute a significant amount of sediment loss, such as 11,000 t km^{-2} yr^{-1} in the Waipaoa catchment in New Zealand (Basher, 2013). By only considering rill and inter-rill erosion through R/USLE, potential soil loss may be underestimated, hence the importance of adding gully erosion to the model (Thorne et al., 1985).

Similar work combining the effect of rill and sheet erosion with gully erosion was done by Momm et al. (2012) in Kansas, and by Zakerinejad and Maeker (2015) in the Mazayjan watershed in Iran. Momm et al. (2012) combined several types of erosion: sheet and rill, gully, and bed and bank erosion, with the sheet and rill erosion estimated using the R/USLE model. They used varying critical CTI thresholds to iteratively generate potential locations of ephemeral gullies, identify sub-watersheds prone to gully erosion, and use scenario analysis to estimate reductions in sediment yields under conservation practices (Momm et al., 2012). One of the limitations Momm et al. (2012) identified was of DEM size; since ephemeral gullies are small features (few metres wide, ~25cm deep), higher-resolution DEMs and LiDAR data would be better for topographic analysis. Another limitation was that topography is only one contributing factor to gully formation, and being able to include the effects of vegetation cover and soil properties could help improve the procedure (Momm et al., 2012). The Unit Stream Power Erosion Deposition Model (USPED), which is similar to the R/USLE model, has also been used to estimate rill and sheet erosion rates with a stream power index (SPI) approach to estimate gully erosion rates (Zakerinejad & Maerker, 2015). Zakerinejad & Maerker (2015) estimated gully erosion in tons hectare^{-1} year^{-1} and combined it with the estimates from the USPED model to produce a map showing potential erosion and deposition within their study area. Hence, there is indeed a precedent and a need to combine erosion estimates from R/USLE with a procedure that accounts for gully erosion for more effective land management.

4.4.2 Seasonal erosion vulnerability

R/USLE applications usually estimate soil loss at the annual timescale, while the MUSLE estimates soil loss from a single storm event (Renard et al., 1997; Sadeghi et al., 2014). As seen in the review of methods to calculate rainfall erosivity, many different studies have attempted to estimate the R-factor, underscoring its importance to soil erosion research. However, estimating the R-factor at the annual timescale does not account for seasonal variations in rainfall. It is useful for land management to understand seasonal variations in soil erosion vulnerability because of the dual effect of rainfall and land cover on soil loss, and the effect of rainfall on land cover (Kulikov et al., 2016). For example, when a season of heavy rainfall coincides with low vegetation cover, the risk of soil erosion increases considerably (Ferreira & Panagopoulos, 2014). Thus, most of the studies around seasonal estimations of soil loss revolve around changes in land cover and rainfall. The soil erodibility (K-factor) can vary too due to changes in permeability and the effects of freezing and thawing, but it is less frequently studied compared to variations in land cover and rainfall (López-Vicente et al., 2008).

Studies that incorporate seasonality in the R/USLE commonly compute R-factors and C-factors at monthly or seasonal time scales. Lu & Yu (2002) computed monthly R-factors in Australia, which was then used in a later study that computed C-factors based on satellite imagery and the NDVI, to produce monthly maps of soil erosion vulnerability over the entire Australian continent (Lu et al., 2003; Lu & Yu, 2002). The method of estimating C-factors using NDVI is popular due to the available of remotely-sensed imagery, and the capability of processing datasets with relative expedience compared to time-consuming fieldwork. Other studies have used the NDVI and similar characteristics to estimate monthly and seasonal C-factors in Brazil, Greece, and Kyrgyzstan (Alexandridis et al., 2015; Durigon et al., 2014; Ferreira & Panagopoulos, 2014; Kulikov et al., 2016; Panagos et al., 2012). The C-factors can also be estimated monthly through the method recommended by R/USLE, but requires knowledge of prior land use, canopy cover, surface roughness, and soil moisture (López-Vicente et al., 2008).

Monthly or seasonal estimations of rainfall factors are more useful to land management planning around crop growth cycles and tillage practices (Diodato, 2004). Studies have used different methods to calculate R-factors, with data requirements ranging from per-storm basis to annual averages. To estimate monthly and seasonal estimations, the required rainfall data can be as fine as individual storm intensity to use the R/USLE method, or be as coarse as average monthly rainfall. Diodato (2004) in Italy and Kavian et al. (2011) used the R/USLE method to calculate storm energy and summed these up per month and season to obtain R-factors. Other studies used daily and monthly rainfall to calculate monthly R-factors and combine them for seasonal R-factors (Alexandridis et al., 2015; Kavian et al., 2011; López-Vicente et al., 2008; Lu et al., 2003; Panagos et al., 2015a; Shamshad et al., 2008). The results of these studies focused on identifying high and low periods of the landscape's vulnerability to soil erosion, depending on combinations of rainfall intensity and land cover.

At the baseline scenario, applying the R/USLE can give management an idea of which areas are vulnerable to soil erosion. Previous work by Alexandridis et al. (2015)

and Ferreira & Panagopoulos (2014) have looked at seasonal variations in soil loss due to land cover using satellite imagery from different times of the year. These approaches are useful in determining soil loss based on previous or existing land cover, but the next step is using scenario analysis to help land management. Scenario analysis can include a myriad of options: expanded urban areas or development, changing crop rotation cycles, or applying support practices in steep or upland areas. By adding seasonal effects, it gives additional knowledge of when these vulnerable areas may be even more vulnerable. Thus, by using scenario analysis, management can test several types of crop and support practices to see their possible effect on soil erosion mitigation. Soil erosion also affects water quality because of sediment delivery to streams and rivers, which raises concerns about access to clean water for drinking and for recreational use. Therefore, understanding seasonal soil erosion is beneficial to local government who can address potential sources of sediment delivery before the problem occurs and be more proactive in their land management.

4.4.3 Consistency in units

The USLE was originally developed using imperial units. Although the handbook provides conversion factors to convert to metric, there are still issues within the scientific literature regarding units. In the process of this review, it was noted that although most studies used the metric units for R-factor and K-factor, there were other studies that did not report their units or had units that were not the imperial or metric units of R/USLE. The problem of unclear or inconsistent units causes problems for future researchers in terms of adapting the rainfall erosivity or soil erodibility equations for their own study sites. To convert from imperial to metric units, Renard et al. (1997) recommends a conversion factor of 17.02 for R-factor and 0.1317 for K-factor. Since the original R/USLE was formulated with US customary units, researchers must be careful to use the correct units and conversions to metric (Renard & Freimund, 1994).

4.5 Summary and conclusion

This chapter reviewed the different components of the Universal Soil Loss Equation (USLE) and its updated form, the Revised Universal Soil Loss Equation (RUSLE). Different studies around the world were collected and analysed to compile how they adapted R/USLE to their unique conditions, how they had calculated rainfall erosivity with only the data available in their study site, and how these methods have been used by subsequent soil erosion studies. At the end of each factor section, a brief summary is given outlining which datasets and equations would be useful for new users depending on their location and data availability. Each factor section also clarifies some of the assumptions and limitations associated with the original R/USLE models.

This chapter also presented some of the model's limitations and outlined a few future directions: incorporating soil loss from other types of soil erosion, importance of estimating soil loss at sub-annual scales and recommended equations, and consistency in reporting units in future literature. At first glance, the USLE and its family of models seems like a relatively straightforward linear model. However, this review shows the difficulty in finding the most appropriate method of calculating its factors depending on location, availability of data, and previous studies done in nearby or similar regions. It is important for future researchers to consider which equations they adapt to their study area and consider testing multiple methods of calculating one factor to see how the results affect soil loss estimates. The main purpose of this chapter was to provide a reference point for future soil researchers by compiling equations for the R/USLE factors, references for C-factors and P-factors, and finding previous studies that may be relevant to their own work for their further investigation and literature review. In the end, the choices made regarding applications of the R/USLE depend on the kind of data that is available for a study area, and how they can adapt or change information from other studies to suit their area's climate, soil type, topography, typical land cover, and support practices. The studies reviewed for this chapter influenced the equations and methodology of the RUSLE applications in the CDO catchment and in the Mangatarere catchment to identify regions vulnerable to soil loss.

5 Estimating soil erosion losses in the Cagayan de Oro catchment (Philippines) using the RUSLE under different land cover scenarios

5.1 Introduction

The previous chapter reviewed the Revised Universal Soil Loss Equation (RUSLE) and its family of models, and their global application. This chapter focuses on soil erosion in the Philippines, specifically testing the RUSLE under three different land cover scenarios. Of the hilly lands of the Philippines, almost half are used for cultivation and the combination of high rainfall, reduced vegetation cover and steep slopes has led to severe problems in soil erosion and agricultural productivity (Paningbatan et al., 1995). The average soil erosion rate in the Philippines was reported to be 80 tons hectare^{-1} year^{-1} (Francisco & Angeles, 1998), with large variation depending on region and land use ranging from 3 tons hectare^{-1} year^{-1} in secondary forest to almost 300 tons hectare^{-1} year^{-1} in grassland and pastureland. Due to the magnitude and gravity of this problem, it is important for land management to identify the area most vulnerable to soil erosion for mitigation options (David, 1988).

Previous RUSLE studies in the Philippines had several common conclusions. The agricultural areas were consistently identified as being vulnerable to soil erosion, especially in areas of upland agriculture. Through scenario analysis, models predicted lower soil loss rates in areas of reforestation and areas that implement conservation measures such as line planting and agroforestry. The limitations across RUSLE studies were also similar: availability of high-resolution temporal and spatial data to calculate RUSLE factors, lack of validation data, and a lack of understanding the sediment transport from typhoons.

David (1988) did an extensive review of soil and water conservation studies in the Philippines, including recommendations on how to calculate the different components of USLE. Previous RUSLE studies in the Philippines have applied the model in watersheds and islands that have large agricultural areas for identifying vulnerable areas, and for scenario analysis (Figure 64). Adornado et al. (2009) used the RUSLE to assess erosion vulnerability in the Quezon Province and to produce a hazard map, citing the dense vegetation as mitigating factors and the existing eroded areas and high rainfall as exacerbating factors for soil erosion in the area. Building on that work, Adornado & Yoshida (2010) applied the RUSLE to the Bukidnon province, which includes parts of the CDO watershed, and identified the steep mountain slopes and agricultural areas as more vulnerable. However, their quantification of soil loss rates in the mountainous region may have been overestimated due to a lack of a robust soil erodibility factor. The areas mapped as undifferentiated mountain soil were given an erodibility factor of 1, the highest possible erodibility value for any given soil within RUSLE (Adornado & Yoshida, 2010).

In terms of scenario analysis, Schmitt (2009) applied the RUSLE over Negros Island and found that the estimated soil erosion rates were lower in the scenario of coconut cultivation adopted on all steep lands compared to conventional farming practices. This study also highlighted limitations of applying RUSLE to a data-poor location: lack of historical field data to validate the model, and the uncertainties in the model results, suggesting that a categorical representation of vulnerability may be more useful (Schmitt, 2009).

The RUSLE was integrated into more complex models and frameworks in the Philippines. Delgado & Canters (2012) applied the WaTEM/SEDEM model, a spatially distributed soil erosion model that utilises a form of RUSLE for its estimates, to three catchments in Claveria. Similar to those of Adornado et al. (2009) and Adornado & Yoshida (2010), they conclude that intense agricultural activity, especially on steep slopes, make the area more vulnerable to soil erosion and they stress the need for conservation practices such as agroforestry. Hernandez et al. (2012) used a combination of RUSLE, SedNet, and a proxy for gully density and erosion to predict soil loss in the Pagsanjan-Lumban catchment. Their research predicted reduced sediment export through reforestation of existing coconut plantations and agriculture areas on steep slopes (Hernandez et al., 2012). Hernandez et al. (2012) also noted that these estimates could contain considerable uncertainty due to data availability, possible underestimation of sediment transport rates, and the inability to account for the effect of sediment transport from typhoons.

An application of Bantayan & Bishop (1998) to the Makiling Forest Reserve integrated RUSLE into a model for ranking land use options and priorities, such as recreation, food production, water sources and soil stability. This application shows the utility of RUSLE in a larger decision-making context when deciding between different priorities, such as analysing trade-offs between ecosystem services.

Table 32. Previous USLE and RUSLE studies in the Philippines, their location, and sources of factors.

Author	Location	R-factor	K-factor	LS-factor	C-factor	P-factor
David (1988)	Various watersheds in the Philippines	Mihara (1951) and Hudson (1971) as cited in David (1988)	Wischmeier and Mannering (1969)	Madarcos (1985) and Smith & Whitt (1947)	Literature	Literature
Adornado et al. (2009)	REINA (Philippines)	El-Swaify et al. (1987) as cited in Post & Hartcher (2006)	Table by Stewart et al. (1975)	Upslope contributing area method	Literature	None observed (P=1)
Schmitt (2009)	Negros Island (Philippines)	RUSLE method	USLE method	RUSLE method at pixel level	Literature	Previous studies
Adornado and Yoshida (2010)	Bukidnon (Philippines) and also REINA (Philippines)	El-Swaify et al. (1987) as cited in Post & Hartcher (2006)	Table by Stewart et al. (1975)	Upslope contributing area method	Literature	None observed (P=1)
Delgado & Canters (2012)	Claveria (Philippines)	Shamshad et al. (2008)	USLE method	RUSLE2 programme, using the upslope contributing area method	Literature	Literature
Hernandez et al. (2012) (used SedNet, which has an USLE component)	Pagsanjan (Philippines)	El-Swaify et al. (1987) as cited in Post & Hartcher (2006)	Wischmeier and Mannering (1969)	Algorithm within SedNet	Literature	

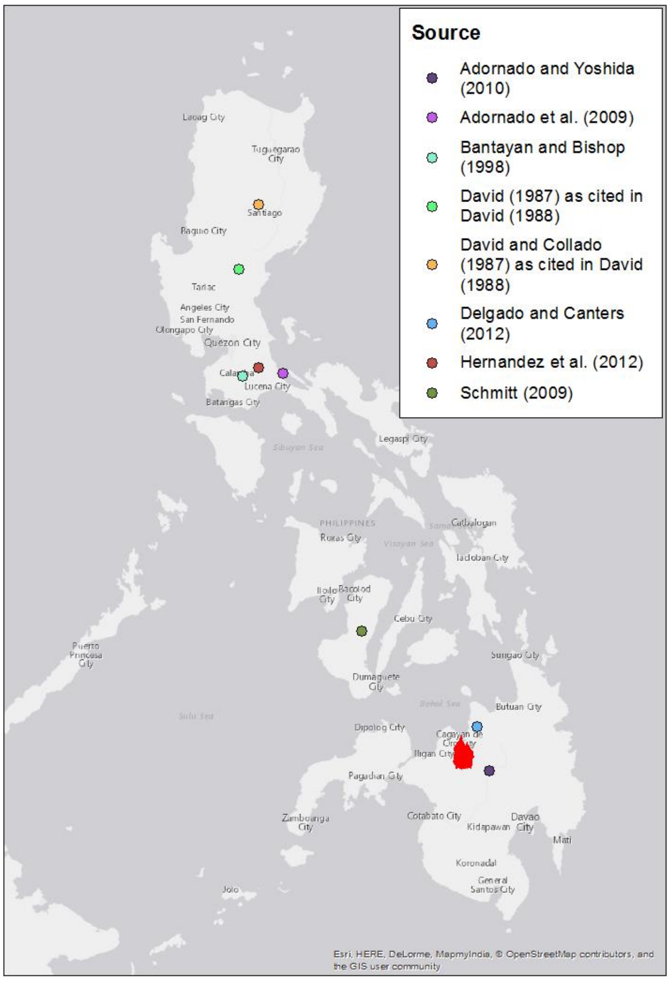

Figure 64. Map of previous RUSLE studies in the Philippines, with the CDO catchment in red.

5.2 Aim and objectives

The research in this chapter builds on the existing work of soil erosion in the Philippines by applying the RUSLE to the CDO catchment. One of the goals of this research is to develop a more robust method of estimating soil erosion and sediment transport within a GIS environment, and to eventually create a Python-based toolbox that can be used within the LUCI framework for its sediment transport operations. Originally, the Compound Topographic Index was intended to be applied to the CDO catchment. The CTI is used to identify areas susceptible to ephemeral gully erosion. However, the application of CTI in CDO would be inappropriate due to a lack of a high-resolution DEM. Ephemeral gullies can be less than a few metres wide, and since the DEM has a spatial resolution of ~30m, it is too coarse to delineate the microtopography and curvature that causes ephemeral gullies to form. Therefore, the focus of this chapter will be on testing RUSLE components in CDO and analysing changes in soil loss over three different land cover scenarios of baseline land cover, and future river basin development plans outlined by the local government. Scenario analysis of changes in land cover and management practices was previously done in the Philippines by Schmitt (2009) and Hernandez et al. (2012), but their research was not in the CDO catchment.

The specific objectives are as follows:

- Assess the sensitivity of different methods for calculating RUSLE factors.
- Use the RUSLE to estimate soil erosion losses for different land use scenarios.

5.3 Methodology

This study was undertaken in CDO catchment in the Philippines, which was described in the introductory chapter (Chapter 1) and whose data sources and land cover scenarios are outlined in the methodology chapter (Chapter 2). After collecting input data and land cover scenarios, equations for calculating the RUSLE factors were gathered from literature, focusing on sources that applied the RUSLE to a tropical climate like Cagayan de Oro. These sources included studies previously undertaken in the Philippines, Malaysia, and Thailand (Table 33). For the land cover and support practice factors, the values were taken from David (1988) or from other studies that focus on specific conservation measures such as line planting or alley cropping. All these combinations were run in ArcMap 10.4.1 to estimate soil loss in tons hectare^{-1} year^{-1}. In addition to these annual runs, monthly RUSLE runs were done for the baseline scenario to assess seasonal variations in soil loss, producing soil loss estimates in tons hectare^{-1} month^{-1}.

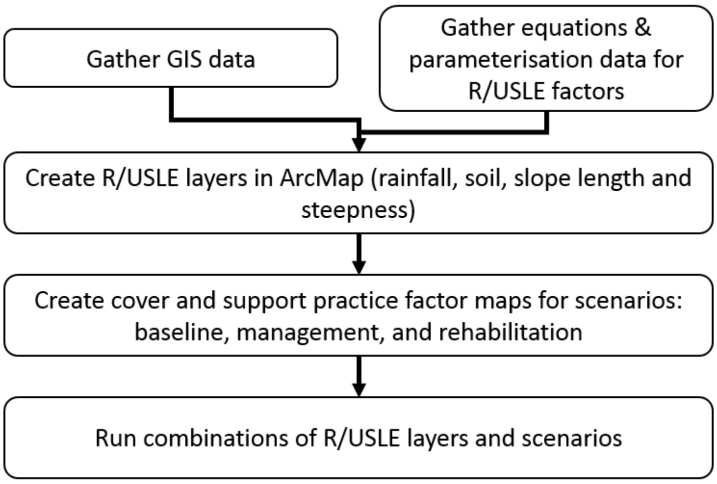

Figure 65. Basic methodology of the modelling runs in this chapter.

5.3.1 USLE equations and sensitivity analysis

5.3.1.1 Rainfall erosivity (R-factor)

The original calculation for the rainfall erosivity factor involves analysing the energy of storm events (EI_{30}) that occurred within the study area, requiring detailed rainfall data that was unavailable for CDO study area due to gauges stopping recording over the course of the study. Instead, multiple equations from other studies were used to calculate a range of possible R-factors from annual or monthly precipitation data.

Table 33. Rainfall erosivity factor equations used in this research.

#	Source	Original Location	Equation	Previous applications in Philippines
1	Shamshad et al. (2008)	Malaysia	$R = \sum_{i=1}^{12} 227 \times \left(\frac{P_i^2}{P}\right)^{0.548}$ P_i = Monthly rainfall P = Annual rainfall Units: Megajoule •millimetre • hectare^{-1} • hour^{-1} • year^{-1}	Delgado and Canters (2012)
2	El-Swaify et al. (1987) as cited in Merritt et al. (2004)	Thailand	$R = 38.5 + 0.35P$ P = Annual rainfall Units: tons • hectare^{-1} • year^{-1}	Adornado et al. (2009); Adornado and Yoshida (2010); Hernandez et al. (2012)
3	Sholagberu et al. (2016)	Malaysia	$R = 0.0003P^{1.771}$ P = Annual rainfall Units: Megajoule •millimetre • hectare^{-1} • hour^{-1} • year^{-1}	
4	Roose (1975) as cited in Morgan (2005)	Malaysia	$R = (9.28 \times P - 8838)\left(\frac{75}{1000}\right)$ P = Annual rainfall Units: Megajoule •millimetre • hectare^{-1} • hour^{-1} • year^{-1}	

These equations were chosen due to the location of their original study: Thailand and Malaysia are two tropical countries also located in Southeast Asia. The equation by El-Swaify et al. (1987) was chosen because it has been used in several studies in the

Philippines. The equation by Shamshad et al. (2008) was applied in the Philippines by Delgado & Canters (2012) and utilises monthly precipitation. This allows the equation to be used for monthly estimates of soil loss which are useful in a catchment that has high temporal variation of rainfall throughout the year.

Panagos et al. (2017) has produced a global rainfall erosivity map at a resolution of ~1km and uses rainfall data from 3,625 stations in 63 countries. This map was also included in this analysis because it gives an idea of the spatial variation of rainfall erosivity within the CDO catchment (Figure 66). The map shows mostly higher rainfall erosivity over most of the catchment, with lower erosivity around the coastal urban area (north) and mountain slopes (southeast).

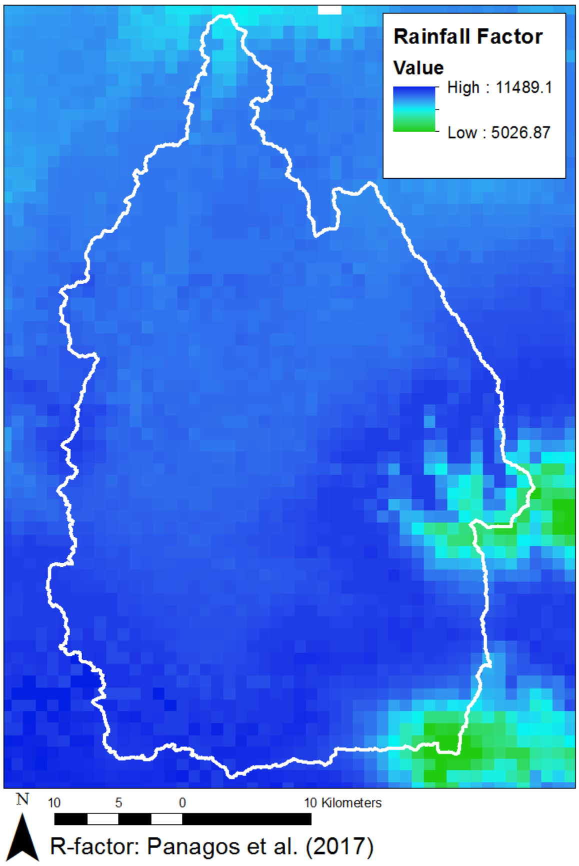

Figure 66. Subset of the Panagos et al. (2017) rainfall erosivity map (R-factor) over the Cagayan de Oro catchment.

5.3.1.2 Soil erodibility (K-factor)

The equation below by David (1988) was chosen due to its relative simplicity of requiring only textural information, organic matter, and pH. By contrast, the original RUSLE K-factor equation also requires information on soil-structure code and profile-permeability that was not available for the soils in the CDO catchment.

$$K = [(0.043 \times pH) + (0.62 \div OM) + (0.0082 \times S) - (0.0062 \times C)] \times Si \times 0.1317$$

Where:

pH	pH of the soil
OM	Organic matter in percent
S	Sand content in percent
C	Clay ratio = % clay / (% sand + % silt)
Si	Silt content = % silt / 100

To calculate the soil erodibility, the following information was taken from the IGBP-PTF dataset for each of the subgroups present in the watershed:

- Textural information (sand, silt, clay, very fine sand)
- pH
- Organic carbon (converted to organic matter by multiplying by 1.72 (Pribyl, 2010))
- Texture class

This alternative method of estimating K-factors based on the relationship between K-factor, textural information, organic matter, and pH proposed by Wischmeier and Mannering (1968). The original imperial units for K-factor are ton × acre × hour × hundreds of acre^{-1} × foot^{-1} × tonf^{-1} × inch^{-1}. Multiplying by 0.1317 gives SI units of metric ton × hectare × hour × hectare^{-1} × megajoule^{-1} × millimetre^{-1}. This equation was used to calculate representative K-factors of Philippine soils based on textural class, ranging from 0.07 to 0.63 (SI: 0.009 to 0.08) (David, 1988).

5.3.1.3 Slope length and steepness (LS-factor)

The equations in Table 34 were chosen for testing due to several reasons. The equation by David (1988) is relatively simple, but only uses slope in percent as an input to account for steepness but does not seem to account for slope length. The equation for Morgan (2005) accounts for slope length and steepness and is very similar to the original method used by RUSLE to calculate the LS-factor. The equation by Desmet & Govers (1996) used slope length, steepness, and flow accumulation to calculate LS-factor and has risen in popularity due to its capability to account for the convergence and divergence of flow, thus allowing for application in more complex terrain.

Table 34. Slope length and steepness factors used in this research.

#	Source	Equation	Previous applications in Philippines
1	David (1988)	$LS = a + bS_L^m$ a = 0.1 b = 0.21 m = 4/3 S_L = slope in percent	
2	Desmet and Govers (1996), similar to equations by Moore & Burch (1986) as cited in Mitasova et al. (1996) and Mitasova et al. (2013)	$LS = (m+1)\left(\frac{U}{L_0}\right)^m \left(\frac{\sin\beta}{S_0}\right)^n$ U (m^2m^{-1}) = upslope contributing area per unit width as a proxy for discharge $U = Flow\ Accumulation \ \times Cell\ Size$ L_0 = length of the unit plot (22.1) S_0 = slope of unit plot (0.09) β = slope m (sheet) and n (rill) depend on the prevailing type of erosion (m= 0.4 to 0.6) and n (1.0 to 1.3)	Adornado et al. (2009); Adornado and Yoshida (2010); Delgado and Canters (2012)
3	Morgan (2005) but previously published in earlier editions	$LS = \left(\frac{l}{22}\right)^{0.5} (0.065 + 0.045s + 0.0065s^2)$ l = slope length (m) s = slope steepness (%)	

5.3.1.4 Cover factor (C-factor) and support practice factor (P-factor)

The values for land cover factors were taken from David (1988) because the paper reports approximate C-factors for land cover typically found in the Philippines. Using cover factors from the original RUSLE sources is common, but a limitation is that the original RUSLE was formulated in the United States and does not have values for crops that are specific to tropical countries.

Table 35. Cover factors from David (1988) for the baseline scenario.

Land cover class	C-factor (David, 1988)	Description (David, 1988)
Other wooded land, shrubs	0.15	Shrubs with patches of open, disturbed grasslands
Other land, natural, grassland	0.3	Grassland, moderately grazed, burned occasionally
Other land, cultivated, annual crop	0.3	Diversified crops
Other land, cultivated, perennial	0.08	Mixed stand of agroforestry species
Other land, built-up area	0.2	Built-up rural areas, with home gardens
Closed forest, broadleaved	0.001	Primary forest with dense undergrowth
Open forest, broadleaved	0.003	Second growth forest with good undergrowth
Inland water	0.001	Same as closed forest
Forest plantation, broadleaved	0.07	Mixed stand of industrial tree plantation (ITP) plant species, 8 years or more
Other wooded land, wooded grassland	0.007	Grasslands, well established and undisturbed
Pineapple	0.35	Annual cash crops, pineapple

Since there is information regarding potential conservation practices in the river basin management report, this research accounts for these practices through the P-factor instead of ignoring it, as was common in previous studies (CESM, 2014). Agricultural Zone 2 has a P-factor of 0.55 because of the planned practice of contour farming in that zone, and Agricultural Zone 3 has a lower C-factor of 0.25 due to the recommendation of fruit orchards within that zone. Similarly, the agroforestry sub-zone has a P-factor of 0.4 due to the recommendation of line planting, while the private agroforestry sub-zone has a P-factor of 0.01 due to the recommendation of Sloping Agricultural Land Technology (SALT). SALT is an agroforestry scheme where crops are planted between hedgerows to reduce soil erosion and increase crop yields through diverse perennial crops and nitrogen-fixing tree species (Tacio, 1993). The P-factor for SALT was estimated from a soil loss study in the Philippines since it is a ratio of soil loss under a particular management practice compared to no management practices occurring (Laquihon & Pagbilao, 1998).

Table 36. Cover and support factors from David (1988) for the management scenario.

Management Land Cover	C-factor (David, 1988)	P-factor (David, 1988)
Agricultural Sub-zone	0.3	
Agricultural Zone 1	0.3	
Agricultural Zone 2	0.3	0.55
Agricultural Zone 3	0.25	
Agroforestry Sub-zone	0.16	0.4
Forest Restoration Sub-zone	0.003	
National Park	0.001	
Natural Park	0.001	
Private Forest Sub-zone	0.003	
Private Agroforestry Sub-zone	0.16	0.01
Private Forest Sub-zone	0.003	
Strict Protection Zone	0.003	
Timber Production Sub-zone	0.03	
Timber Regeneration Sub-zone	0.075	

Similar to the management scenario, the cover and support factors (Table 37) for the rehabilitation scenario were chosen based on information about the recommended conservation strategies in those areas (CESM, 2015). The agroforestry zones have a P-factor of 0.4 based on David (1988), and the conservation farming zones have a P-factor of 0.05 due to the recommendation of using alley cropping in those zones. This P-factor was estimated from a study in the Philippines that published soil loss rates for plots that had conventional and alley cropping treatments (Paningbatan et al., 1995).

Table 37. Cover and support factors from David (1988) for the rehabilitation scenario.

Rehabilitation Land Cover	C-factor (David, 1988)	P-factor
City	0.2	
Agroforestry	0.08	0.4
Reforestation	0.003	
Recommend Agroforestry	0.08	0.4
Recommend Reforestation	0.003	
Practice Conservation Farming	0.3	0.05
Protection	0.001	
Assisted Natural Regeneration	0.003	
Recommend Conservation Farming	0.3	0.05

5.3.2 Estimating soil erosion losses

After all the RUSLE factors were calculated, they were converted to raster layers and multiplied together in the Raster Calculator to obtain an estimate of annual soil loss using only the RUSLE equation over several different combinations. For the monthly RUSLE runs, the Shamshad et al. (2008) equation was used to calculate rainfall erosivity for each month using CESM and WorldClim data. At the monthly time-step, only the baseline scenario was used as cover input.

Table 38. Summary of RUSLE factors used for in this research.

Rainfall Erosivity Factor	Soil Erodibility Factor	Slope Length and Steepness Factor	Cover and Support Practice Factor
• Panagos et al. (2017) • Shamshad et al. (2008) using CESM Data • Shamshad et al. (2008) using WorldClim Data • Sholagberu et al. (2016) using CESM Data • Sholagberu et al. (2016) using WorldClim Data • El-Swaify et al. (1987) using CESM Data • El-Swaify et al. (1987) using WorldClim Data • Roose (1975) using CESM Data • Roose (1975) using WorldClim Data	• David (1988)	• David (1988) • Desmet and Govers (1996) • Morgan (2005)	• Baseline • Management • Rehabilitation

Previous RUSLE studies in the Philippines have highlighted the considerable uncertainties associated with soil erosion modelling, since the RUSLE's relative simplicity cannot capture all the processes associated with soil erosion and sediment transport. Hence, work by Adornado et al. (2009) and Adornado & Yoshida (2010) has recommended a focus on making maps showing risk categories of soil erosion may be more useful than a graduated map of soil loss estimates. Their categorisation (Table 39) is used in the maps of soil loss risk produced by this research.

Table 39. Erosion risk classes and ranges as recommended by Adornado et al. (2009) and Adornado & Yoshida (2010).

Erosion Risk Class	Erosion Range (ton hectare^{-1} year^{-1})
None to slight	0 to 5
Moderate	5 to 15
High	15 to 50
Very high	50 to 150
Severe	150 to 300
Very severe	> 300

5.4 Results & Discussion

This section is divided into two parts: the results of using different equations for RUSLE components and how they differ between equations, and the actual soil loss estimates under the different combinations of factors and scenarios (Table 38).

5.4.1 USLE factors and sensitivity analysis

5.4.1.1 Rainfall erosivity (R-factor)

The estimated R-factors across the different equations have a wide range, between 286 MJ mm ha^{-1} hr^{-1} yr^{-1} for the lowest and 13,251 MJ mm ha^{-1} hr^{-1} yr^{-1} for the highest estimated value (Table 40). The rainfall erosivity in the CDO catchment from Panagos et al. (2017) ranges from 5,026 to 11,489 with a mean of 10,252.

Table 40. Estimated rainfall erosivity from the different R-factor equations and rainfall data.

Equation Source	R-factor from CESM Data	R-factor from WorldClim Data
Shamshad et al. (2008)	12,777	13,251
Sholagberu et al. (2016)	286	324
El-Swaify et al. (1987) as cited in Merritt et al. (2004)	870	931
Roose (1975) as cited in Morgan (2005)	991	1,112

By comparison, the range of R-factors for different watersheds in the Philippines reported by David (1988) ranged from 1,821 and 5,600. Shamshad et al. (2008) and

Panagos et al. (2017) provided estimates above this range, while the other erosivity equations provided estimates below this range. The rainfall erosivity estimates of David (1988) use an equation that requires daily rainfall, but also ignores any days that have less than 25mm of precipitation. This means that areas that experience intense storms over short periods are treated differently in the equation compared to areas that experience lighter rain over a longer period. In the CDO catchment, the climate is characterised by a dry season lasting between one to three months, with the rainy season not as pronounced as the other climate types in the Philippines (CESM, 2015). In terms of intense rainfall, the area experiences less tropical cyclones compared to the northern part of the Philippines, meaning that the way that rainfall affects soil erosion in CDO may be driven by lighter but frequent rainfall events compared to more intense one-off storm events. This difference of short-intense rainfall events or long-light rainfall events being more frequent in an area is important when applying R-factor equations from a different study site.

The results from the Shamshad et al. (2008) equation are high within the CDO catchment, but their study area in Malaysia had a mean annual rainfall of 2,500mm and runs over multiple years produced R-factors ranging from 9,000 to 14,000. This is similar to the annual rainfall that occurs in CDO and the estimated R-factors from the Shamshad et al. (2008) equation still fall within the expected range of R-factors for a location similar to Malaysia (Chapter 4).

In terms of the results from the Panagos et al. (2017) dataset, the lowest R-factor predicted for CDO is in the upper range of R-factors reported by David (1988). The erosivity map was generated through relating R-factors calculated from high-resolution rainfall data and climatic covariates from the global WorldClim dataset regarding rates of precipitation and seasonality (Panagos et al., 2017). One drawback is that the Panagos et al. (2017) analysis did not include rainfall data from the Philippines, but the closest weather stations used were in Peninsular Malaysia. In terms of tropical locations around the world, Panagos et al. (2017) reported a mean of 7,105 with a range of ~5,000 to ~11,000. Given the similarities and overlapping values, and the fact that the Panagos et al. (2017) map relates R-factors with local climate variables that have spatial and temporal variation, the Panagos et al. (2017) results may be more suitable for RUSLE modelling in CDO but will require further testing and comparison with R-factors calculated in the Philippines.

The other three equations (Sholagberu et al. (2016), El-Swaify et al. (1987), Roose (1975)) all produce R-factors for CDO that are very low compared to the range of R-factors reported by David (1988). The Sholagberu et al. (2016) equation was derived from time-series analysis that ignores days below 10mm of rainfall, bringing back the original question of whether short-intense rainfall events or long-light rainfall events are the driving factor of erosion in a particular area. The estimated R-factor for CDO (286 and 324) was much lower than the estimated R-factor range for the Malaysian study site (690 to 1,924) even though the annual precipitation rates were similar (Sholagberu et al., 2016). When compared to global R-factors of Panagos et al. (2017), these values of 286 and 324 for CDO are similar to values for arid areas in the Middle East and Northern Africa. The El-Swaify et al. (1987) equation was used by previous studies in the Philippines, which is why it was chosen for analysis in this research, and again produced R-factors that were low compared to the ranges reported by David (1988) and global range of tropical R-factors reported by Panagos et al. (2017). Another oddity of this equation is the reporting of units: previous studies that used it do not report the units and the English source of Merritt et al. (2004) reports the units for this equation to be in tons hectare^{-1} year^{-1}. This inconsistency with the original RUSLE units causes problems when plugged into the RUSLE model. Lastly, the Roose (1975) equations predicts similar results to the El-Swaify et al. (1987) equation, far below estimated ranges of R-factors in the Philippines and in tropical areas (David, 1988; Panagos et al., 2017).

Monthly rainfall erosivity followed the same pattern of highs and lows as the rainfall (Figure 67). The most vulnerable months were when the monsoon season occurs in the Philippines, while the drier periods had lower rainfall erosivity. The dry season in the CDO catchment occurs during December to April, with rainfall being evenly distributed during the rest of the year (CESM, 2014). Despite this, the typhoons Washi (2011), Bopha (2012), Jangmi (2014) and Tembin (2017) all occurred in December during the drier season. The occurrence of these extreme events is an important component of soil erosion research due to event-based erosion. Hence, one of the components of future work is to model the event-based erosion in CDO which can cause landslides and issues with water quality.

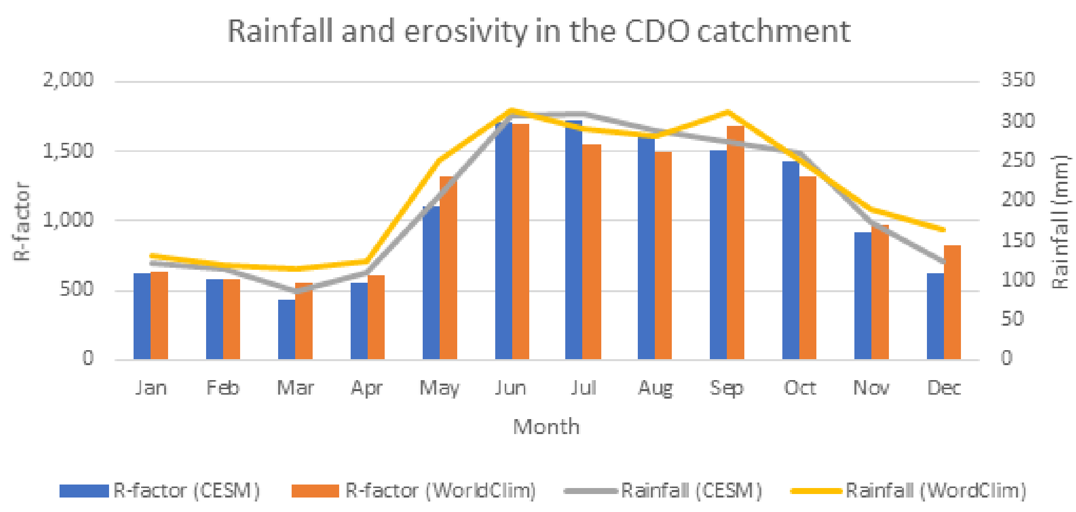

Figure 67. Monthly rainfall and erosivity in the CDO catchment.

It is difficult to compare these R-factor estimates with previous RUSLE studies in the Philippines because they tend to report overall soil loss estimates rather than the results for each factor. Therefore, the points of reference for R-factors obtained in this study are the R-factors reported by David (1988), and the resulting soil loss estimates compared to published rates of soil loss in the Philippines.

5.4.1.2 Soil (K-factor)

The equation proposed by David (1988) produced some K-factors that exceeded 1.0, which is beyond the range of the K-factor. This may be due to some limitations of the original equation involving the textural characteristics, pH, and organic matter. These values were excluded before converting them to SI units, and the mean K-factor for each group was taken as the K-factor used in this analysis (Table 41). The range of K-factors for Philippine soils reported by David (1988) was from 0.009 to 0.083 while the range used by Adornado et al. (2009) was from 0.013 to 0.036 in SI units. The K-factors used in CDO fall within the range specified by David (1988) but is above the range reported by Adornado et al. (2009).

Table 41. Estimated K-factors for the different soils present in the CDO watershed.

USDA Subgroup	Local Soil Name	K-factor (David, 1988)
Fluventic Eutropepts	San Manuel loam	0.048
Typic Hapludalfs	Bolinao clay Alimodian clay	0.044
Typic Hapludults	Jasaan silt loam Jasaan clay loam	0.047
Typic Paleudults	Adtuyan clay Mountain soil (undifferentiated)	0.038

Over the soils present in the CDO watershed, the K-factors were quite similar to each other. San Manuel loam, Jasaan silt loam, and Jasaan clay loam have higher values compared to the other soil types. Loams and silt loams are more vulnerable to detachment compared to the other soil types, and these results are consistent with that: San Manuel loam and Jasaan silt loam having a slightly higher K-factor compared to the clays (Morgan, 2005). The clay soils have lower K-factors, also consistent with the principle that finer soils are more resistant to detachment (Morgan, 2005).

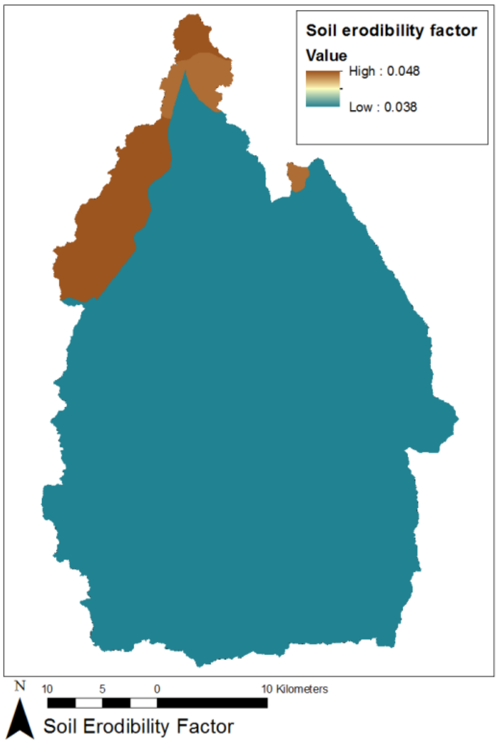

Figure 68. Soil erodibility over the CDO watershed.

5.4.1.3 Topography (LS-factor)

Across the three LS-factor equations, the mean values were 19 for David (1988), 11 for Morgan (2005), and 23 for Desmet & Govers (1996). By comparison, the mean LS-factors for countries in the EU using the Desmet & Govers (1996) method ranged from 0.32 to 5.20 (Panagos et al., 2015b). These LS-factors for the EU were limited to slopes less than 50%, hence the lower LS-factor values compared to the CDO estimates. Although the means do not differ by large amounts, the maximum LS-factor produced by the method of Desmet & Govers (1996) is higher than the other two methods by two orders of magnitude (Figure 69). This is due to the fact that Desmet & Govers (1996) uses flow accumulation as one of the variables in its equation, leading to high maximum values of LS-factors in large watersheds.

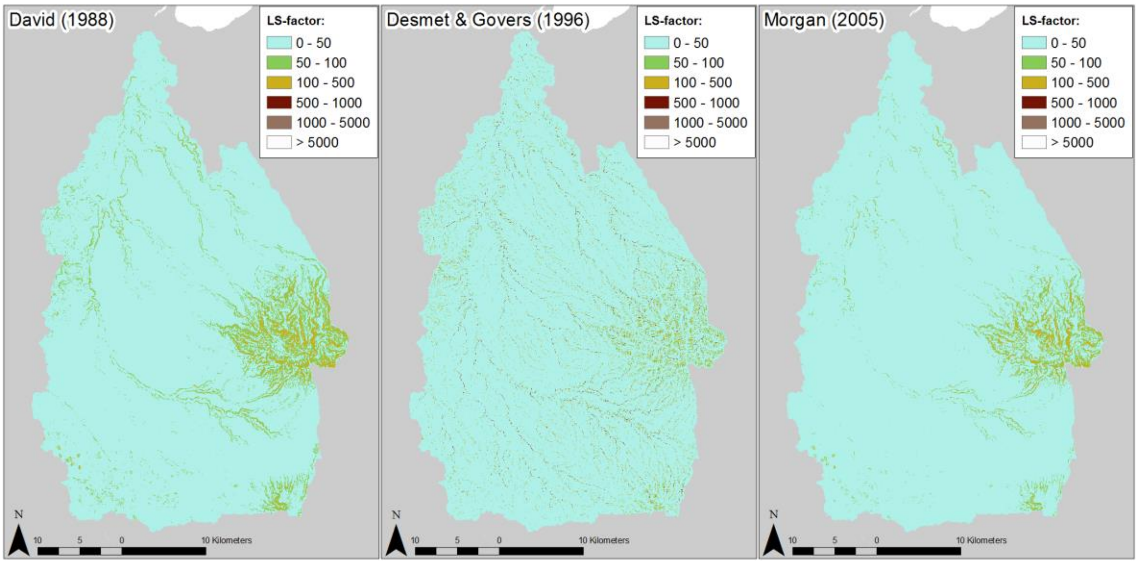

Figure 69. LS-factor maps for the three different methods of calculating LS-factor.

Although the actual values produced by the David (1988) and Morgan (2005) techniques are different, a visual analysis of the maps shows they are identifying similar areas of high and low LS-factors. These areas are steep slopes associated with river valleys and mountainous areas in the eastern part of the CDO catchment. The highest LS-factor values produced by Desmet & Govers (1996) are also associated with the stream network that are the areas of high flow accumulation. This method, and similar methods incorporating flow accumulation, are popular in the RUSLE literature because of their ability to account for complex terrain. However, at the watershed level with high flow accumulation, the large LS-factors may skew the estimated soil loss and lead to over-prediction of soil loss estimates. At smaller scales such as the sub-watershed level and with a finer resolution DEM, the Desmet & Govers (1996) technique allows pixel-level assessment of soil loss vulnerability. At the watershed level with a coarse resolution DEM, the Morgan (2005) technique is more suitable for outlining large areas that can be targeted for management interventions.

5.4.1.4 Land cover and support practice (C-factor and P-factor)

Based on the C-factor maps (Figure 70), the development and rehabilitation scenarios look very similar in terms of how the watershed is going to be divided into zones of different land use. The main exception is the area at the south of the watershed, which is zoned for agricultural use in the management scenario but for reforestation in the rehabilitation scenario. Across all scenarios, the highest C-factor values correspond to agricultural activities while the lowest values correspond to forested areas. In the management and rehabilitation scenario, since conservation measures were recommended, P-factor maps (Figure 71) were produced with appropriate values relating to alley-cropping, contour-farming, and line-planting. Although the P-factor is ignored in much of the RUSLE literature, it is important in research involving scenario analysis when considering different support practice factors over the same land cover.

One of the limitations in the rehabilitation scenario relates to areas where forest rehabilitation is currently taking place or planned to take place in the future. The rehabilitation scenario assumes that the trees have already been planted and established, which gives them a lower C-factor compared to newly-planted trees or a reforested area that is still being established. This can be addressed in the future through approximating values for tree growth that range between the value for newly-planted/young trees and the value for mature and well-established trees. David (1988) has some approximate values for Philippine hardwood trees between 3 to 8 years (0.05 to 0.10) and the same species of trees older than 8 years (0.01 to 0.05).

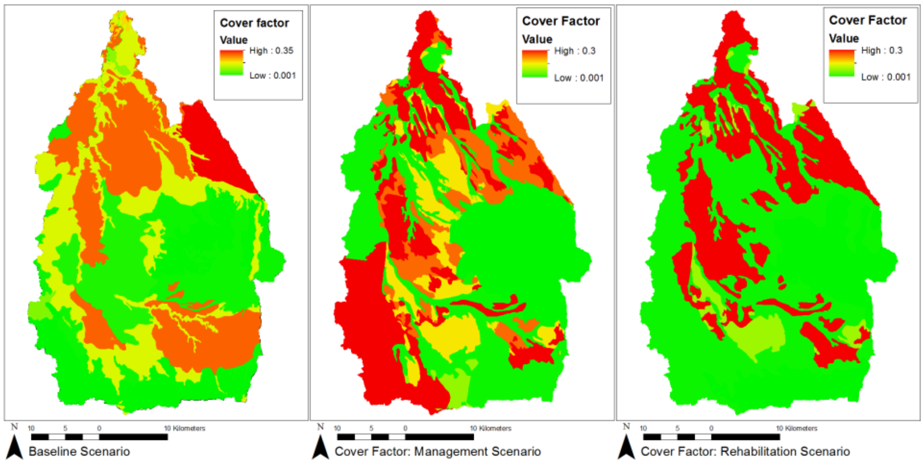

Figure 70. C-factor maps for baseline, development, and rehabilitation scenarios.

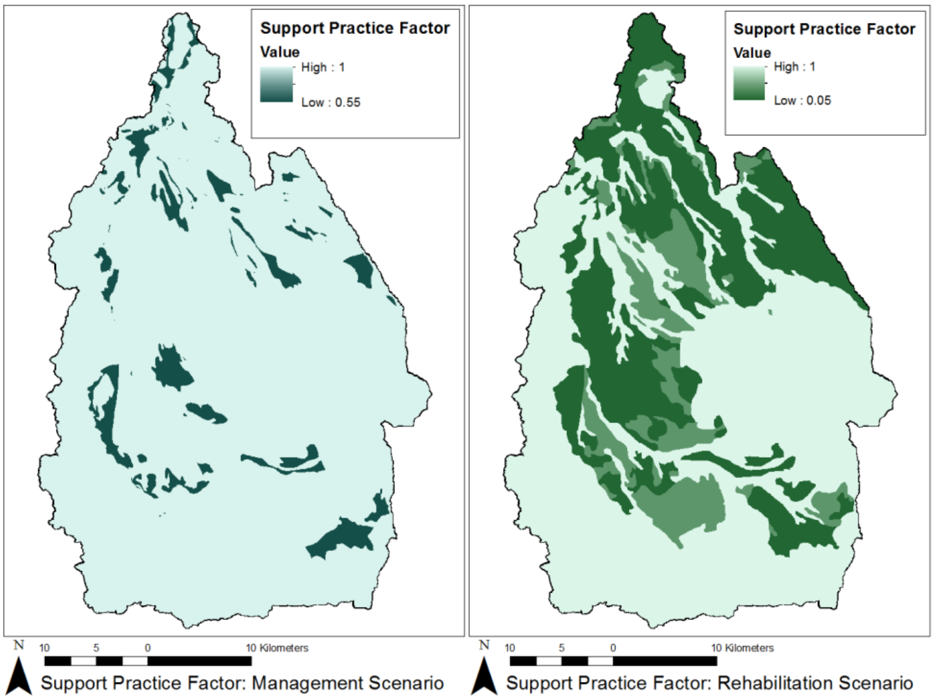

Figure 71. P-factor maps for the development and rehabilitation scenarios.

5.4.2 Soil loss

According to previous studies on soil erosion in the Philippines, the national average soil erosion rate is 80 ton ha^{-1} yr^{-1} (Francisco & Angeles, 1998). In the review by David (1988), some reported soil loss estimates are 308 to 414 ton ha^{-1} yr^{-1} over different types of grassland and crops, and estimates of 50 ton ha^{-1} yr^{-1} and 108 ton ha^{-1} yr^{-1} in different watersheds that used the USLE model. In-situ soil erosion work in areas close to the CDO watershed have found erosion rates of 185 ton ha^{-1} yr^{-1} in cropland and grazing areas (Marin & Jamis, 2013).

The mean soil loss of the CDO watershed depending on the approach used for each factor, especially the R-factor and LS-factor. In the baseline scenario, the estimated soil loss ranged between 11 ton ha^{-1} yr^{-1} to 1,462 ton ha^{-1} yr^{-1} (Figure 72). In the development scenario, the lowest estimate was 7 ton ha^{-1} yr^{-1} while the highest was 965 ton ha^{-1} yr^{-1} (Figure 73). In the rehabilitation scenario, the range of soil loss was 1 ton ha^{-1} yr^{-1} to 77 ton ha^{-1} yr^{-1} (Figure 74).

The R-factor equation that constantly produced the highest estimates of soil loss across all three scenarios was using the Shamshad et al. (2008) equation on WorldClim data. Similarly, the LS-factor equation that constantly produced the highest estimates of soil loss across all three scenarios was using the method by Desmet & Govers (1996). This method produces large estimates of the LS-factor because it uses flow accumulation as one of its inputs, and given the size and topography of the CDO watershed, some cells have very large LS-factor values. One of the suggested methods to prevent the LS-factor from becoming too large is to assign a cut-off value for slope percentage to deal with slopes that are very steep, such as in the case of constructing LS-factors for continental Europe (Panagos et al., 2015b). Conversely, the R-factor that produced the lowest soil loss estimates was the equation by Sholagberu et al. (2016) that excluded days below 10mm of rainfall. The LS-factor that produced the lowest soil loss estimates was the equation by Morgan (2005).

The mean soil losses that used the factors from Panagos et al. (2015a) and Shamshad et al. (2008) are much higher than the other soil losses, showing that the rainfall factor is one of the more crucial factors in the RUSLE equation. The R-factor from Panagos et al. (2015a) was based on rainfall data from thousands of rainfall gauges all over the globe and was interpolated using rainfall data from the WorldClim climate surfaces. This extensive dataset of rainfall gauges and actual R-factors could point to the dataset by Panagos et al. (2015a) as the more reliable rainfall factor dataset compared to the other methods of deriving rainfall erosivity. The Shamshad et al. (2008) method predicts a larger soil loss, but a value that is close to that given by Panagos et al. (2015a). The El-Swaify et al. (1987) also uses an equation that has the R-factor in units of tons hectare^{-1} year^{-1}, which is not consistent with the other rainfall factor equations in the RUSLE literature.

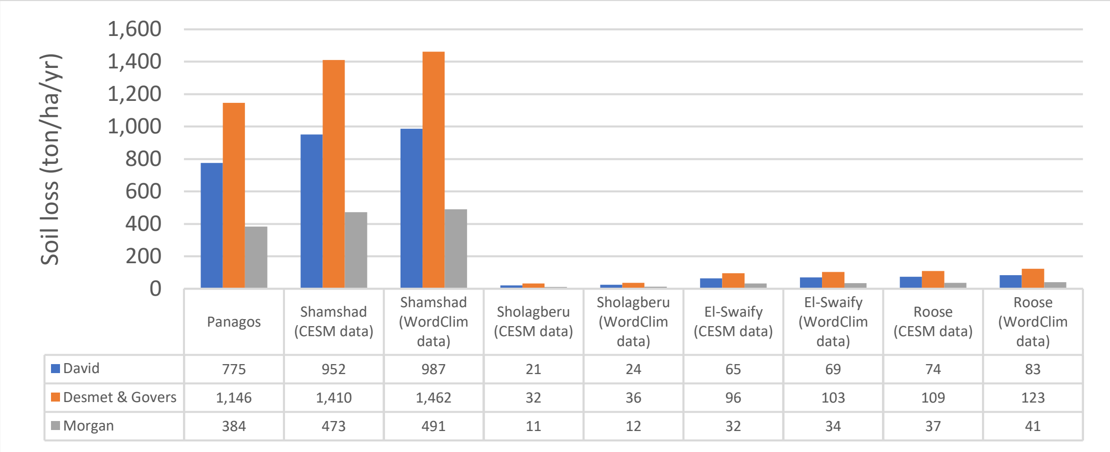

	Panagos	Shamshad (CESM data)	Shamshad (WordClim data)	Sholagberu (CESM data)	Sholagberu (WordClim data)	El-Swaify (CESM data)	El-Swaify (WordClim data)	Roose (CESM data)	Roose (WordClim data)
David	775	952	987	21	24	65	69	74	83
Desmet & Govers	1,146	1,410	1,462	32	36	96	103	109	123
Morgan	384	473	491	11	12	32	34	37	41

Figure 72. Mean soil loss for the CDO watershed in the baseline scenario across different methods for calculating R-factors and LS-factors.

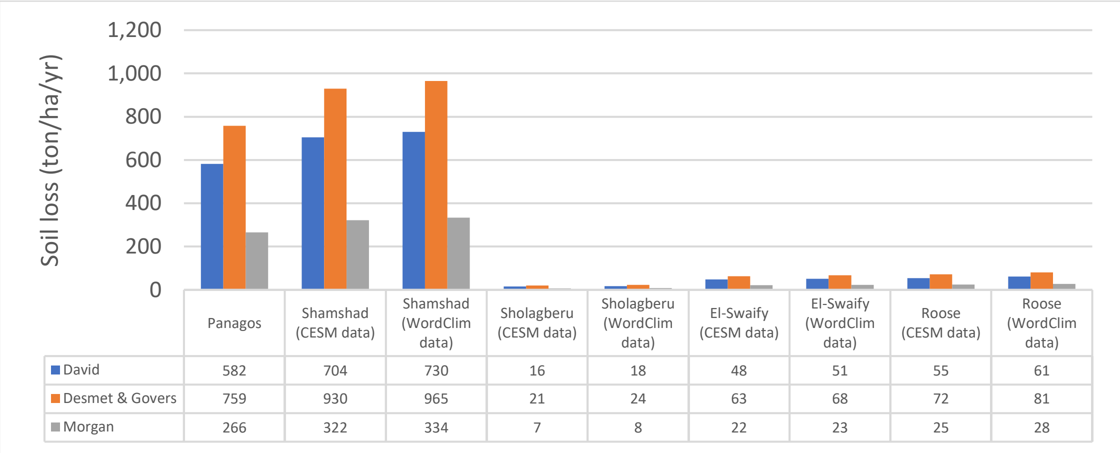

	Panagos	Shamshad (CESM data)	Shamshad (WordClim data)	Sholagberu (CESM data)	Sholagberu (WordClim data)	El-Swaify (CESM data)	El-Swaify (WordClim data)	Roose (CESM data)	Roose (WordClim data)
David	582	704	730	16	18	48	51	55	61
Desmet & Govers	759	930	965	21	24	63	68	72	81
Morgan	266	322	334	7	8	22	23	25	28

Figure 73. Mean soil loss for the CDO watershed in the development scenario across different methods for calculating R-factors and LS-factors.

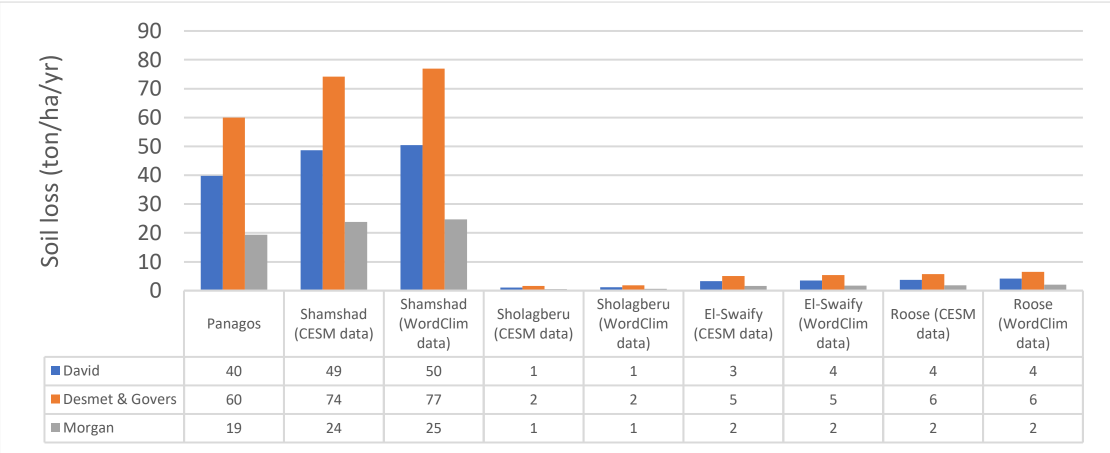

	Panagos	Shamshad (CESM data)	Shamshad (WordClim data)	Sholagberu (CESM data)	Sholagberu (WordClim data)	El-Swaify (CESM data)	El-Swaify (WordClim data)	Roose (CESM data)	Roose (WordClim data)
David	40	49	50	1	1	3	4	4	4
Desmet & Govers	60	74	77	2	2	5	5	6	6
Morgan	19	24	25	1	1	2	2	2	2

Figure 74. Mean soil loss for the CDO watershed in the rehabilitation scenario across different methods for calculating R-factors and LS-factors.

Given that the CDO watershed is heavily utilised for agriculture and is very mountainous, the estimated soil loss rates are expected to be high. Although it is difficult to verify these soil loss estimates because of the relatively low number of previously published soil erosion rates in the Philippines, areas utilised for agriculture or grassland have estimates ranging from 185 to 414 ton ha^{-1} yr^{-1} (David, 1988; Marin & Jamis, 2013). In the baseline scenario, even across different LS-factors, the equations by Sholagberu et al. (2016), El-Swaify et al. (1987), and Roose (1975) produced soil loss estimates that fell below this range. Conversely, the R-factors produced by Panagos et al. (2017) and Shamshad et al. (2008) produced soil loss estimates either in the upper bound of this range or beyond it. Because the RUSLE only accounts for sheet and rill erosion, ignoring gully erosion or mass wasting, these overestimates of soil loss are more useful for management because it more clearly shows the priority areas for rehabilitation or intervention measures. Conservative estimates of soil loss using the RUSLE can lead to vulnerable areas being classified as low-risk areas. Despite this large uncertainty in what might be an accurate R-factor, testing these different equations was useful to see any changes in the resulting soil vulnerability maps for the baseline scenario (Figure 75). All the runs identified the areas classified as agriculture and grassland as vulnerable to soil erosion, with the actual magnitude of the soil loss varying across R-factors.

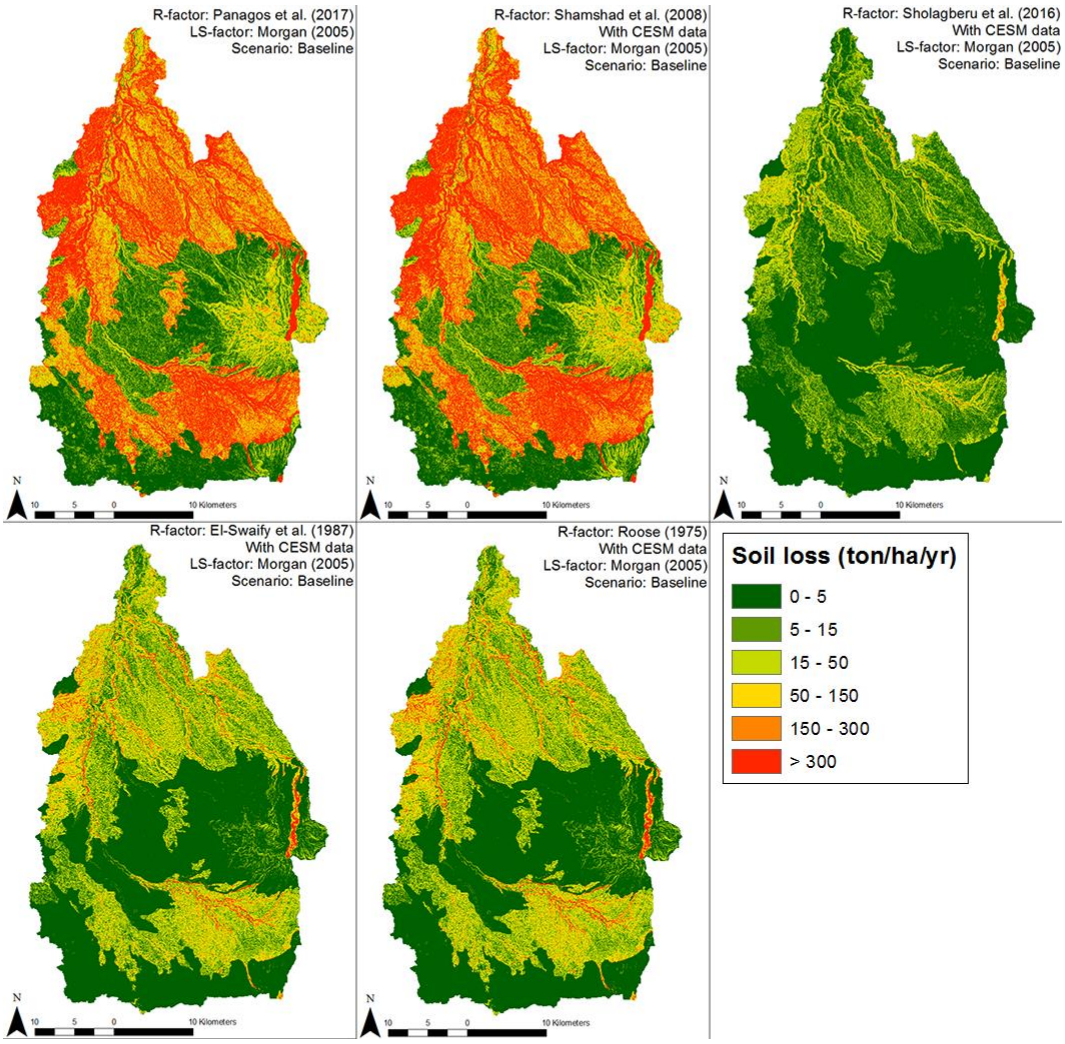

Figure 75. Soil vulnerability map over the CDO catchment in the baseline scenario using different methods of calculating the R-factor.

Even the most conservative estimates of soil loss identified the steep river valleys within the agricultural areas as priority areas of management. At the national, regional, or catchment scale, these extreme estimates are useful for identifying which broad classifications of land use are vulnerable to soil erosion. At the sub-watershed or field scale, using a lower estimate of R-factor can help management narrow down the smaller but still critical areas of soil vulnerability.

Regarding the spatial distribution of vulnerable areas across different LS-factors, the agricultural and grassland areas were consistently identified as at-risk areas, with the Morgan (2005) method classifying fewer areas as extremely (>300 tons ha^{-1} yr^{-1}) vulnerable compared to the David (1988) method (Figure 76). At the catchment scale, the maps produced by the Desmet & Govers (1996) method are more difficult to interpret due to the high granularity of soil loss. Hence, to make the visual interpretation of differences between scenarios easier, the maps presented in the scenario comparisons will be utilising the Morgan (2005) method for LS-factor.

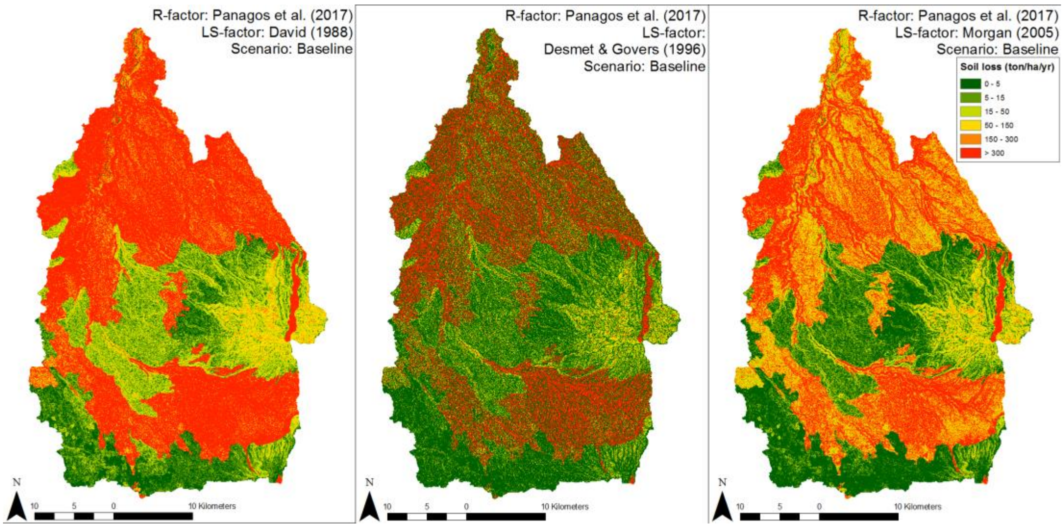

Figure 76. Soil loss maps under the baseline scenario across different methods of calculating LS-factors.

In comparing the management and rehabilitation scenarios with the baseline scenario, there is always a decrease in the estimated mean soil loss across all the combinations of R-factors and LS-factors (Table 42). The mean relative difference between the baseline and management scenario is 31% while the difference between the baseline and rehabilitation scenario is 95%. This suggests a potential decrease in the mean annual soil loss in the CDO catchment if these scenarios were pursued by management and with a larger decrease if the rehabilitation scenario occurred.

Table 42. Differences in mean soil loss over between baseline and management, and baseline and rehabilitation scenarios over different combinations of R-factor and LS-factor.

		Differences in Mean		Relative Differences in Mean	
		ton/ha/yr		%	
R-factor	**LS-factor**	**Base vs Mgmt**	**Base vs Rehab**	**Base vs Mgmt**	**Base vs Rehab**
Panagos et al. (2017)	David (1988)	193	735	25	95
	Desmet & Govers (1996)	388	1,086	34	95
	Morgan (2005)	118	365	31	95
Shamshad et al. (2008) with CESM data	David (1988)	247	903	26	95
	Desmet & Govers (1996)	480	1,336	34	95
	Morgan (2005)	151	449	32	95
Shamshad et al. (2008) with WorldClim data	David (1988)	257	936	26	95
	Desmet & Govers (1996)	497	1,385	34	95
	Morgan (2005)	157	466	32	95
Sholagberu et al. (2016) with CESM data	David (1988)	6	20	26	95
	Desmet & Govers (1996)	11	30	34	95
	Morgan (2005)	3	10	32	95
Sholagberu et al. (2016) with WorldClim data	David (1988)	6	23	26	95
	Desmet & Govers (1996)	12	34	34	95
	Morgan (2005)	4	11	32	95
El-Swaify et al. (1987) with CESM data	David (1988)	17	61	26	95
	Desmet & Govers (1996)	33	91	34	95
	Morgan (2005)	10	31	32	95
El-Swaify et al. (1987) with WorldClim data	David (1988)	18	66	26	95
	Desmet & Govers (1996)	35	97	34	95
	Morgan (2005)	11	33	32	95

Table 42. Differences in mean soil loss over between baseline and management, and baseline and rehabilitation scenarios over different combinations of R-factor and LS-factor. (continued)

		Differences in Mean		**Rel. Differences in Mean**	
		ton/ha/yr		**%**	
R-factor	**LS-factor**	**Base vs Mgmt**	**Base vs Rehab**	**Base vs Mgmt**	**Base vs Rehab**
Roose (1975) with CESM data	David (1988)	19	70	26	95
	Desmet & Govers (1996)	37	104	34	95
	Morgan (2005)	12	35	32	95
Roose (1975) with WorldClim data	David (1988)	22	79	26	95
	Desmet & Govers (1996)	42	116	34	95
	Morgan (2005)	13	39	32	95
			Mean	**31**	**95**

The areas classified as at-risk to soil erosion changed between the baseline and the two scenarios (Figure 77). The southern part of the watershed is classified in the baseline scenario as forest but is classified as agricultural area in the management scenario. In both the development and rehabilitation scenarios, the western part of the watershed is planned to be used as a protection zone for regenerating forest, hence its change to a less vulnerable area of soil erosion. The steep river valleys have also been classified as less vulnerable because of the management plans of practicing conservation farming such as alley-cropping, agroforestry, line-planting, and contour farming.

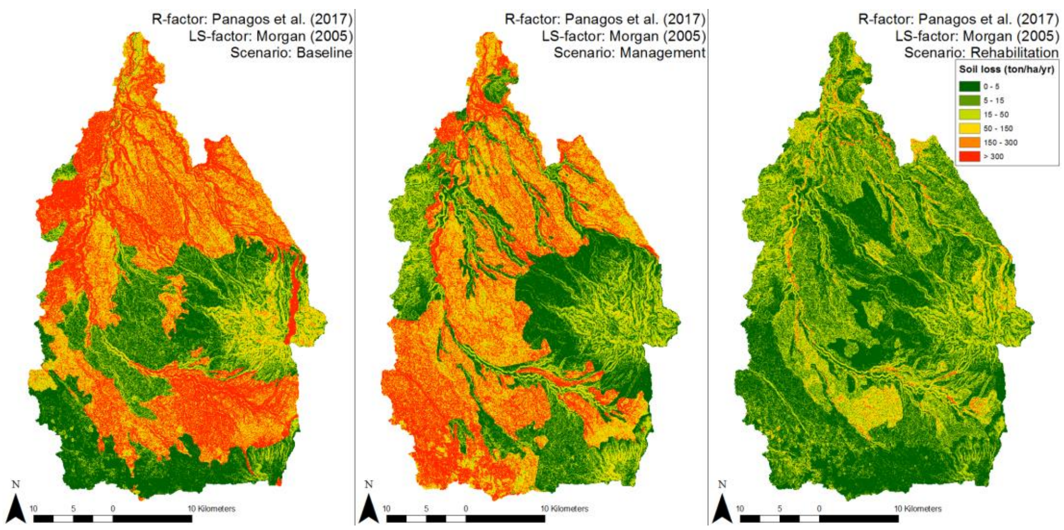

Figure 77. Soil loss under different scenarios.

In terms of intra-annual soil loss, the monthly soil loss follows the pattern of rainfall throughout the year (Figure 78). Higher soil loss rates are expected over the course of June to September, which corresponds with the monsoon season in the Philippines.

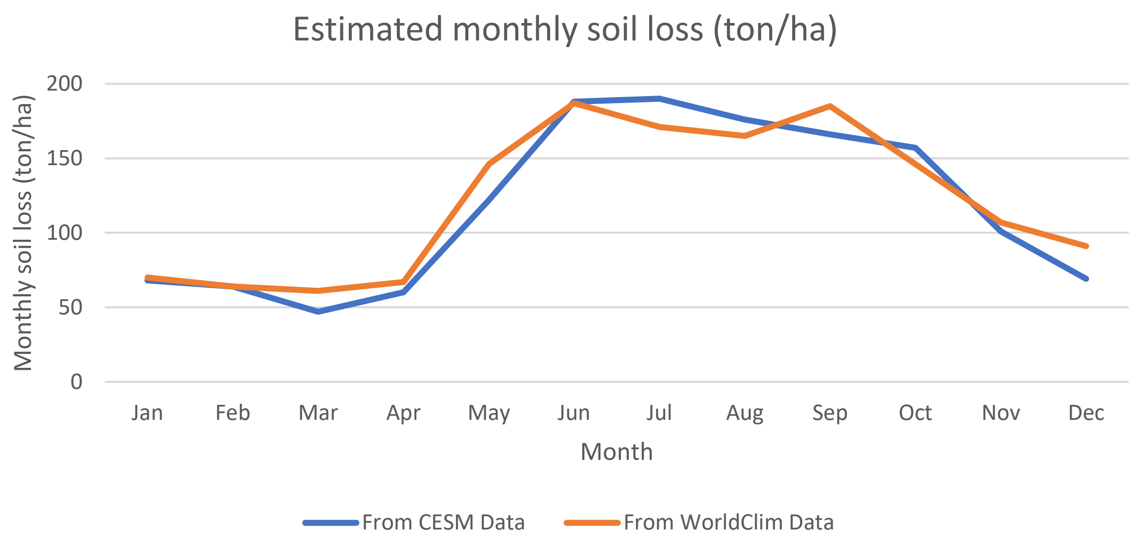

Figure 78. Estimated monthly soil loss in the CDO catchment.

5.5 Limitations and future work

One of the main limitations of this study, and arguably all RUSLE studies in the Philippines, is the availability of data as input and as validation. Without long-term soil erosion records around the country, it is difficult to truly assess the accuracy of the RUSLE in the Philippines. Even so, the model is useful for identifying areas that are vulnerable to soil erosion, which is a suitable start for catchment management plans. The model is also useful for performing scenario analysis with future catchment development plans, showing potential decreases in the mean soil loss under different conditions of land cover and conservation measures. Building on to the soil loss estimates, sediment delivery can be added to the model to assess the impact on water quality, a critical issue in the Philippines. The global rainfall erosivity dataset developed by Panagos et al. (2017) was identified as a reliable resource for future RUSLE applications, but analysis of long-term rainfall records available in the Philippines would be a good first step in creating a similar raster layer at the national scale. This could then be verified against Panagos et al. (2017) to check for differences and to elucidate the effect of using local-scale rainfall against global rainfall datasets.

Given that the Philippines is vulnerable to typhoons, event-based erosion is a potential future direction. By estimating the sediment loss associated with typhoons, and determining the quantity of sediment delivered to waterways, there are potential applications in assessing river siltation and water quality post-disasters. The Modified Universal Soil Loss Equation (MUSLE) uses the same factors as the RUSLE except the rainfall factor which is replaced by an equation that uses the peak flow rate (cumecs), flow volume (m^3), and location coefficients to predict event-based soil loss (Sadeghi et al., 2014). The hydrological modelling capability of LUCI (Chapter 8) produces flow hydrographs (cumecs) that can be used to derive peak flow rate and flow volume. Further work can be done to calibrate the location coefficients needed by MUSLE by reviewing previous MUSLE studies in areas similar to CDO.

Another limitation of this study was the inability to include the Compound Topographic Index (CTI), in order to assess gully erosion in CDO. The coarse resolution of the DEM and the relatively small widths of ephemeral gullies meant the CTI was not able to be applied in CDO. In the future, with higher resolution DEMs such as those available through LiDAR, it is possible that the CTI can be used with RUSLE to estimate the combined soil loss from sheet/rill and gully erosion.

5.6 Summary and conclusion

This chapter showed the utility and difficulty of applying the RUSLE to the Cagayan de Oro catchment where the agricultural activity, steep slopes, and heavy rainfall make it vulnerable to soil erosion. Different methods of calculating the RUSLE factors were tested to see how the resulting annual soil loss estimates were affected. For the rainfall factors, using the higher rainfall factors were useful in identifying broad categories of land use that were vulnerable to soil erosion while using the lower rainfall factors were useful in pinpointing smaller areas for more targeted management. Similarly, deciding which slope length and steepness factors to use was dependent on scale. Methods involving only slope length and steepness were more useful at the catchment scale compared to the method involving flow accumulation, because of the high granularity associated with the latter. At the sub-watershed or field scale, the method involving flow accumulation was more useful to pinpoint areas for management. Even though the accuracy of the RUSLE could not be compared with actual soil erosion records, it was also useful to see how changing land cover would affect mean soil loss through scenario analysis. In all scenarios, those areas classified as agriculture and areas with steep slopes were considered the most vulnerable to soil erosion. However, conservation practices outlined in the management and rehabilitation scenarios have the potential to mitigate soil erosion, especially on steeper slopes.

Priority future directions for RUSLE work in the Philippines include sediment delivery for water quality analysis, assessing the erosion associated with extreme events such as typhoons, and including the Compound Topographic Index (CTI) for gully erosion in areas were high-resolution elevation data is available. Sediment delivery to streams can affect water quality, and thus is a principal issue for a heavily populated city like Cagayan de Oro. Although typhoons are rarer in CDO compared to the northern areas of the Philippines, analysing the siltation associated with typhoons is important for post-disaster water quality and to analysing the effectiveness of downstream flood inundation defences. Lastly, RUSLE specifically considers sheet and rill erosion but ignores gully erosion Future development of RUSLE in LUCI could allow the inclusion of the CTI which would explicitly account for gully erosion. However as stated in Chapter 6, CTI and RUSLE both use slope and flow accumulation and care must be taken to avoid double-counting.

6 Improving the estimation of soil loss using a combination of the Revised Universal Soil Loss Equation (RUSLE) and the Compound Topographic Index (CTI) in the Mangatarere watershed

6.1 Introduction

Although the main scope of this thesis is ecosystem services modelling in the Cagayan de Oro catchment in the Philippines, this section applies the RUSLE to the Mangatere catchment in New Zealand. This is due to the availability of more detailed data to test different sub-factors within the RUSLE, such as high-resolution DEMs and a daily rainfall time-series. The highest resolution DEM publicly available for the CDO is the 30m ASTER DEM, while the Mangatarere catchment has two high-resolution DEMs at 15m and 5m. Having these DEMs allowed for testing of how spatial resolution affected different approaches to estimating the slope length and steepness factor within the RUSLE, which was not possible for the CDO. The availability of a daily rainfall time-series in the Mangatarere was used to test different rainfall erosivity equations from those used in the CDO catchment. In the CDO, only annual and monthly rainfall were used to estimate soil erosion. Additionally, the relatively coarse ASTER DEM in CDO is not sufficient to apply the Compound Topographic Index (CTI) accurately due to dependence on accurately representing slope curvature. CTI uses upstream drainage area, slope, and planform curvature to identify areas susceptible to gully erosion and to calculate soil loss rates (Thorne et al., 1985). It was originally applied at the field scale, but was applied in a GIS environment within LUCI to calculate areas susceptible to erosion (Jackson et al., 2013). Using a high-resolution DEM is important for identifying gully-prone areas due to the size of ephemeral gullies, commonly 0.5 to 50cm in depth (Momm et al., 2012). The predictive ability of the CTI is affected by DEM resolution, with analysis finding its ability degrading at ~10m resolution (Parker et al., 2007).

Due to the mountainous topography, erodible volcanic soils, and high rainfall activity in New Zealand, the country experiences high rates of soil erosion (Rodda et al., 2001). Anthropogenic activity has exacerbated the problem, especially in pastoral and agricultural hill country (Basher, 2013). Previous studies on soil erosion have used modelling to understand the extent of the problem in hopes of finding ways to mitigate erosion (Cogle et al., 2003; Elliott et al., 2012; Rodda et al., 2001). As of 2012, the highest total estimated soil loss was in the West Coast region (50 million tons year^{-1}) while the highest estimated soil loss rate was in the Gisborne region (4,844 tons km^{-2} year^{-1}) (Stats NZ, 2015).

The Revised Universal Soil Loss Equation (RUSLE), or slightly modified versions of it, have been applied to New Zealand. Work by Rodda et al. (2001) used the RUSLE as part of a decision support system in the Ngongotaha catchment to assess potential sediment yields under different land use scenarios, highlighting the utility of riparian planting to reduce sediment load. Similarly, work by Fernandez & Diagneault (2016) used the RUSLE and the New Zealand Empirical Erosion Model to estimate soil loss, which were used in an economic model to assess the potential implications of erosion control in the Waikato region. Their results underscored the highly spatial nature of soil erosion, indicating that targeting the critical areas for erosion would maximise the cost-effectiveness of measures such as shelter belts, riparian planting (M. A. Fernandez & Daigneault, 2016).

At the national scale, work by Klik et al. (2015) on the rainfall erosivity factor produced a New Zealand-wide map of R-factor and equations to estimate the R-factor from annual and seasonal precipitation. The R-factor ranged from less than 550 MJ mm ha^{-1} h^{-1} in locations such as Central Otago to above 16,000 MJ mm ha^{-1} h^{-1} in the Southern Alps, highlighting the large potential influence of precipitation on sediment yield (Klik et al., 2015). Using nationally available data, work by Dymond (2010) produced the NZUSLE which considers an area's rainfall, slope, soil, land cover, and management factors (Dymond et al., 2010). This approach uses broad classifications of land cover and soil texture, but at the catchment scale, more detailed parameterisation accounting for several types of land cover and structural integrity of the soil may provide more accurate soil loss estimates.

The NZUSLE by Dymond (2010) is shown below:

$$\bar{e}_s(x,y) = \alpha P^2(x,y)K(x,y)L(x,y)Z(x,y)U(x,y)$$

Where:

$\bar{e}_s$	Mean annual erosion rate due to surficial processes (t km^{-2} yr^{-1})
A	Constant calibrated with published surficial erosion rates (1.2×10^{-3})
P	Mean annual rainfall (mm)
K	Soil erodibility factor depending on texture (Sand: 0.05; Silt: 0.35; Clay: 0.20; Loam: 0.25)
L	Slope length factor where λ is slope length (m) in $L = \left(\frac{\lambda}{22}\right)^{0.5}$
U	Vegetation cover factor (Bare ground: 1.0; Pasture: 0.01; Scrub: 0.005; Forest: 0.005)
Z	$Z = 0.065 + 4.56\frac{dz}{dx} + 65.41\left(\frac{dz}{dx}\right)^2$ Where dz/dx is the slope gradient

The NZUSLE uses broad classifications of soil and land cover, and mean annual rainfall to determine its rainfall erosivity, which makes it a relatively simple model to apply. However, the influence of land cover is dependent on more than just the broad categories proposed in the NZUSLE, as factors such as type of forest, crop growth, or tillage practice can influence soil erosion (Panagos et al., 2015d). The soil erodibility factor of the NZUSLE is also unclear about how to handle soils of mixed textures (e.g. clay loam) which can affect how susceptible the soil is to erosion. Part of this research is to parameterise the RUSLE for more specific cover and crop types, and eventually lead to farm-scale applications that can take crop growth and stage into account.

One of the limitations of RUSLE is that it estimates soil loss through sheet and rill erosion (through the length-slope and steepness factor), but not from other types of erosion such as gully erosion, channel erosion, or from mass wasting events such as landslides (Nagle et al., 1999; Wischmeier & Smith, 1978). By not including ephemeral gully erosion, soil loss estimates can be under-estimated (Thorne et al., 1985). The model also does not account for deposition or sediment routing (Desmet & Govers, 1996; Wischmeier & Smith, 1978). Since it does not predict the sediment pathways from hillslopes to water bodies, it is difficult to analyse possible effects on downstream areas, such as pollution or sedimentation (Jahun et al., 2015). These two limitations have implications for being able to adequately identify areas vulnerable to erosion and more accurately estimate soil loss in more topographically complex terrain, like many areas of New Zealand.

6.2 Aim and objectives

The main aim of this chapter is to further parameterise the RUSLE approach for application to New Zealand conditions and data, and to allow monthly or seasonal estimates of erosion to be determined. The specific objectives are as follows:

- Apply the RUSLE to the Mangatarere catchment using different equations for the rainfall erosivity factor and the slope length and steepness factor.

Given there are several methods for calculating RUSLE factors (Chapter 4), this research will also test the sensitivity of these equations to produce a range of RUSLE factors for the Mangatarere.

6.3 Methodology

The Mangatarere catchment (~157km^2) is located in the central Wairarapa region of New Zealand and is covered by forest in the northern area (Tararua Forest Park) and agricultural activity such as dairy and drystock farming in the plains (Milne et al., 2010) (Figure 80). This catchment was chosen as the study site due to the high rainfall in the forested part of the catchment, and the extensive anthropogenic activity in the plains area. The rainfall data was extracted from the OVERSEER nutrient budget model which uses rainfall data representative of the typical daily rainfall over one year for the region wherein the Mangatarere is located (Wheeler, 2016b). Using rainfall at a daily resolution would allow for monthly and seasonal estimates of soil loss. The soil shapefile was taken from the Fundamental Soils layer[10] and uses the New Zealand Soil Classification at the highest level (order) (Hewitt, 2010). Soil physicochemical characteristics at the order level were taken from the OVERSEER nutrient budget model (Wheeler, 2016a).

Two DEMs of differing resolution were chosen for this study to test differences in slope-length and steepness factor and resulting soil loss estimates. The Wellington 15m DEM (NZSoSDEM v1.0) is part of a larger DEM dataset with national coverage that

[10] http://lris.scinfo.org.nz/layer/48079-fsl-new-zealand-soil-classification/

was produced from topographic vector data (Columbus et al., 2011). The 5m DEM was created from interpolating the Wellington LiDAR 1m DEM (2013) from Land Information New Zealand[11]. Lastly, the land cover for the study area was taken from the Land Cover Database version 4.1[12] which is a national-scale map of land cover and land use that was produced by Landcare Research and is updated at ~5 year intervals (Landcare Research, 2013).

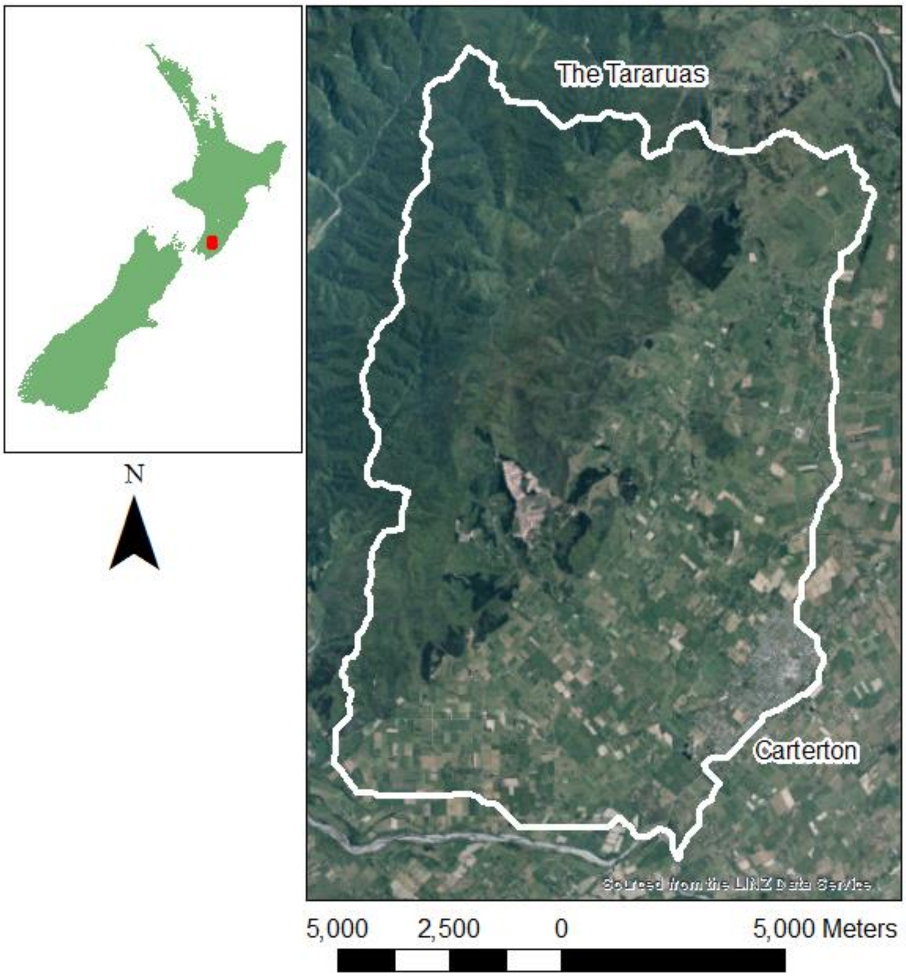

Figure 79. Location of the Mangatarere catchment in red relative to New Zealand, and the Mangatarere catchment showing the forested and agricultural areas.

[11] http://data.linz.govt.nz/layer/53621-wellington-lidar-1m-dem-2013/
[12] http://lris.scinfo.org.nz/layer/48423-lcdb-v41-land-cover-database-version-41-mainland-new-zealand/

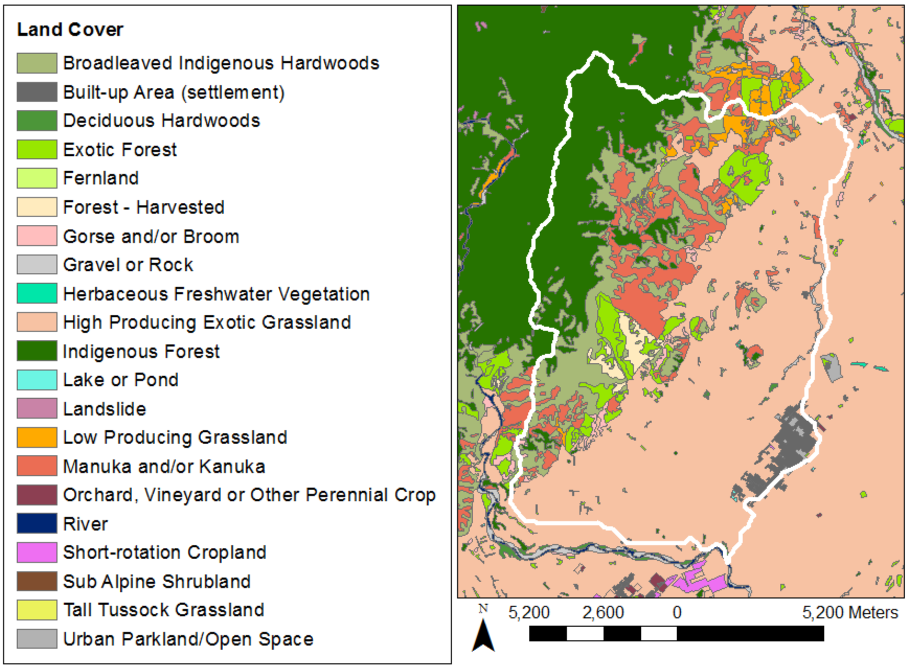

Figure 80. Land cover map for the Mangatarere using the LCDB 4.1 classification.

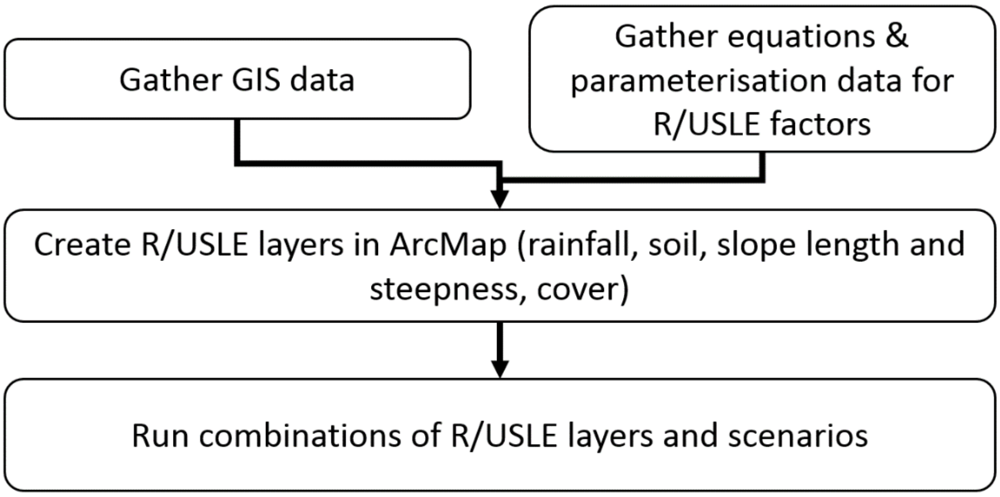

Figure 81. Methodology of the study.

Different parameterisation equations were gathered for the different RUSLE factors, focusing on sources in New Zealand and using daily or monthly rainfall data. For more detail on the RUSLE factors and methods to calculate them, refer to the review chapter (Chapter 4). The high temporal resolution allows for monthly and seasonal soil erosion estimates instead of the annual soil erosion commonly estimated with RUSLE. The K-factor was estimated using an equation by David (1988) which uses textural information and organic material to estimate soil erodibility. Two different LS-factor equations were taken from Desmet & Govers (1996) and Morgan (2005) to test their applicability at the watershed scale. The values for C-factors were taken from literature and are more detailed compared to the vegetation cover factor proposed by Dymond et al. (2010). The support practice factor was not included due to the lack of information regarding management practices or future plans for management interventions.

After the RUSLE parameterisation, these layers were used to estimate mean annual soil loss in tons hectare^{-1} year^{-1} and seasonal soil loss in tons hectare^{-1} season^{-1}. For easier comparison to previous soil loss estimates in New Zealand, the maps were also converted to tons km^{-2}.

6.3.1 RUSLE equations

6.3.1.1 Rainfall erosivity (R-factor)

The high rainfall in New Zealand has been cited as one of the main drivers of soil erosion (Basher, 2013). In the Mangatarere, mean annual rainfall varies between ~900mm on the Wairarapa Plains up to ~3,000mm on the forested part of the catchment in the foothills of the Tararua Ranges (Milne et al., 2010). Given the availability of daily rainfall data, the equations from Loureiro & Coutinho (2001) and Ferreira & Panagopolous (2014) were chosen (Table 43). The annual and seasonal R-factor equations by Klik et al. (2015) were chosen due to their application in New Zealand, being derived from New Zealand rainfall data, and because of the objective of doing seasonal soil loss estimates.

Table 43. Rainfall erosivity factor equations used in this research.

#	Source	Original Location	Equation
1	Loureiro & Coutinho (2001)	Portugal	$EI_{30\,(monthly)} = 7.05 rain_{10} - 88.92 days_{10}$ $$R = \frac{1}{N}\sum_{i=1}^{N}\sum_{m=1}^{12} EI_{30(monthly)}$$ Rain$_{10}$ = Monthly rainfall for days with > 10.0mm of rain Days$_{10}$ = Monthly number of days with rainfall > 10.0mm of rain N = Number of years Units: Megajoule •millimetre • hectare^{-1} • hour^{-1} • year^{-1}

Table 43. Rainfall erosivity factor equations used in this research. (continued)

#	Source	Original Location	Equation
2	Ferreira & Panagopolous (2014)	Portugal	$$R = \sum_{i=1}^{12} 6.56rain_{10} - 75.09days_{10}$$ $Rain_{10}$ = Monthly rainfall for days with > 10.0mm of rain $Days_{10}$ = Monthly number of days with rainfall > 10.0mm of rain Units: Megajoule •millimetre • hectare^{-1} • hour^{-1} • year^{-1}
3	Klik et al. (2015)	New Zealand	Equation 1: $R = aP^b$ Equation 2: $R = aP + b$ P = Annual or seasonal precipitation a & b = Constants depending on location defined by Klik et al. (2015) • Mangatarere located in Region 2 • Annual a & b: 0.026 & 1.536 (eq 1) • Spring a & b: 0.08 & 1.435 (eq 1) • Summer a & b: 0.078 & 1.537 (eq 1) • Fall a & b: 2.508 & -284.4 (eq 2) • Winter a & b: 0.021 & 1.633 (eq 1)

6.3.1.2 Soil erosivity (K-factor)

The equation below by David (1988) was chosen due to its relative simplicity of requiring only textural information, organic matter, and pH. By contrast, the original RUSLE K-factor equation also requires information on soil structure and profile-permeability that was not available for the soils in the Mangatarere catchment.

$$K = [(0.043 \times pH) + (0.62 \div OM) + (0.0082 \times S) - (0.0062 \times C)] \times Si \times 0.1317$$

Where:

pH	pH of the soil
OM	Organic matter in percent
S	Sand content in percent
C	Clay ratio = % clay / (% sand + % silt)
Si	Silt content = % silt / 100

6.3.1.3 Slope length and steepness factor (LS-factor)

The equations in Table 44 were chosen because of their ubiquity in RUSLE literature and to test the strengths and weaknesses of each method. The method by Desmet & Govers (1996) is widely used because of its capability to account for the convergence and divergence of flow, thus allowing for application in more complex terrain. The method by Morgan (2005) is like the original RUSLE calculation for LS-factor and was chosen because of its relative simplicity.

Table 44. Slope length and steepness factors used in this research.

#	Source	Equation
1	Desmet and Govers (1996), like equations by Moore & Burch (1986) as cited in Mitasova et al. (1996) and Mitasova et al. (2013)	$$LS = (m+1)\left(\frac{U}{L_0}\right)^m \left(\frac{\sin\beta}{S_0}\right)^n$$ U (m^2m^{-1}) = upslope contributing area per unit width as a proxy for discharge $$U = Flow\ Accumulation\ \times Cell\ Size$$ L_0 = length of the unit plot (22.1) S_0 = slope of unit plot (0.09) β = slope m (sheet) and n (rill) depend on the prevailing type of erosion (m= 0.4 to 0.6) and n (1.0 to 1.3)
2	Morgan (2005) but previously published in earlier editions	$$LS = \left(\frac{l}{22}\right)^{0.5} (0.065 + 0.045s + 0.0065s^2)$$ l = slope length (m) s = slope steepness (%)

6.3.1.4 Cover factor (C-factor) and support practice factor (P-factor)

To determine the C-factor, the land cover classification of the LCDB 4.1 was compared to the land cover classes reported by Morgan (2005), Dymond (2010), and Panagos et al. (2015d). The values taken for C-factor were based on the average reported C-factor for similar land cover classes found in these studies. The areas classified as harvested forest and landslide were given the value for bare soils (1.0), although the classification did not specify if the harvested forest left any debris behind, which could influence soil erosion. The land cover classifications from 1996, 2001, and 2008 were also used as land cover scenarios to determine any changes in soil erosion compared to 2012.

The support practice factor (P-factor) is included in the original RUSLE to account for the effect of diverse types of land management. However, detailed information about specific land management (e.g. mulching, contour cropping, etc.) was not available for this application of RUSLE to the Mangatarere catchment. Thus, the P-factor was excluded but can be included for more detailed farm-scale applications where information on management is more easily accessible.

Table 45. C-factor values for the land cover classifications present in the Mangatarere catchment.

LCDB4 Land Classification	C-factor	Notes
Broadleaved Indigenous Hardwoods	0.002	Average for forest classes
Built-up Area (Settlement)	0.015	Average for built-up areas
Deciduous Hardwoods	0.002	Erosion control trees, large trees
Exotic Forest	0.002	Average for forest classes
Forest - Harvested	1	Described as predominantly bare ground
Gorse and/or Broom	0.0445	Scrubby weeds
Gravel or Rock	0	No soil to erode
Herbaceous Freshwater Vegetation	0.0445	Reed-like
High Producing Exotic Grassland	0.055	Grazing activity, pasture
Indigenous Forest	0.002	Average for forest classes
Lake or Pond	0	No soil to erode
Landslide	1	Same as bare soil
Low Producing Grassland	0.055	Also associated with grazing
Manuka and/or Kanuka	0.002	Large trees with smaller scrub beneath
Orchard, Vineyard or Other Perennial Crop	0.002	Average for forest classes
River	0	No soil to erode
Short-rotation Cropland	0.25	Agriculture, used average of wheat and maize
Sub Alpine Shrubland	0.0445	Shrubland
Tall Tussock Grassland	0.0445	Brush, grassland
Urban Parkland/Open Space	0.0445	Like scrub, described as grassed and “sparsely-treed”

6.3.2 Annual and seasonal estimates of soil loss

After all the RUSLE factors were calculated, they were converted to raster layers and multiplied together in the *Raster Calculator* of ArcMap 10.4.1 to obtain an estimate of annual soil loss over several different combinations. Annual and seasonal estimates of soil loss were done for each of the R-factors and C-factors, giving soil loss in tons hectare^{-1} year^{-1}, but the maps were converted to tons kilometre^{-2} year^{-1} for easier comparison to national estimates of soil loss.

$$\frac{ton}{ha\ yr} \times \frac{1\ ha}{0.01\ km^2}$$

The maps were then classified into the following categories following the work of Dymond (2010) (tons kilometre^{-2} year^{-1}). The estimated average soil erosion in the Wellington region is approximately 729 tons km^{-2} yr^{-1} (Stats NZ, 2015), and the erosion rates above 501 tons km^{-2} yr^{-1} are considered vulnerable to extreme regions of soil erosion.

- 0 to 50
- 51 to 200
- 201 to 500
- 501 to 2,000
- 2,001 to 5,000
- 5,001 to 20,000
- > 20,000

Table 46. Summary of the equations used in this application of RUSLE to the Mangatarere.

Rainfall Erosivity Factor	**Soil Erodibility Factor**	**Slope Length and Steepness Factor (on 15m and 5m DEMs)**	**Cover and Support Practice Factor**
• Klik et al. (2015) • Loureiro & Coutinho (2001) • Ferreira & Panagopolous (2014) • Panagos et al. (2017)	• David (1988)	• Desmet and Govers (1996) • Morgan (2005)	• 2012 • 2008 • 2001 • 1996

6.4 Results and discussion

The more detailed parameterisation of RUSLE allows more representative estimates of soil loss and can be used to examine monthly or seasonal variability in soil erosion vulnerability. Due to use of monthly rainfall and land cover scenarios depending on agricultural activity, we highlight the utility of RUSLE at a finer temporal scale. The addition of the temporal aspect can aid in identifying which months in the year erosion management would be more useful.

6.4.1 Differences in RUSLE factors

6.4.1.1 Rainfall erosivity (R-factor)

Of the different R-factor equations, the one by Klik et al. (2015) produced the largest estimate of rainfall erosivity while Loureiro & Coutinho (2001) produced the lowest (Table 47). The Panagos et al. (2017) erosivity map was clipped to the study area and shows the spatial variability of rainfall erosivity between the agricultural plains and the foothills of the mountain range where the rainfall erosivity is higher (Figure 82).

The work by Klik et al. (2015) used pluviographic data from rainfall stations across New Zealand at sub-hourly (10min) temporal resolution to calculate R-factor values, creating a national dataset by relating these to annual precipitation. The rainfall erosivity produced by this equation was the highest at 2607 MJ mm ha^{-1} hr^{-1} for the Mangatarere catchment, higher than the average for that region (~1900 MJ mm ha^{-1} hr^{-1}). This could be due to the influence of the high rainfall associated with the mountain ranges in the north of the catchment. Meanwhile, Loureiro & Coutinho (2001) and Ferreira & Panagopolous (2014) produced lower estimates of the R-factor compared to Klik et al. (2015), likely due to their equations excluding days that had less than 10mm of rainfall. In the dataset used for this research, 310 out of 365 days (85%) recorded less than 10mm of rainfall. The dataset by Panagos et al. (2017) had a range of 266 to 2,277 (mean: 1,221) MJ mm ha^{-1} hr^{-1} for the Mangatarere catchment due to the difference in rainfall between the plains and hilly areas. The dataset by Panagos et al. (2017) is important to capture that spatial variation and was produced by relating other climate variables to R-factors, not just precipitation amount.

Table 47. R-factors calculated from the different equations and the average of Panagos et al. (2017) (MJ mm ha^{-1} hr^{-1}).

Source	Klik et al. (2015)	Loureiro & Coutinho (2001)	Ferreira & Panagopolous (2014)	Panagos et al. (2017)
Annual R	2607	1391	1715	1221

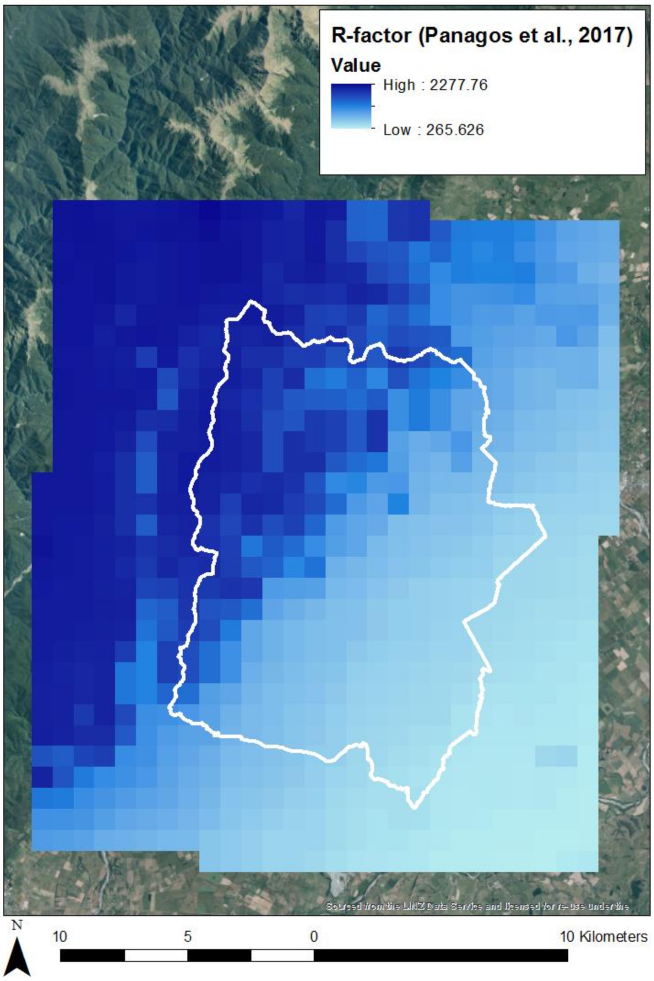

Figure 82. R-factor map from Panagos et al. (2017) for the Mangatarere.

The equations by Klik et al. (2015), Loureiro & Coutinho (2001), and Ferreira & Panagopolous (2014) were used to produce seasonal R-factor estimates for the catchment (Figure 83). The trend produced by Klik et al. (2015) was completely different from the trend predicted by the other two equations. For Klik et al. (2015), the highest erosivity occurs in summer and the lowest in winter/spring. For the other two, the opposite is true with the highest erosivity occurring in winter/spring and the lowest in summer. In the region where the Mangatarere is located, Klik et al. (2015)

reports that although there is high rainfall in both winter and summer, there are more storms occurring in summer. This stark difference in seasonal R-factor trends shows the importance of testing R-factor equations from multiple sources instead of using only one. Aside from testing different equations, another way of refining R-factor for the Mangatarere is to test those equations on more years of rainfall data to see if the monthly and seasonal trends still hold. These monthly and seasonal estimates can then be aggregated to produce annual soil estimates that can be compared to the annual soil estimates that were produced using only annual precipitation data.

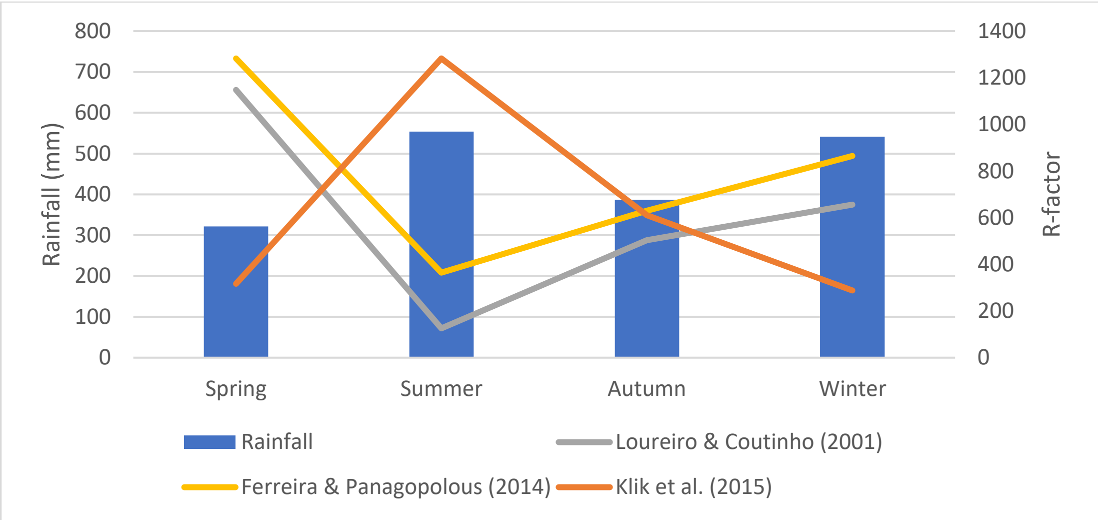

Figure 83. Seasonal rainfall and erosivity estimates.

6.4.1.2 Soil erodibility (K-factor)

For the areas classified as urban and gravel, soil erodibility is assumed to be zero. Outside of these areas, K-factors ranged from 0.0277 (Gley) up to 0.0379 (Pallic) (Table 48). The gley soils have the lowest estimated K-factor, which is consistent with their characteristics of minimal erosion due to ponding and higher possibility of deposition in areas where gley soils are found (Hewitt, 2010). The other three soil orders in the study area of brown, pallic, and recent, all have similar soil erodibility factors. These soils have relatively stable topsoils, but can be subject to erosion and sedimentation after periods of tillage or usage of heavy machinery (Hewitt, 2010).

The classification at the soil order level is useful at large scales such as national, regional, and for larger catchments. At smaller scales such as sub-watershed or field scale, more specific soil classification levels such as groups and sub-groups would be more useful to observe differences in the spatial distribution of soil erodibility.

Another method of refining the K-factor parameterisation in future work is to incorporate the structural integrity characteristic that uses top soil clay content, top soil carbon content, and the anion storage capacity as a measure of soil strength (Wheeler, 2016a). Structural integrity is a modified form of the structural vulnerability characteristics for New Zealand soils, which was formulated through reviewing and analysing physical information about NZ soils to assess their erodibility against commonly measured soil attributes (Hewitt & Shepherd, 1997).

Table 48. K-factor values for different soils in the Mangatarere (ton hr MJ^{-1} mm^{-1}).

Soil Order	**K-factor**
Brown	0.0324
Gley	0.0277
Pallic	0.0379
Recent	0.0356

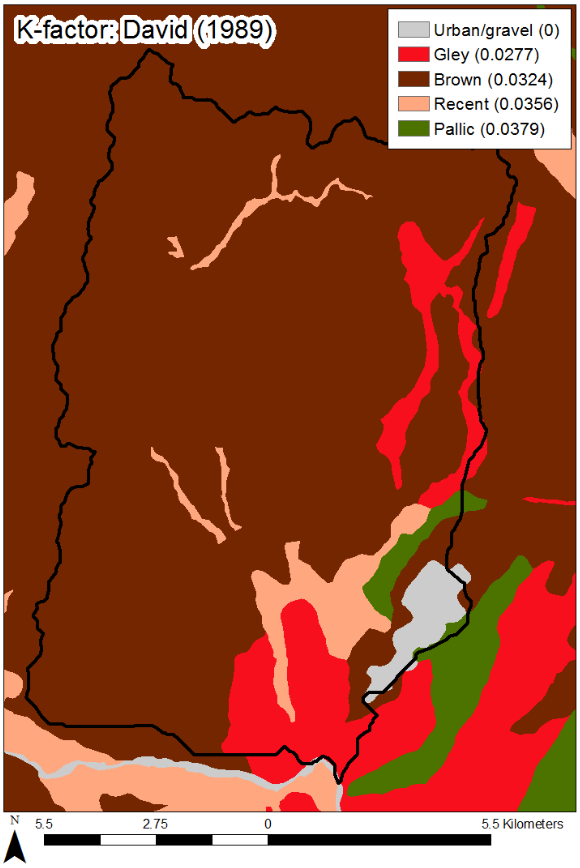

Figure 84. K-factor map for the Mangatarere.

6.4.1.3 Slope length and steepness factor (LS-factor)

For the 15m DEM, the mean values of LS-factor are 10 for Morgan (2005) and 12 for Desmet & Govers (1996). For the 5m DEM, the mean values of LS-factor are 6 for Morgan (2005) and 9 for Desmet & Govers (1996). Although the mean values are similar, the spatial distribution of LS-factors across both methods are slightly different (Figure 85 and Figure 86). The main similarities in the spatial distribution are the high values in the hilly areas while the lower areas are in the plains area, due to the hilly areas having steeper slope gradients. The main difference is that Desmet & Govers (1996) predict the highest LS-factors predicted by Desmet & Govers (1996) along the stream network due to the high flow accumulation whereas Morgan (2005) predicts the highest LS-factors on steep mountainous slopes.

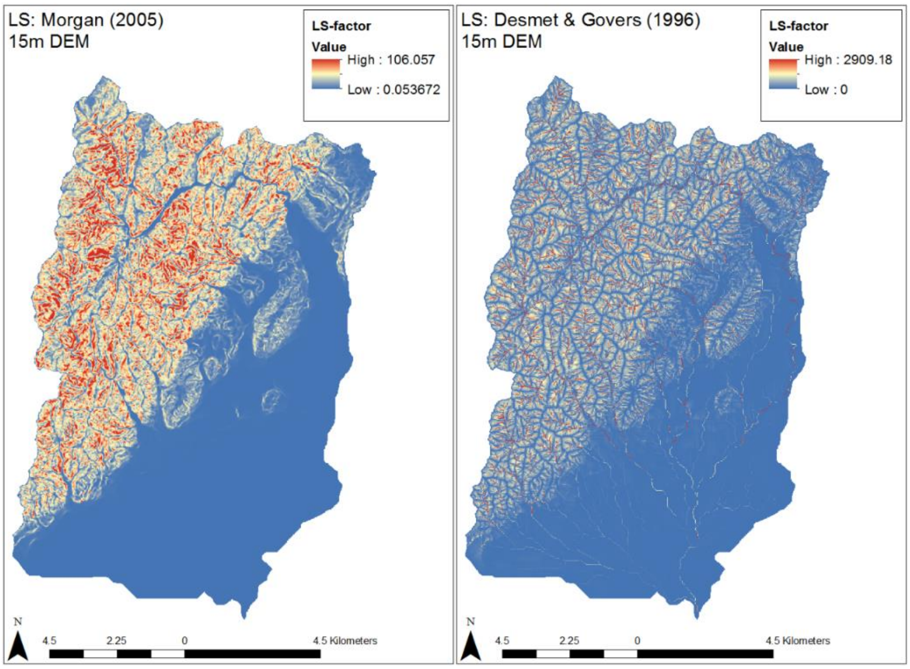

Figure 85. LS-factor maps for the 15m DEM using Morgan (2005) and Desmet & Govers (1996) methods.

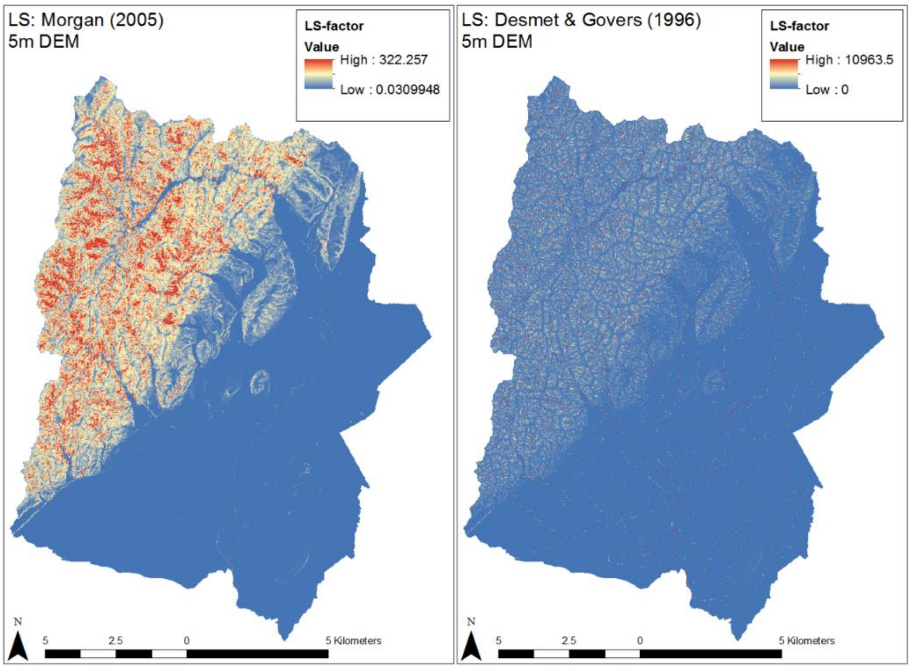

Figure 86. LS-factor maps for the 5m DEM using Morgan (2005) and Desmet & Govers (1996) methods.

6.4.2 Annual estimates of soil loss

The Mangatarere catchment is located within the Wellington region, whose long-term soil erosion rate is estimated to be 792 t km^{-2} yr^{-1} (Stats NZ, 2015). In the nearby Manawatu catchment, the measured sediment yield ranged from 137 to 978 t km^{-2} yr^{-1} and the modelled sediment yield ranged from 368 to 978 t km^{-2} yr^{-1} (Dymond, 2010). The Manawatu is like the Mangatarere catchment in terms of having hilly topography in the Tararua mountain ranges and pasture farming in the flat areas.

The mean soil loss of the Mangatarere watershed varied between the various factors, especially between different values for R-factor and LS-factor. For the R-factor, the equation that produced the highest mean soil loss estimate was Klik et al. (2015) (2,877 ton km^{-2} yr^{-1}) while Panagos et al. (2017) produced the lowest mean soil loss estimate (775 ton km^{-2} yr^{-1}) (Figure 87). This follows the expected trend of higher rainfall erosivities leading to higher estimates of mean soil loss, as Klik et al. (2015) produced the highest R-factor values.

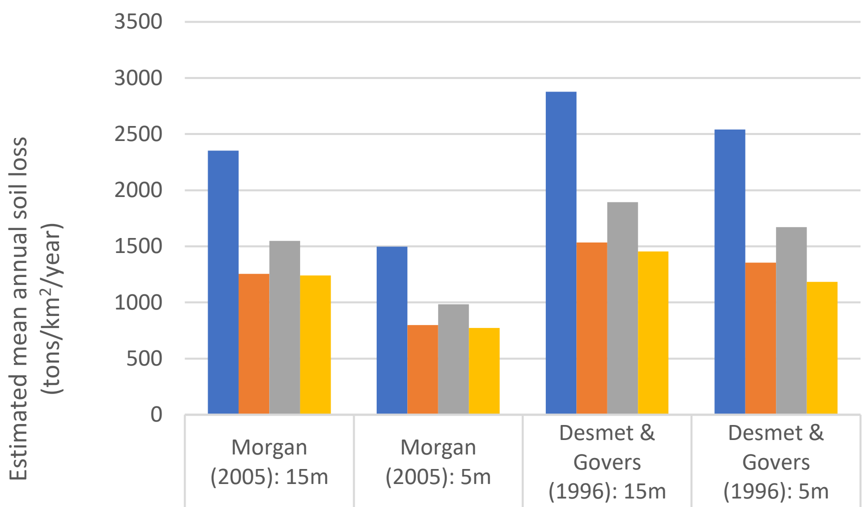

	Morgan (2005): 15m	Morgan (2005): 5m	Desmet & Govers (1996): 15m	Desmet & Govers (1996): 5m
Klik et al. (2015)	2353.18926	1497.44217	2877.36843	2539.65012
Loureiro & Coutinho (2001)	1254.66639	798.40491	1534.16013	1354.08672
Ferreira & Panagopolous (2014)	1548.02814	985.08966	1892.85825	1670.69352
Panagos et al. (2017)	1241.2	774.5	1454.1	1182.4

Figure 87. Soil estimates of the different combinations of R-factor, LS-factor, and DEM resolution.

Although mean soil loss values are very different (775 to 2,877 ton km^{-2} yr^{-1}), the distribution of the areas considered extremely vulnerable to soil loss are similar across the different R-factor equations (Figure 88 and Figure 89). The areas classified as harvested forest are described as predominantly bare ground and have the highest estimated soil loss due to lack of vegetation cover and the other vulnerable areas are exotic grassland, and gorse/broom. Exotic grassland areas are commonly used for pasture grazing and are dominated by short vegetation. In general, the hilly areas are classified as more vulnerable to soil loss compared to the plains areas due to the presence of steep slopes.

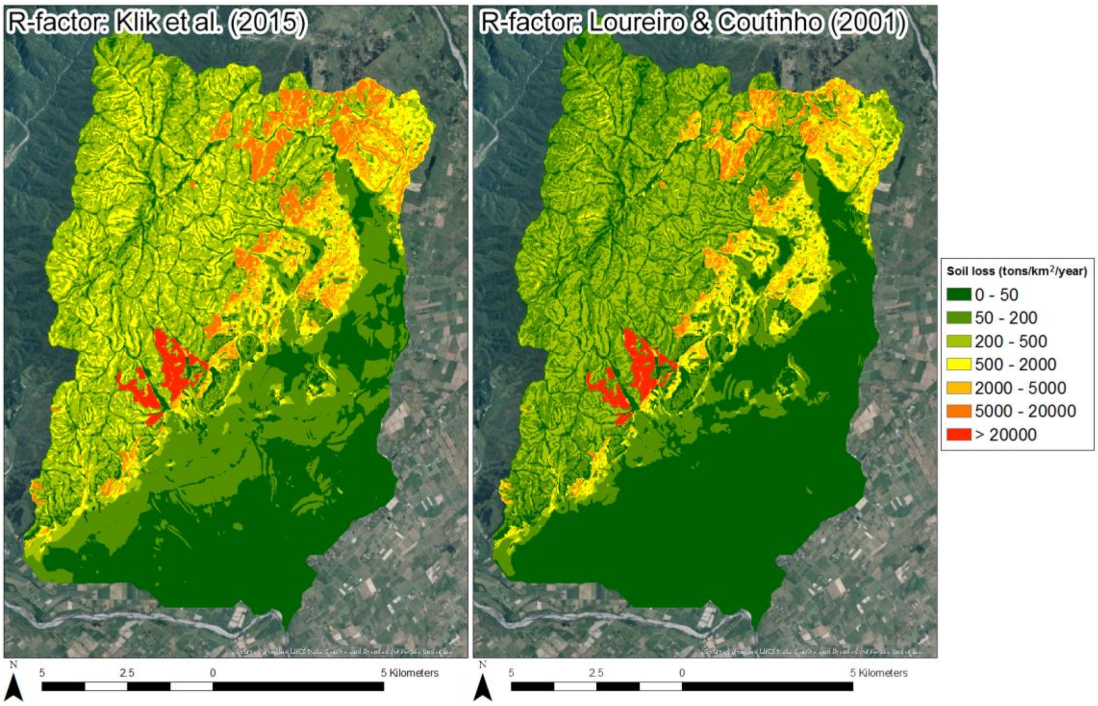

Figure 88. Soil loss maps for R-factor estimated with Klik et al. (2015) and Loureiro & Coutinho (2001).

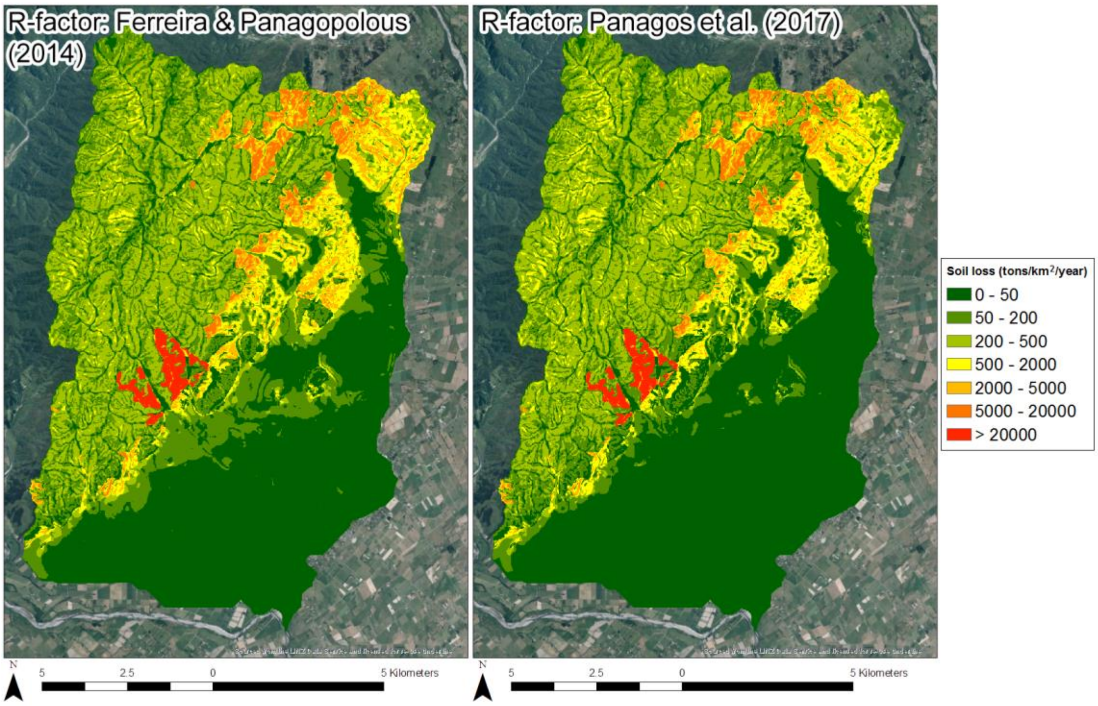

Figure 89. Soil loss maps for R-factor estimated with Ferreira & Panagopolous (2014) and Panagos et al. (2017).

In terms of absolute and relative differences, the difference between Klik et al. (2015) and the other two equations is similar. Klik et al. (2015) predicts higher soil loss in all areas of the catchment, specially the area classified as harvested forest which is the most vulnerable to soil erosion. This is because of the R-factor estimated by Klik et al. (2015) is higher compared to the one estimated by Loureiro & Coutinho (2001) and Ferreira & Panagopoulous (2014). In terms of relative differences, there is a mean difference of ~47% between the Klik et al. (2015) predictions and the Loureiro & Coutinho (2001) predictions. Similarly, the mean relative difference between the Klik et al. (2015) predictions and the Ferreira & Panagopoulous (2014) predictions is 34%. Loureiro & Coutinho (2001) estimated a lower R-factor, hence the lower soil erosion estimates produced. The mean relative difference between Loureiro & Coutinho (2001) and Ferreira & Panagopoulous (2014) soil loss estimates was -23%.

The rainfall factor is a key component of the RUSLE because of the driving force of precipitation to trigger soil erosion and related events. In the RUSLE literature, a common method of calculating R-factor in data-sparse areas is to utilise equations from other study areas. However, researchers must be mindful of the differences in soil loss estimates produced by different R-factor equations. Through testing multiple R-factor equations, researchers are then able to compare the estimates of soil loss to previous work and data to pick the most appropriate equation.

In terms of the LS-factor, the areas classified as extremely vulnerable to soil erosion are the same for the two different LS-factor equations. These are the areas classified as harvested forest or exotic grassland. However, the inclusion of flow accumulation causes the areas with very low/no flow accumulation to appear more clearly on the map while the areas of high flow accumulation, such as the flow pathways on the plains area are classified as more vulnerable. This difference is seen clearly in the 15m DEM (Figure 90), where the plains areas show more areas vulnerable to soil loss using the Desmet & Govers (1996) method.

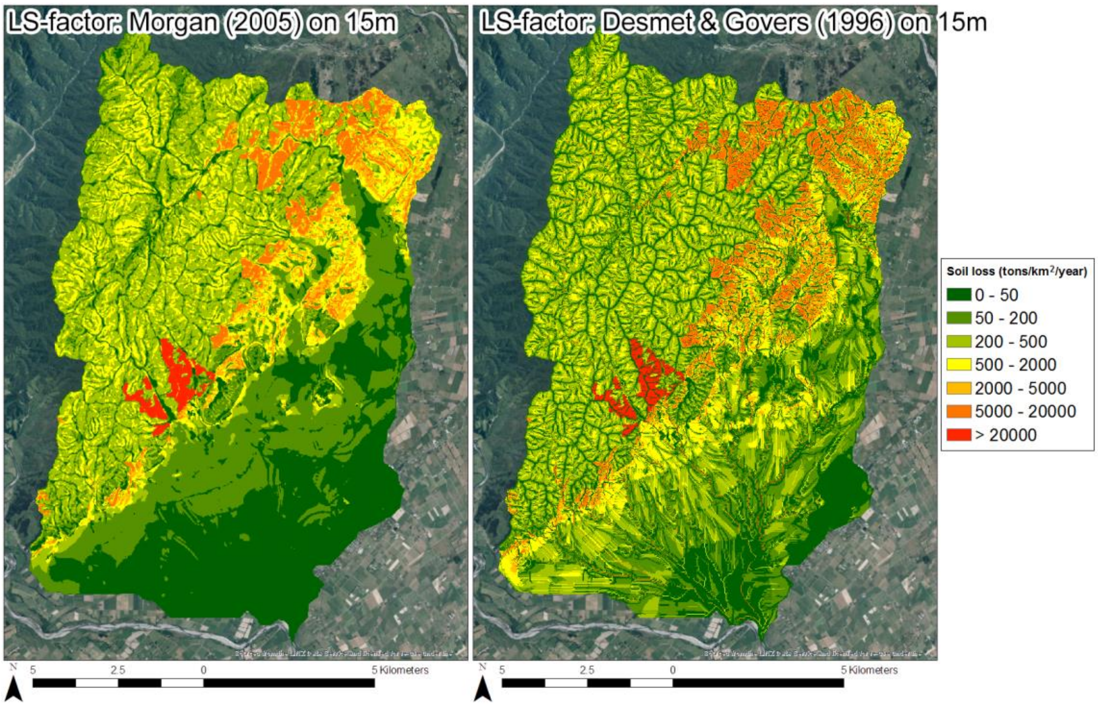

Figure 90. Soil loss maps for LS-factor estimated with Morgan (2005) and Desmet & Govers (1996) on the 15m DEM with R-factor equation Klik et al. (2015).

For the 5m DEM, the difference between the LS-factor of Morgan (2005) and Desmet & Govers (1996) at the watershed scale are more difficult to see (Figure 91). There is more granularity in the flat plains area, but the model is still identifying the same areas as most vulnerable to soil erosion: harvested forest and exotic grasslands. At a smaller scale (Figure 92), the differences of the two LS-factors for the 5m DEM are clearer. The inclusion of flow accumulation allows the RUSLE to identify finer areas to target, using information about the movement of water and its erosive force to delineate the areas that are most vulnerable to soil erosion. At the watershed scale, the slope gradient approach by Morgan (2005) is useful for targeting areas of land for large-scale interventions or future management planning. At the sub-watershed and field scale, the method by Desmet & Govers (1996) is more useful to identify the areas that are vulnerable to soil erosion based on land cover and flow pathways.

In terms of differences between DEM resolutions, the higher-resolution can identify areas on the flat plains area as vulnerable to soil erosion that the 15m DEM could not. The 5m DEM can pick up on the microtopography of the plains areas, which could be important in study areas that have seemingly flat topography but whose smaller topographic features could contribute to soil erosion. This is due to the improvements in vertical resolution associated with using LiDAR over coarse DEMS, which affects how slope and the subsequent hydrological attributes are represented in the DEM.

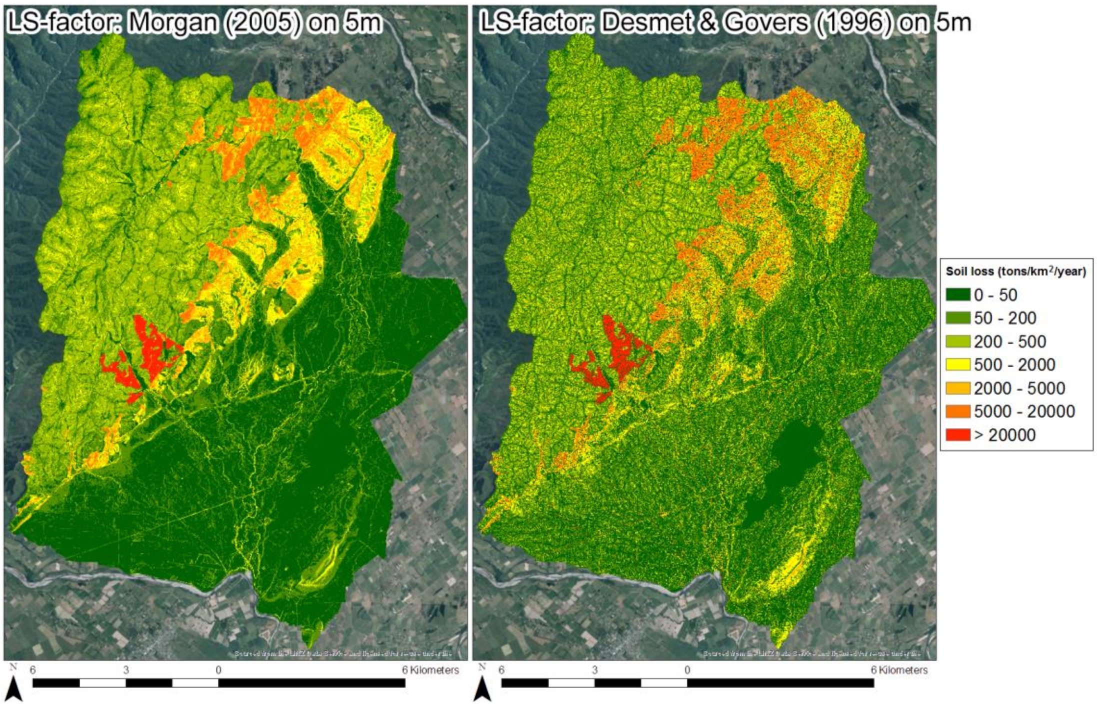

Figure 91. Soil loss maps for LS-factor estimated with Morgan (2005) and Desmet & Govers (1996) on the 5m DEM at the watershed scale.

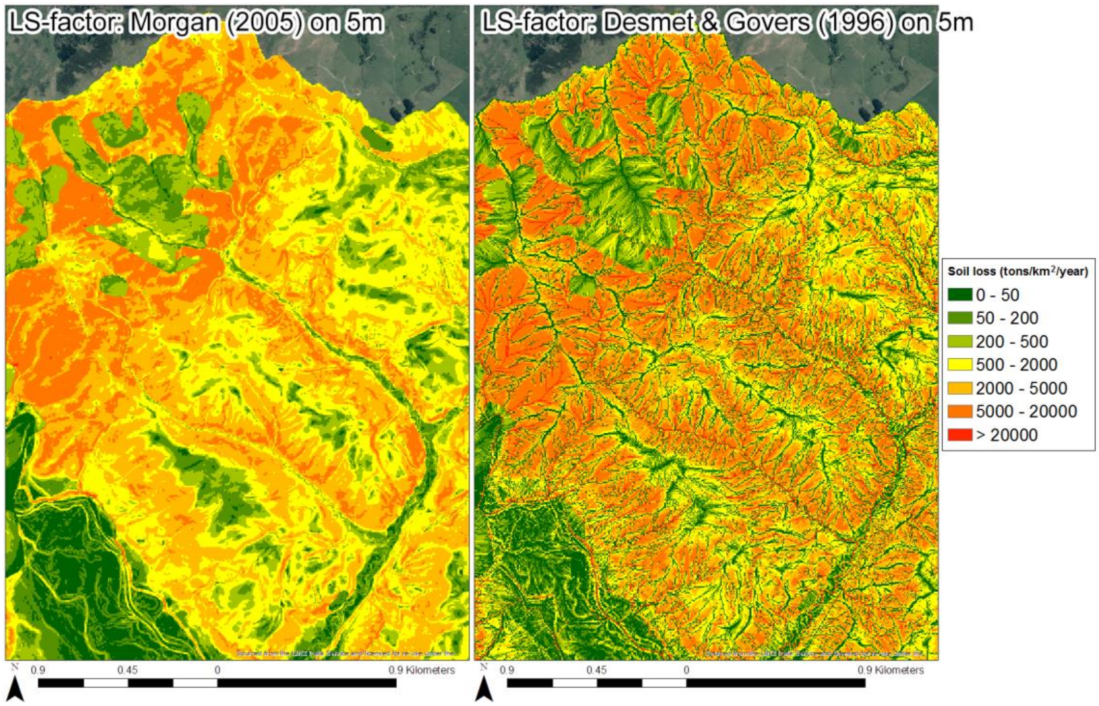

Figure 92. Soil loss maps for LS-factor estimated with Morgan (2005) and Desmet & Govers (1996) on the 5m DEM at a closer scale.

Like the difference maps for the R-factors, the main difference for the LS-factor maps manifested in the areas vulnerable to soil erosion. The values for total soil loss (Table 49) differ by 18% in the 15m DEM and 41% in the 5m DEM. As shown by the maps (Figure 93 and Figure 94), this difference is due to the equation by Morgan (2005) using slope steepness as one of the main drivers of soil erosion by the equation by Desmet & Govers (1996) uses both steepness and flow accumulation. The areas with the smallest differences are the flat areas while the areas with the largest differences are the areas with either steep slopes or high flow accumulation. This difference in predicted soil loss between the methods by Morgan (2005) and Desmet & Govers (1996) underscores the importance of further comparing these results not only to previous soil loss modelling work but also relating model predictions to observational values. Such validation work includes comparing the estimated to measured surficial erosion rates (Dymond, 2010), using water quality records to elucidate sediment loads as detailed in Section 4.3, or ground-truthing the areas identified as vulnerable to soil erosion to check for physical evidence of erosion.

One suggested method of generating arguably more realistic LS-factor estimates is to assign a maximum value for slope steepness due to shallow soils or absence of soil on slopes beyond a certain threshold, such as above 26.6 degrees for soils in the European Union (Panagos et al., 2015b). The resulting sediment supply and soil loss predictions are likely to be significantly lower than predictions that used an equation for LS-factor with no maximum slope steepness threshold.

Given the influence on slope on soil loss, future work can include an in-depth review focusing on the LS-factor, the different methods used to calculate it, and the common values and thresholds used by other studies. As outlined in the review (Chapter 4), the LS-factor and the Compound Topographic Index (CTI) both account for slope steepness and flow accumulation. Thus, a more thorough review of LS-factor and CTI and how they would be combined to prevent double-counting would greatly contribute to understanding how to account for both sheet/rill erosion and gully erosion.

Table 49. Comparisons of total estimated soil loss in tons/yr produced by RUSLE when using LS-factor equations from Morgan (2005) or Desmet & Govers (1996).

	Total soil loss (ton/yr)		
LS-factor used	**Morgan (2005)**	**Desmet and Govers (1996)**	**Difference (%)**
15m DEM	357,101	436,646	18
5m DEM	280,225	475,260	41

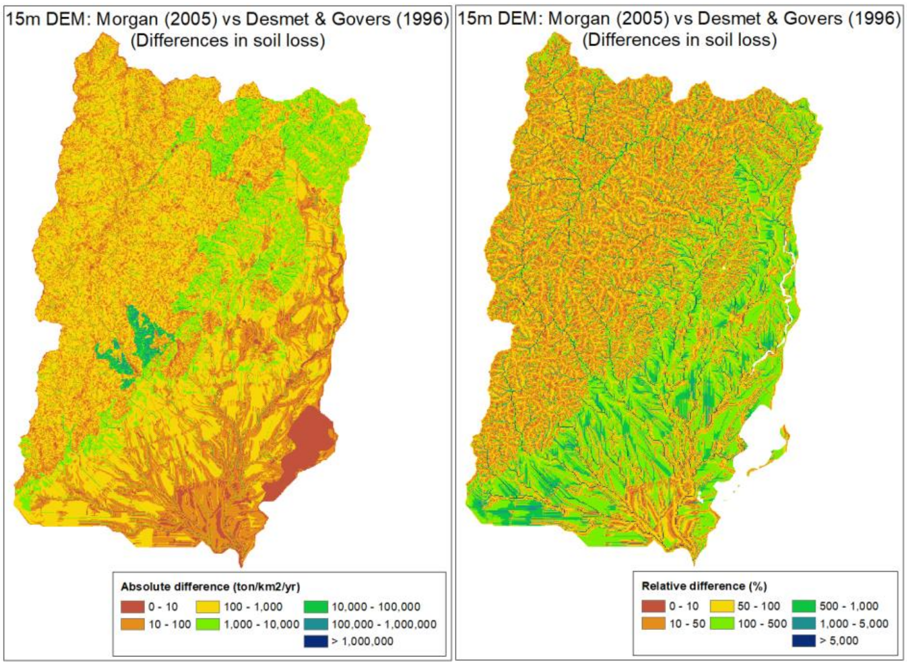

Figure 93. Absolute and relative difference maps of soil loss comparing Morgan (2005) and Desmet & Govers (1996) on the 15m DEM.

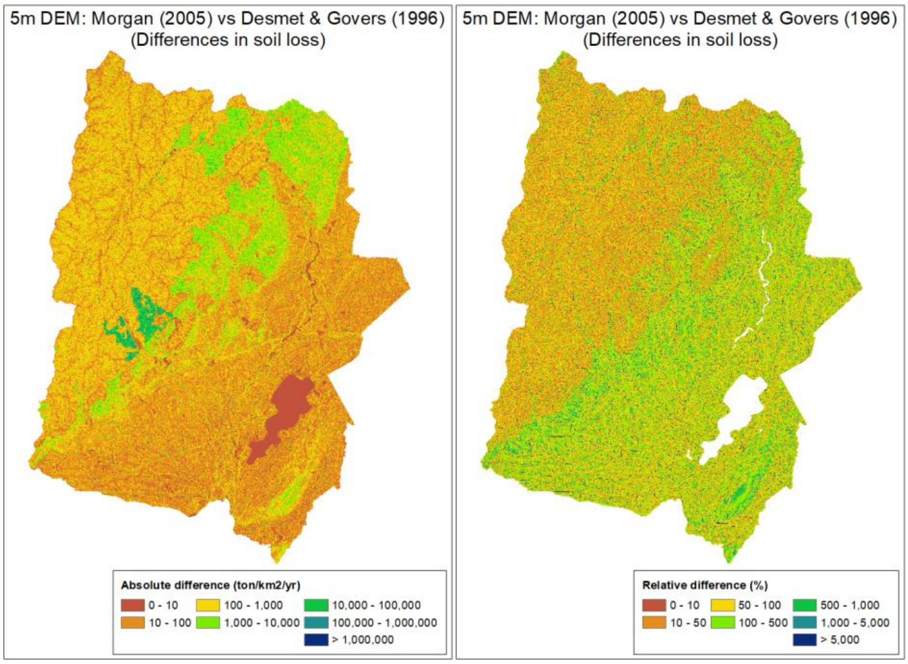

Figure 94. Absolute and relative difference maps of soil loss comparing Morgan (2005) and Desmet & Govers (1996) on the 5m DEM.

Within the LCDB are classifications of the same area over different years: 1996, 2001, 2008 and 2012. Over those changes in land cover, the areas consistently identified as vulnerable to soil erosion are the exotic grassland areas in the hilly regions (Figure 95). However, the most vulnerable area changes because of the area classified as harvested forest changed between surveys. In 2001, there were no areas within the Mangatarere classified as harvested forest, hence leading to 2001 having the lowest estimates of soil loss across the four land cover scenarios.

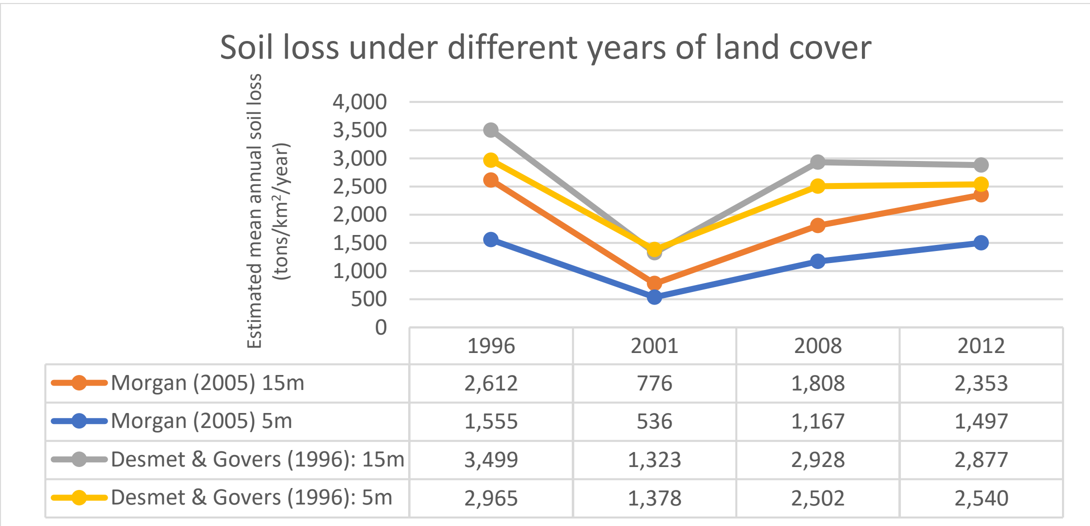

	1996	2001	2008	2012
Morgan (2005) 15m	2,612	776	1,808	2,353
Morgan (2005) 5m	1,555	536	1,167	1,497
Desmet & Govers (1996): 15m	3,499	1,323	2,928	2,877
Desmet & Govers (1996): 5m	2,965	1,378	2,502	2,540

Figure 95. Estimates of soil loss under different years of land cover using different LS-factor methods (15m and 5m DEM) with the R-factor of Klik et al. (2015).

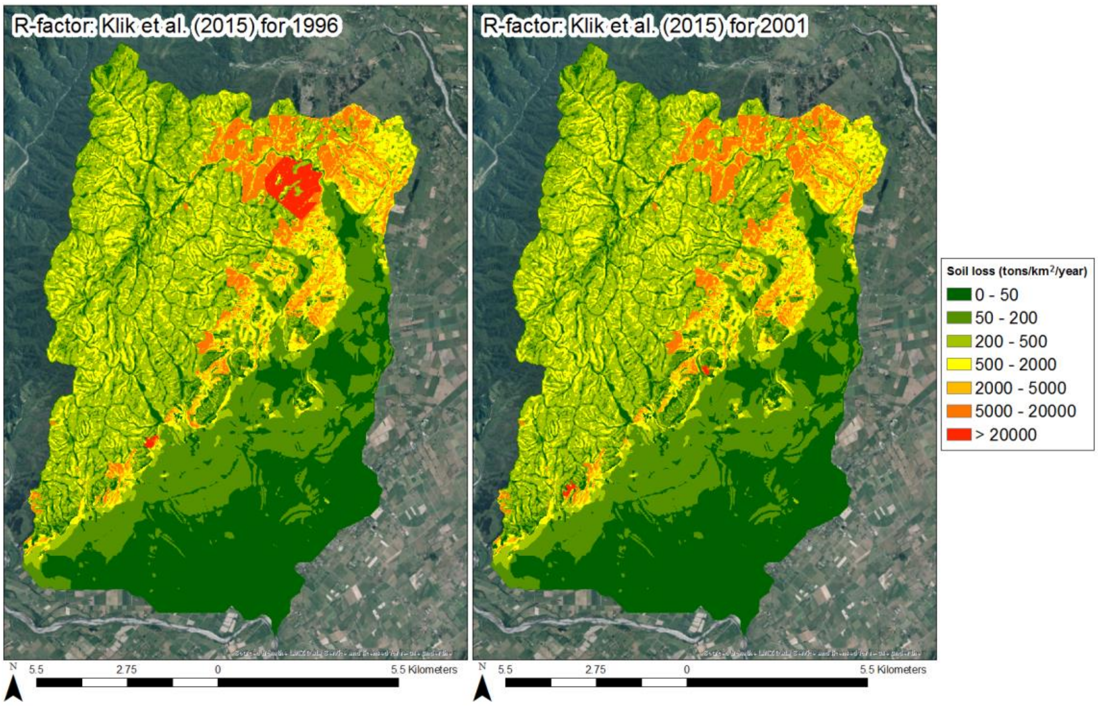

Figure 96. Soil loss maps under Klik et al. (2015) using LCDB1 (1996) and LCDB2 (2001).

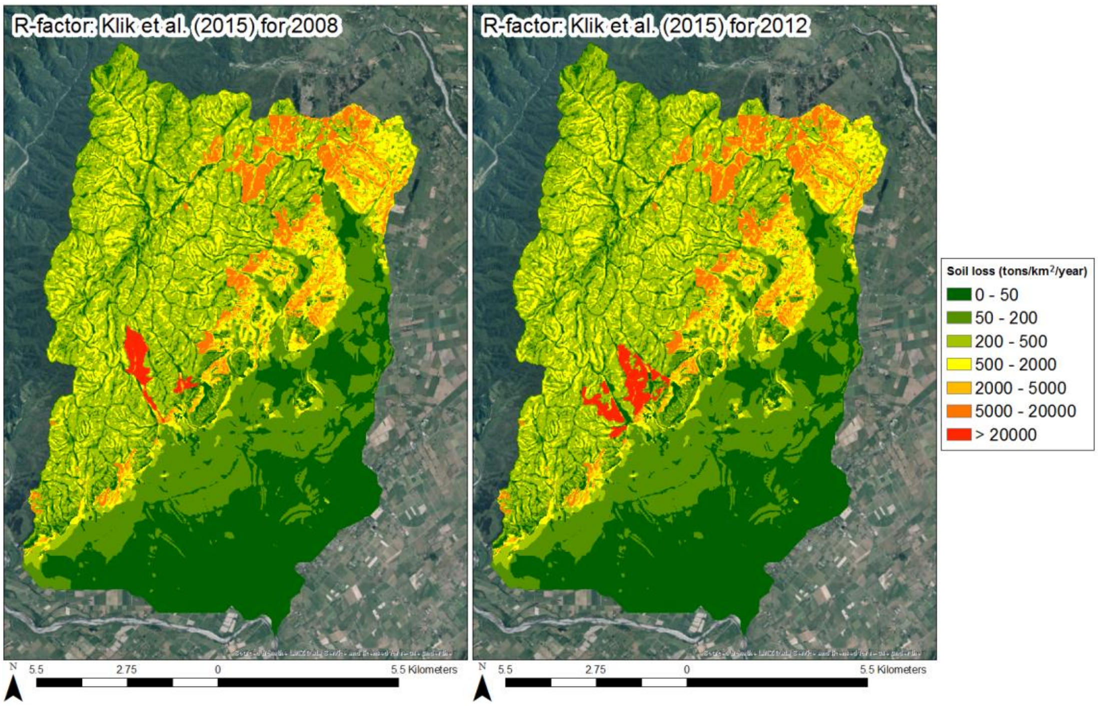

Figure 97. Soil loss maps under Klik et al. (2015) for LCDB3 (2008) and LCDB4 (2012).

6.4.3 Seasonal estimates of soil loss

Like the rainfall erosivity factor estimates, the seasonal soil loss estimates follow the same pattern. The soil loss predicted by Klik et al. (2015) was highest in the summer while the lowest occurred during spring. The opposite trend is seen in the seasonal soil loss estimates produced by the other two equations (Figure 98). Since more erosive storms occur during summer for the Mangatarere, the Klik et al. (2015) equation is the most appropriate to use for estimating seasonal soil loss. In terms of spatial variation, a larger proportion of the catchment is classified as vulnerable during the summer season (Figure 99). At the catchment scale, this inclusion of seasonal soil loss is useful because it allows management to see which seasons are more likely to bring erosion events and possibly exacerbate sediment delivery to streams, and impacts water quality. These seasonal results can be aggregated to annual soil loss, allowing for comparison between using monthly precipitation and annual precipitation to produce soil loss estimates.

At the farm scale, these seasonal estimates of soil loss have more utility. With changes in crops and agricultural practices, it is important for land management to understand which areas of their farm are vulnerable to soil erosion in each season. By refining the parameterisation of land cover (C-factor) and support practice (P-factor), the monthly estimates of soil loss can be improved, and more extensive scenario analysis can be undertaken to test which combinations of crop and practices will produce the most or least amount of soil loss. As stated in the review of R/USLE (Chapter 4), verifying the seasonal soil loss estimates could be done through observing variations in recorded water quality data in order to attain information about realistic patterns of seasonal soil loss.

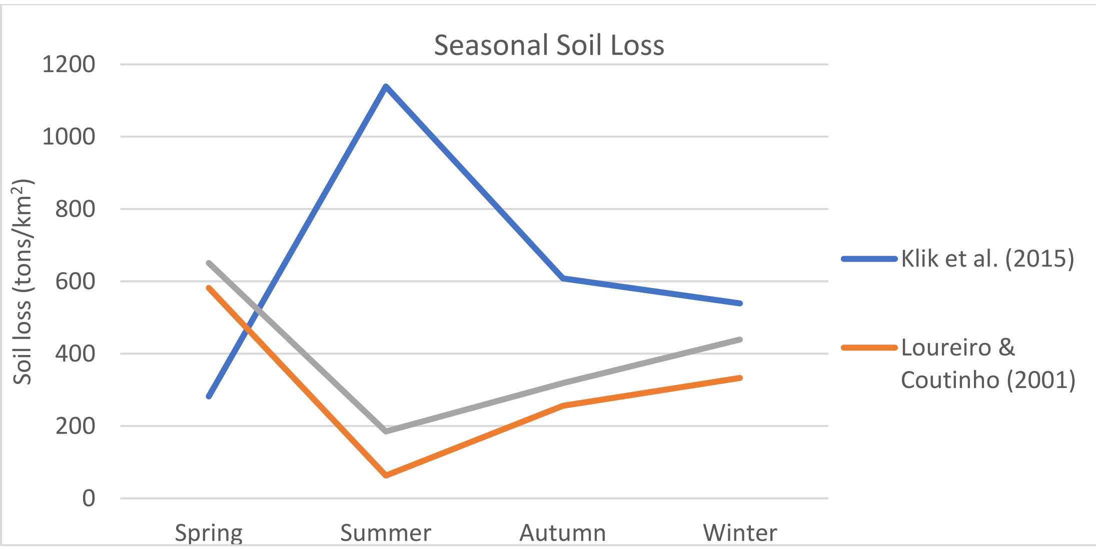

Figure 98. Seasonal estimates of soil loss using the three different R-factor equations.

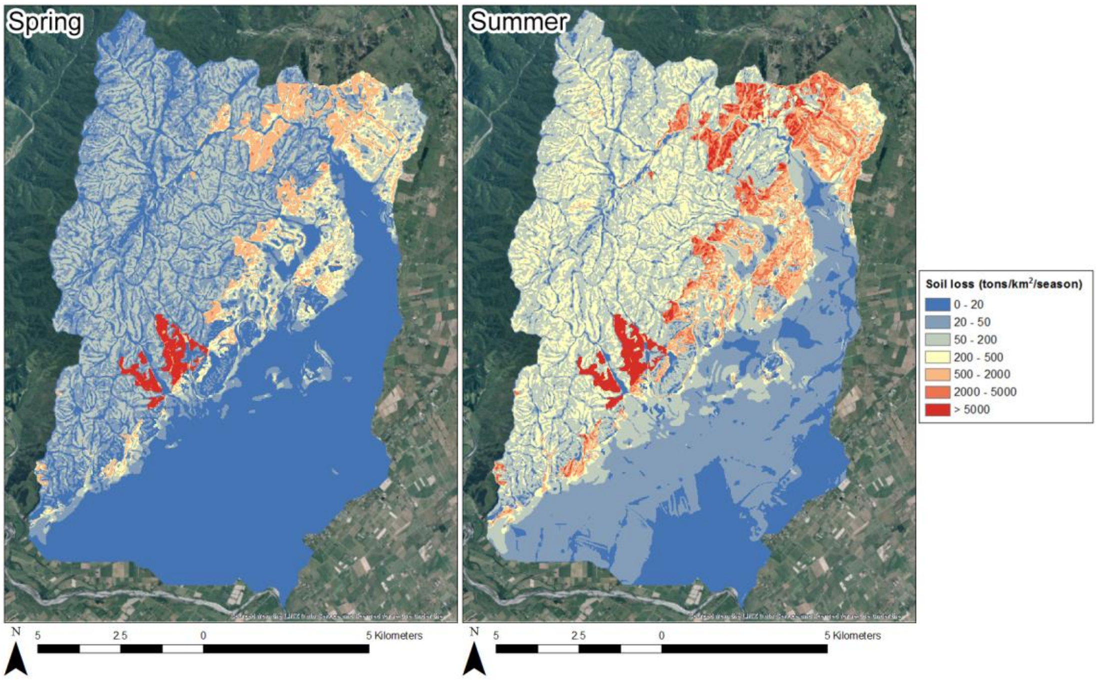

Figure 99. Soil loss maps under Klik et al. (2015) for Spring and Summer.

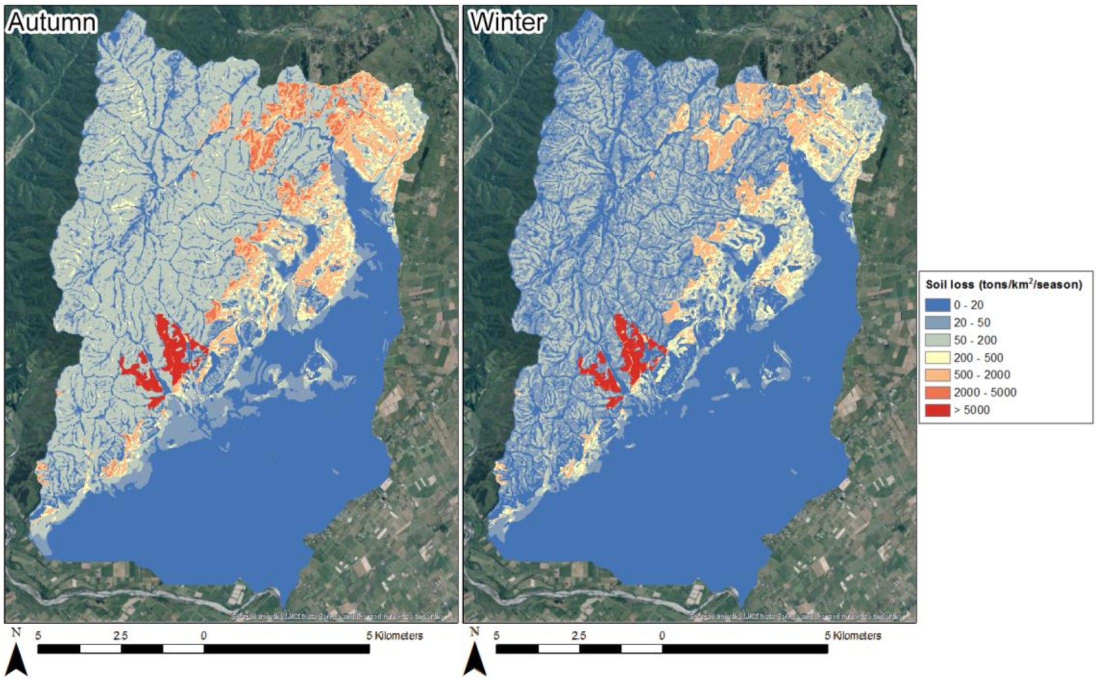

Figure 100. Soil loss maps under Klik et al. (2015) for Autumn and Winter.

6.4.4 Utility of the Compound Topographic Index (CTI)

At the catchment scale, the RUSLE is useful for identifying large areas vulnerable to soil erosion but does not yet account for erosion at much smaller scales, such as ephemeral gullying at the field scale. Gully erosion can be estimated through analysing aerial photographs and satellite imagery to observe temporal changes in gully size and thus estimate volume, but this technique requires pre-existing knowledge about gullies in the area of interest and may be tedious at larger scales (Daba et al., 2003; Gomez et al., 2003). The Ephemeral Gully Erosion Model (EGEM) uses rainfall-runoff and soil erosion modelling to estimate gully width, volume, and rates but requires detailed parameterisation data (Capra et al., 2005; Woodward, 1999).

As stated in Chapter 4, the Compound Topographic Index (CTI) uses three characteristics to identify areas susceptible to gully erosion: upstream drainage area, slope, and planform curvature (Thorne et al., 1985). These characteristics can be estimated from the DEM alone, making it a relatively simple model that has already been included in the LUCI model and to easier coupling with another empirical models, like RUSLE.

There are several ideas of how to include the CTI into the soil erosion estimates. One of these is to calculate sheet and rill erosion through the RUSLE, calculate gully erosion through the CTI, and add these two together. This can be the first step in including the CTI as it allows for comparison of soil eroded by sheet and rill erosion and soil eroded by gully erosion. However, it is important to note that this can lead to overestimation of soil loss or "double-counting" because of the interactions between the different mechanisms of soil erosion, such as sheet and rill erosion contributing to gully erosion (Lentz et al., 1993). Additionally, the CTI already includes slope and flow accumulation, which is included in the LS-factor method proposed by Desmet & Govers (1996). This means that simply adding the results of RUSLE and CTI will lead to the model account for slope and flow accumulation twice, which will affect soil erosion estimates.

The key to combining the CTI and the RUSLE may lie in the planform curvature, which is present in the CTI but not in the LS-factor. In an analysis of different topographic characteristics, the planform curvature was one of the most useful characteristics to predict ephemeral gullying, as channel cross-sectional area was positively correlated with planform curvature (Lentz et al., 1993). Since the LS-factor already accounts for slope and flow accumulation, combining it with the planform curvature could be an effective way of predicting ephemeral gully erosion. However, like the critical value for CTI that was proposed by Thorne et al. (1985), there must be a threshold for the LS-factor over which ephemeral gullying is likely. This threshold factor will depend not just on the topography of the site but can also account for the site's climate and erodibility. Further testing of the CTI and various combinations with the LS-factor are beyond the scope of this thesis and are recommended for future work.

The initial application of CTI to the Mangatarere identified more spots of erosion-prone land using the 5m DEM (Figure 101). The areas identified were those associated with the stream network and thus high values for flow accumulation. A user-defined threshold value can be used to identify the areas critical for gully erosion mitigation depending on the statistical distribution of CTI values (Momm et al., 2012). Figure 102 shows the spots within the Mangatarere where the CTI values were in the 90th percentile of all non-zero positive values for the catchment. Defining this threshold value is difficult and is dependent on the catchment's characteristics (e.g. flatter terrain requires higher threshold values), thus underscoring the need for further testing of the CTI within the Mangatarere. As stated previously, more research must be done to understand how the RUSLE and CTI can be combined to identify areas of soil erosion in the Mangatarere.

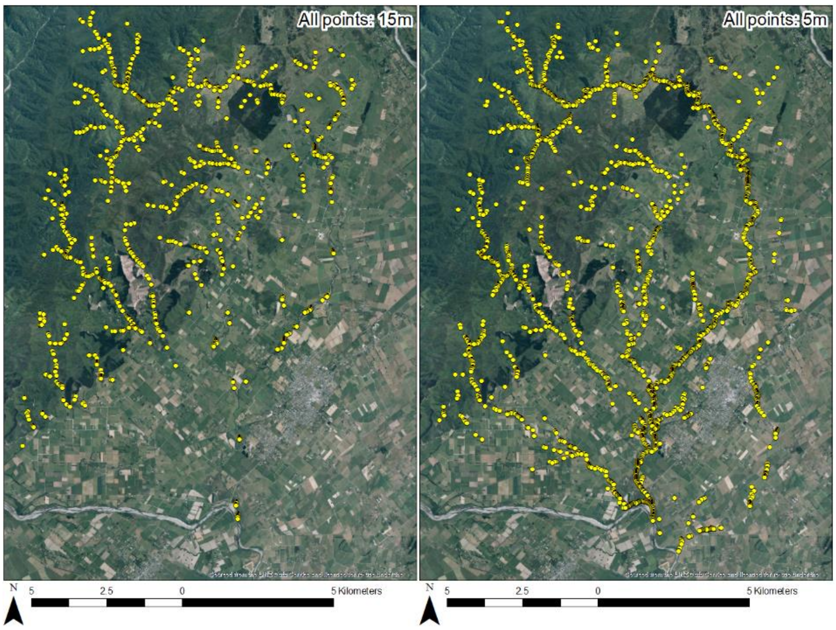

Figure 101. Sample map of erosion-prone locations in the Mangatarere based on all non-zero positive CTI values using the 15m DEM (left) and the 5m DEM (right).

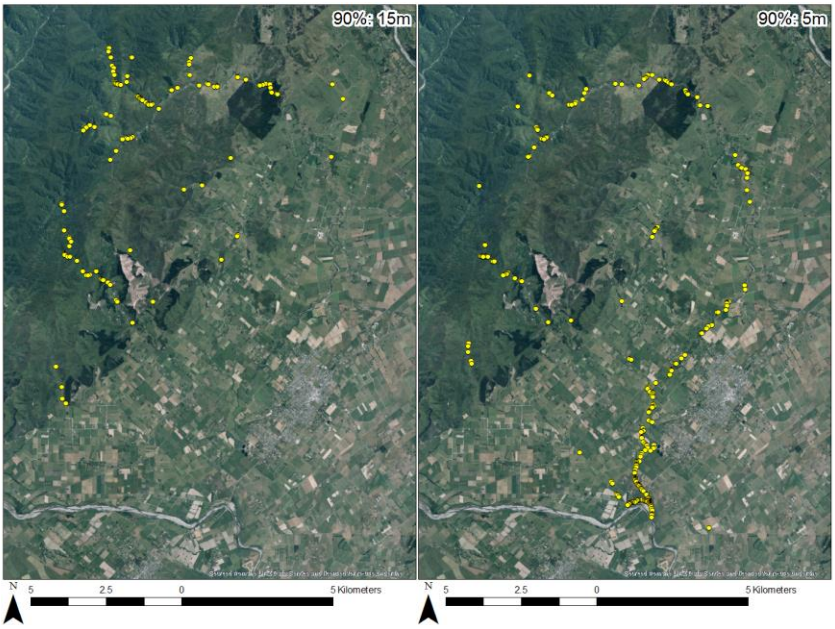

Figure 102. Sample map of erosion-prone locations in the Mangatarere showing the 90th percentile of non-zero positive CTI values using the 15m DEM (left) and the 5m DEM (right).

6.5 Limitations and future work

One of the objectives of this case study was to study the spatial variation of rainfall over the catchment using local rainfall data and how it affected the spatial variability of the rainfall erosivity factor. Although the work by Panagos et al. (2017) did produce a map that accounted for spatial variability, data from more local rain gauges can have be tested in future work with the other three R-factor equations to see if their pattern of spatial variability is similar. Aside from spatial variability, another direction for future work regarding the R-factor is to test all the equations on more years of rainfall data to get a range of possible R-factors for the Mangatarere, and to analyse the seasonal trends from year to year. Regarding the land cover, more specific parameterisation at the crop level and farm support practice scale can lead to more nuanced estimates of soil loss. Combining this with seasonal and monthly rainfall erosivity would allow farm management to estimate which areas of the farm would be at risk of soil erosion over different seasons, allowing them to time their management interventions accordingly. Going even finer with crop parameterisation would include accounting for the growing stages of plants, through analysing their rooting depth and how their ability to stabilise the soil changes over their growth cycle. Lastly, an important limitation of the RUSLE is its exclusion of other types of soil erosion such as gully erosion and mass wasting. Section 6.4.4 outlined some key ideas for incorporating gully erosion, and mass wasting can be included through a of threshold factor where landslides are triggered should it be exceeded.

6.6 Summary and conclusion

In this case study of the Mangatarere catchment and the RUSLE, the regional specificity of R-factor equations was outlined and tested by using several different equations. At the annual scale, the R-factor ranged from 1,221 to 2,607 MJ mm ha^{-1} hr^{-1}. At the seasonal scale, the trends in rainfall erosivity were completely different for the equation by Klik et al. (2015) and the equations by Loureiro & Coutinho (2001) and Ferreira & Panagopolous (2014). This underscores the importance of testing different equations for one study site to ascertain which equation is most appropriate. In terms of DEM resolution and the LS-factor, the slope gradient approach by Morgan (2005) on the 15m DEM was more useful at the catchment scale for identifying large areas of vulnerability. At the sub-watershed or farm scale, the approach by Desmet & Govers (1996) on the 5m DEM that includes flow accumulation is more useful because it delineates those vulnerable areas even further. In terms of land cover, those areas in the Mangatarere that are most vulnerable to soil loss are the ones classified as harvested forest and exotic grassland. This chapter shows the results of testing those different equations and outlines potential future work regarding the RUSLE and its parameterisation for New Zealand conditions.

7 Incorporating and extending a flatwater inundation model for the Land Utilisation and Capability Indicator (LUCI) Framework

7.1 Introduction

As established in Chapter 1, mapping flood hazards from extreme typhoon events is a critical component of the disaster risk mitigation programmes in the Philippines. This process estimates inundation extent and depths depending on the relationship between river water level, terrain elevation, and the influence of land cover roughness (Alaghmand et al., 2010). This process elucidates the connections between river level, flood volume and flood extent, thus allowing urban planners to identify areas that are vulnerable to flooding under different rainfall extremes. Since a component of this thesis is to create inundation maps of the CDO floodplain under different land cover and rainfall scenarios, it is important to understand the different kinds of methods used to estimate inundation under different conditions. The aim of this chapter is to extend and document the raster-based algorithm described in Ballinger et al. (2011) used for flood inundation within the Land Utilisation and Capability Indicator (LUCI) framework. The LUCI framework assists decision-making regarding sustainable land use management through its ecosystem services modelling capabilities, and identifying potential areas where management interventions can enhance ecosystem services (Jackson et al., 2013). One of the ecosystem services included in the LUCI framework is flood mitigation, and a more detailed hydrological and hydraulic modelling module is in development.

The possible applications of inundation modelling have led to the development of different types of computer models for estimating flood inundation, depending on the availability of data (Teng et al., 2017). These flood inundation models (FIMs) generally use discharge data, among other inputs, to estimate water depth and spatial extent of inundation on a floodplain (Castro-Bolinaga & Diplas, 2014). Since FIMs are used in scenario analysis under different flood scenarios, running a large number of different scenarios requires the FIM to be computationally efficient (Bernini & Franchini, 2013). There are several types of FIMs available, and Teng et al. (2017) identified three main approaches to flood inundation modelling: empirical methods, hydrodynamic models of varying complexity, and the emerging approach of simplified conceptual models.

The main aim of this chapter is to review the different methods of flood inundation modelling and to explain the inundation approach used by LUCI that was originally coded within MATLAB. This first iteration of the LUCI FIM was developed to test the utility of a new computationally efficient parsimonious flatwater inundation model that can be used in data-sparse regions (Ballinger et al., 2011). This flatwater inundation approach falls under the purview of simplified conceptual models which are explained in Section 7.1.3.

Although this thesis mainly focuses on the Philippines, this chapter uses the Lower Hutt floodplain to test the FIM Python code to replicate the results produced by the FIM MATLAB code presented by Ballinger et al. (2011). This site was chosen because of the availability of a high-resolution DEM (5m) and information about the areas along the river where water is expected to breach when the flow exceeds channel capacity. In the CDO, this information about breach locations and overtopping flow is not available. However, this chapter is included in this thesis because flatwater inundation model is planned to be coupled with the rainfall-runoff model within LUCI that has compared well with the HEC-HMS model already within CDO (Chapter 8).

To help improve the applicability of the LUCI FIM, it was translated into Python to allow for implementation into ArcMap 10.4.1 and the LUCI framework. The LUCI FIM complements the existing LUCI framework by using flow data to estimate inundation depths and extent, which has applications for testing the effect of land cover changes, response to extreme events and potential inundation under climate change.

7.1.1 Empirical methods

Empirical methods use satellite imagery to derive flood inundation maps from previous flooding events, which can be compared to recorded gauge heights to build a library of maps for a range of events (Bhatt et al., 2016). With the advent of cloud-computing technology such as Google Earth Engine, satellite data from different sources can be more easily accessed and processed to map historical floods (Schwarz et al., 2018). The utility of this method is to give an estimation of flood extent based on past flood events, which can assist in city planning. Rating curves that relate flood extent and stage or discharge measurements can be created for scenario analysis, but their accuracy is dependent on the type of satellite imagery used (Smith, 1997). Bhatt et al. (2016) used satellite Radarsat-1 and Radarsat-2 satellite imagery to map historical floods in India while Schwarz et al. (2018) used the resources of Google Earth Engine to do the same in Senegal. These satellite observations may be insufficient to predict future flood events, especially those that are larger than previous floods (Teng et al., 2017). Thus, empirical methods may be useful in areas where only satellite imagery and historical flood data are available. However, in the presence of more detailed data, hydrodynamic models can be applied to give a more accurate representation of flood inundation.

7.1.2 Inundation models

To predict the response of a watershed to rainfall and the resulting floodplain inundation, two types of models are usually used in combination: hydrological models and hydraulic/hydrodynamic models. Hydrological models are used to simulate the response of a watershed to a given pattern of rainfall intensity in order to produce a hydrograph of discharge against time (Bedient et al., 2013). Hydrodynamic models approximate fluid dynamics through solving equations based on the physics of flow (Teng et al., 2017). These approximations of fluid dynamics are used in hydraulic models, which use discharge information (along with cross-sectional geometry and roughness information) from hydrological models to compute water surface depths and spatial extent (Castro-Bolinaga & Diplas, 2014). This combination of models can then be used for flood forecasting, scenario analysis and hazard mapping (Teng et al., 2017).

Hydrodynamic and hydraulic models are usually classified based on the dimensions they are capable of representing: one-dimensional, two-dimensional, and three-dimensional (Hunter et al., 2007). Although increasing dimensionality of these models allows for more in-depth and detailed analysis of flood inundation, the trade-offs are high computational costs for large floodplains and detailed data requirements that may not be available or are costly to obtain (Bernini & Franchini, 2013). As the model complexity increases, factors of computational cost, input data collection costs and the requirements of the user influence the type of model that is most suitable for the modelling application (Hunter et al., 2007). This chapter presents an overview of several types of inundation models: hydrodynamic models and simplified conceptual models.

7.1.2.1 One-dimensional

One-dimensional models represent flow processes within the river channel going in the direction of flow, and have some functions to roughly represent the floodplain (Falter et al., 2013). The river and floodplain are represented as a series of cross-sections that require information about floodplain topography, the location of the riverbank and the shape of the river bed. At each time step, the model solves the one-dimensional Saint-Venant equations to estimate flow discharge and water depth between each cross-section (Teng et al., 2017). These models can be used in locations where the available information consists of floodplain topography, river bathymetry and land cover.

Due to their efficiency and relative simplicity, these models are widely-used in tandem with hydrologic models for scenario analysis. For example, the Hydrologic Engineering Center's River Analysis System (HEC-RAS) has been applied with HEC's Hydrologic Modeling System (HEC-HMS) to assess the effect of changing land use on flood peak and inundation in places such as Malaysia, China and the United States of America (Alaghmand et al., 2010; Du et al., 2012; McColl & Aggett, 2007). HEC-HMS is a rainfall-runoff model that uses mathematical representations of infiltration, runoff, flow and routing to produce a flow hydrograph (Scharffenberg, 2013). The hydrograph from the HEC-HMS model can then be used as input to HEC-RAS to produce inundation maps. HEC-RAS estimates water surface profiles by calculating the water surface elevation and flow characteristics at each cross-section, then interpolating between cross-sections, and extracting final water depth by comparing it to the original digital elevation model (DEM) (Tayefi et al., 2007). HEC-RAS solves several equations that represent steady flow, unsteady flow, routing and land cover roughness to produce its inundation maps (Brunner, 2010a). Another one-dimensional hydraulic model is MIKE 11 from DHI which can use three different flow descriptions: dynamic wave approach that solves the full momentum equation to simulate fast flows; diffusive wave approach that accounts for downstream boundary conditions and backwater effects; and the kinematic wave approach based on balancing friction and gravity effects (DHI, 2009).

One-dimensional models are advantageous for study sites with relatively sparse data (DEM, river cross-sections, and land cover) and are more computationally efficient compared to two- and three-dimensional models. However, an assumption of these models is that flow moves in one direction which is parallel to the main channel, which may not always be true (Pender,f2006). Although these models can capture one-dimensional flow within a river channel and the resulting floodplain inundation, modelling inundation over more complex and wide terrain necessitates the use of a two-dimensional model.

7.1.2.2 Two-dimensional

Two-dimensional models generally use simplified shallow water equations to better represent flood inundation over wide floodplains by estimating water level and depth-average velocity in two perpendicular directions (Pender, 2006; F8(ter a1)a5(a)-6(i)100 0 1 4als 0 0-3 2013). These models may use the 1D St. Venant equations for computing in-channel flow, but then solve the full 2D shallow water equations for estimating floodplain flow (Krupka & Wallis,od(, Tmo0.0l reW*864 4 353.09 Tm g G(K)] TJETQq0.000008871 0 595.32 841.92 reW* compared to simpler models, making them suitable for small-scale applications with fine DEM resolution or large-scale applications with coarse DEM resolution (Bates et al., 2013; Falter et al., 2013).

Two-dimensional models have an advantage over one-dimensional models due to their capability to model varying flows within a channel and not just at each cross-section. Another advantage is their more robust representation of lateral flow over a floodplain. However, they are more computationally intensive. In a comparison between the one-dimensional MIKE11 and the coupled 1D/2D MIKEFLOOD model over a 17km^2 floodplain, the computational time for MIKE11 was 2 minutes while the MIKEFLOOD model at the coarsest DEM resolution took 3 hours and 43 minutes (Chatterjee et al., 2008). They found that the storage space required by MIKE11 was significantly less compared to the storage space required by MIKEFLOOD for its computations, with 22MB for MIKE11 and 1.1 GB for MIKEFLOOD.

For applications that require an even more detailed representation of flow, particularly around structures such as bridges or dams, three-dimensional models are required.

7.1.2.3 Three-dimensional

Applications that utilise three-dimensional models require complex modelling of detailed flow dynamics, usually to assess the integrity of dams and other structural measures against flash floods or tsunamis (Teng et al., 2017). Three-dimensional models solve the 3D Reynolds-averaged Navier-Stokes (RANS) equations for steady incompressible turbulent flows to estimate water levels and velocity fields within the channel and on the floodplains (Lai et al., 2003; Néelz et al., 2009). This approach goes beyond two-dimensional modelling because it can simulate vertical flow patterns, which has applications in testing structural integrity and sediment transport.

Lai et al. (2003) used three-dimensional flow simulation to assess flow in a hydroturbine draft tube and a fish passage facility. Work by Kheiashy et al. (2010) used three different 3D models for one application in a large alluvial river: ECOMSED which simulates both flow and sediment transport, MIKE 3 which solves continuity and momentum conservation equations in three dimensions, and H3D which solves the 3D RANS equations.

Three-dimensional models can represent more complex flow dynamics, but at the cost of computational efficiency. In large areas with sparse data, there is an emerging method: simplified conceptual models that represent physical processes through simplified hydraulic concepts (Teng et al., 2017).

7.1.3 Simplified conceptual models

Simplified conceptual models do not fall under the previous categories of one-dimensional, two-dimensional, and three-dimensional hydraulic models because their algorithms do not solve physics-based equations such as the Saint-Venant or RANS equations. These are raster-based models which represent the floodplain DEM as a series of grid cells or topographic depressions where water can accumulate, and where the flood behaviour and exchange between these grid cells is governed by mass conservation equations (Bernini & Franchini, 2013). These are used for large-scale assessment of flood spatial extent and depth due to their relative computational efficiency and low data requirements (Pender, 2006).

One technique in simplified conceptual modelling is the Rapid Flood Spreading Model (RFSM), which represents the floodplain as a system of storage reservoirs which are natural depressions in the ground where water accumulates, defined as impact zones (IZs) or accumulation zones (AZs) (Bernini & Franchini, 2013; Gouldby et al., 2012; Lhomme et al., 2009). GIS pre-processing is achieved on a DEM of the floodplain to divide it into AZs, and each AZ has an associated volume and volume-level curve, which determines the amount of water the AZ can hold before it spills into adjacent AZs. The cells in-between AZs are called boundary cells, and the one with the lowest elevation is defined as the “communication point”, where water will spill into the adjacent AZ once the initial AZ has been filled up (Bernini & Franchini, 2013; Lhomme et al., 2009). Although not called RFSM, a similar approach was used by Krupka & Wallis (2007) to represent the floodplain as a series of flood storage cells, which spill into neighbouring cells when the water level reaches the elevation of the adjacent cells. Similar approaches of delineating depressions or accumulation zones to represent the floodplain have also been applied in urban floodplains in China (Z. Li et al., 2014; Shen et al., 2016; Zhang & Pan, 2014).

Another technique in simplified conceptual modelling is flatwater inundation, which represents the floodplain as a series of regular grid cells instead of topographic depressions, and is suitable for study sites where detailed data on floodplain characteristics is unavailable (Ballinger et al., 2011). This method requires a high-resolution DEM and knowledge of locations along the river where water is likely to spill when the flow reaches a certain discharge rate, called “breach points”. DEM cells adjacent to these breach points are defined as “wet cells,” and water is iteratively added to these wet cells and to the surrounding cells which have a lower elevation and are considered “dry cells” (Chen et al., 2009). Unlike RFSM, flatwater inundation models do not require extensive pre-processing of the floodplain DEM because it does not need to divide the floodplain into accumulation zones. Pre-processing can involve identifying the cells with the lowest elevation, or the highest contributing area, and creating a sorted list of cells based on those two characteristics to increase the computational efficiency of the inundation model (Yang et al., 2015).

This technique has been applied to the Lower Hutt floodplain in New Zealand, and is being developed for use in the Land Utilisation and Capability Indicator (LUCI) model as its inundation routine (Ballinger et al., 2011). The algorithm runs within the MATLAB R2015a. Starting with the breach points, iteratively spill water from wet cells to dry cells and end once all the water has spilled from all the breach points. Work by Chen et al. (2009) has applied a similar algorithm to the University of Memphis, Tennessee, using elevation data in the form of contour maps and sewer system data to estimate inundation using runoff from a storm-runoff model.

Although the utility of these simplified conceptual models is clear, there are some criticisms of these techniques. The main drawback is that these models lack the representation of flow dynamics represented in hydrodynamic models, making them unsuitable for applications such as determining velocity within the channel (1D), in the lateral flow over the floodplain (2D) and against structures such as dams or bridges (3D) (Teng et al., 2017). For applications that require velocity, hydrodynamic models are a more suitable choice of inundation model. Simplified conceptual models are also unable to represent the temporal evolution of a flood event, making them more suitable for applications where the final or maximum flood inundation is required, such as hazard zoning or extreme flood scenario analysis (Zhang & Pan, 2014).

Another criticism of simplified conceptual models is that they are unable to approximate the temporal evolution of a flood, because applications have mostly been concerned with final inundation extent. Bernini & Franchini (2013) were able to approximate the temporal evolution by a gradual “spilling” of total flood volume into AZs instead of instantaneously filling AZs. This was done by splitting the volume into a large number of fractions and gave results that were in better agreement with the reference inundation produced by the FLO-2D model compared to instantaneous filling (Bernini & Franchini, 2013).

Since mass conservation is the governing equation of simplified conceptual models, they do not explicitly account for the effects of gravity and friction. Surface friction causes a time lag before reaching maximum inundation depth, which may allow flood water to infiltrate into the ground or be carried away by sewer systems (J. Chen et al., 2009). Lhomme et al. (2009) represents the effect of friction on inundation using the Manning coefficient of friction to raise the threshold before water spreads, because friction can affect flood wave movement. Future developments of the LUCI FIM can include coefficients to account for the effect of friction and infiltration under several types of land cover, as the infiltration capacity of of different land covers could affect the flood wave differently.

The criticisms of simplified conceptual models can be addressed by extending the existing algorithm to approximate temporal evolution based on dividing spill volumes, and accounting for friction based on coefficients of friction. Algorithms can also account for the effect of storm drains, where in the study by Chen et al. (2009), water was removed from the floodplain based on a function that includes the permanent conveyable flow rate of the sewer system (cumecs hr^{-1}), the time (s), and the drainage area of the study site (ha).

The first iteration of the LUCI FIM ran mainly in the MATLAB environment and calls several ArcMap functions. Conversion to Python allows the code to be more widely-utilised by potential users that do not have access to MATLAB. By using Python instead of MATLAB, the FIM can then be integrated into the existing LUCI toolbox so that users perform their own scenario analysis for creating hazard maps. This chapter builds on the work by Ballinger et al. (2011) in Lower Hutt, New Zealand, and contributes to the growing body of research surrounding more simplified inundation models.

7.2 The LUCI Floodplain Inundation Model

This inundation model was originally developed for a study investigating flooding in the Lower Hutt floodplain in New Zealand and is being developed for inclusion in the Land Utilisation and Capability Indicator (LUCI) framework. The LUCI FIM is a raster-based algorithm that requires elevation data, and flood runoff or sea level rise data (Ballinger et al., 2011).

At the base level, the LUCI FIM requires the following datasets: a digital elevation model (DEM) of the floodplain, a polygon shapefile of the river, and a polyline shapefile of the breaches. The shapefile of the breaches must contain the following information for each of the breaches:

- ID (unique for each breach);
- Overtop volumes (in cumecs);
- Reachcode (for breaches that are associated with each other, such as those on opposite sides of the river); and
- Length of breach (in metres).

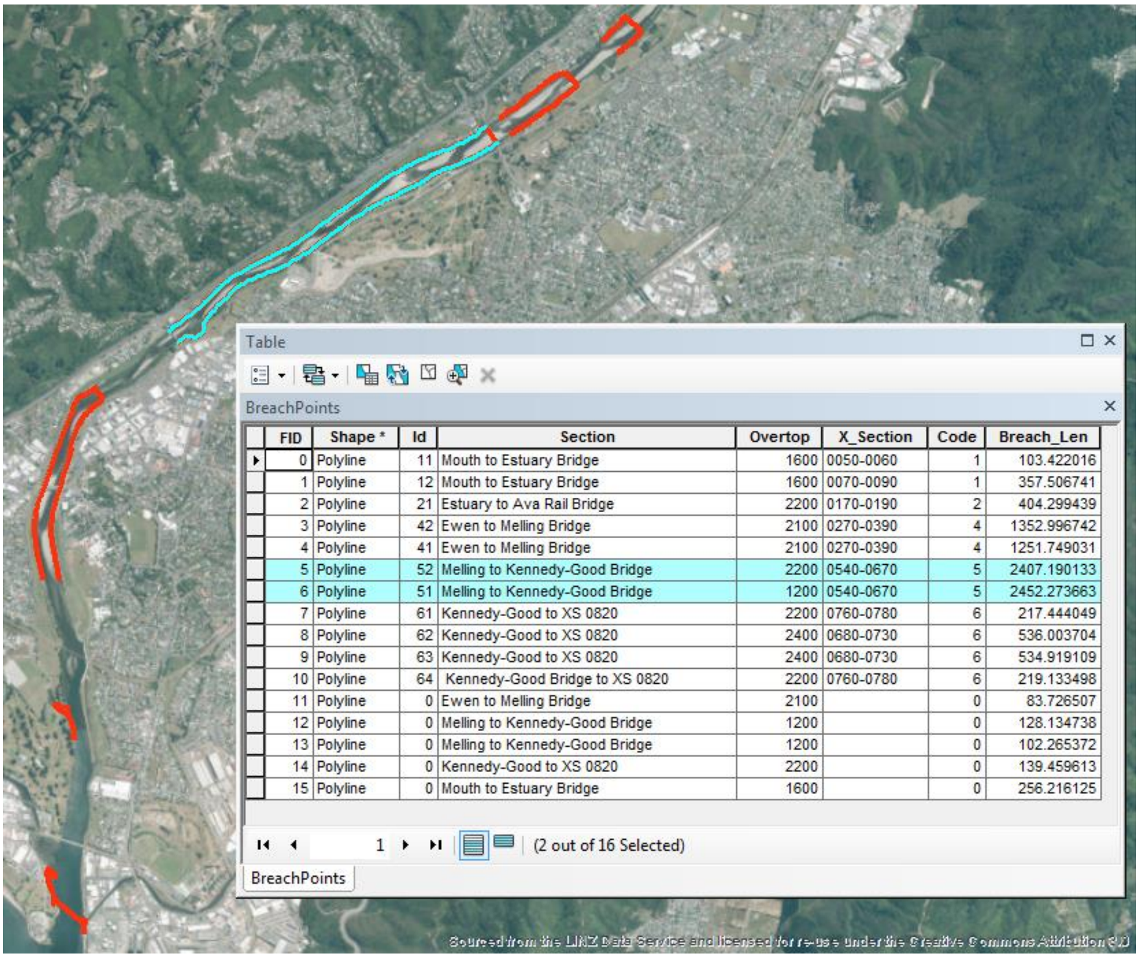

Figure 103. Screenshot of the breach shapefile and attribute table for Lower Hutt floodplain inundation.

The shapefile for the breaches is important in order to estimate the volume of water that will be spilled from a reach. Each breach should have an associated Id, Reach Code, and overtopping volume. The overtopping volume is the flow volume where the water is expected to go over the breach and spill into the floodplain. This information can be taken from previous observations of the breach during flooding or from the technical specifications of constructed stopbanks. The preprocessing to calculate the volume spilled is as follows:

First, multipliers were calculated for each breach. Since some breaches are associated with each other (e.g. on opposite river banks), these multipliers are used to predict the proportion of flood volume expected to spill from that breach. For breach with Id A associated with Reach Code B:

$$Multiplier = \frac{Length\ of\ breach\ Id\ A}{(Total\ length\ of\ breaches\ with\ Code\ B)}$$

Next, the potential volume that will be spilled was calculated on a per-scenario basis. For the initial testing of the LUCI FIM in the Lower Hutt floodplain, 17 scenarios of different flood volumes were defined ranging from 1500 cumecs to 3200 cumecs. For each of the flood scenarios (Flood):

$$Volume\ to\ spill = (Flood\ - overtopping\ volume) \times Multiplier\ \times 60\ \times 60$$

From a flow volume in cubic metres per second, the volume of spill is converted into cubic metres depending on the appropriate flow from the hydrograph or design flood. If the resulting volume is negative, the volume to spill is set to zero. In addition to the input data, there are several boundary conditions and parameters that can be set in the LUCI FIM (Table 50). The programme is capable of batch-running over several different scenarios (Scenario). The flood defences (Flooddef) can be either the flood defences as of 2011 or the flood defences after the proposed upgrades (Ballinger et al., 2011).

Table 50. LUCI FIM inputs, boundary conditions, and parameters.

Input	Definition	Default value
inputDir	Pathway to where the files are located	
DEM	Filename of the digital elevation model	
River	Filename of the shapefile of the river	
Breach	Filename of the shapefile of the breach points	
Inundation_opt	Inundation scenarios from TopNet (1) or reference (2)	2
Scenario	Pulls the flood volumes from the inundation scenarios	From 1 to 17
Seaheight	Height of the sea	0
Flooddef	Whether the flood defences are not upgraded (1) or upgraded (2)	1
Breach_link_opt	Whether to allow water exchange across river	0
Sea_tolerance	Tolerance to water building on boundary between the river and the sea	0.01
output_type	ESRI grid (1) or ASCII file (2)	1
incrmRate	Amount of water depth added to each of the wet cells on each iteration (m)	0.005

7.2.1 Simplified Description of the LUCI FIM (MATLAB)

In the first version of the LUCI FIM, the code was primarily used in MATLAB R2015a with ArcPy functions to import and export the results. Starting from each breach, water is iteratively "spilled" into the cells adjacent to the breaches and cells that are already "wet". The programme finishes "spilling" once the maximum volume that can be spilled is reached, or the inundated area reaches the sea.

A simplified flowchart of the LUCI FIM is shown in Figure 104. The final water depths are estimated by the difference between the final water surface elevations and the elevation of the original DEM and exported by default as ESRI grid files.

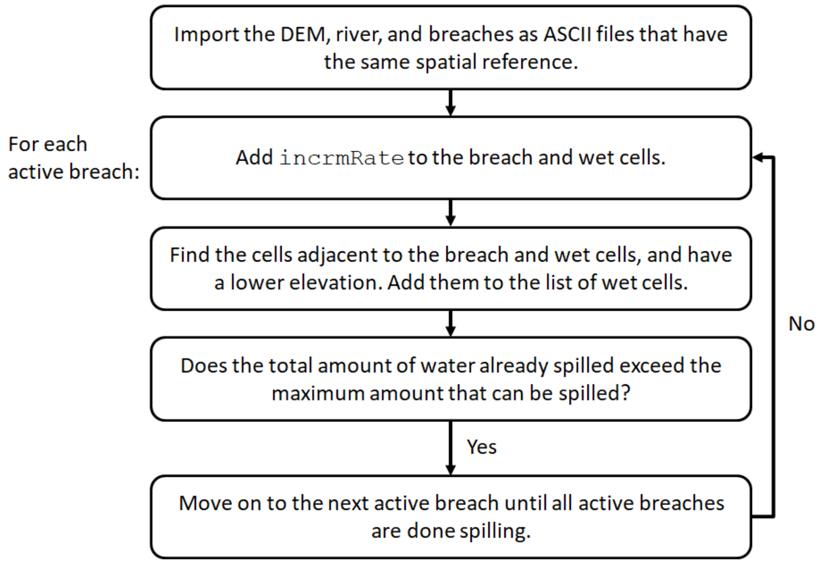

Figure 104. Simplified flowchart of the LUCI FIM.

7.2.2 Detailed Description of the LUCI FIM (MATLAB)

The input files of DEM, river shapefile and breaches shapefile are converted to ASCII format, with the spatial reference being that of the DEM. These ASCII files are then imported into MATLAB as an array of values, with all three arrays having the same number of rows and columns as the DEM.

The DEM data is copied into another variable (DDEM). Within DDEM, any cells where the river is located are assigned a high value (9999) to prevent spillage into the river. The FIM keeps track of the indices of cells that are considered "wet" and their corresponding elevation. The breach cells are classified as "wet" and are where the water begins to spread.

The FIM begins spilling from one breach at a time, if the breach is considered "active" because it has been overtopped by the flood water. The FIM keeps track of the maximum amount of water that can be spilled by that breach, and how much water has already been spilled by that breach.

During each iteration, the volume of water already spilled on the floodplain is checked against the maximum amount of water expected to spill from that breach. If the floodwater has not yet reached the sea, the programme also checks that the volume of water expected to spill in the next iteration will not be above the maximum amount expected to spill. If more water can be spilled, an increment rate (default: 5mm) of water is added to each of the “wet” cells. The algorithm then looks for the cells adjacent to the “wet” cells and spills water into the cells that have a lower elevation. If the volume of water to be spilled in the next iteration will cause exceedance of the maximum volume of water, the algorithm moves into the final increment. The amount of water added to each “wet” cell is the difference between the maximum and spilled volume of water divided by the number of wet cells.

After the last increment for that breach is complete, the DEM including water depths (the “wet DEM”) is updated and the algorithm moves on to spilling from the next active breach. Once the spilling is complete for all the active breaches, the final water depths are calculated by getting the difference between the final “wet DEM” and the original DEM. The resulting matrix is rewritten as an ASCII file and then exported as an ESRI grid file to allow for visualisation in ArcMap.

7.2.3 Differences between the MATLAB version (FIM MATLAB) and Python version (FIM Python) of the LUCI FIM

The main difference between FIM MATLAB and FIM Python is that the latter can run as a Python script within the ArcGIS environment. The FIM MATLAB code ran mainly within the MATLAB programme but also used ArcGIS commands to import and export the results. This is useful because FIM MATLAB required the user to have access to both MATLAB and ArcGIS, but since FIM Python runs solely within the ArcGIS environment, ArcGIS would be the only software required. Additionally, the LUCI framework runs as a toolbox solely within the ArcGIS environment, so FIM Python can be fully integrated into the LUCI framework and distributed to its users that already use ArcGIS. Future work on the FIM Python will include a user interface within ArcMap that will allow users to enter their own input and flood scenarios. This makes the LUCI

FIM more accessible to users who are familiar with ArcMap but not necessarily with MATLAB or Python coding script. Since the LUCI FIM was originally applied to Lower Hutt (New Zealand), the novelty of this work through updating and converting it from MATLAB to Python allows it to be tested and applied in new study areas. Although the scope of this thesis is mainly the CDO catchment in the Philippines, the LUCI FIM has not been fully parameterised for the CDO floodplain and comparing it to the already established HEC-RAS model is a key component of future work (Chapter 8).

7.3 Application: Lower Hutt, New Zealand

As stated previously, the FIM MATLAB was developed and applied to the Lower Hutt floodplain in New Zealand. The purpose of applying the FIM Python to the same floodplain is to validate it against the original FIM MATLAB results. The Hutt River catchment (~655km^2) is located at the southern part of the North Island of New Zealand (Figure 105) with the main Hutt River running for 54km through the mainly forested headwaters and through the heavily urbanised valley and floodplain (GWRC, 2001). With its long history of destructive flood events and the potential of climate change to exacerbate these floods, local government has made it a priority to use structural measures such as stopbanks to protect communities and infrastructure (GWRC, 2001; Lawrence et al., 2013). Previous inundation work in Lower Hutt has contributed to the development of the Lower Hutt Floodplain Management plan that produced flood extent maps to guide decision-making, and to the development of the LUCI flatwater inundation method detailed in the previous sections (Ballinger et al., 2011; GWRC, 2001).

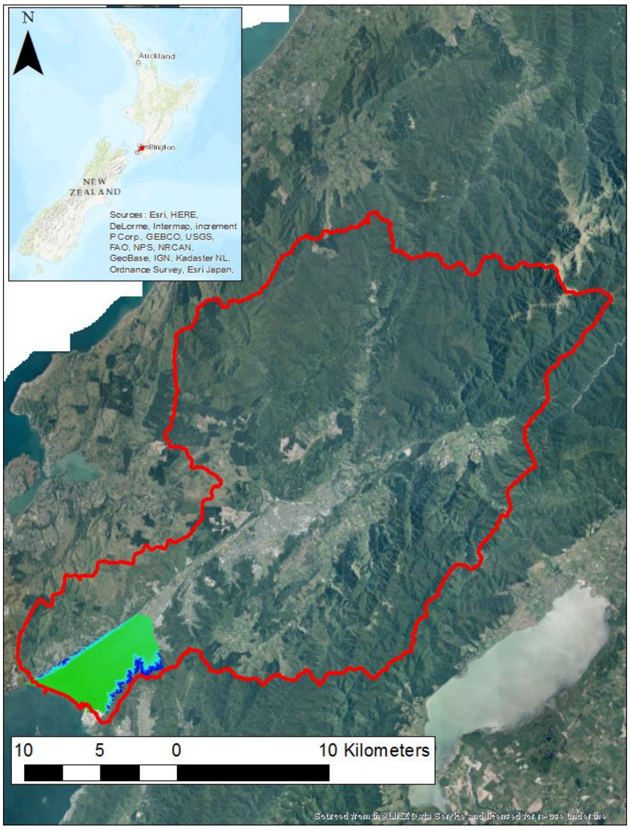

Figure 105. Map of the Hutt catchment (red) showing its location within New Zealand and the extent of the LiDAR-derived DEM on the floodplain (green) (Catchment shapefiles taken from the GWRC Open Data Portal: http://data-gwrc.opendata.arcgis.com/).

The DEM (5m resolution) was derived from LiDAR information and covers the mainly urbanised area of the Lower Hutt floodplain (Figure 106). Although an updated LiDAR-derived DEM is available for the entire Greater Wellington Region, this study was limited to the floodplain to replicate the geographical extent used by Ballinger et al. (2011). Modelling the urbanised area of the Lower Hutt floodplain is important to disaster risk management because of the river's proximity to populated areas and the estimated cost of NZD 1 billion in damages from an extreme flood event (GWRC, 2001). The breach points were compiled by Ballinger et al. (2011) using information about the sections of the Hutt River vulnerable to overtopping, and the scenarios tested ranged from a flood event of 1,500 m^3 sec^{-1} to 3,200 m^3 sec^{-1} (cumecs) of water. Risk modelling has indicated that a flood event exceeding 2,300 cumecs would lead to a significant increase in physical and financial damage compared to a 2,100 cumecs flood event (Lawrence et al., 2011).

Figure 106. Extent of LiDAR-derived DEM (black) over the Lower Hutt floodplain and modelling extent.

This section briefly presents results of flood inundation modelling from the LUCI FIM MATLAB and Python versions. Seven scenarios were compared between the MATLAB and Python code. For scenarios 1 to 7 (Table 51), the programme ran successfully and produced similar inundation results. However, the Python code ran slower compared to the MATLAB code. At larger flows (>2,100 cumecs), the first draft of the Python code experienced much longer computation times compared to the MATLAB code and requires more improvements to the computational efficiency. The scope of this thesis is to update the existing LUCI FIM code from 2010 to be run within MATLAB, and future work will include improving the new Python version to run more efficiently for larger flood volumes.

Table 51. Inundation depths for different scenarios using the LUCI FIM in MATLAB and Python.

Scenario #	Peak flow (cumecs or m^3 sec^{-1})	Inundation depth from FIM MATLAB (m)			Inundation depth from Python (m)		
		Min	Mean	Max	Min	Mean	Max
1	1,500	0.001	0.444	0.862	0.020	0.468	0.891
2	1,600	0.001	0.444	0.862	0.020	0.468	0.891
3	1,700	0.023	0.485	1.367	0.023	0.485	1.367
4	1,800	0.015	0.389	1.974	0.015	0.572	1.974
5	1,900	0.003	0.566	2.143	0.002	0.579	2.043
6	2,000	0.001	0.275	2.143	0.002	0.281	2.043
7	2,100	0.001	0.477	2.143	0.001	0.477	2.143
8	2,200	0.001	0.640	3.233			
9	2,300	0.001	0.872	3.233			
10	2,400	0.002	0.546	3.233			
11	2,500	0.001	0.563	3.233			
12	2,600	0.005	0.579	3.233			
13	2,800	0.005	0.579	3.233			
14	2,900	0.005	0.579	3.233			
15	3,000	0.005	0.579	3.233			
16	3,100	0.005	0.579	3.233			
17	3,200	0.005	0.579	3.233			

For Scenario 1 at 1,500 cumecs, flooding occurred near Melling where the overtopping volume of that breach is 1,200 cumecs (Figure 107). This section of the Hutt River was proposed for upgrades in flood protection against a peak flow of 2,800 cumecs (Ballinger et al., 2011). Scenario 2 (1,600 cumecs) shows the same amount of flooding to Scenario 1 where only the area near the Melling Link experiences any breaching (Figure 108). Comparing the inundation extent, the results produced by FIM MATLAB and FIM Python are almost the same. Flooding occurs in the same area for both versions of the FIM code, with an extra cell of flooding in the FIM Python code (Figure 107). In terms of differences in flooding depths, the FIM MATLAB predicted a lower minimum flood depth (0.001m) compared to the FIM Python depth of 0.020m. The mean flood depth and maximum depths were similar between FIM MATLAB (0.444 mean and 0.862 max) and FIM Python (0.468 mean and 0.891 max).

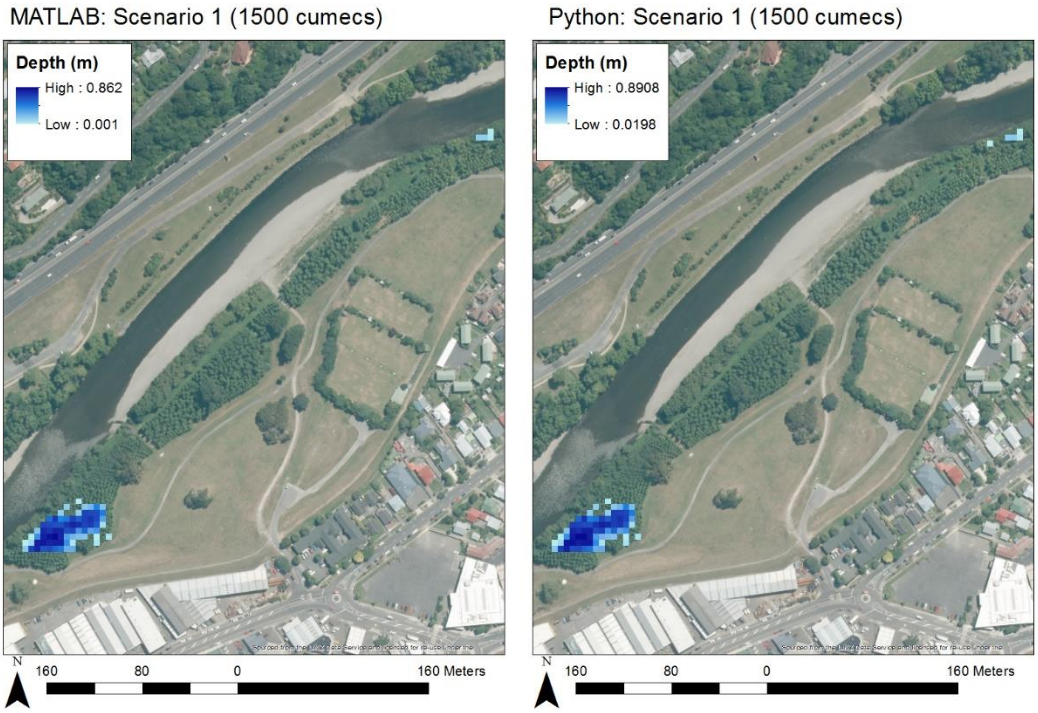

Figure 107. Comparison of the Scenario 1 (1,500 cumecs) showing flooding near Melling Road.

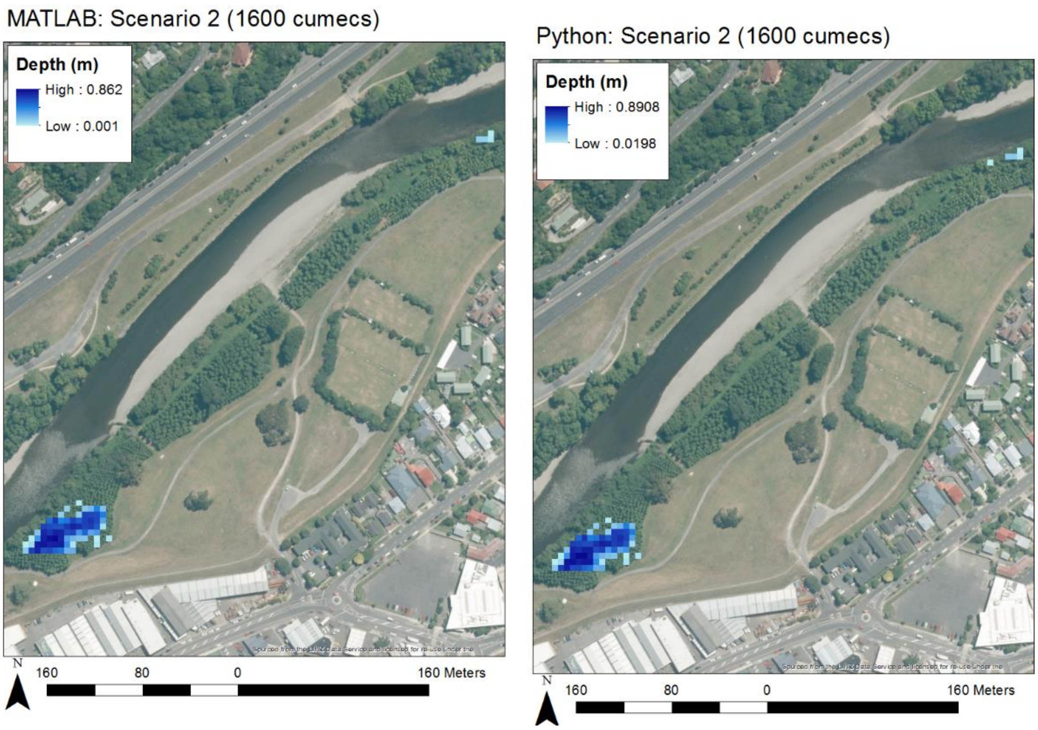

Figure 108. Comparison of the Scenario 2 (1,600 cumecs) showing flooding near Melling Road similar to Scenario 1.

In Scenario 3 (1,700 cumecs), the inundation results from FIM MATLAB and FIM Python are the same, showing flooding near Melling and near the mouth of the Hutt River (Figure 109). This area at the mouth of the river has an overtopping volume of 1,600 cumecs, hence inundation occurring at 1,700 cumecs. In terms of inundation extent, the areas predicted by FIM MATLAB and FIM Python to be flooded are similar. The minimum, mean, and maximum flood depths are also the same between the two codes: 0.023m (min), 0.485m (mean), and 1.367m (max) (Table 51).

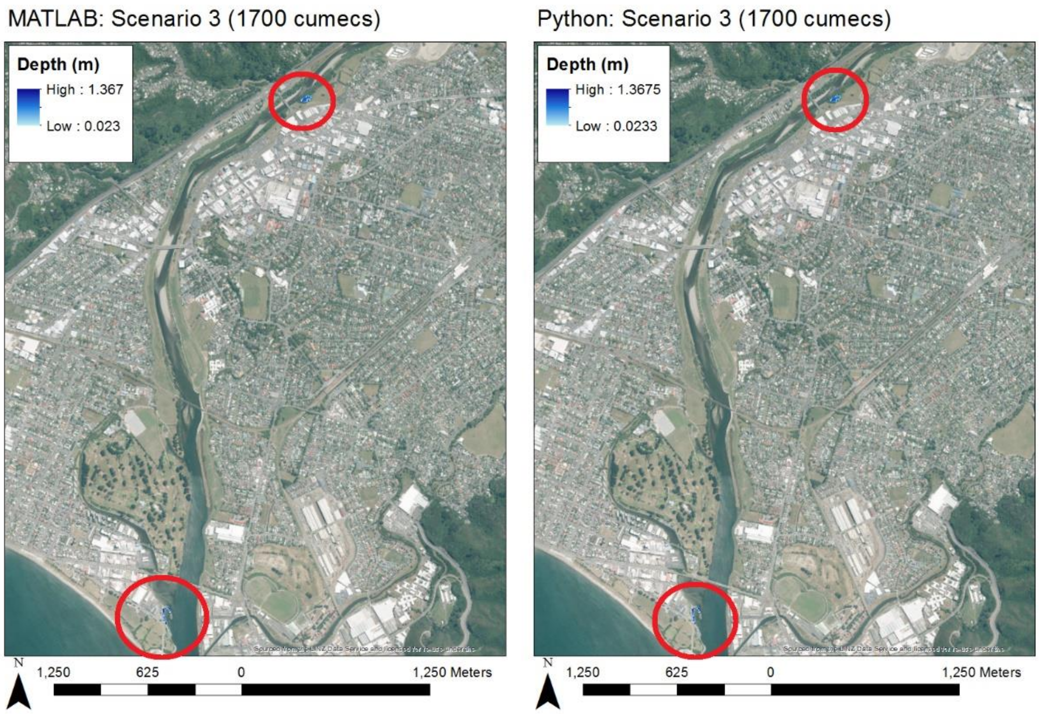

Figure 109. Comparison of the Scenario 3 (1,700 cumecs) showing flooding near Melling Road similar and at the mouth of the Hutt River.

In Scenario 4, the areas inundated are similar to Scenario 3, but with more flooding occurring at the mouth of the Hutt River (Figure 110). On closer inspection, there is little difference in the area around the mouth of the Hutt River; the inundation extent predicted by FIM MATLAB and FIM Python is the same (Figure 111). In terms of flooding depths, the minimum and maximum values predicted by both codes is the same: 0.015m (min) and 1.974 (max). However, the estimated mean flooding depth is higher in the FIM Python code (0.572m) compared to the FIM MATLAB code (0.389m).

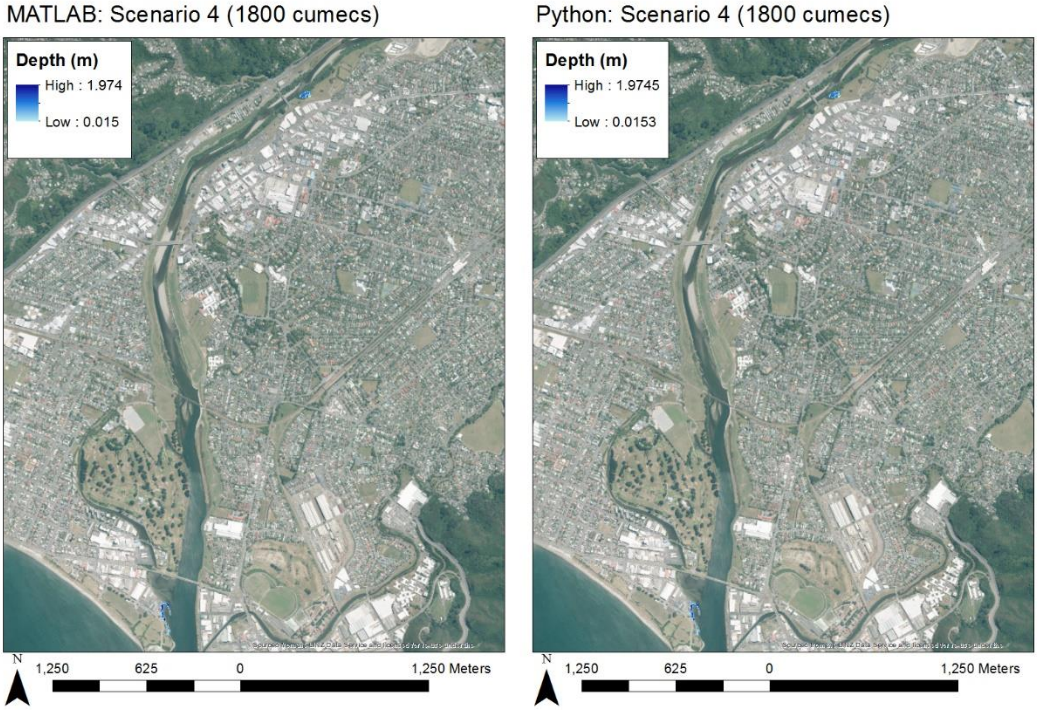

Figure 110. Comparison of the Scenario 4 (1,800 cumecs) showing flooding near Melling Road similar and at the mouth of the Hutt River.

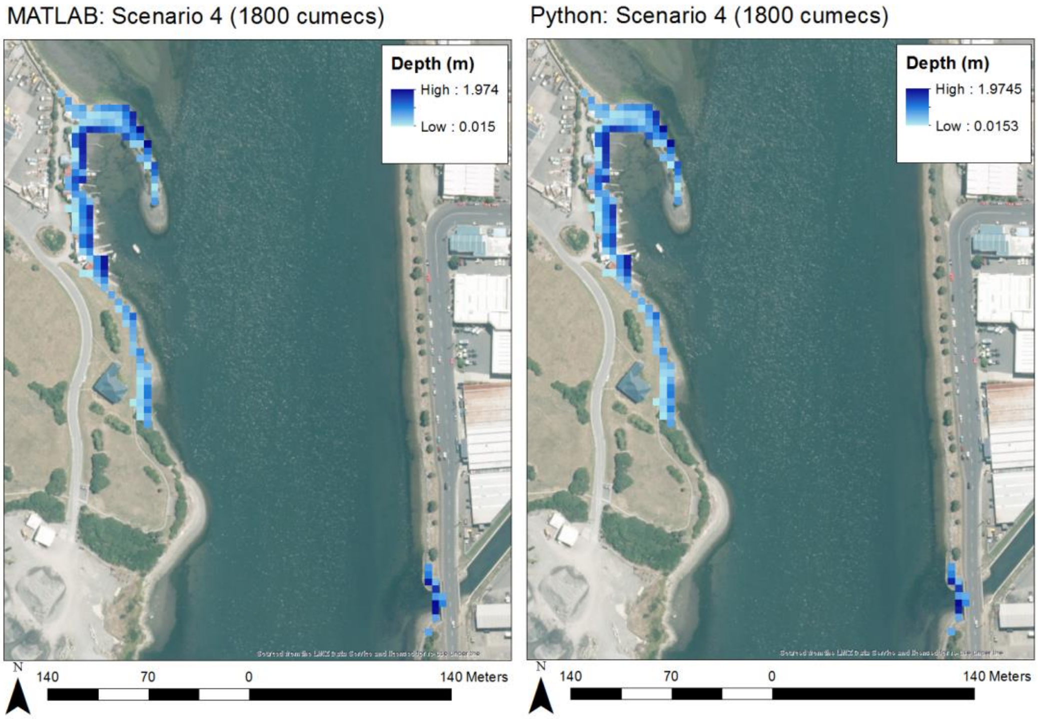

Figure 111. A zoom in on the mouth of the Hutt River where flooding occurs in Scenario 4.

Scenario 5 (1,900 cumecs) shows inundation similar to Scenario 3 and 4, but with a larger inundation extent at the mouth of the Hutt River (Figure 113). The FIM MATLAB and FIM Python produced comparable results for inundation extent but differences in depths (Table 51).

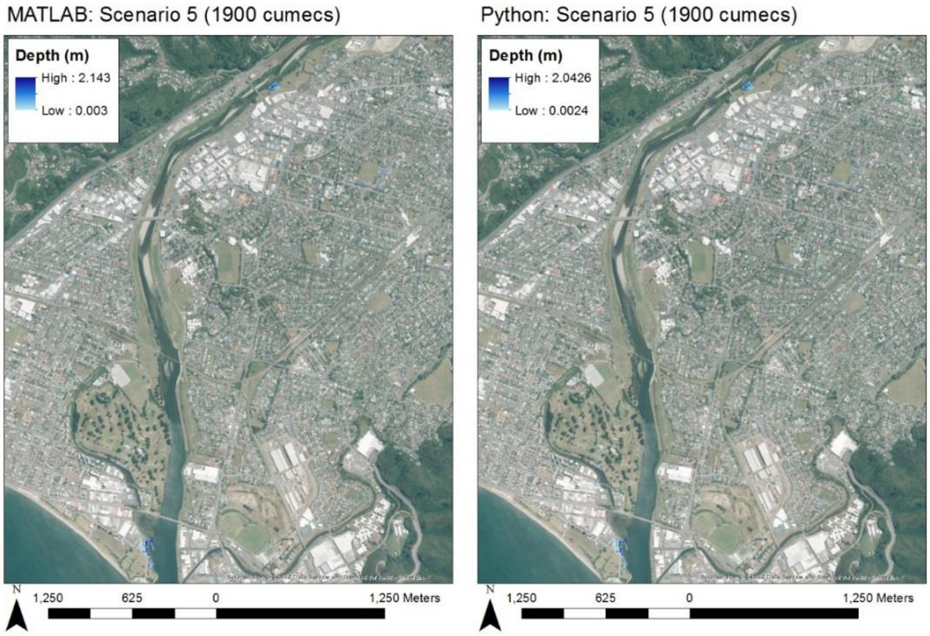

Figure 112. Comparison of the Scenario 5 (1,900 cumecs) showing flooding near Melling Road similar and at the mouth of the Hutt River.

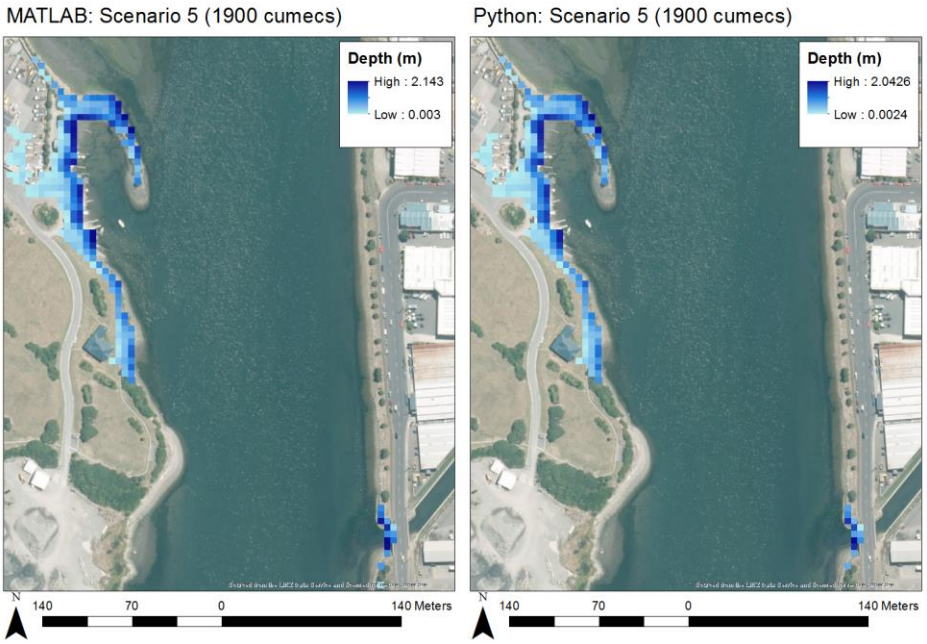

Figure 113. A zoom in on the mouth of the Hutt River where flooding occurs in Scenario 5.

Scenario 6 shows greater inundation predicted at the river mouth than previous scenarios, including a section of Marine Parade as flooded (Figure 114). Overall, the inundation extent is similar between MATLAB FIM and MATLAB Python. When zooming in to the inundated area of the river mouth (Marine Parade), the two codes are predicting the same inundation extent. In terms of flooding depths, the minimum, mean, and maximum flooding depths differ between codes. The FIM MATLAB predicted a lower minimum and mean flooding depth (0.001m and 0.275m) compared to the FIM Python (0.002m and 0.281m). Conversely, the FIM MATLAB predicted a higher maximum flooding depth (2.143m) compared to the FIM Python (2.043m).

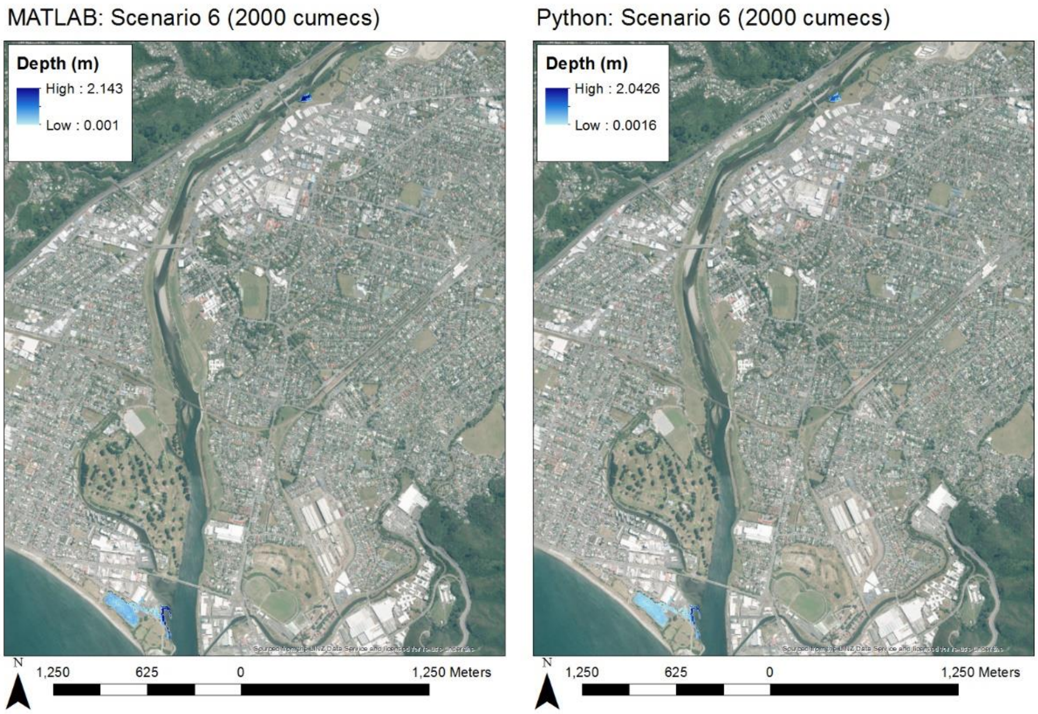

Figure 114. Comparison of the Scenario 6 (2,000 cumecs) showing flooding near Melling Road similar and at the mouth of the Hutt River.

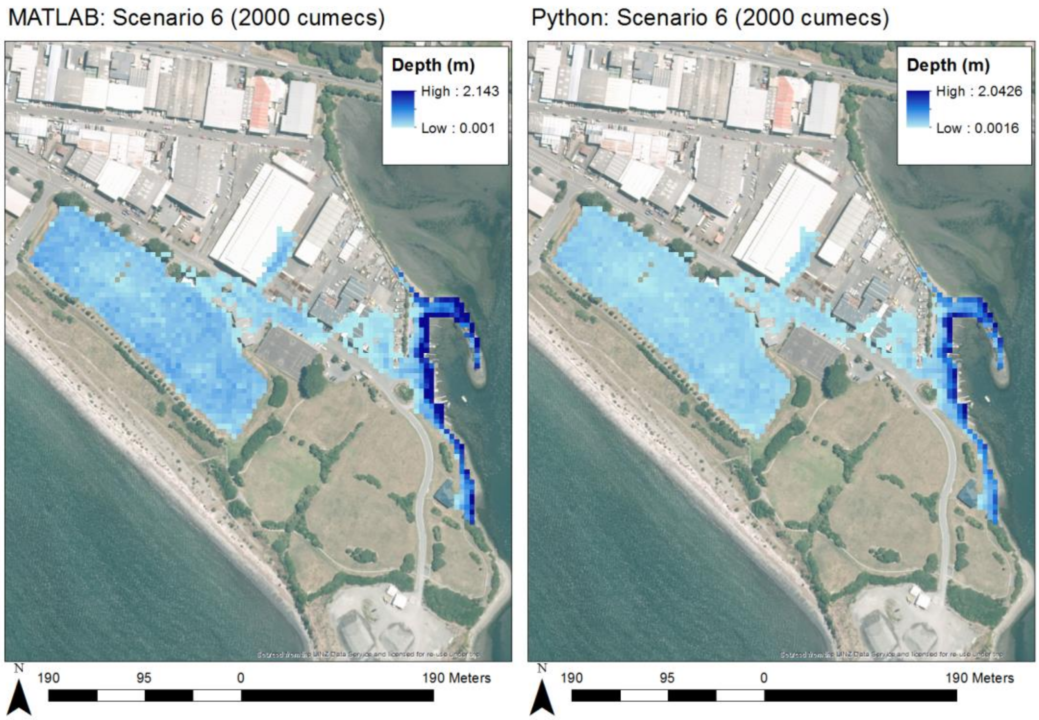

Figure 115. A zoom in on the mouth of the Hutt River and Marine Parade where flooding occurs in Scenario 6.

For Scenario 7 (2,100 cumecs), the inundation extent was the same for FIM MATLAB and FIM Python but the depth of the inundated area halfway up the river (Woburn) is different between the two codes (Figure 116 and Figure 117). In FIM MATLAB, the inundation depth of that small area ranged from 0.07m to over 1m, while FIM Python had an average depth of 0.03m. In terms of flooding depth statistics, the minimum, mean and maximum values are the same between the FIM MATLAB and the FIM Python for Scenario 7. This difference in spatial distribution of flood volume is an indication of further testing needing to be done on the FIM Python.

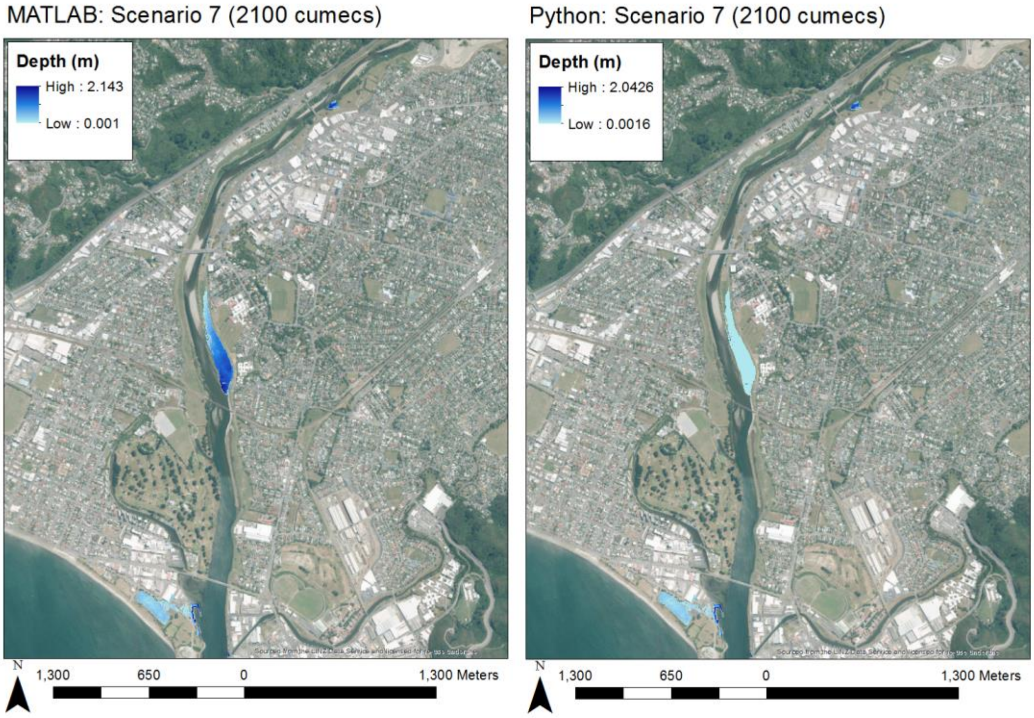

Figure 116. Comparison of the Scenario 7 (2,100 cumecs) showing additional inundation at Woburn.

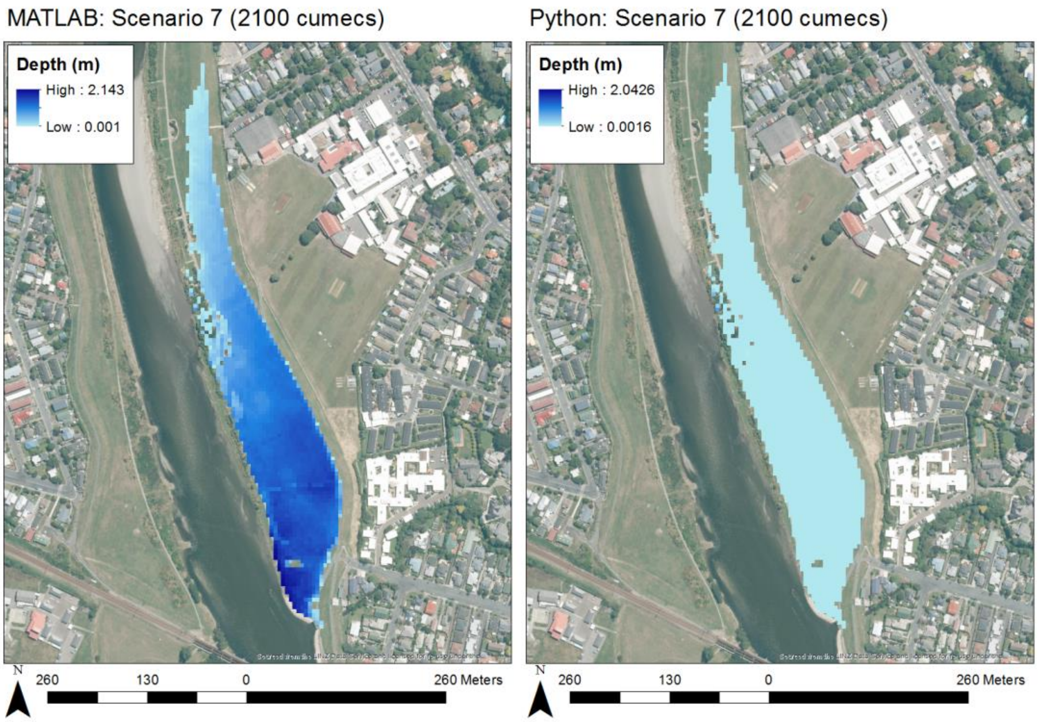

Figure 117. A zoom in on the area of Woburn where flooding occurs in Scenario 7.

Table 52. Summary of the absolute and relative differences between the FIM MATLAB and FIM Python results for flooding depth.

Scenario #	Peak flow (cumecs)	Absolute difference (m)			Relative difference (%)		
		Min	Mean	Max	Min	Mean	Max
1	1,500	-0.019	-0.024	-0.029	-1,900.000	-5.405	-3.364
2	1,600	-0.019	-0.024	-0.029	-1,900.000	-5.405	-3.364
3	1,700	0.000	0.000	0.000	0.000	0.000	0.000
4	1,800	0.000	-0.183	0.000	0.000	-47.044	0.000
5	1,900	0.001	-0.013	0.100	33.333	-2.297	4.666
6	2,000	-0.001	-0.006	0.100	-100.000	-2.182	4.666
7	2,100	0.000	0.000	0.000	0.000	0.000	0.000
Mean differences		-0.005	-0.036	0.020	-552.381	-8.905	0.372

When comparing the FIM MATLAB and the FIM Python, the inundated area produced by both versions of the LUCI FIM is the same. However, in terms of flood depth statistics, the FIM Python produced slightly different values compared to FIM MATLAB (Table 52). On average, the minimum flood depth predicted by FIM Python was 0.005m higher compared to FIM MATLAB. The larger differences are in the mean and maximum flood depths. FIM Python predicted mean flood depths higher by 0.036m and maximum flood depths lower by 0.020m compared to FIM MATLAB. Overall, the differences in flood depth statistics are only slight numerical differences that may be due to how the two programmes handle mathematical arrays.

Given that future LUCI FIM development includes coefficients to estimate roughness and infiltration, reconciling the values between FIM MATLAB and FIM Python is less important than improving the efficiency of the code since the estimates of flooding depth may change due to these physical representations of land cover. In terms of real-world consequences, at relatively low flows where the areas inundated are mostly riverbanks and low-lying non-urbanised areas, these differences in predicted flood depth may not be very significant for management. However, when protecting infrastructure and communities, it is important for management to what level of flood protection is the difference between virtually no flooding or even shallow flood occurring in urbanised and residential areas.

For larger flows, the computational time required for FIM Python was longer compared to the time required for FIM MATLAB. With larger arrays of wet cells, the

Python code takes longer to run because it iterates through all the wet cells and checks the adjacent cells to determine whether water spills into these cells. For large arrays, this process leads to longer computation times and thus the comparisons between the FIM MATLAB and FIM Python could not be done for the larger flow volumes. Future work on the LUCI FIM will be to use more efficient methods of processing large arrays and comparing the computation requirements of array to loop processing.

At 2,200 and 2,300 cumecs, flood inundation extends to large areas by the river (Figure 118). Beyond 2,400 cumecs, the flood flows into the highly urbanised area of Lower Hutt and causes damage to communities and infrastructure (Figure 119). As the flow peak moves higher than 2,400 cumecs, the area inundated remains largely the same and even the estimated flood depths flatten out at 2,600 cumecs (Table 51). Based on the modelling results, the stopbanks and structural flood protection measures are sufficient for up to a peak flow of 2,300 cumecs (1 in 440 year flood). Beyond this flood peak, there is considerable risk to the Lower Hutt floodplain. To compound this problem, climate change could lead to an increased risk of inundation due to changes in flood frequency and extreme events (Lawrence et al., 2011). These future risks to the Lower Hutt floodplain are important to consider, especially for management to protect communities and infrastructure, and shows the utility of using floodplain inundation models.

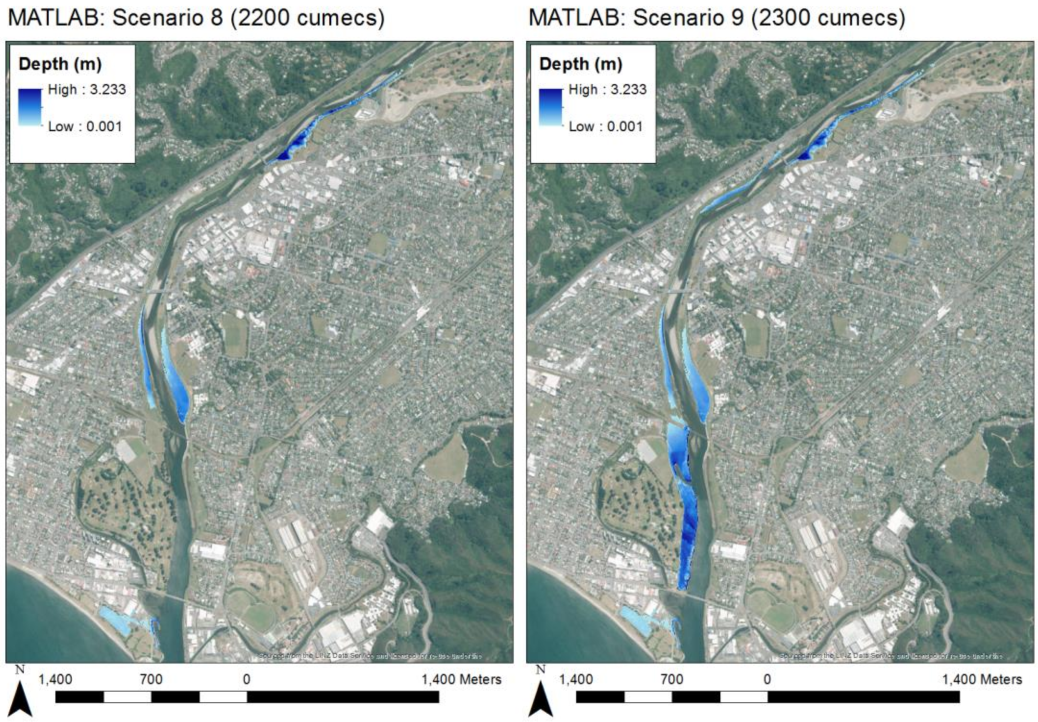

Figure 118. At Scenario 8 (2,200 cumecs) and Scenario 9 (2,300 cumecs), additional flooding occurs at Ava and Moera.

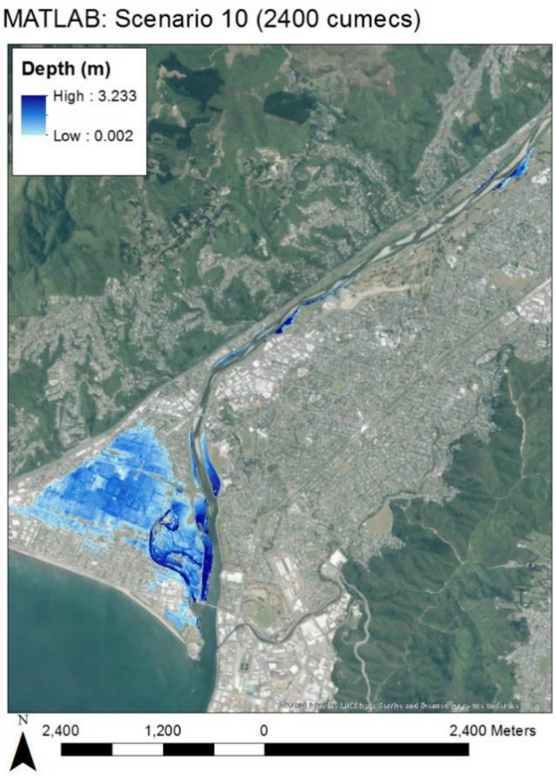

Figure 119. Beyond 2,300 cumecs, flooding occurs in the urbanised area of the Lower Hutt floodplain.

7.4 Summary, conclusion, and future work

The purpose of creating the LUCI FIM was to create a programme capable of estimating floodplain inundation with relatively low data requirements. Instead of detailed hydraulic information about stopbanks and structures, the LUCI FIM requires a digital elevation model (DEM) of high resolution (~5m), a polygon shapefile of the river, and a polyline shapefile of the breach points. These breach points are the banks of the river where the water is known to overtop if the peak flow goes above a certain volume. The original LUCI FIM was created in 2010 and the purpose of this work was to update the LUCI FIM for compatibility with later versions of MATLAB and ArcMap, and to test the code with the Hutt River as a case study. Going further, the LUCI FIM was recoded to work in the Python script. The purpose of converting it to Python is for implementation solely within ArcMap 10.4.1 and integrate it as part of the LUCI framework. Between the FIM MATLAB and FIM Python, the inundation extents and flooding depths were similar for most of the compared scenarios. For the scenarios where flood depths differed, more testing and improvements to efficiency will be carried out. At larger flood volumes, the computational time for the FIM Python was longer compared to the FIM MATLAB. This computational inefficiency can be improved through future work regarding more efficient handling of larger arrays. This work with the LUCI FIM links into the broader scope of this thesis by continuing the development of LUCI in the following ways:

- **Updated the FIM MATLAB code to be compatible with ArcMap 10.4.1:** The FIM MATLAB was parameterised for the CDO floodplain and tested against HEC-RAS, the inundation programme currently used for disaster risk management in CDO
- **Converted the MATLAB code to Python:** Although more improvements to efficiency are required, the initial results of the new Python version are promising and future implementation of the LUCI FIM into the LUCI framework will expand LUCI's utility for testing the effects of changing land cover and rainfall events.

Beyond the scope of this thesis, the relative simplicity of the LUCI FIM will allow implementation in other places that have high-resolution DEMs and information about the breach points along a river. In addition to improvements in efficiency, future work on the LUCI FIM could include accounting how different land cover (e.g. vegetation versus concrete) and urban storm drainage networks can affect flood extent.

8 Extreme events modelling in the Cagayan de Oro catchment

8.1 Introduction

The vulnerability of the Philippines to extreme events and their devastating effects on communities and infrastructure has driven more research regarding real-time forecasting, and predictions of runoff and flow under different land cover scenarios and rainfall events. Simulation models have two main aims: exploring the implications of the assumptions around how a real-world system is represented in models, and to predict the behaviour of that system under naturally-occurring circumstances (Beven, 1989). This chapter focuses on testing the LUCI model against the HEC-HMS through simulating the catchment hydrology of Cagayan de Oro (CDO) under the baseline land cover scenario during Typhoon Bopha. The specific objectives of this chapter are:

- Use HEC-HMS and LUCI to model the flood hydrograph of the CDO catchment under the baseline land cover scenario with Typhoon Bopha rainfall; and
- Use the resulting flood hydrographs from LUCI and HEC-HMS as input to HEC-RAS to map floodplain inundation

Both HEC models are well-used and established for watershed and inundation modelling applications, while LUCI is a more recent ecosystem services model with strong but novel and less-tested rainfall-runoff capabilities. The LUCI model is highly spatially resolved, working at the sub-field scale (Jackson et al., 2013). The LUCI model can perform event-based rainfall-runoff modelling, and this application allowed that aspect of LUCI to be tested against HEC-HMS. An emerging development within LUCI is the flatwater inundation model (Chapter 7) and the testing of the LUCI FIM against HEC-RAS is a key component of future work. This comparison of LUCI and the HEC models allows for further development of the LUCI framework, especially for the inundation model which will be implemented into the ArcMap model of LUCI in future work. By understanding LUCI's performance against more established models, the framework can be further developed to account for more complex components of rainfall-runoff modelling and inundation mapping. An important part of model development is to find a balance between accurately representing real-world processes and making it simple/computationally efficient to run on standard computing resources (Carlaw, 2000).

The HEC-HMS and HEC-RAS models were briefly described in the introduction (Chapter 1) and the inundation chapter (Chapter 7). The HEC-HMS model simulates the precipitation-runoff processes of a catchment through representing the infiltration, runoff, flow and routing with mathematical models that the user can select based on their data and catchment characteristics (Scharffenberg, 2013). This high level of flexibility allows for the use of HEC-HMS in many applications with differing levels of data and information of the catchment's physical characteristics (McColl & Aggett, 2007). The limitations of HEC-HMS arise from the simplified formulation of the models and simplified representation of flow, as all the mathematical models are deterministic in order to keep the programme's computation time relatively expedient (Scharffenberg, 2013). HEC-RAS is a one-dimensional inundation model used to simulate steady flow, unsteady flow, sediment transport, and water temperature (Brunner, 2010a). The HEC-RAS model was also used by Project NOAH for its floodplain modelling, but has been replaced by the FLO-2D and ISIS-2D models for inundation (Lagmay et al., 2017). It is a one-dimensional model that mainly simulates in-stream channel flow and can approximate floodplain inundation through roughness coefficients (Paringit et al., 2015). FLO-2D and ISIS-2D are used for one-dimensional channel flow simulation and two-dimensional floodplain inundation simulation (Lagmay et al., 2017). Two-dimensional models are more complex and can represent physical processes in a more robust manner compared to one-dimensional models, and more information about these differences in found in the inundation review (Chapter 7). Since HEC-HMS does watershed modelling and HEC-HMS does floodplain inundation modelling, these two are commonly paired for rainfall-runoff and inundation applications.

In order to simulate the response of the catchment to extreme events, two things are required at the minimum: a loss function and a routing function (Beven, 1989). The DREAM (2015) parameterisation of HEC-HMS for the CDO catchment uses the Soil Conservation Service Curve Number method to simulate loss and Muskingum-Cunge method for routing (UP TCAGP, 2015). The LUCI model uses a form of soil moisture accounting (soil as a bucket) to account for water going in/out of the system with spatially-explicit routing between hydrological response units (HRUs) at the sub-field scale (Jackson et al., 2013).

The Soil Conservation Service Curve Number method (SCS CN) is one of the ways that HEC-HMS can simulate infiltration loss, whether at the sub-watershed level or through a gridded approach (Scharffenberg, 2013). The SCS CN method converts precipitation into runoff based on the influence of soils, vegetation, impervious areas, interception, and storage (USDA NRSC, 1986). The SCS CN method is mainly used for simulating the associated runoff of storm events, such as the framework of Project NOAH for real-time flood forecasting (Kannan et al., 2008; Paringit et al., 2015). The SCS CN method has also been previously used to perform scenario analysis of the effect of changing land cover on runoff (Du et al., 2012; McColl & Aggett, 2007). However, this method has several limitations: it does not account for rainfall intensity or duration because it does not contain an expression for time, and applies only to direct surface runoff without considering subsurface flow or ground water contributions (USDA NRSC, 1986).

The Soil Moisture Accounting method (SMA) represents soil as a storage unit (or several units) and tracks the amount of water that flows in (e.g. precipitation) and out (e.g. evapotranspiration) of that unit (Alley, 1984). SMA is also available in HEC-HMS as a method for simulating loss/water movement by representing the soil as several layers through which water can move or be stored (Scharffenberg, 2013). Other methods of estimating the soil's water balance are the use of empirical models that are heavily-reliant on field observations and through hydrodynamic models that require detailed soil hydraulic information and plant properties (Ma et al., 2013). Soil moisture accounting is a lumped conceptual model based on the mass balance of soil water, making it relatively simple compared to mathematically-based complex models that solve Richard's equation for soil moisture dynamics at a point scale (Ma et al., 2013; Nunzio Romano, 2014). However, this simplicity does not account for more complex soil dynamics such as the vertical movement of water through the soil matrix, which affects the plant available water and would help in irrigation scheduling (Laio et al., 2001; Ma et al., 2013).

HEC-RAS is a one-dimensional inundation model that estimates channel flow and inundation, while the LUCI FIM is a conceptual model that uses flatwater inundation to estimate flood extent. More detail about these two types of models, their strengths and weaknesses, and differences can be found in the inundation review (Chapter 7).

8.2 Methodology

Figure 120 summarises the methodology specific to this chapter. The three different land cover scenarios are the baseline, development, and rehabilitation scenarios that were detailed in Chapter 2. To parameterise the HEC-HMS model for the scenarios, the curve numbers of the sub-watersheds were calculated and changed under different scenarios, similar to work by McColl & Aggett (2007). The HEC-HMS and HEC-RAS models were parameterised and calibrated by the Project NOAH team (Disaster Risk and Exposure Assessment for Mitigation Program, 2015).

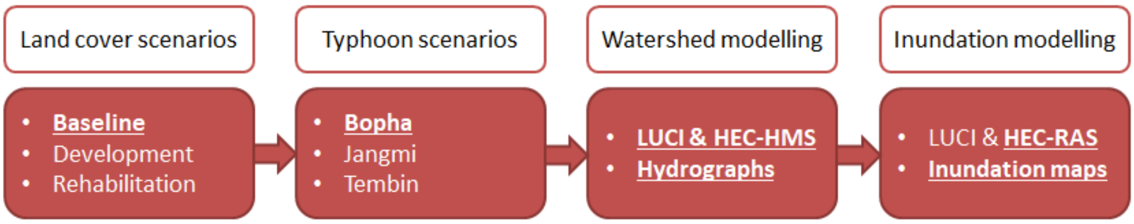

Figure 120. Overview of the methodology of this chapter, items emphasised are presented in this thesis.

The main rainfall scenario considered for this thesis is Typhoon Bopha (local name: Pablo) which hit CDO in 2012 causing the city to be declared under a state of calamity and affected over 50,000 people (NDRRMC, 2012b). Over December 4 and 5 2012, Typhoon Bopha brought 139.5mm of rainfall to Cagayan de Oro City, corresponding to a 1 in 14-year rainfall event (JICA, 2014). The other extreme events that are potential scenarios for future research are Jangmi (Seniang) in 2014 and Tembin (Vinta) in 2017. In 2014, Jangmi caused 66 casualties in all affected regions and, within CDO city, over 2,000 families were affected by evacuation operations (NDRRMC, 2014a). Over 51 hours, the total rainfall recorded for all affected regions was ~500 mm (Wiltgen, 2014). In 2017, the warnings associated with Tembin prompted the evacuation of communities living along the CDO river (NDRRMC, 2017). All of these typhoons had devastating effects that reached further than the CDO catchment and the city.

The rainfall data for Bopha was verified by DREAM (2015) while the rainfall data for Jangmi and Tembin required infilling to account for gauges that had gone down during these events. Infilling missing values from nearby gauges is achieved through several methods: station-average, normal-ratio, inverse-distance weighting, regression, and isohyetal methods (Dingman, 2008; Maxwell, 2013). The normal-ratio estimates missing values at the target gauge through the ratio of annual precipitation of the target gauge to the donor gauges as follows (Dingman, 2008):

$$\hat{p}_0 = \frac{1}{G} \times \sum_{g=1}^{G} \frac{P_0}{P_g} \times p_g$$

Where:

$\hat{p}_0$	Missing precipitation value at target gauge for a point in time (t)
G	Nearby "donor" gauges
P_0	Annual average precipitation at target gauge
P_g	Annual average precipitation at donor gauge
p_g	Observed precipitation value at donor gauge for a point in time (t)

This infilling was done with the different rainfall gauges within and around the CDO catchment (Figure 121). Infilling was required to create a continuous set of rainfall data over the time of the different rainfall events, and to create a gridded raster layer for use within LUCI. Although the rainfall for Jangmi and Tembin was not modelled in this research, the infilled rainfall datasets can be used for additional modelling runs to compare LUCI to the HEC models in the future.

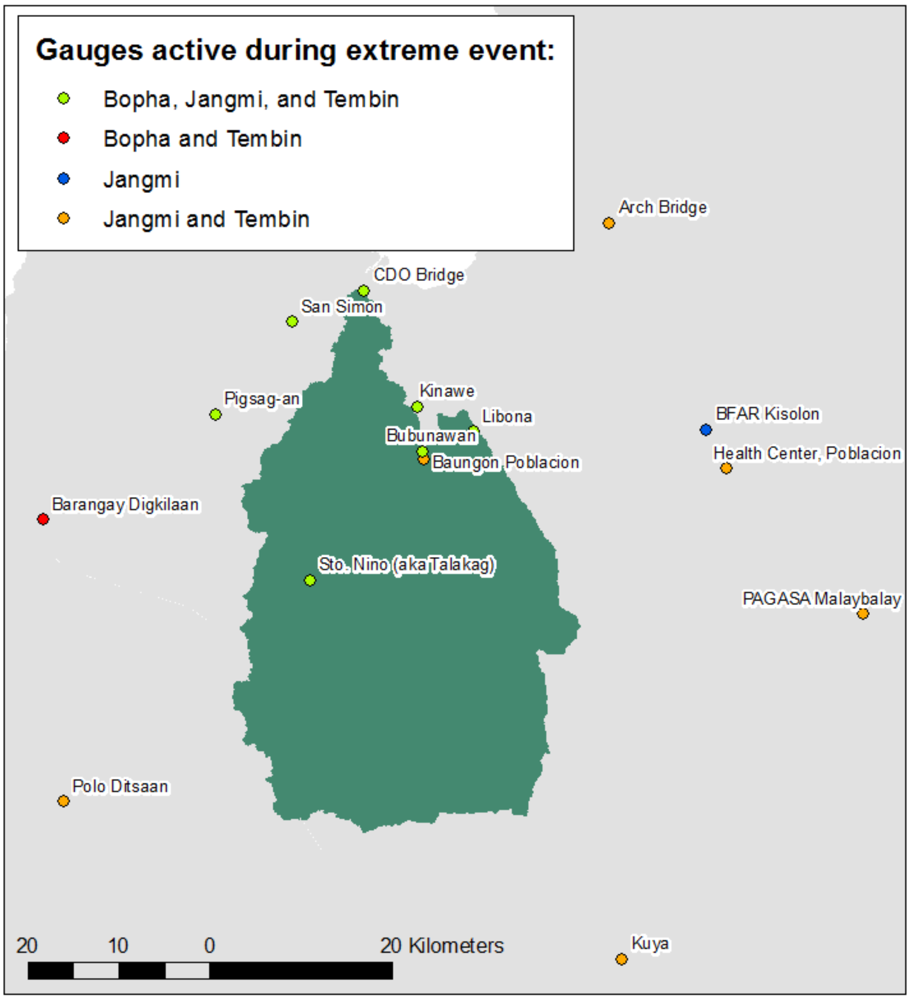

Figure 121. Map of gauges within and around the CDO catchment, and their activity during the three extreme events.

8.2.1 Watershed modelling in HEC-HMS

Within the HEC-HMS model, there are different mathematical model options for representing catchment characteristics, infiltration losses, transformation of precipitation to runoff, baseflow contribution, routing, and water diversion (Scharffenberg, 2013). For the DREAM (2015) programme parameterisation of HEC-HMS the SCS Curve Number method is used to simulate infiltration losses. Each sub-basin is assigned one composite number to represent its different combinations of soil and land cover (Scharffenberg, 2013).

The curve numbers of the different scenarios were assigned based on land use type and hydrologic soil group (HSG). The HSG of a soil is determined by its minimum infiltration rate, which will influence its response to different rainfall intensities (USDA

NRSC, 1986). Lower curve numbers are associated with forests and vegetation while higher curve numbers are associated with agricultural and built-up areas.

Table 53. Curve number lookup table used in assigning curve numbers (Paringit et al., 2015).

Land Use Code	Land Use Description	Hydrologic Soil Group			
		A	B	C	D
1	Closed Canopy	17	40	59	68
2	Open Canopy Forest	50	68	80	84
3	Mangrove	98	98	98	98
4	Tree Plantation and Perennial	30	53	68	77
5	Brushland	17	33	52	63
6	Grassland	17	44	60	70
7	Cultivated Area	55	70	80	85
8	Built-up	85	90	93	94
9	Marshland	61	74	84	88
10	Fishpond	99	99	99	99
11	Inland Water	99	99	99	99
13	Open Areas	63	77	85	88

The baseline land cover was previously parameterised in HEC-HMS by DREAM (2015) and is currently used for real-time flood forecasting in CDO (Paringit et al., 2015). To parameterise the development and rehabilitation scenarios for future modelling work, their land use types were correlated with the land use descriptions used by DREAM (2015) and Paringit et al. (2015) for curve number assignment. Under the development and rehabilitation scenarios, each of the zones has distinct types of land management specified in the development plans such as contour farming, Sloping Agricultural Land Technology (SALT), or agroforestry. These land management practices were parameterised in the RUSLE application to CDO (Chapter 5) but are not specifically present in Table 53. Therefore, the areas in the rehabilitation scenario of conservation farming and recommend conservation farming are parameterised as tree plantation and perennial instead of agricultural areas in HEC-HMS. The original SCS Curve Number method accounts for distinct types of land management and hydrological conditions, but since this chapter focuses on testing the existing HEC-HMS parameterisation against LUCI, the DREAM (2015) curve number table was used in the extreme events modelling.

Table 54. Correlation table between the different scenarios and the USGS land cover classifications.

Original land cover classification	USGS land cover classification
Baseline	
Other wooded land, shrubs	Brushland
Other wooded land, wooded grassland	
Other land, natural, grassland	Grassland
Other land, cultivated, annual crop	Cultivated area
Pineapple plantation	
Other land, cultivated, perennial	Tree Plantation and Perennial
Forest plantation, broadleaved	
Other land, built-up area	Built-up
Closed forest, broadleaved	Closed canopy
Open forest, broadleaved	Open canopy forest
Inland water	Inland water
Development	
Agricultural Sub-zone	Cultivated Area
Agricultural zone1	
Agricultural zone2	Tree Plantation and Perennial
Agricultural zone3	
Agroforestry Sub-zone	
Private Agroforestry Sub-zone	
Timber Production Sub-zone	
Timber Regeneration Sub-zone	
Forest Restoration Sub-zone	Open Canopy Forest
National Park	Closed Canopy
Natural Park	
Private Forest Sub-zone	
Strict Protection Zone	
Rehabilitation	
Agroforestry	Tree Plantation and Perennial
Recommend Agroforestry	
Assisted Natural Regeneration	Open Canopy Forest
City	Built-up
Practice Conservation Farming	Tree Plantation and Perennial
Recommend Conservation Farming	
Protection	Closed Canopy
Recommend Reforestation	
Reforestation	

The land use and soil shapefiles were then combined using the *Union (Analysis)* tool in ArcMap 10.4.1 to produce polygons that have information about both the land use and the soil hydrologic properties. Each of these polygons were compared with the lookup table that assigned curve numbers based on land use and soil hydrologic group (Table 53). After each polygon was assigned a curve number, the next step was to assign weighted curve numbers to each sub-catchment within CDO. Using the sub-catchment file supplied by DREAM (2015), the *Split (Analysis)* function was used to separate the soil and land use polygons into the sub-watersheds.

$$WCN_{sub} = \frac{\sum CN_i * Area_i}{Area_{sub}}$$

Where:

WCN_{sub}	Weighted curve number for the sub-watershed
CN_i	Curve number for soil/land use polygon i
$Area_i$	Area for soil/land use polygon i
$Area_{sub}$	Total area of the subwatershed

The weighted curve number is essentially a method of accounting for different combinations of soil and land use present in the sub-watershed. The more area a particular polygon has within the sub-watershed, the more influence it has on the weighted curve number. The WCN influences the initial retention after runoff begins (S) and the initial abstraction (I_a), which were calculated for the CDO catchment scenarios following the methodology of Paringit et al. (2015):

$$S_{sub} = \frac{25400}{WCN_{sub}} - 254$$

$$I_a = 0.05 \times S$$

Given the rainfall (P), HEC-HMS calculates the runoff (Q) for the sub-watershed through the following formula:

$$Q = \frac{(P - I_a)^2}{(P - I_a) + S}$$

8.2.2 Watershed modelling in LUCI

To perform watershed modelling in LUCI, rainfall rasters were created within ArcMap 10.4.1 using the *Inverse Distance Weighting (IDW)* tool with 15-minute temporal resolution and ~1 km spatial resolution. The 15-minute temporal resolution was chosen to capture the variation of rainfall over the time of the event, while the ~1km spatial resolution was chosen for computational efficiency.

8.2.3 Inundation modelling

The flow hydrographs from HEC-HMS and LUCI were used as input into HEC-RAS to estimate the inundation extent under the baseline scenario for Typhoon Bopha. This parameterisation of HEC-RAS was set up and calibrated by DREAM (2015) for Project NOAH.

The LUCI FIM requires a floodplain DEM (raster), a river polygon (shapefile) and polylines showing the potential breach points (shapefile). The LiDAR-based floodplain DEM was detailed in the methodology (Chapter 2) while the river polygon was derived from the HEC-RAS parameterisation provided by DREAM (2015). The breach points and associated overtopping volumes were based on previous studies that analysed the vulnerability of the CDO floodplain to floods of different peak flows (JICA, 2014; Mabao & Cabahug, 2014). Future work to parameterise the LUCI FIM in CDO would be through analysing the historical flood record and determining the breach points based on those floods of known peak flow. Another way to improve the LUCI FIM application in CDO would be building on the future directions outlined in the inundation review (Chapter 7) and adding the influence of land cover in the model. After further testing and parameterisation of the LUCI FIM in CDO, the model can then be compared to HEC-RAS in future modelling runs.

8.3 Results and Discussion

This section presents the results of the different curve numbers, flood hydrographs, and flood inundation maps for the baseline scenario under Typhoon Bopha.

8.3.1 Curve number parameterisation

The baseline scenario had the lowest minimum, maximum, and mean WCN compared to the development and rehabilitation scenarios (Table 55). The rehabilitation and development scenarios had higher mean and maximum WCN values compared to the baseline scenario. In the baseline scenario, a large part of the catchment is defined as brushland/grassland, which has a lower curve number compared to agricultural land. However, these areas are more likely to be a mixture of agriculture and brushland/grassland, which would result in a higher curve number, hence the WCN values for the development and rehabilitation scenarios are generally higher than the baseline scenario. As outlined in the methodology (Section 8.2), more detailed curve number parameterisation of these practices can be done in the future to account for the effect of specific practices such as SALT or line-planting. There are more detailed curve number parameterisations available for urban areas, different types of management (e.g. contouring vs straight row crops), and hydrological conditions (USDA NRSC, 1986). Future testing of HEC-HMS against LUCI under all the land cover scenarios should use the curve number tables from USDA NRSC (1986) for more detailed land cover management scenarios.

Table 55. Minimum, maximum, and mean weighted curve numbers for the different land cover scenarios.

Weighted Curve Numbers (WCN)	Baseline	Development	Rehabilitation
Min	23.90	49.80	45.11
Max	71.89	85.00	84.00
Mean	36.62	69.75	66.99

8.3.2 Watershed modelling

The modelled flow hydrographs of HEC-HMS and LUCI compare well with the observed flow at the CDO outlet (Figure 122 and Table 56). Both hydrographs from HEC-HMS and LUCI show similar peak flow volumes and occurrence times, as well as a smaller peak occurring after the event during December 5 after the main flood event. The hydrograph produced by LUCI had a flashier catchment response and a later peak flow occurrence compared to the hydrograph produced by HEC-HMS on December 4 2012 by 10 minutes. However, the falling limb of the LUCI hydrograph is more like the observed flow compared to the HEC-HMS hydrograph. LUCI can better capture the abrupt rise and fall of the flood peak.

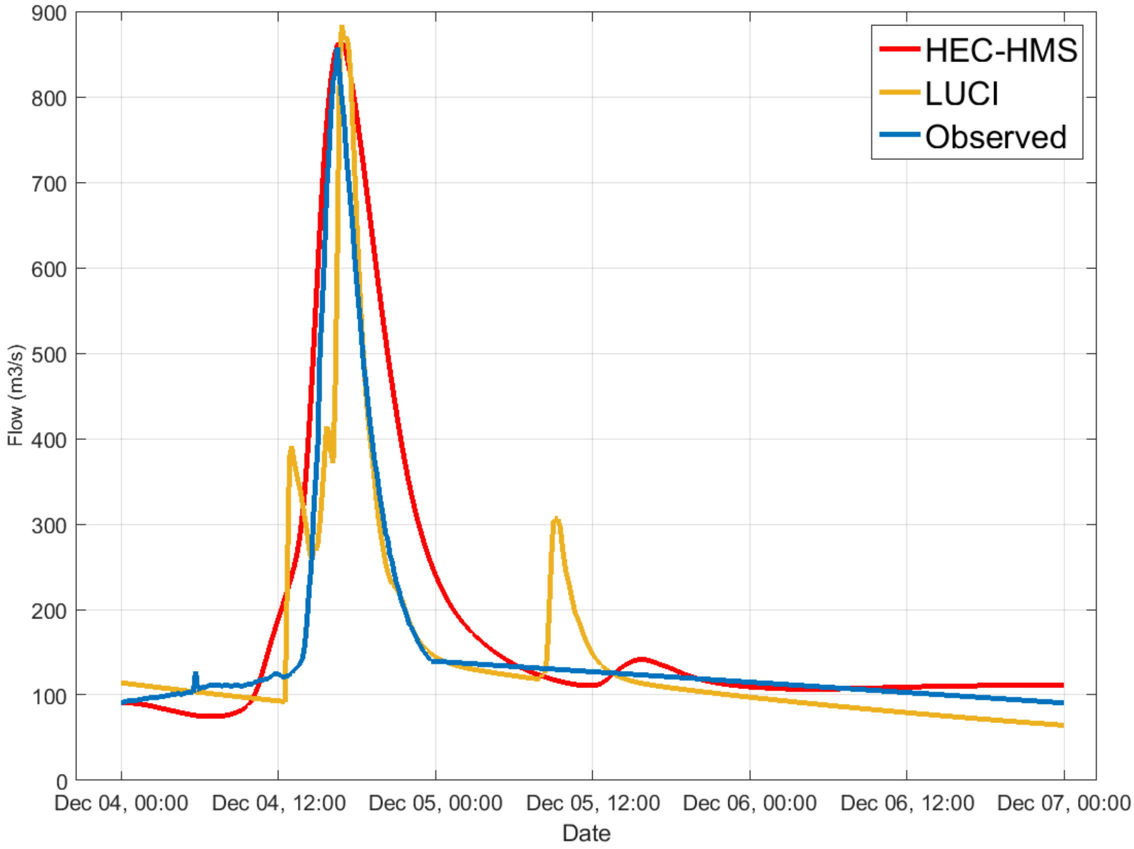

Figure 122. The modelled (HEC-HMS in red, LUCI in orange) and observed (blue) flow hydrographs at CDO bridge for Typhoon Bopha under the baseline land cover scenario.

Table 56. Peak flows and total flow volumes for Typhoon Bopha under the baseline land cover scenario.

	Peak flow (cumecs)	**Total flow volumes (m^3)**
HEC-HMS	864.7	55,280
LUCI	884	45,418
Observed	858.3	44,366

This test of LUCI against HEC-HMS shows promising results from the rainfall-runoff model within the LUCI framework for Typhoon Bopha. However, this is only for one event and the rainfall-runoff model has not been properly validated against other events or a longer time-series. Further testing of the LUCI rainfall-runoff model with a longer time-series would be useful to further calibrate the model to the flow regime of the CDO catchment. Additionally, testing under different extreme events at the baseline scenario using both LUCI and HEC-HMS will allow for further calibration of the LUCI rainfall-runoff model. To run the different land cover scenarios, the curve numbers within the HEC-HMS model should be calculated using the USDA NRSC (1986) guidelines to allow parameterisation of specific land management practices such as contouring or agroforestry. Previous land cover scenario analyses in the Philippines have predicted increased runoff with decreased forest area and increased agricultural areas (Alibuyog et al., 2009; Santillan et al., 2011). This agrees with a long-term monitoring study in the nearby Mapawa catchment where increased runoff was observed with increased maize areas (Valentin et al., 2008).

The inclusion of specific land management practices in the HEC-HMS and LUCI parameterisation is important because of their potential impacts on runoff. In Valentin et al. (2008), conservation technologies such as riparian planting and bamboo cultivation had soil conservation and runoff reduction outcomes compared to traditional up-and-down tillage. As stated in the ecosystem services chapter (Chapter 3), parameterising for these conservation technologies is important due to the future plans of the catchment management to promote riparian planting and bamboo cultivation on riverbank slopes (CESM, 2014). In the RUSLE application (Chapter 5), including the conservation technologies showed decreases in the potential soil loss over the entire catchment.

Aside from looking at the flow hydrograph at the catchment outlet, understanding which sub-catchments had the biggest contribution to runoff is another potential direction for future work (Amini et al., 2011). Through determining the individual contributions of sub-catchments to peak flow, it would help land management decide which sub-catchments to focus mitigation efforts.

8.3.3 Inundation modelling

Both hydrographs from HEC-HMS and LUCI were used as input in the unsteady flow simulation of HEC-RAS to produce floodplain inundation maps. The flooding within the river was removed to show only the water that encroached on the floodplain. The flooding extents were similar but LUCI hydrograph predicted less coverage compared to the HEC-HMS hydrograph (Figure 123). The maximum inundation depths were 4.82m (HEC-HMS) and 4.63m (LUCI). Both hydrographs produced inundation occurrences at similar areas: at the mouth of the river (Figure 124), and locations where the river meanders (Figure 125 and Figure 126). The likely reason for this difference is the larger flood peak and volume predicted by HEC-HMS compared LUCI (Table 56). The resulting maps from HEC-HMS hydrograph were less patchy compared to the LUCI hydrograph because of this larger peak and volume.

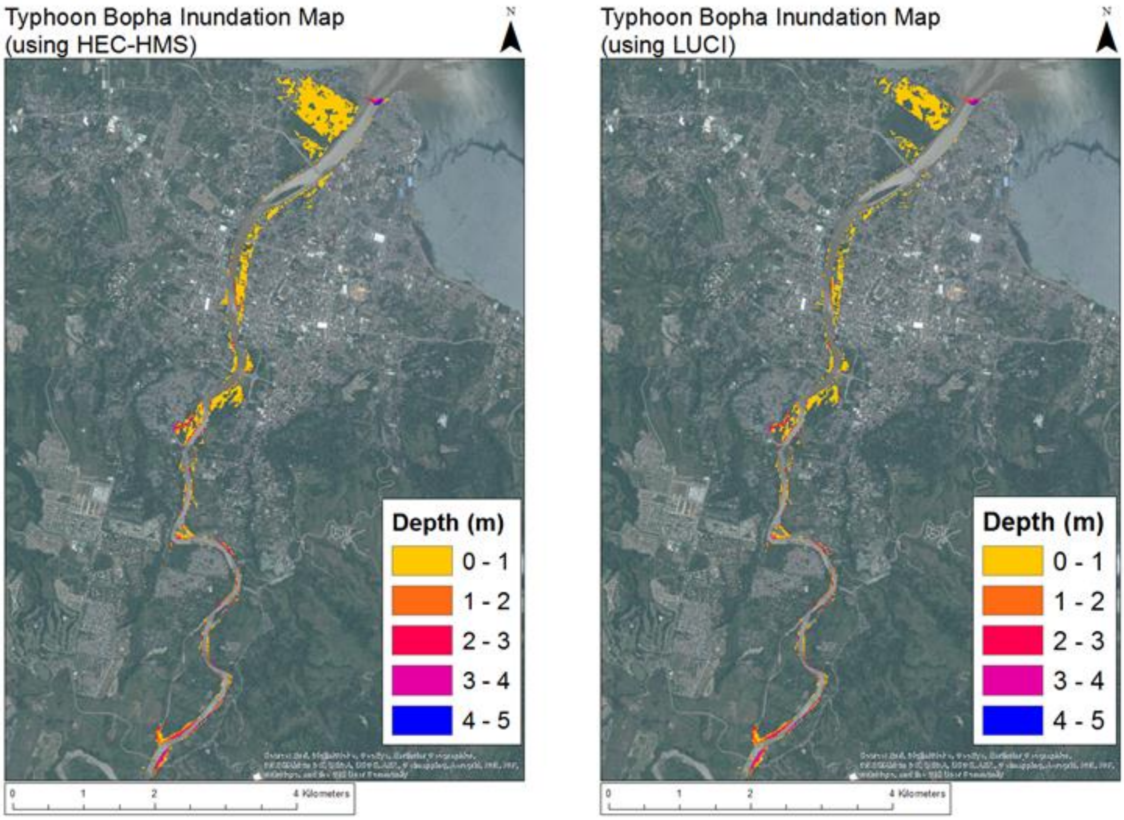

Figure 123. Inundation maps produced by HEC-RAS using the flood hydrographs from HEC-HMS (left) and LUCI (right) with the river and inundation below one centimetre excluded.

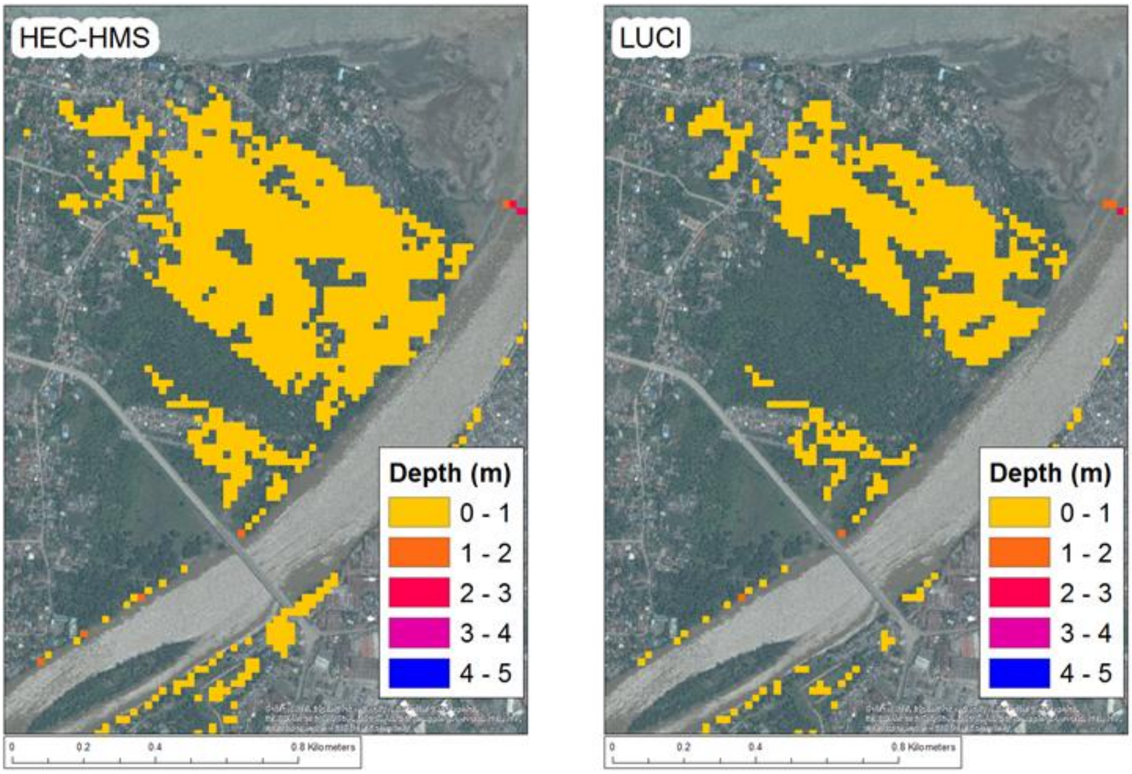

Figure 124. Inundation maps at the mouth of the river produced by HEC-RAS using the flood hydrographs from HEC-HMS (left) and LUCI (right) with the river and inundation below one centimetre excluded.

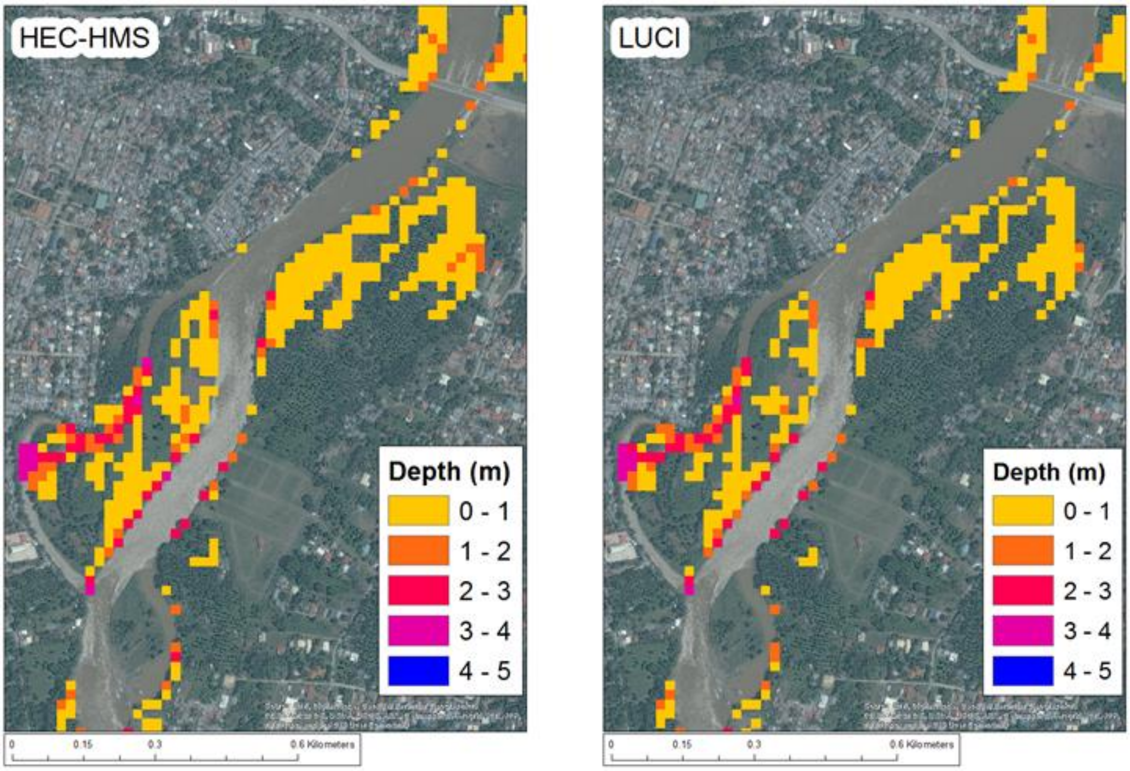

Figure 125. Inundation maps at a river meander produced by HEC-RAS using the flood hydrographs from HEC-HMS (left) and LUCI (right) with the river and inundation below one centimetre excluded.

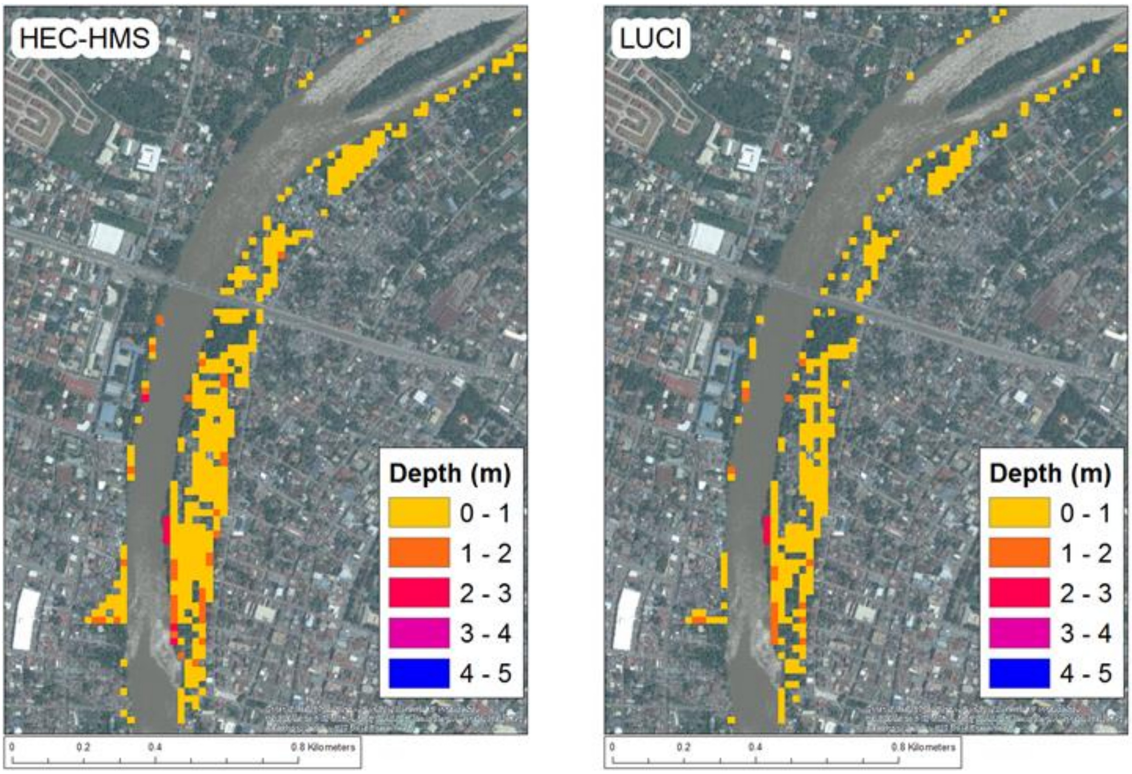

Figure 126. Inundation maps at another river meander produced by HEC-RAS using the flood hydrographs from HEC-HMS (left) and LUCI (right) with the river and inundation below one centimetre excluded.

One of the limitations of this research was the verification of the flooding extent. Although disaster reports and anecdotal evidence are available, there is a lack of the satellite imagery associated with these events. The disaster reports and anecdotal evidence (e.g. news reports, surveys) are important sources of information to pinpoint which specific areas within the CDO floodplain were impacted by flooding. By cross-referencing the location of reported incidents with the inundation extent, the modelled hazard maps can be verified. Anecdotal evidence and surveys were also important in verifying the flooding extent of Typhoon Washi in 2011 (JICA, 2014).

Increased availability of satellite imagery and emerging technologies such as Google Earth Engine are a potential priority for future research to verify flooding extent (Gorelick et al., 2017). Google Earth Engine has been previously utilised to map rice paddies, small reservoirs, and seasonal inundation of wetlands (Dong et al., 2016; Jones et al., 2017; Tang et al., 2016). Hence, future work around hazard mapping in CDO can use past satellite imagery to verify model results if there is appropriate imagery captured during the time of the event.

8.4 Future work

For the development of the LUCI rainfall-runoff model, one of the future developments common to this chapter, the ES chapter (Chapter 3), and the soil erosion chapter (Chapter 5) is more detailed parameterisation for the different land cover and vegetation types common in the CDO catchment. The LUCI rainfall-runoff model would benefit from more detailed parameterisation that accounts for distinct types of land management practises, such as those used by the RUSLE. The development of a crop water production model combined with the soil moisture accounting method accounts for the effect of crop water usage and can elucidate the effect of water surplus or deficits on crop yields (Ma et al., 2013). The robustness of the CDO crop water model can be increased through analysing soil moisture records within/near the CDO catchment to get a broad understanding of intra-annual changes in catchment water balance. For further comparison with the SCS CN method, the original curve number handbook has values for varying types of hydrological conditions and support practices that can be used to re-parameterise the land cover scenarios in HEC-HMS. This re-parameterisation can then be tested against the less detailed HEC-HMS parameterisation used in this chapter, the classification-based LUCI parameterisation, and the future more detailed LUCI parameterisation that also accounts for vegetation effects.

Some of the future directions for the LUCI inundation model were outlined in the inundation review (Chapter 7), mainly the addition of factors to account for the effect of land cover roughness and friction. This would elucidate the possible effects of green infrastructure such as riparian planting on floodplain inundation compared to grey infrastructure such as retaining walls.

Another aspect of future work for extreme events modelling in CDO is to understand and quantify the flood risk based on the social dimensions of the CDO floodplain. The risks to communities are not purely spatial and are affected by the community's socioeconomic status, demographics, dependence on natural resources, and access to public infrastructure (Pati et al., 2014). By understanding the complex interactions between communities, the river, and potential disasters, these communities can be more involved in the decision-making processes around creating disaster risk mitigation programmes before, during, and after disaster events.

8.4.1 Extreme events under climate change

As established in the introduction (Chapter 1), there is strong regional variability in the potential effects of climate change, underscoring the need for downscaling and testing climate change at the regional or catchment level. CDO is located within Region 10 where projections show temperature increase for all seasons, increases to rainfall during the northeast monsoon (December to February), but decreases in rainfall for the other seasons (Hilario et al., 2011). This seasonal variation in climate change effects is important because of the occurrence of typhoons in CDO during the northeast monsoon season. Washi, Bopha, Jangmi, and Vinta all hit the CDO catchment during the month of December. Hence, an important future direction is perturbing the existing event rainfall under different scenarios of climate change to test the potential effects on the flow hydrograph and inundation. The rainfall under climate change should be modelled under the different land cover scenarios to elucidate the potential interactions between climate, ecosystems and resulting floods. The peak flows under climate change and different land cover scenarios can then be checked against the capacity of the existing structural measures within the CDO floodplain. This increases the adaptive capacity of management and better decisions can be made around the long-term resilience of the ecosystem and city (Ty et al., 2012).

8.5 Summary and conclusions

The LUCI model is commonly used for ecosystem service analysis and has already been used to model the distribution of ES in CDO under different land cover scenarios. LUCI is highly spatially resolved as it can be applied at the sub-field scale with strong but novel and less-tested rainfall-runoff capabilities. Since the HEC-HMS and HEC-RAS models are widely used and applied in the Philippines, this chapter aimed to test LUCI's rainfall-runoff modelling to that of HEC-HMS and to use the flood hydrographs as input into HEC-RAS for floodplain mapping. Under the baseline land cover scenario with Typhoon Bopha rainfall, the LUCI and HEC-HMS hydrographs showed good agreement with each other and with the observed flow during the event. The inundation maps produced by HEC-RAS also showed similar areas of inundation from the hydrographs from both rainfall-runoff models. Since LUCI predicted a slightly lower peak flow and flood volume, the resulting HEC-RAS inundation map had a smaller inundation extent compared to the hydrograph produced by HEC-HMS. Although the LUCI inundation model is operational (Chapter 7), more testing and parameterisation must be achieved for CDO before comparing it to HEC-RAS.

Future work involves comparing LUCI against HEC-HMS for additional extreme events: Jangmi (2014) and Tembin (2017). The rainfall for these two events has already been obtained and undergone infilling to correct for gaps in the data. The weighted curve number for the other two land cover scenarios have also been calculated at the sub-catchment level, but the parameterisation must be improved through using the original USDA NRCS (1986) curve number table that accounts for different land management and hydrological conditions. This is a more detailed parameterisation that can account for the specific mitigation interventions (e.g. riparian planting and bamboo cultivation) detailed in the development and rehabilitation scenarios that impacted the results of the ES (Chapter 3) and soil erosion modelling (Chapter 5). After parameterising the different land cover scenarios, downscaling climate change predictions and perturbing the extreme event rainfall allows for testing the combined effect of land cover and climate changes in CDO.

Given the reasonable comparison between the LUCI and HEC-HMS, this chapter also lays the groundwork for predicting soil erosion at the event scale through its development and parameterisation of the LUCI rainfall-runoff model. Through combining the capability of the LUCI rainfall-runoff model with the RUSLE application in CDO, this chapter also lays the groundwork for event-based soil erosion modelling in the future.

9 Synthesis of understanding the effect of changing land use on floods and soil erosion in the Cagayan de Oro catchment

9.1 Summary of the rationale and aims

As discussed in detail in Chapter 1, the destructive capability of natural disasters such as tropical storms, earthquakes, droughts, volcanoes, etc. have had a significant impact on communities and infrastructure all over the world (Guha-sapir et al., 2014). Of these disasters, the most devastating were those associated with tropical storms, flooding, and landslides (Guha-sapir et al., 2014). Due to the destruction associated with flooding and extreme events in the Philippines, considerable attention is given to increasing the resilience of communities and ecosystems through real-time flood warnings, construction of structural flood protection, and promoting sustainable land use management. This thesis fits into the broader context of disaster risk management and resilience through understanding how different types of land cover affect the CDO catchment, specifically regarding the spatial distribution of ecosystem services and the catchment's response to extreme rainfall events. The CDO catchment has experienced extreme flooding as a result of typhoons (Sendong in 2011, Bopha in 2012, Jangmi in 2014, and Tembin in 2017), and the current disaster-risk framework in CDO includes a real-time flood forecasting and warning system, and the construction of a retaining wall on the floodplain (JICA, 2014; Paringit et al., 2015). This mitigation framework includes rehabilitation, protection, and comprehensive land use planning through proper zoning of the CDO catchment (CESM, 2014). This research applied the Land Utilisation and Capability Indicator (LUCI) framework and the Revised Universal Soil Loss Equation (RUSLE) to the CDO catchment for the following objectives:

- Understand the spatial distribution of ecosystem services and help identify priority areas for management
- Assess the effect of development and rehabilitation plans on ecosystem services (soil conservation and flood mitigation) and on flooding regimes under extreme rainfall
- To contribute to future development of LUCI through developing and testing new components of the LUCI framework (i.e. sediment delivery, floodplain inundation, and rainfall-runoff modelling)

The main ecosystem services chosen for this research were soil conservation and flood mitigation, although LUCI runs were also achieved for agricultural productivity and nutrient delivery. Future work includes further parameterisation for the CDO catchment to run the additional services within LUCI: carbon sequestration, habitat connectivity, and habitat suitability. Soil conservation was assessed through the RUSLE, which delineates the areas of the catchment most vulnerable to soil erosion, hence marking those areas as priority for management to apply soil conservation measures. Flood mitigation modelling used LUCI to delineate the areas that were providing good mitigating services, but also the areas where management such as rehabilitation can be applied to enhance flood mitigation. Through scenario analysis, the effect of changing land cover on the potential soil erosion and flood mitigation was also analysed. Finally, extreme events modelling was carried out to elucidate the effect of changing land cover on peak flows and floodplain inundation. Aside from modelling results, this thesis contributed to the development of the LUCI model through the testing and addition of RUSLE and updates to the existing floodplain inundation code.

9.2 Ecosystem services and extreme events

There were several overarching results common to both the soil erosion modelling and the flood mitigation modelling. The rehabilitation of the CDO catchment led to decreases in estimates of soil erosion rates and to increases in the ability of the catchment to provide flood mitigation services. The steep slopes of the CDO catchment, combined with agricultural activity with no conservation measures, cause these areas to be more vulnerable to soil erosion and making them targets for potential management interventions to increase flood mitigation. In the RUSLE scenario analysis, conservation measures such as agroforestry and contour farming showed potential for decreasing the annual soil erosion rate compared with the baseline scenario. The LUCI model results also indicate these steep slopes and valleys as areas of high flood accumulation, but with high opportunity to enhance flood mitigation through different management strategies. One of the recommendations in the catchment management plan is to rehabilitate these slopes with bamboo, thus increasing the capacity to absorb and intercept the water before entering the stream network (Barth & Döll, 2016; CESM, 2014). The results of both RUSLE and LUCI align with that of the basin management, showing synergistic opportunities to enhance both soil conservation and flood mitigation services within CDO. Identifying synergies and trade-offs in ecosystem services is important because of the complex interactions between services, such as where enhancing one service may lead to a degradation of a different service provided by the same area. Future parameterisation and coding work with LUCI will lead to an eventual incorporation of RUSLE into the framework and ability to run the other ecosystem services (agricultural productivity, nutrient transport, carbon sequestration) for the CDO catchment, creating maps to help land zoning and deciding management strategies.

Aside from spatial variations in soil erosion, temporal variations in soil erosion were also analysed. Using monthly rainfall data in the RUSLE, monthly estimates of soil loss showed higher likelihood of soil loss occurring during the months of June to November, which fall within the southwest monsoon season for CDO. The months with the lowest likelihood of soil loss were December to May, which have lower monthly rainfall and fall within the weaker northeast monsoon season. The intra-annual variations in soil erosion help guide management in determining when intervention strategies are likely to have the most benefit, as well as when there may be water quality issues associated with sediment transport. Aside from soil erosion, future work can incorporate running the nutrient delivery tools within LUCI at the monthly or seasonal scale to elucidate temporal variations in the presence of nitrogen and phosphorus in the stream network.

Although the December to May months have the lowest estimated sediment transport, extreme rainfall events have struck the CDO catchment in December most notably in recent years: Washi (2011), Bopha (2012), Jangmi (2014), and Tembin (2017). These typhoons have the ability to cause flooding that exacerbates sediment transport through the CDO catchment and increases the possibility of mass movement events such as landslides. Event-based sediment transport underscores those complex interactions between ecosystem services, and shows the benefit of synergistic approaches to land management. By using soil conservation measures in tandem with flood mitigation strategies, the long-term problem of soil erosion and the short-term problem of event floods is addressed.

The extreme events modelling was done under Typhoon Bopha for the baseline land cover scenario to compare LUCI's novel rainfall-runoff model with the more established curve number method used by the DREAM (2015) parameterisation of HEC-HMS. Both models had good agreement with each other and with the observed flow, showing the strengths of LUCI's model working at the sub-field scale. The next steps for extreme event modelling in LUCI is to run a greater number of extreme events (Jangmi and Tembin), a wider range of land cover scenarios (development and rehabilitation), and under rainfall affected by climate change. The application of the LUCI rainfall-runoff model at the event scale also lays the groundwork for future coupling with the MUSLE to produce sediment delivery estimates during typhoon events.

The looming threat of climate change is also prevalent in the Philippines, as there are projected rainfall increases in both the southwest monsoon season (June to August) and the weaker monsoon season (December to January) (CESM, 2014; Hilario et al., 2011). Downscaling climate change predictions and modelling the potential effect on the ecosystem services of CDO is an important direction for future work, especially under different scenarios of land use and land cover, to elucidate the complex interactions between the ecosystem and climate (Villarin et al., 2016). This increase in rainfall can lead to increased sediment transport and flooding; modelling the potential effects of climate change on erosion and flooding is one of the future recommendations for the CDO catchment. By understanding the effect rainfall increases can have on ecosystem services and flood events, the adaptive capacity increases as management can plan to place more management interventions in the most vulnerable areas or design structural measures that account for increased peak flows under climate change.

With further improvements to the parameterisation details for the CDO catchment, running the carbon tool would elucidate potential carbon storage in catchment and any fluxes associated with changing land cover. There have been previous studies within and near the CDO catchment that have tested the carbon stock potential of different types of agroforestry systems (Canencia et al., 2015; Labata et al., 2012). As shown by the scenario-based soil erosion and ecosystem services modelling (Chapter 5 and 3), agroforestry techniques increase soil conservation and provide flood mitigation over traditional agricultural methods. Field-based tests showed the utility of agroforestry systems for climate change mitigation by sequestering more carbon compared to grassland or pastureland systems (Canencia et al., 2015; Labata et al., 2012). Agroforestry can potentially provide livelihood for upland communities where agricultural productivity is hampered by soil degradation or erosion (Canencia et al., 2015).

The ability to identify synergies and trade-offs to understand the links between ecosystem services and how they are affected by climate change is clearly a critical area of study. One of the services within the LUCI framework is modelling carbon sequestration and future work to parameterise specific tree species would allow this model to be run for CDO and potentially the rest of the Philippines. As shown by Labata et al. (2012) and Canencia et al. (2015), the carbon sequestered by different tree species and agroforestry systems varies, and using their work as parameterisation for LUCI, scenario analysis can be used to determine which species or systems provide larger carbon stock benefits. “Climate-smart reforestation” requires an understanding of how both the spatial distribution of trees and tree species will affect the hydrological cycle and provision of related services such as flood mitigation, soil erosion, and habitat refugia (Locatelli et al., 2015). LUCI is already spatially explicit and can explore scenarios around spatial distribution of trees, and parameterising the carbon sequestration ability and water needs of different tree species will be useful for the model’s role in climate-smart reforestation (Dierick & Hölscher, 2009; Jackson et al., 2013).

The human interactions with climate change, the ecosystem, and its services are another crucial area of future study (Cruz et al., 2017). Working with stakeholders to promote sustainable land use management and education around the potential effects of climate change can increase their resilience and disaster preparedness (Eugenio et al., 2016; Japos & Lubos, 2014). The work already contributed by this thesis around ecosystem services can be further enhanced to include the effect of climate perturbations on ES and the hydrological cycle under different land cover scenarios, increasing the utility of the LUCI framework for decision-making.

The habitat connectivity and suitability tools would link the landscape and vegetation with the protection of the fauna and biodiversity of the CDO catchment. More future work would revolve around collecting information about the habitat requirements of the various animals present in the catchment, thus outlining possible areas that can be managed specifically for their protection and conservation.

9.3 Model development

Aside from understanding the effect of land cover on ecosystem services and floods, this thesis also contributed to the testing and development of the LUCI framework. This section summarises the work around the RUSLE and its eventual incorporation into LUCI, identification of limitations in the land cover parameterisation and potential solutions, and improvements in the LUCI inundation model. As climate change can severely affect the hydrology of the CDO catchment, this thesis also outlined some ways forward to better incorporate spatial detail in climate drivers such as rainfall and potential evapotranspiration.

Since the RUSLE is used around the world, there are many possible sub-equations to use within the model to estimate the effects of rainfall, topography, soil erodibility, etc. but not as much guidance as to which equations are appropriate to use depending on regional specificity or data availability. The RUSLE review (Chapter 4) compiled many of these sub-equations and their sources, including the availability of national and global datasets for future applications of RUSLE. Out of this review came the case studies of the CDO catchment and in the Mangatarere catchment (New Zealand), which analysed the different sub-equations to test their effect on the resulting soil erosion estimates. These case studies identified biases in the equations, such as rainfall erosivity equations that ignored days where rainfall was below a certain amount. These equations and the RUSLE account for high-intensity erosive storms, but may not account for periods of lighter rainfall with longer durations. In the Mangatarere application, using DEMs of different resolutions and different methods to account for topography showed the utility of each equation at different scales. At the catchment scale, topography equations based on slope length and steepness were useful for delineating large areas vulnerable to soil erosion. At the sub-catchment or field scale, topography equations that used flow accumulation on high-resolution

DEMs identified only the most critical areas for soil erosion due to their micro-topography. The temporal variability of soil erosion due to rainfall variation was already discussed (Section 9.2), but the temporal variability of soil erosion due to differences in vegetation growth stages could also be investigated. At the catchment scale, there may be plans for rehabilitation and tree-planting, but more detailed information about the ability of vegetation to mitigate soil erosion at the sapling or mature stage would be useful to land management. By understanding the relationship of soil erosion to tree growth and stage, the model can indicate at what timeframes the trees are still vulnerable and require monitoring, and when the trees could mitigate soil erosion. At the field scale, a crop growth and stage model would be useful for the farmer to know what stages in the crop development cycle would have increases in the potential soil loss and where to put management interventions.

This inclusion of a tree/crop development model is also a future direction for more detailed land cover parameterisation within LUCI. As the plant rooting depth and water needs change with stage, so does its ability to mitigate floods or sequester carbon. Similar to how this detailed parameterisation would benefit soil loss and sediment delivery modelling, adding a plant development model elucidates the timeframes of when rehabilitated areas are still vulnerable, and when the area's ability to mitigate floods increases due to changes in rooting depth and water needs. Although the broad classification used in this research was appropriate to produce ecosystem service maps for CDO (Chapter 3), using more specific crop characteristics helps to more robustly represent the complexity of the landscape. For example, rice paddies were observed in CDO and their use of standing water at different crop stages can affect the hydrological response of the landscape to rainfall events. Other tropical vegetation to be included in future parameters are palm trees, coconuts, and mangroves. Mangroves are of particular importance due to their ability to sequester carbon and the future plans of the CDO management to establish mangrove plantations along the coastal areas (Castillo et al., 2017; CESM, 2014).

The LUCI inundation model was first developed in 2011 and was updated in this thesis to run through MATLAB R2015a by calling functions from ArcMap 10.4.1. The code was also converted to Python for future direct integration into the LUCI software that solely requires ArcMap 10.x, although requires more improvements to computational efficiency. One possible method of increasing computation efficiency is through preprocessing the DEM and dividing the floodplain into depression zones of known volume and stage, thus allowing the flood to spread to adjacent zones ones a threshold value of volume is reached (Chapter 7). Since the current version of the LUCI inundation model relies on mass conservation, future versions can incorporate the effect of land cover through roughness and friction coefficients to test the effect of non-structural measures such as riparian planting.

9.4 Limitations and future work

One of the biggest limitations of this thesis was the lack of validation data to quantitatively test the accuracy of the soil erosion and flood modelling. Previous work included water quality monitoring that was previously recorded for the CDO river from 2001 to 2006 with the total suspended solids (TSS) seen as an indicator for the amount of sediment transported into the waterways from erosive activities (CESM, 2014). Since the RUSLE models the potential soil erosion per unit area (tons hectare^{-1} year^{-1}), more work is needed to convert these rates into water quality indicators to compare against water quality records. Long-term water quality records are needed to understand the monthly and seasonal variations in water quality and the potential link to soil erosion. Another way to validate soil erosion data would be to compare modelled soil loss with data from other studies that were done in similar geoclimatic regions or on similar land covers. One of the future contributions to soil erosion research is to review published soil erosion literature to compile a database of potential soil loss categorised by climate type, land cover, and region.

The flow hydrographs produced by LUCI and HEC-HMS were compared with the observed flow data, which was based on a rating curve relating flow and stage height of a station at the outlet of the catchment. Validating the inundation extent was more difficult and required relying on soft data such as recorded incidents of flooding in disaster reports and news articles. With the availability of satellite imagery, future work to validate inundation extent could involve the usage of Google Earth Engine to process imagery and produce inundation maps from observations (Gorelick et al., 2017).

Another limitation of the RUSLE was the inability to account for gully erosion, hence the discussion of how to incorporate RUSLE and CTI together into an enhanced soil erosion model used by the LUCI framework (Chapter 6). Currently, the LUCI framework uses the CTI to delineate areas vulnerable to soil erosion by using information about slope steepness, contributing area, and planform curvature (Thorne et al., 1985). This approach does not account for the different effects of land cover or management practices. The RUSLE accounts for land cover, slope steepness, and contributing area. This overlap in what both models account for would mean the danger of double counting or overestimation if their resulting erosion rates were added together. Hence, developing a method to balance the factors accounted for by RUSLE and those accounted for by CTI is a good future direction and can lead to more robust representation of complex soil erosion processes. From the case studies in this thesis, the manual steps required to apply RUSLE are being converted to automated Python toolboxes that can be used by future users of LUCI.

In terms of ecosystem service modelling, the areas providing flood mitigation in CDO were identified in this research. However, it is also important to delineate the flow of a service (e.g. water supply) from the source to the sink in order to understand if the demand for that service is being met (Bagstad et al., 2014). Studies involving the valuation and willingness-to-pay for ecosystem services have been accomplished previously in the CDO catchment (Baig et al., 2015; ILC, 2013), but incorporating an economic valuation model into LUCI would be useful for cost-benefit-analysis as land managers may have to work within a certain budget. In the LUCI application, using different thresholds of flood mitigation was useful in identifying which areas are the most critical for management interventions. Depending on budgetary constraints, land managers may want to prioritise those critical areas for interventions.

9.5 Implications

This thesis mainly contributed to the field of ecosystem services modelling in the Philippines through LUCI application in the Cagayan de Oro catchment, and to the technical development of the LUCI model through improvements in the soil erosion model and through parameterising the model for a tropical catchment. Although ecosystem services have been previously studied in CDO (Chapter 1), these studies have focused on the stakeholder perception and economic valuation of ecosystem services. The novel contribution of this research is the use of the LUCI framework to delineate the areas in the catchment providing flood mitigation services, areas vulnerable to soil erosion, areas to improve for agricultural productivity, and areas contributing to high nutrient delivery. This study also used scenario analysis to understand the potential changes of these services under different land cover plans of development and rehabilitation. This information assists stakeholders and local government in understanding the potential consequences of their land management plans as compared to the current or baseline land cover. Understanding soil erosion and flood mitigation are important in the CDO catchment because it is heavily utilised for agriculture and experiences flooding brought on by extreme events, hence the need to perform ecosystem services modelling. Future work around improving the soil and land cover parameterisation in CDO will add more detail to the unique vegetation of tropical areas (e.g. rice paddies, mangroves) and allow for more Philippines-based detail in the LUCI framework to run its models of agricultural productivity and sediment delivery.

This application in the CDO catchment was the first application of the LUCI framework to the Philippines and was used as a stepping stone to understand the data availability and limitations associated with applying the model to a new country. A database has been built with soil, land cover, and vegetation characteristics of the CDO catchment, which is a stepping stone for a larger database for more study areas in the Philippines. Soil erosion is a problem in the Philippines due to its mountainous topography, anthropogenic activities in upland areas, and high annual rainfall (Paningbatan et al., 1995). Flooding is a devastating problem, as established in Chapter 1. Understanding the agricultural productivity and nutrient delivery ecosystem services in the Philippines would contribute to potentially more optimal agricultural strategies and improves to the associated water quality issues. As established in Section 9.2, parameterising the carbon stock model using information on vegetation in the Philippines would contribute to “climate-smart reforestation” where the benefits of trees are for flood mitigation, soil conservation, and carbon sequestration.

National-scale LUCI applications have been previously achieved in Wales (Emmett et al., 2017), and with a large parameterisation database and high computing power, a national-scale LUCI application is possible for the Philippines in the future. LUCI could potentially be used to produce ecosystem services maps, synergy maps, and trade-off maps at the national scale, helping land managers and regional authorities understand the services provided by their local region.

Expanding beyond the Philippines, this research outlines the challenges of applying the LUCI framework to tropical areas and other geoclimatic regions as pilot sites. This thesis showed what type of data is needed in terms of fieldwork, plans from local government, the availability of global databases for soil characteristics, etc. Correlating to the New Zealand parameterisation is possible for study areas with scarce data due to the New Zealand soil and land cover types having the most detail within the LUCI framework. Tropical areas were begun through this study, and both hot and cold arid areas have interesting challenges around evapotranspiration and the resilience of arid plants. This research identified freely available global datasets of rainfall, evapotranspiration, and rainfall erosivity, and future work around building a database of datasets with global coverage will lead to a global-scale LUCI application given sufficient computational power.

Although this research is primarily focused on physical sciences, it can be part of a larger cross-disciplinary study. As established in Chapter 1, ecosystem services research includes economic components through valuation, cost-benefit analysis, and willingness-to-pay. This is important for drafting management interventions that fit within a budget, and for understanding how stakeholders value services to elucidate priority management directions. The social dimension of ecosystem services research shows that the importance of participatory decision-making through engaging directly with stakeholders such as local and indigenous communities. These stakeholders are the most likely beneficiary of services and whose local actions directly affect the distribution and supply of services, hence the need for their participation.

9.6 Summary and conclusion

The overall aim of this study was to understand the changes to ecosystem services and hydrological responses of the CDO catchment associated with changes in land cover from the baseline scenario to plans involving catchment development and rehabilitation. The specific objectives were as follows:

1. To apply LUCI to the CDO catchment to understand the spatial aspect of its ecosystem services and help identify priority areas for land management;
2. To assess how development and rehabilitation plans will affect the soil erosion and flood mitigation within the watershed; and
3. To contribute to future development of LUCI through developing and testing new components of the LUCI framework (i.e. sheet/rill erosion modelling, floodplain inundation, and rainfall-runoff modelling)

The aims and objectives were achieved through applying the LUCI framework the CDO catchment to delineate areas providing flood mitigation, agricultural productivity, and nutrient delivery services. The priority areas for management to improve flood mitigation were on steeper slopes associated with agricultural land use and river valleys. These steep agricultural slopes were also identified as vulnerable erosion areas by RUSLE, which could be mitigated also by riparian planting. The provision of flood mitigation services was better in the rehabilitation scenario compared to the development scenario. In terms of nutrient delivery, the development and rehabilitation scenarios had lower loads of nitrogen and phosphorous compared to the baseline. The identification of areas vulnerable to soil erosion was accomplished using the RUSLE model, which was tested to find the best factor equations for the CDO catchment and will be converted into a Python toolbox to be used by future LUCI users.

This research also contributed to the technical development of the LUCI framework through developing the floodplain inundation model from MATLAB into Python, building a database of parameterisation information for CDO which can be expanded to the Philippines and eventually to other tropical areas, through testing the RUSLE model for future integration into LUCI, and through testing LUCI's rainfall-runoff modelling capabilities against HEC-HMS.

The potential land cover changes caused significant differences in the areas providing ecosystem services, areas vulnerable to soil erosion, and the hydrological response of the catchment to extreme events. This research showed that it is important to understand these potential changes to prevent degradation of these services and to increase the resilience of ecosystems, communities, and infrastructure to extreme events. By providing and enhancing tools to engage with stakeholders, local government, and local communities, this research contributes to the participatory decision-making necessary for the continued maintenance of ecosystem services, well-being of communities, and sustainable management of catchments.

In summary, this research contributed to the field of ecosystem services modelling by producing spatially-explicit maps showing the existing distribution of services in the CDO catchment, and the areas where these services can be improved through management strategies. Additionally, modelling the potential land cover change and showing the resulting effect on ecosystem services and soil erosion is of use to land management and policy-makers. This type of ecosystem services modelling has never been previously accomplished in CDO, thus underscoring the novelty of this research. Through parameterising the model for CDO, the LUCI model's applicability is extended to tropical areas such as other areas in the Philippines, Southeast Asia, and other islands. In terms of model development, this research also contributed to the field of soil erosion through a thorough review of the RUSLE and its applications in the Philippines and New Zealand, and to inundation modelling through the continued development on the flatwater inundation model.

Appendix 1. Summary of previous studies that have applied the USLE and RUSLE

Author	Location	R-factor	K-factor	LS-factor	C-factor	P-factor
David (1988)	Various watersheds in the Philippines	Mihara (1951) and Hudson (1971) as cited in David (1988)	Wischmeier and Mannering (1969)	Madarcos (1985) and Smith & Whitt (1947)	Literature	Literature
Eiumnoh (2000)	Sakae Krang watershed (Thailand)	El-Swaify et al. (1987) as cited in Post & Hartcher (2006)	USLE method	USLE method	Literature	None observed (P=1)
Fernandez et al. (2003)	Lawyers Creek Watershed (USA)	USDA-ARS (2002)	From the SSURGO database (USDA)	Upslope contributin g area method	Database from RUSLE software	Database from RUSLE software
Merritt et al. (2004)	Mae Chem watershed (Thailand)	El-Swaify et al. (1987) as cited in Post & Hartcher (2006)	Previous studies in area	USLE method	Previous studies in area	Previous studies in area
Post and Hartcher (2005)	Mae Chem watershed (Thailand)	El-Swaify et al. (1987) as cited in Post & Hartcher (2006)	Previous studies in area	L = 1 S = derived from DEM	Previous studies in area	None observed (P=1)
Dumas and Fossey (2009)	Efate Island (Vanuatu)	Roose (1975) and Morgan (1994) as cited in Morgan (2005)	USLE method	RUSLE method at pixel level	Literature	None observed (P=1)
Adornado et al. (2009)	REINA (Philippines)	El-Swaify et al. (1987) as cited in Post & Hartcher (2006)	Table by Stewart et al. (1975)	Upslope contributin g area method	Literature	None observed (P=1)
Schmitt (2009)	Negros Island (Philippines)	RUSLE method	USLE method	RUSLE method at pixel level	Literature	Previous studies
Jayasinghe et al. (2010)	Nuwaraeliya (Sri Lanka)	El-Swaify et al. (1987) as cited in Post & Hartcher (2006)	Table by Stewart et al. (1975)	Upslope contributin g area method	Literature	None observed (P=1)
Jain and Das (2010)	Jharkhand (India)	Ram et al. (2004), as cited in Jain and Das (2010)	USLE method and previous studies	Upslope contributin g area method	Literature	None observed (P=1)
Adornado and Yoshida (2010)	Bukidnon (Philippines) and also REINA (Philippines)	El-Swaify et al. (1987) as cited in Post & Hartcher (2006)	Table by Stewart et al. (1975)	Upslope contributin g area method	Literature	None observed (P=1)

Boyle et al. (2011)	California (USA)	From previous studies	From previous studies	Upslope contributing area method	Literature	N/A
Chen et al. (2011)	Xiangxi watershed (China)	Wischmeier and Smith (1978)	Williams and Renard (1983) nomograph	Upslope contributing area method	Using NDVI	N/A
Demirci & Karaburun (2012)	Buyukcekmece Lake watershed (Turkey)	Arnoldus (1980)	Torri et al. (1997) equation	Upslope contributing area method	Using NDVI	None observed (P=1)
Nontananandh and Changnoi (2012)	Songkhran watershed (Thailand)	LDD (2000)	Values from LDD (2000)	Modified RUSLE method	Literature	None observed (P=1)
Ozsoy et al. (2012)	Mustafakemalpasa River Basin (Turkey)	From previous studies	USLE method	RUSLE method, using a 3rd party programme	Literature	None observed (P=1)
Delgado & Canters (2012)	Claveria (Philippines)	Shamshad et al. (2008)	USLE method	RUSLE2 programme, using the upslope contributing area method	Literature	David (1988)
Hernandez et al. (2012) (used SedNet, which has an USLE component)	Pagsanjan (Philippines)	El-Swaify et al. (1987) as cited in Post & Hartcher (2006)	Wischmeier and Mannering (1969)	Algorithm within SedNet	Literature	N/A
Sinha & Joshi (2012)	Maharashtra (India)	Roose (1975)	USLE method	Morgan (1986)	Literature	Literature
Nigel & Rughooputh (2012)	Mauritius	Arnoldus (1980), as cited in Le Roux et al. (2005)	From previous studies	Upslope contributing area method	Literature	Literature
Životić et al. (2012)	Nisava river basin (Serbia)	Wischmeier and Smith (1978)	USLE method	RUSLE method	Using NDVI	None observed (P=1)
Rozos et al. (2013)	Euboea Island (Greece)	Flabouris (2008)	Based on geological characteristics	Morgan (1986)	Literature	None observed (P=1)
Bagherzadeh (2014)	Masshad plain (Iran)	Wischmeier and Smith (1978)	USLE method	USLE method		None observed (P=1)
Ferreira and Panagopoulos (2014)	Alqueva (Portugal)	Similar to Loureiro and Coutinho (2001)	USLE method	Upslope contributing area method	Using NDVI	None observed (P=1)
Li et al. (2014)	Guangdong (China)	Zhou et al. (1995)	USLE method	Similar to RUSLE method	Using NDVI	1 for wasteland and built-up 0.5 for forested

						0.2 for orchard land 0.35 for cropland
Zakerinejad and Maerker (2015) (used USPED, which has USLE components)	Mazayjan (Iran)	Ferro et al. (1991); Renard & Freimund (1994); Sadeghifard et al. (2004)	RUSLE method	Algorithm within USPED	Literature	None observed (P=1)
Jahun et al. (2015)	Crete (Greece)	Fu et al. (2006)	RUSLE method	Upslope contributin g area method	Using NDVI	Previous studies
Farhan and Nawaiseh (2015)	Wadi Kerak catchment (Jordan)	Eltaif et al. (2010)	Similar to USLE nomograph	Upslope contributin g area method	Literature	Literature
Panagos et al. (2015c) and related papers	Europe	Rainfall Intensity Summarisatio n Tool (RIST)	USLE method	3rd party programme	Literature	Literature
Russo (2015)	Brunei Darussalam	Rosewell & Turner (1992)	Rosewell (1997)	RUSLE method	Based on ground covered	None observed (P=1)
Nakil and Khire (2016)	Gangapur (India)	Nakil (2014)	USLE method	RUSLE method	Literature	Literature
Raissouni et al. (2016)	Smir Dam (Morocco)	Similar to Arnoldus (1980) methods	Merzouk (1985)	Upslope contributin g area method	Literature	None observed (P=1)
Fernandez and Daigneault (2016)	Waikato (New Zealand)	Institute of Water Research (2015)	Dymond et al. (2010)	Upslope contributin g area method	Range between 1 (wood vegetation) and 10 (herbaceou s vegetation or bare ground)	
Duarte et al. (2016)	Montalegre (Portugal)	Loureiro and Coutinho (2001)	USLE method	USLE method	Literature	Literature
Gaubi et al. (2017)	Lebna watershed (Tunisia)	Rango and Arnoldus (1987)	USLE method	Upslope contributin g area method	Literature	None observed (P=1)

References

Abon, C. C., David, C. P. C., & Pellejera, N. E. B. (2011). Reconstructing the Tropical Storm Ketsana flood event in Marikina River, Philippines. *Hydrology and Earth System Sciences*, *15*(4), 1283–1289. https://doi.org/10.5194/hess-15-1283-2011

Acutis, M., & Donatelli, M. (2003). SOILPAR 2.00: Software to estimate soil hydrological parameters and functions. *European Journal of Agronomy*, *18*, 373–377. https://doi.org/10.1016/S1161-0301(02)00128-4

Adornado, H. A., & Yoshida, M. (2010). Assessing the Adverse Impacts of Climate Change: A Case Study in the Philippines. *Journal of Developments in Sustainable Agriculture*, *5*, 141–146.

Adornado, H. A., Yoshida, M., & Apolinares, H. (2009). Erosion Vulnerability Assessment in REINA, Quezon Province, Philippines with Raster-based Tool Built within GIS Environment. *Agricultural Information Research*, *18*(1), 24–31. https://doi.org/10.3173/air.18.24

Aksoy, H., & Kavvas, M. L. (2005). A review of hillslope and watershed scale erosion and sediment transport models. *Catena*, *64*(2–3), 247–271. https://doi.org/10.1016/j.catena.2005.08.008

Alaghmand, S., Abdullah, R., Abustan, I., & Vosoogh, B. (2010). GIS-based River Flood Hazard Mapping in Urban Area (A Case Study in Kayu Ara River Basin, Malaysia). *International Journal of Engineering and Technology*, *2*(6), 488–500.

Alexandridis, T. K., Sotiropoulou, A. M., Bilas, G., Karapetsas, N., & Silleos, N. G. (2015). The Effects of Seasonality in Estimating the C-Factor of Soil Erosion Studies. *Land Degradation and Development*, *26*(6), 596–603. https://doi.org/10.1002/ldr.2223

Alibuyog, N. R., Ella, V. B., Reyes, M. R., Srinivasan, R., Heatwole, C., & Dillaha, T. (2009). Predicting the effects of land use change on runoff and sediment yield in Manupali River subwatersheds using the SWAT model. *International Agricultural Engineering Journal*, *18*(1), 15.

Alley, W. M. (1984). On the Treatment of Evapotranspiration, Soil Moisture Accounting, and Aquifer Recharge in Monthly Water Balance Models. *Water Resources Research*, *20*(8), 1137–1149. https://doi.org/10.1029/WR020i008p01137

Alvim, P. D. T., & Kozlowski, T. T. (1977). *Ecophysiology of tropical crops*. Academic Press: Elsevier. https://doi.org/10.1016/c2013-0-07134-4

Amadore, L., Bolhofer, W. C., Cruz, R. V. O., Feir, R. B., Freysinger, C. A., Guill, S., Jalal, K. F., Iglesias, A., Jose, A., Leatherman, S., Lenhart, S., Mukherjee, S., Smith, J. B., & Wisniewski, J. (1996). Climate change vulnerability and adaptation in Asia and the Pacific: Workshop Summary. *Water, Air, and Soil Pollution*, *92*, 1–12.

Amini, A., Ali, T. M., Ghazali, A. H. B., Aziz, A. a., & Akib, S. M. (2011). Impacts of Land-Use Change on Streamflows in the Damansara Watershed, Malaysia. *Arabian Journal for Science and Engineering*, *36*, 713–720. https://doi.org/10.1007/s13369-011-0075-3

Armitage, F. B., & Burley, J. (1980). Pinus Kesiya. *Tropical Forestry Papers*. Oxfordshire: University of Oxford.

Arnoldus, H. M. J. (1977). Methodology used to determine the maximum potential average annual soil loss due to sheet and rill erosion in Morocco. *FAO Soils Bulletin*, *34*, 39–51.

Arnoldus, H. M. J. (1980). An approximation of the rainfall factor in the Universal Soil Loss Equation. In M. De Boodt & D. Gabriels (Eds.), *Assessment of Erosion* (pp. 127–131). Chichester, UK: Wiley.

Atu, L. L. (2013). *Studies on Propagation Materials and Growing Conditions for Sweetpotato [Ipomoea Batatas (L .) Lam] Production*. *Masters Thesis*. University of Queensland.

Badilla, R. A. (2008). *Flood Modelling in Pasig-Marikina River Basin*. (Master's thesis). International Institute for Geo-information Science and Earth Observation. Enschede, Netherlands.

Bagherzadeh, A. (2014). Estimation of soil losses by USLE model using GIS at Mashhad plain, Northeast of Iran. *Arabian Journal of Geosciences*, *7*(1), 211–220. https://doi.org/10.1007/s12517-012-0730-3

Bagstad, K. J., Semmens, D. J., Waage, S., & Winthrop, R. (2013). A comparative assessment of decision-support tools for ecosystem services quantification and valuation. *Ecosystem Services*, *5*, 27–39. https://doi.org/10.1016/j.ecoser.2013.07.004

Bagstad, K. J., Villa, F., Batker, D., Harrison-Cox, J., Voigt, B., & Johnson, G. W. (2014). From theoretical to actual ecosystem services: Mapping beneficiaries and spatial flows in ecosystem service assessments. *Ecology and Society*, *19*(2). https://doi.org/10.5751/ES-06523-190264

Baig, S., Rizvi, A., Josella, M., & Palanca-Tan, R. (2015). *Cost and Benefits of Ecosystem Based Adaptation: the case of the Philippines*. Gland, Switzerland: IUCN.

Ballinger, J., Jackson, B., Pechlivanidis, I., & Ries, W. (2011). *Potential flooding and inundation on the Hutt River*. Wellington, New Zealand: Victoria University of Wellington.

Bantayan, N. C., & Bishop, I. D. (1998). Linking objective and subjective modelling for landuse decision-making. *Landscape and Urban Planning*, *43*(1–3), 35–48. https://doi.org/10.1016/S0169-2046(98)00101-7

Battista, W., Karr, K., Sarto, N., & Fujita, R. (2017). Comprehensive Assessment of Risk to Ecosystems (CARE): A cumulative ecosystem risk assessment tool. *Fisheries Research*, *185*, 115–129. https://doi.org/10.1016/j.fishres.2016.09.017

Barth, N. C., & Döll, P. (2016). Assessing the ecosystem service flood protection of a riparian forest by applying a cascade approach. *Ecosystem Services*, *21*, 39–52. https://doi.org/10.1016/j.ecoser.2016.07.012

Barwick, M. (2004). *Tropical & Subtropical Trees: A Worldwide Encyclopaedic Guide*. High Holborn, London: Thames & Hudson.

Basher, L. R. (2013). Erosion Processes and Their Control in New Zealand. *Ecosystem Services in New Zealand: Conditions and Trends*, 363–374.

Bates, P., Trigg, M., Neal, J., & Dabrowa, A. (2013). *LISFLOOD-FP User manual*. Bristol, United Kingdom: University of Bristol.

Bedient, P. B., Huber, W. C., & Vieux, B. E. (2013). *Hydrology and Floodplain Analysis* (5th ed.). New York, United States of America: Prentice Hall.

Bellu, A., Sanches Fernandes, L. F., Cortes, R. M. V., & Pacheco, F. A. L. (2016). A framework model for the dimensioning and allocation of a detention basin system: The case of a flood-prone mountainous watershed. *Journal of Hydrology*, *533*, 567–580. https://doi.org/10.1016/j.jhydrol.2015.12.043

Benavidez, R., Jackson, B., Maxwell, D., & Paringit, E. (2016). Improving predictions of the effects of extreme events, land use, and climate change on the hydrology of watersheds in the Philippines. *Proceedings of the International Association of Hydrological Sciences*, *373*, 147–151. https://doi.org/10.5194/piahs-373-147-2016

Bernini, A., & Franchini, M. (2013). A Rapid Model for Delimiting Flooded Areas. *Water Resources Management*, *27*(10), 3825–3846. https://doi.org/10.1007/s11269-013-0383-3

Beven, K. J. (1989). Changing ideas in hydrology - The case of physically-based models. *Journal of Hydrology*, *105*(1–2), 157–172. https://doi.org/10.1016/0022-1694(89)90101-7

Beven, K. J., & Kirkby, M. J. (1979). A physically based, variable contributing area model of basin hydrology. *Hydrological Sciences*, *24*(1), 43–69.

Bhatt, C. M., Rao, G. S., Diwakar, P. G., & Dadhwal, V. K. (2016). Development of flood inundation extent libraries over a range of potential flood levels: a practical framework for quick flood response. *Geomatics, Natural Hazards and Risk*, *5705*(November), 1–18. https://doi.org/10.1080/19475705.2016.1220025

Bien, F. E., & Plopenio, J. C. (2017). Hydrologic modeling of Guinale River Basin using HEC-HMS and synthetic aperture radar. In K. Themistocleous, S. Michaelides, G. Papadavid, V. Ambrosia, G. Schreier, & D. G. Hadjimitsis (Eds.), *Fifth International Conf. on Remote Sensing and Geoinformation of the Environment*. Paphos, Cyprus. https://doi.org/10.1117/12.2277690

Bonilla, C. A., & Vidal, K. L. (2011). Rainfall erosivity in Central Chile. *Journal of Hydrology*, *410*(1–2), 126–133. https://doi.org/10.1016/j.jhydrol.2011.09.022

Boongaling, C. G. K., Faustino-Eslava, D. V., & Lansigan, F. P. (2018). Modeling land use change impacts on hydrology and the use of landscape metrics as tools for watershed management: The case of an ungauged catchment in the Philippines. *Land Use Policy*, *72*(August 2016), 116–128. https://doi.org/10.1016/j.landusepol.2017.12.042

Boyle, J. F., Plater, A. J., Mayers, C., Turner, S. D., Stroud, R. W., & Weber, J. E. (2011). Land use, soil erosion, and sediment yield at Pinto Lake, California: Comparison of a simplified USLE model with the lake sediment record. *Journal of Paleolimnology*, *45*(2), 199–212. https://doi.org/10.1007/s10933-010-9491-8

Bradshaw, C. J. A., Giam, X., & Sodhi, N. S. (2010). Evaluating the relative environmental impact of countries. *PLoS ONE*, *5*(5). https://doi.org/10.1371/journal.pone.0010440

Briones, R. U., Ella, V. B., & Bantayan, N. C. (2016). Hydrologic impact evaluation of land use and land cover change in Palico Watershed, Batangas, Philippines Using the SWAT model. *Journal of Environmental Science and Management*, *19*(1), 96–107.

Brunner, G. (2010a). *HEC-RAS User's Manual*. Davis, United States of America: Hydrologic Engineering Center.

Brunner, G. (2010b). *River Analysis System HEC-RAS Release Notes*. Davis, United States of America: Hydrologic Engineering Center.

Buan, R. D., Maglinao, A. R., Evangelista, P. P., & Pajuelas, B. G. (1996). Vulnerability of rice and corn to climate change in the Philippines. *Water, Air, and Soil Pollution*, *92*, 41–51.

Bulayog, M. S. B., Montes Jr, H. R., Lina, S. B., Patindol, T. A., Diola, A. C., Espinosa, E. D., & Modina, R. M. R. (2015). *Assessment of Natural Assets in the Agricultural and Aquatic*

Ecosystems in Sogod Bay, Southern Leyte. EEPSEA Research Report No. 2015-RR.

BSWM (Bureau of Soils and Water Management). (2013). *Soil Type*. Quezon City, Philippines, Department of Agriculture.

Burkhard, B., Müller, A., Müller, F., Grescho, V., Anh, Q., Arida, G., Bustamante, J. V., Chien, H. V., Heong, K. L., Escalada, M., Marquez, L., Truong, D. T., Villareal, S., & Settele, J. (2015). Land cover-based ecosystem service assessment of irrigated rice cropping systems in southeast Asia-An explorative study. *Ecosystem Services*, *14*, 76–87. https://doi.org/10.1016/j.ecoser.2015.05.005

Camacho, L. D., Tolentino, E. L., Rebugio, L. L., & Camacho, S. C. (2007). Economics of using water use efficient forest landscape restoration tree species. *Forest Science and Technology*, *3*(2), 101–107. https://doi.org/10.1080/21580103.2007.9656325

Campostrini, E., & Glenn, D. M. (2007). Ecophysiology of papaya: A review. *Brazilian Journal of Plant Physiology*, *19*(4), 413–424. https://doi.org/10.1590/S1677-04202007000400010

Canadell, J., Jackson, R. B., Ehleringer, J. B., Mooney, H. A., Sala, O. E., & Schulze, E.-D. (1996). Maximum rooting depth of vegetation types at the global scale. *Oecologia*, *108*(4), 583–595. https://doi.org/10.1007/BF00329030

Canencia, O. P., Palma, R. A., Ansigbat, V., Lacang, G., Osio, A., Tulang, R., Tamang, R., & Arnejo, B. (2015). Carbon Sequestration Potentials for Agro-forestry System and Grasslands in Bukidnon and Cagayan de Oro Landscape. *Mindanao Journal of Science and Technology*, *13*, 152–169.

Capra, A., Mazzara, L. M., & Scicolone, B. (2005). Application of the EGEM model to predict ephemeral gully erosion in Sicily, Italy. *Catena*, *59*(2), 133–146. https://doi.org/10.1016/j.catena.2004.07.001

Carating, R. B., Galanta, R. G., & Bacatio, C. D. (2014). *The Soils of the Philippines*. Dordrecht, Netherlands: Springer.

Carandang, A. P., Camacho, L. D., Gevaña, D. T., Dizon, J. T., Camacho, S. C., de Luna, C. C., Pulhin, F. B., Combalicer, E. A., Paras, F. D., Peras, R. J. J., & Rebugio, L. L. (2013). Economic valuation for sustainable mangrove ecosystems management in Bohol and Palawan, Philippines. *Forest Science and Technology*, *9*(3), 118–125. https://doi.org/10.1080/21580103.2013.801149

Carlaw, S. M. (2000). *Soil Moisture Accounting in Distributed Hydrologic Modelling*. (Master's thesis). University of Waterloo. Waterloo, Canada.

Carroll, M. L., DiMiceli, C. M., Sohlberg, R. A., & Townshend, J. R. G. (2004). 250m MODIS Normalized Difference Vegetation Index, Collection 4. University of Maryland, College Park, Maryland.

Castillo, J. A. A., Apan, A. A., Maraseni, T. N., & Salmo, S. G. (2017). Soil C quantities of mangrove forests, their competing land uses, and their spatial distribution in the coast of Honda Bay, Philippines. *Geoderma*, *293*, 82–90. https://doi.org/10.1016/j.geoderma.2017.01.025

Castonguay, A. C., Burkhard, B., Müller, F., Horgan, F. G., & Settele, J. (2016). Resilience and adaptability of rice terrace social-ecological systems: A case study of a local community's perception in Banaue, Philippines. *Ecology and Society*, *21*(2). https://doi.org/10.5751/ES-08348-210215

Castro-Bolinaga, C. F., & Diplas, P. (2014). Hydraulic Modeling of Extreme Hydrologic Events: Case Study in Southern Virginia. *Journal of Hydraulic Engineering*, *140*(12), 05014007. https://doi.org/10.1061/(ASCE)HY.1943-7900.0000927

CESM. (Center for Environmental Studies and Management). (2014). *Formulation of an Integrated River Basin Management and Development Master Plan for Cagayan de Oro River Basin*. San Juan City, Philippines: CESM.

CESM. (Center for Environmental Studies and Management). (2015). *Integrated River Basin Management and Development Master Plan for Cagayan de Oro River Basin: Implications on Regional and Spatial Development in Mindanao. Research Forum on Integrated River Basin Management and Development Master Plan and River Basin Flood Modelling in Northern Mindanao*. San Juan City, Philippines: CESM.

CGIAR-CSI. (2005). *Global Aridity and Global PET – Methodology*. CGIAR Consortium for Spatial Information. Retrieved November 21, 2018, from https://cgiarcsi.community/data/global-aridity-and-pet-database/.

Chan, E., & Elevitch, C. R. (2006). *Cocos nucifera (coconut)*. *Species Profiles for Pacific Island Agroforestry*. https://doi.org/10.1007/978-90-481-8661-7

Chatterjee, C., Forster, S., & Bronstert, A. (2008). Comparison of hydrodynamic models of different complexities to model floods with emergency storage areas. *Hydrological Processes*, *22*, 2267–2274. https://doi.org/10.1002/hyp

Chen, J., Hill, A. A., & Urbano, L. D. (2009). A GIS-based model for urban flood inundation. *Journal of Hydrology*, *373*(1–2), 184–192. https://doi.org/10.1016/j.jhydrol.2009.04.021

Chen, L., Qian, X., & Shi, Y. (2011). Critical Area Identification of Potential Soil Loss in a Typical Watershed of the Three Gorges Reservoir Region. *Water Resources Management*, *25*(13), 3445–3463. https://doi.org/10.1007/s11269-011-9864-4

Christensen, J. H., Kumar, K. K., Aldrian, E., An, S. I., Cavalcanti, I. F. A., de Castro, M., Dong, W., Goswami, P., Hall, A., Kanyanga, J. K., Kitoh, A., Kossin, J., Lau, N. C., Renwick, J., Stephenson, D. B., Xie, S. P., &Zhou, T. (2013). Climate Phenomena and their Relevance for Future Regional Climate Change. In T. F. Stocker, D. Qin, G. K. Plattner, M. Tignor, S. K. Allen, J. Boschung, Nauels, A., Xia, Y., Bex, V., & P. M. Midgley (Eds.), *Climate Change 2013: The Physical Science Basis. Contribution of Working Group I to the Fifth Assessment Report of the Intergovernmental Panel on Climate Change* (pp. 1217–1308). Cambridge, United Kingdom and New York, NY, USA: Cambridge University Press.

Cinco, T. A., de Guzman, R. G., Ortiz, A. M. D., Delfino, R. J. P., Lasco, R. D., Hilario, F. D., Juanillo, E. L., Barba, R., & Ares, E. D. (2016). Observed trends and impacts of tropical cyclones in the Philippines. *International Journal of Climatology*, *36*(14), 4638–4650. https://doi.org/10.1002/joc.4659

Cogle, A. L., Lane, L. J., & Basher, L. (2003). Testing the hillslope erosion model for application in India, New Zealand and Australia. *Environmental Modelling and Software*, *18*(8–9), 825–830. https://doi.org/10.1016/S1364-8152(03)00082-3

Columbus, J., Sirguey, P., & Tenzer, R. (2011). A free, fully assessed 15-m DEM for New Zealand. *Survey Quarterly*, *66*, 16–19.

Combalicer, E. A., Cruz, R. V. O., Lee, S., & Im, S. (2010). Assessing climate change impacts on water balance in the Mount Makiling forest, Philippines. *Journal of Earth Systems Sciences*, *119*(3), 265–283.

Cremaschi, D. G., D. Lasco, R., & Jane P. Delfino, R. (2012). Payments for Watershed Protection Services: Emerging Lessons from the Philippines. *Journal of Sustainable Development*, *6*(1), 90–103. https://doi.org/10.5539/jsd.v6n1p90

Cruz, R. V. O. (1999). Integrated Land Use Planning and Sustainable Watershed Management. *Journal of Philippine Development*, *16*(47), 27–49.

Cruz, R. V. O., Aliño, P. M., C, C. O., David, C. P. C., David, L. T., Lansigan, F. P., Lasco, R. D., Licuanan, W. R. Y., Lorenzo, F. M., Mamauag, S. S., Peñaflor, E. L., Perez, R. T., Pulhin, J. M., Rollon, R. N., Samson, M. S., Siringan, F. P., Tibig, L. V., Uy, N. M., & Villanoy, C. L. (2017). *2017 Philippine Climate Change Assessment: Impacts, Vulnerabilities and Adaptation.* Pasig City, Philippines: The Oscar M. Lopez Center for Climate Change Adaptation and Disaster Risk Management Foundation, Inc.

da Silva, A. M. (2004). Rainfall erosivity map for Brazil. *Catena*, *57*(3), 251–259. https://doi.org/10.1016/j.catena.2003.11.006

Daba, S., Rieger, W., & Strauss, P. (2003). Assessment of gully erosion in eastern Ethiopia using photogrammetric techniques. *Catena*, *50*(2–4), 273–291. https://doi.org/10.1016/S0341-8162(02)00135-2

David, W. P. (1988). Soil and Water Conservation Planning: Policy Issues and Recommendations. *Journal of Philippine Development*, *15*(1), 47–84.

Davies, H. N., & Bell, V. A. (2009). Assessment of methods for extracting low-resolution river networks from high-resolution digital data. *Hydrological Sciences Journal*, *54*(1), 17–28. https://doi.org/10.1623/hysj.54.1.17

De Almeida, A. A. F., & Valle, R. R. (2007). Ecophysiology of the cacao tree. *Brazilian Journal of Plant Physiology*, *19*(4), 425–448. https://doi.org/10.1590/S1677-04202007000400011

de Asis, A. M., & Omasa, K. (2007). Estimation of vegetation parameter for modeling soil erosion using linear Spectral Mixture Analysis of Landsat ETM data. *ISPRS Journal of Photogrammetry and Remote Sensing*, *62*(4), 309–324. https://doi.org/10.1016/j.isprsjprs.2007.05.013

de Mello, C. R., Norton, L. D., Pinto, L. C., Beskow, S., & Curi, N. (2016). Agricultural watershed modeling: a review for hydrology and soil erosion processes. *Ciencia e Agrotecnologia*, *40*(1), 7–25. https://doi.org/10.1590/S1413-70542016000100001

de Vente, J., & Poesen, J. (2005). Predicting soil erosion and sediment yield at the basin scale: Scale issues and semi-quantitative models. *Earth-Science Reviews*, *71*(1–2), 95–125. https://doi.org/10.1016/j.earscirev.2005.02.002

DeFries, R., & Eshleman, K. N. (2004). Land-use change and hydrologic processes: a major focus for the future. *Hydrological Processes*, *18*(11), 2183–2186. https://doi.org/10.1002/hyp.5584

Delgado, M. E. M., & Canters, F. (2012). Modeling the impacts of agroforestry systems on the spatial patterns of soil erosion risk in three catchments of Claveria, the Philippines. *Agroforestry Systems*, *85*(3), 411–423. https://doi.org/10.1007/s10457-011-9442-z

Demirci, A., & Karaburun, A. (2012). Estimation of soil erosion using RUSLE in a GIS framework: A case study in the Buyukcekmece Lake watershed, northwest Turkey. *Environmental Earth Sciences*, *66*(3), 903–913. https://doi.org/10.1007/s12665-011-1300-9

DAFF. (Department of Agriculture, Forestry and Fisheries). (2009). *Cultivating Papayas*.

Pretoria, South Africa: Department of Agriculture, Forestry and Fisheries.

Desmet, P. J. J., & Govers, G. (1996). A GIS procedure for automatically calculating the USLE LS factor on topographically complex landscape units. *Journal of Soil and Water Conservation*, *51*, 427–433. Retrieved from http://www.jswconline.org/content/51/5/427.short

DHI. (2009). *MIKE 11 Reference Manual*. Hørsholm, Denmark: DHI.

Dierick, D., & Hölscher, D. (2009). Species-specific tree water use characteristics in reforestation stands in the Philippines. *Agricultural and Forest Meteorology*, *149*(8), 1317–1326. https://doi.org/10.1016/j.agrformet.2009.03.003

Dierick, D., Kunert, N., Michael, K., & Schwendenmann, L. (2010). Tropical Rainforests and Agroforests under Global Change, 293–308. https://doi.org/10.1007/978-3-642-00493-3

Dingman, S. L. (2008). *Physical Hydrology* (2nd Edition). Long Grove, Illinois: Waveland Press Inc.

Diodato, N. (2004). Estimating RUSLE's rainfall factor in the part of Italy with a Mediterranean rainfall regime. *Hydrology and Earth System Sciences*, *8*(1), 103–107. https://doi.org/10.5194/hess-8-103-2004

Disaster Risk and Exposure Assessment for Mitigation Program. (2015). HEC-RAS and HEC-HMS Model Parameterised for Cagayan de Oro, Philippines. Quezon City, Philippines: University of the Philippines Diliman.

Dong, J., Xiao, X., Menarguez, M. A., Zhang, G., Qin, Y., Thau, D., Biradar, C., & Moore, B. (2016). Mapping paddy rice planting area in northeastern Asia with Landsat 8 images, phenology-based algorithm and Google Earth Engine. *Remote Sensing of Environment*, *185*, 142–154. https://doi.org/10.1016/j.rse.2016.02.016

Du, J., Qian, L., Rui, H., Zuo, T., Zheng, D., Xu, Y., & Xu, C. Y. (2012). Assessing the effects of urbanization on annual runoff and flood events using an integrated hydrological modeling system for Qinhuai River basin, China. *Journal of Hydrology*, *464–465*, 127–139. https://doi.org/10.1016/j.jhydrol.2012.06.057

Duke, J. A. (1998). *Handbook of Energy Crops*. Indiana, United States of America: Center for New Crops & Plants Products. Retrieved November 21, 2018, from https://hort.purdue.edu/newcrop/duke_energy/dukeindex.html.

Dumas, P., & Fossey, M. (2009). Mapping potential soil erosion in the Pacific Islands: A case study of Efate Island (Vanuatu). *11th Pacific Science Inter-Congress: Pacific Countries and Their Ocean, Facing Local and Global Changes*.

Duncan, C., Primavera, J. H., Pettorelli, N., Thompson, J. R., Loma, R. J. A., & Koldewey, H. J. (2016). Rehabilitating mangrove ecosystem services: A case study on the relative benefits of abandoned pond reversion from Panay Island, Philippines. *Marine Pollution Bulletin*, *109*(2), 772–782. https://doi.org/10.1016/j.marpolbul.2016.05.049

Durigon, V. L., Carvalho, D. F., Antunes, M. A. H., Oliveira, P. T. S., & Fernandes, M. M. (2014). NDVI time series for monitoring RUSLE cover management factor in a tropical watershed. *International Journal of Remote Sensing*, *35*(2), 441–453. https://doi.org/10.1080/01431161.2013.871081

Dymond, J. R. (2010). Soil erosion in New Zealand is a net sink of CO2. *Earth Surface Processes and Landforms*, *35*(15), 1763–1772. https://doi.org/10.1002/esp.2014

Dymond, J. R., Betts, H. D., & Schierlitz, C. S. (2010). An erosion model for evaluating regional land-use scenarios. *Environmental Modelling and Software*, *25*(3), 289–298. https://doi.org/10.1016/j.envsoft.2009.09.011

Easton, S. (2015). *Irrigation and Ecosystem Services: development of an irrigation model for the LUCI ecosystem services framework*. (Master's thesis). Wellington, New Zealand: Victoria University of Wellington.

Eiumnoh, A. (2000). *Integration of Geographic Information Systems (GIS) and Satellite Remote Sensing (SRS) for Watershed Management*. *Technical Bulletin 150*. Pathumthani, Thailand: Asian Institute of Technology.

El-Sharkawy, M. A. (2006). International research on cassava photosynthesis, productivity, eco-physiology, and responses to environmental stresses in the tropics. *Photosynthetica*, *44*(4), 481–512. https://doi.org/10.1007/s11099-006-0063-0

El-Swaify, S. A., & Dangler, E. W. (1976). Erodibilities of selected tropical soils in relation to structural and hydrologic parameters. In *Soil Erosion: Prediction and Control* (pp. 105–114). Ankeny, Iowa: Soil Conversation Society of America.

El-Swaify, S. A., Gramier, C. L., & A, L. (1987). Recent advances in soil conservation in steepland in humid tropics. In *Proceedings of the International Conference on Steepland Agriculture in the Humid Tropics* (pp. 87–100). Kuala Lumpur: MADI.

Elliott, A. H., Oehler, F., Schmidt, J., & Ekanayake, J. C. (2012). Sediment modelling with fine temporal and spatial resolution for a hilly catchment. *Hydrological Processes*, *26*(24), 3645–3660. https://doi.org/10.1002/hyp.8445

Emmett, B. E., & the GMEP team (2017). *Glastir Monitoring and Evaluation Programme Final Report to Welsh Government: Executive Summary (Contract reference: C147/2010/11)*. Lancaster, United Kingdom: Centre for Ecology & Hydrology.

EPA. (Environmental Protection Agency). (2013). *Principles of Watershed Management*. Washington D.C., United States of America: Environmental Protection Agency.

Estoque, R. C., & Murayama, Y. (2016). Quantifying landscape pattern and ecosystem service value changes in four rapidly urbanizing hill stations of Southeast Asia. *Landscape Ecology*, *31*(7), 1481–1507. https://doi.org/10.1007/s10980-016-0341-6

Eugenio, E. A., Acosta, L. A., Macandog, D. B. M., Macandog, P. B. M., Lin, E. K. H., Eugenio, J. M. A., & Manuta, J. B. (2016). Adaptive capacity of Philippine communities vulnerable to flash floods and landslides: assessing loss and damage from typhoon Bopha in Eastern Mindanao. *International Journal of Sustainable Development*, *19*(3), 279. https://doi.org/10.1504/IJSD.2016.078290

Eyles, A., Drake, P., Quang, L. T., Bon, P. Van, Mendham, D., White, D., Dat, K. T., Dung, P. T., & Beadle, C. (2015). Ecophysiology of Acacia species in wet–dry tropical plantations. *Southern Forests*, *77*(4), 287–296. https://doi.org/10.2989/20702620.2015.1063030

Falter, D., Vorogushyn, S., Lhomme, J., Apel, H., Gouldby, B., & Merz, B. (2013). Hydraulic model evaluation for large-scale flood risk assessments. *Hydrological Processes*, *27*(9), 1331–1340. https://doi.org/10.1002/hyp.9553

Farhan, Y., & Nawaiseh, S. (2015). Spatial assessment of soil erosion risk using RUSLE and GIS techniques. *Environmental Earth Sciences*, *74*(6), 4649–4669. https://doi.org/10.1007/s12665-015-4430-7

Feldman, A. D. (2000). *Hydrologic Modeling System HEC-HMS Technical Reference Manual*. *US Army Corps of Engineers*. https://doi.org/CDP-74B

Fernandez, C., Wu, J., McCool, D., & Stoeckle, C. (2003). Estimating water erosion and sediment yield with GIS, RUSLE, and SEDD. *Journal of Soil and Water Conservation*, *58*, 128–136.

Fernandez, M. A., & Daigneault, A. (2016). Erosion mitigation in the Waikato District, New Zealand: economic implications for agriculture. *Agricultural Economics*, *48*, 1–21. https://doi.org/10.1111/agec.12338

Ferreira, V., & Panagopoulos, T. (2014). Seasonality of soil erosion under Mediterranean conditions at the Alqueva dam watershed. *Environmental Management*, *54*(1), 67–83. https://doi.org/10.1007/s00267-014-0281-3

FLO-2D Software Inc. (2012). *FLO-2D Reference Manual*. Arizona, United States of America: FLO-2D Software Inc.

Floresca, J. P., Alcantara, A. J., Lamug, C. B., Rapera, C. L., & Adalla, C. B. (2009). Assessment of Ecosystem Services of Lowland Rice Agroecosystems in Echague, Isabela, Philippines. *Journal of Environmental Science and Management*, *12*(1), 25–41. https://doi.org/ISSN 0119-1144

FAO. (Food and Agriculture Organization of the United Nations). (2007). *Ecocrop: Terminalia catappa*. Retrieved March 2, 2018, from http://ecocrop.fao.org/ecocrop/srv/en/cropView?id=2062.

FAO. (Food and Agriculture Organization of the United Nations). (2018). *CROPWAT*. Retrieved February 26, 2018, from http://www.fao.org/land-water/databases-and-software/cropwat/en/.

Foster, G. R., Toy, T. E., & Renard, K. G. (2003). Comparison of the USLE, RUSLE1.06c, and RUSLE2 for Application to Highly Disturbed Lands. In *First Interagency Conference on Research in Watersheds, October 27–30* (pp. 154–160). United States Department of Agriculture.

Francisco, H. A., & Angeles, M. S. de L. (1998). *Soil Resource Depreciation and Deforestation: Philippine case study in resource accounting*. Rome, Italy: Food and Agriculture Organization of the United Nations.

Fuentes, R. U., & Concepcion, R. (2007). Implementation of Initiatives for Addressing Climate Change and Land Degradation: A Look at the Philippine Context. In M. V. K. Sivakumar & N. Ndiang'ui (Eds.), *Climate and Land Degradation* (pp. 447–467). Springer Science & Business Media.

Garcia, J. N. M., Aguilar, E. A., Sangalang, J. B., Alcantara, A. J., Habito, R. C. F., Medina, C. P., & Malayang III, B. S. (2009). Valuation of Ecosystem Services of Coconut Types: Framework and Methodology Development. *Journal of Environmental Science and Management*, *12*(1), 68–78.

Gassman, P., Reyes, M., Green, C., & Arnold, J. (2007). The Soil and Water Assessment Tool: historical development, applications, and future research directions. *Asabe*, *50*(4), 1211–1250. https://doi.org/10.13031/2013.23637.Rights

Global Invasive Species Database. (2010a). Species profile: Leucaena leucocephala. Retrieved March 2, 2018, from http://www.iucngisd.org/gisd/speciesname/Leucaena+leucocephala

Global Invasive Species Database. (2010b). Species profile: Mimosa pudica. Retrieved March 2, 2018, from http://www.iucngisd.org/gisd/speciesname/Mimosa+pudica

Gomez, B., Banbury, K., Marden, M., Trustrum, N. A., Peacock, D. H., & Hoskin, P. J. (2003). Gully erosion and sediment production: Te Weraroa Stream, New Zealand. *Water Resources Research*, *39*(7), 1–8. https://doi.org/10.1029/2002WR001342

Gorelick, N., Hancher, M., Dixon, M., Ilyushchenko, S., Thau, D., & Moore, R. (2017). Google Earth Engine: Planetary-scale geospatial analysis for everyone. *Remote Sensing of Environment*, *202*, 18–27. https://doi.org/10.1016/j.rse.2017.06.031

Gouldby, B., Lhomme, J., Mcgahey, C., Panzeri, M., Hassan, M., Burgada, N. K., Orue, C. M., Jamieson, S., Wright, G., Damme, M. V., & Morris, M. (2012). A flood system risk analysis model with dynamic sub-element 2D inundation model, dynamic breach growth and life-loss. In *Proceedings of the 2nd European Conference on Flood Risk Management, FLOODrisk2012*. Rotterdam.

GWRC. (Greater Wellington Regional Council). (2001). *Hutt River Floodplain Management Plan: For the Hutt River and its Environment*. Wellington, New Zealand: Greater Wellington Regional Council.

Guha-sapir, D., Hoyois, P., & Below, R. (2013). *Annual Disaster Statistical Review 2012*. Brussels, Belgium: Center for Research on the Epidemiology of Disasters.

Guha-sapir, D., Hoyois, P., & Below, R. (2014). *Annual Disaster Statistical Review 2013*. Brussels, Belgium: Center for Research on the Epidemiology of Disasters.

Hellweger, F. (1997). *AGREE - DEM Surface Reconditioning System*. Texas, United States of America: University of Texas. Retrieved March 28, 2018, from http://www.ce.utexas.edu/prof/maidment/gishydro/ferdi/research/agree/agree.html

Hernandez, E. C., Henderson, A., & Oliver, D. P. (2012). Effects of changing land use in the Pagsanjan–Lumban catchment on suspended sediment loads to Laguna de Bay, Philippines. *Agricultural Water Management*, *106*, 8–16. https://doi.org/10.1016/j.agwat.2011.08.012

Hewitt, A. E. (2010). *New Zealand Soil Classification*. Canterbury, New Zealand: Manaaki Whenua Press.

Hewitt, A. E., & Shepherd, T. G. (1997). Structural vulnerability of New Zealand soils. *Australian Journal of Soil Research*, *35*(3), 461–474. https://doi.org/10.1071/S96074

Hijmans, R. J., Cameron, S. E., Parra, J. L., Jones, P. G., & Jarvis, A. (2005). Very high resolution interpolated climate surfaces for global land areas. *International Journal of Climatology*, *25*(15), 1965–1978. https://doi.org/10.1002/joc.1276

Hilario, F. D., Cinco, T. A., de Guzman, R., & Ares, E. D. (2011). *Climate Change in the Philippines*. Quezon City, Philippines: Philippine Atmospheric, Geophysical and Astronomical Services Administration.

Hudson, N. W. (1971). *Soil Conservation*. Ithaca, New York: Cornell University Press.

Hunter, N. M., Bates, P. D., Horritt, M. S., & Wilson, M. D. (2007). Simple spatially-distributed models for predicting flood inundation: A review. *Geomorphology*, *90*(3–4), 208–225. https://doi.org/10.1016/j.geomorph.2006.10.021

ILC. (International Land Coalition). (2013). *Payment for ecosystem services connects urban community with indigenous people*. Bukidnon, Philippines: Xavier Science Foundation, Inc.

IPCC. (Intergovernmental Panel on Climate Change). (2012). *Managing the Risks of Extreme Events and Disasters to Advance Climate Change Adaptation*. Cambridge, UK, and New York, USA.

IPCC. (Intergovernmental Panel on Climate Change). (2013). Annex I: Atlas of Global and Regional Climate Projections [van Oldenborgh, G.J., M. Collins, J. Arblaster, J.H. Christensen, J. Marotzke, S.B. Power, M. Rummukainen and T. Zhou (eds.)]. In T. F. Stocker, D. Qin, G. K. Plattner, M. Tignor, S. K. Allen, J. Boschung, Nauels, A., Xia, Y., Bex, V., & P. M. Midgley (Eds.), *Climate Change 2013: The Physical Science Basis. Contribution of Working Group I to the Fifth Assessment Report of the Intergovernmental Panel on Climate Change*. Cambridge, United Kingdom and New York, NY, USA: Cambridge University Press.

İrvem, A., Topaloğlu, F., & Uygur, V. (2007). Estimating spatial distribution of soil loss over Seyhan River Basin in Turkey. *Journal of Hydrology*, *336*(1–2), 30–37. https://doi.org/10.1016/j.jhydrol.2006.12.009

Jackson, B., Pagella, T., Sinclair, F., Orellana, B., Henshaw, A., Reynolds, B., Mcintyre, N., Wheater, H., & Eycott, A. (2013). Polyscape: A GIS mapping framework providing efficient and spatially explicit landscape-scale valuation of multiple ecosystem services. *Landscape and Urban Planning*, *112*, 74–88. https://doi.org/10.1016/j.landurbplan.2012.12.014

Jackson, B., Wheater, H. S., McIntyre, N. R., Chell, J., Francis, O. J., Frogbrook, Z., Marshall, M., Reynolds, B., & Solloway, I. (2008). The impact of upland land management on flooding: insights from a multiscale experimental and modelling programme. *Journal of Flood Risk Management*, *1*(2), 71–80. https://doi.org/10.1111/j.1753-318X.2008.00009.x

Jahun, B. G., Ibrahim, R., Dlamini, N. S., & Musa, S. M. (2015). Review of Soil Erosion Assessment using RUSLE Model and GIS. *Journal of Biology, Agriculture and Healthcare*, *5*(9), 36–47.

Jain, M. K., & Das, D. (2010). Estimation of sediment yield and areas of soil erosion and deposition for watershed prioritization using GIS and remote sensing. *Water Resources Management*, *24*(10), 2091–2112. https://doi.org/10.1007/s11269-009-9540-0

Jamaludheen, V., Kumar, B. M., Wahid, P. A., & Kamalam, N. V. (1997). Root distribution pattern of the wild jack tree (Artocarpus hirsutus Lamk.) as studied by 32P soil injection method. *Agroforestry Systems*, *35*, 329–336.

JICA. (Japan International Cooperation Agency). (2014). *Preparatory Survey for Flood Risk Management Project for Cagayan de Oro River (FRIMP-CDOR)*. Cagayan de Oro, Philippines: Department of Public Works and Highways.

Japos, G. V., & Lubos, L. C. (2014). Practices, Behaviors, and Action on Climate Change and Environmental Protection and Conservation of Settlers along the Banks of Oro River, Northern Mindanao, Philippines. *Asian Journal of Biodiversity*, *5*. https://doi.org/10.7718/ijec.v6i1.623.g820

Jayasinghe, P. K. S. C., Adornado, H. A., Yoshida, M., & Leelamanie, D. a. L. (2010). A Web-Based GIS and Remote Sensing Framework for Spatial Information System (SIS): A Case Study in Nuwaraeliya, Sri Lanka. *Agricultural Information Research*, *19*(4), 106–116. https://doi.org/10.3173/air.19.106

Johnes, P. J. (1996). Evaluation and management of the impact of land use change on the nitrogen and phosphorus load delivered to surface waters: The export coefficient modelling approach. *Journal of Hydrology*, *183*(3–4), 323–349. https://doi.org/10.1016/0022-1694(95)02951-6

Jones, S. K., Fremier, A. K., DeClerck, F. A., Smedley, D., Pieck, A. O., & Mulligan, M. (2017). Big data and multiple methods for mapping small reservoirs: Comparing accuracies for applications in agricultural landscapes. *Remote Sensing*, *9*(12). https://doi.org/10.3390/rs9121307

Jose, A. M., & Cruz, N. A. (1999). Climate change impacts and responses in the Philippines: water resources. *Climate Research*, *12*, 77–84.

Juarez-Lucas, A. M., Kibler, K. M., Ohara, M., & Sayama, T. (2016). Benefits of flood-prone land use and the role of coping capacity, Candaba floodplains, Philippines. *Natural Hazards*, *84*(3), 2243–2264. https://doi.org/10.1007/s11069-016-2551-2

Kannan, N., Santhi, C., Williams, J. R., & Arnold, J. G. (2008). Development of a continuous soil moisture accounting procedure for curve number methodology and its behaviour with different evapotranspiration methods. *Hydrological Processes*, *22*(13), 2114–2121. https://doi.org/10.1002/hyp.6811

Kavian, A., Fathollah Nejad, Y., Habibnejad, M., & Soleimani, K. (2011). Modeling seasonal rainfall erosivity on a regional scale: A case study from Northeastern Iran. *International Journal of Environmental Research*, *5*(4), 939–950.

Kheiashy, K. E. L., Mccorquodale, J., Georgiou, I., & Meselhe, E. (2010). Three dimensional hydrodynamic modeling over bed forms in open channels. *International Journal of Sediment Research*, *25*(4), 431–440. https://doi.org/10.1016/S1001-6279(11)60010-3

Kim, J. B., Saunders, P., & Finn, J. T. (2005). Rapid assessment of soil erosion in the Rio Lempa Basin, Central America, using the universal soil loss equation and geographic information systems. *Environmental Management*, *36*(6), 872–885. https://doi.org/10.1007/s00267-002-0065-z

Kinnell, P. I. A. (2010). Event soil loss, runoff and the Universal Soil Loss Equation family of models: A review. *Journal of Hydrology*, *385*(1–4), 384–397. https://doi.org/10.1016/j.jhydrol.2010.01.024

Kittur, B. (2011). *Bamboo (Dendrocalamus strictus (Roxb.) Nees) based agroforestry system: planting density effects on biomass accumulation, carbon sequestration, root distribution pattern and understorey crop productivity*. Thrissur, India: Kerala Agricultural University.

Klik, A., Haas, K., Dvorackova, A., & Fuller, I. C. (2015). Spatial and temporal distribution of rainfall erosivity in New Zealand. *Soil Research*, *53*, 815–825.

Krupka, M., & Wallis, S. (2007). Some practical aspects of flood inundation modelling. *Publications of the Institute of Geophysics, Polish Academy of Sciences*, *7*(401). Retrieved from http://agp2.igf.edu.pl/agp/files/E-7/Krupka et al.pdf

Kubiszewski, I., Anderson, S. J., Costanza, R., & Sutton, P. C. (2016). The Future of Ecosystem Services in Asia and the Pacific. *Asia and the Pacific Policy Studies*, *3*(3), 389–404. https://doi.org/10.1002/app5.147

Kulikov, M., Schickhoff, U., & Borchardt, P. (2016). Spatial and seasonal dynamics of soil loss ratio in mountain rangelands of south-western Kyrgyzstan. *Journal of Mountain Science*, *13*(2), 316–329. https://doi.org/10.1007/s11629-1

Labata, M. M., Aranico, E. C., & Tabaranza, A. C. E. (2012). Carbon stock assessment of three selected agroforestry systems in Bukidnon, Philippines. *AES Bioflux*, *4*(1), 5–11. Retrieved from http://www.cabdirect.org/abstracts/20123279807.html

Lagmay, A. M. F. A., Racoma, B. A., Aracan, K. A., Alconis-Ayco, J., & Saddi, I. L. (2017). Disseminating near-real-time hazards information and flood maps in the Philippines through Web-GIS. *Journal of Environmental Sciences*, *59*, 13–23. https://doi.org/10.1016/j.jes.2017.03.014

Lai, Y. G., Weber, L. J., & Patel, V. C. (2003). Nonhydrostatic Three-Dimensional Model for Hydraulic Flow Simulation. I: Formulation and Verification. *Journal of Hydraulic Engineering*, *129*(3), 196. https://doi.org/10.1061/(ASCE)0733-9429(2003)129:3(196)

Laio, F., Porporato, A., Fernandez-Illescas, C., & Rodriguez-Iturbe, I. (2001). Plants in water-controlled ecosystems: active role in hydrologic processes and response to water stress II. Probabilistic soil moisture dynamics. *Advances in Water Resources*, *24*(7), 745–762. https://doi.org/10.1016/S0309-1708(01)00007-0

Landcare Research. (2013). Land Cover Database. Retrieved April 26, 2018, from https://www.data.govt.nz/case-studies/land-cover-database/

Langerwisch, F., Václavík, T., von Bloh, W., Vetter, T., & Thonicke, K. (2018). Combined effects of climate and land-use change on the provision of ecosystem services in rice agro-ecosystems. *Environmental Research Letters*, *13*(1), 015003. https://doi.org/10.1088/1748-9326/aa954d

Laquihon, W. A., & Pagbilao, M. V. (1998). Sloping Agricultural Land Technology (SALT) in the Philippines. In R. C. Gutteridge & H. M. Shelton (Eds.), *Forage Tree Legumes in Tropical Agriculture*. St Lucia: The Tropical Grassland Society of Australia Inc.

Lasco, R. D., Espaldon, M. L. O., & Habito, C. M. D. (2016). Smallholder farmers’ perceptions of climate change and the roles of trees and agroforestry in climate risk adaptation: evidence from Bohol, Philippines. *Agroforestry Systems*, *90*(3), 521–540. https://doi.org/10.1007/s10457-015-9874-y

Lasco, R. D., Pulhin, F. B., Jaranilla-Sanchez, P. A., Delfino, R. J. P., Gerpacio, R., & Garcia, K. (2009). Mainstreaming adaptation in developing countries: The case of the Philippines. *Climate and Development*, *1*(2), 130. https://doi.org/10.3763/cdev.2009.0009

Lawrence, J., Reisinger, A., Mullan, B., & Jackson, B. (2013). Exploring climate change uncertainties to support adaptive management of changing flood-risk. *Environmental Science and Policy*, *33*, 133–142. https://doi.org/10.1016/j.envsci.2013.05.008

Lawrence, J., Reisinger, A., Tegg, S., & Quade, D. (2011). *Vulnerability and adaptation to increased flood risk with climate change — Hutt Valley summary*. Wellington, New Zealand: Victoria University of Wellington.

LDD. (Land Development Department). (2002). *Assessment of Soil Loss using the Equation of Soil Loss*. Bangkok, Thailand: Land Development Department.

Lentz, R. D., Dowdy, R. H., & Rust, R. H. (1993). Soil property patterns and topographic parameters associated with ephemeral gully erosion. *Journal of Soil and Water Conservation*, *48*(4).

Lhomme, J., Sayers, P., Gouldby, B., Samuels, P., Wills, M., & Mulet-marti, J. (2009). Spreading Method. In *Flood Risk Management: Research and Practice*. London: Taylor & Francis Group.

Li, L., Wang, Y., & Liu, C. (2014). Effects of land use changes on soil erosion in a fast developing area. *International Journal of Environmental Science and Technology*, *11*(6), 1549–1562. https://doi.org/10.1007/s13762-013-0341-x

Li, Z., Wu, L., Zhu, W., Hou, M., Yang, Y., & Zheng, J. (2014). A new method for urban storm flood inundation simulation with fine CD-TIN surface. *Water (Switzerland)*, *6*(5), 1151–1171. https://doi.org/10.3390/w6051151

Lindsay, J. B. (2016). The practice of DEM stream burning revisited. *Earth Surface Processes and Landforms*, *41*(5), 658–668. https://doi.org/10.1002/esp.3888

Locatelli, B., Catterall, C. P., Imbach, P., Kumar, C., Lasco, R., Marín-Spiotta, E., Mercer, B., Powers, J. S., Schwartz, N., & Uriarte, M. (2015). Tropical reforestation and climate change: Beyond carbon. *Restoration Ecology*, *23*(4), 337–343. https://doi.org/10.1111/rec.12209

López-Vicente, M., Navas, A., & Machín, J. (2008). Identifying erosive periods by using RUSLE factors in mountain fields of the Central Spanish Pyrenees. *Hydrology and Earth System Sciences Discussions*, *12*, 2111–2142. https://doi.org/10.5194/hessd-4-2111-2007

Loureiro, N. D. S., & Coutinho, M. D. A. (2001). A new procedure to estimate the RUSLE EI30 index, based on monthly rainfall data and applied to the Algarve region, Portugal. *Journal of Hydrology*, *250*(1–4), 12–18. https://doi.org/10.1016/S0022-1694(01)00387-0

Lu, H., Prosser, I. P., Moran, C. J., Gallant, J. C., Priestley, G., & Stevenson, J. G. (2003). Predicting sheetwash and rill erosion over the Australian continent. *Australian Journal of Soil Research*, *41*(6), 1037–1062. https://doi.org/10.1071/SR02157

Lu, H., & Yu, B. (2002). Spatial and seasonal distribution of rainfall erosivity in Australia. *Australian Journal of Soil Research*, *40*, 887. https://doi.org/10.1071/SR01117

Ma, Y., Feng, S., & Song, X. (2013). A root zone model for estimating soil water balance and crop yield responses to deficit irrigation in the North China Plain. *Agricultural Water Management*, *127*, 13–24. https://doi.org/10.1016/j.agwat.2013.05.011

Ma, H. L., Wang, Z. L., & Zhou, X. (2001). Estimation of soil loss based on RUSLE in Zengcheng, Guangdong Province. *Yangtze River*, *41*, 90–93.

Mabao, K., & Cabahug, R. G. (2014). Assessment and Analysis of the Floodplain of Cagayan De Oro River Basin. *Mindanao Journal of Science and Technology*, *12*, 147–170.

Macandog, P. B. M. (2016). *An Overview of PES Implementation in the Philippines. EEPSEA SRG Report No. 2016-SRG6. Economy and Environment Programe for Southeast Asia, Laguna, Philippines.* Laguna, Philippines: Economy and Environment Program for Southeast Asia (EEPSEA)..

Madarcos, B. S. (1985). *Soil Erosion in Four Cashew-based Crops Under Two Slope Categories*. Los Banos, Philippines: Food and Agriculture Organization of the United Nations.

Mahapatra, B. S., Mitra, S., Ramasubramanian, T., & Sinha, M. K. (2009). Research on jute (Corchorus olitorius and C. capsularis) and kenaf (Hibiscus cannabinus and H. sabdariffa): Present status and future perspective. *Indian Journal of Agricultural Sciences*, *79*(12), 951–967.

Malaguit, J. C., Makahiya, M. F., & De Lara, M. L. D. (2017). Event-Based Rainfall-Runoff Forecasting in Pampanga River Basin, Philippines using Artificial Neural Networks (ANN). *International Journal of Environmental and Rural Development*, *8*(1), 33–38.

Marapara, T. (2016). *Eco-hydrology interactions between trees, soil and water in terrestrial and wetland areas: The effect of tree planting on water flow dynamics in Wairarapa Wetlands, New Zealand*. (Doctoral dissertation). Wellington, New Zealand: Victoria University of Wellington.

Marin, R. A., & Jamis, C. V. (2013). Soil erosion status of the three sub-watersheds in Bukidnon Province, Philippines. *AES Bioflux*, *5*(1), 116–123. Retrieved from http://www.aes.bioflux.com.ro

Maxwell, D. H. (2013). *A rainfall-runoff model for the highly regulated Lake Taupo catchment , using a constrained Ensemble Kalman Filter to improve the accuracy and reliability of model output*. (Doctoral dissertation). Wellington, New Zealand: Victoria University of Wellington.

Mayavel, A., Soosai Raj, J., Gurudev Sigh, B., & Krishnakumar, N. (2014). Cultivation Techniques for Gmelina arborea. In *Transfer of Tree Cultivation Technologies* (pp. 23–27). Coimbatore, India: Institute of Forest Genetics and Tree Breeding. https://doi.org/10.1080/0269249X.2006.9705652

McColl, C., & Aggett, G. (2007). Land-use forecasting and hydrologic model integration for improved land-use decision support. *Journal of Environmental Management*, *84*, 494–512. https://doi.org/10.1016/j.jenvman.2006.06.023

MEA. (Millennium Ecosystem Assesment). (2005). *Ecosystems and human well-being*. *Ecosystems* (Vol. 5). Island Press. https://doi.org/10.1196/annals.1439.003

Merritt, W. S., Croke, B. F. W., Jakeman, A. J., Letcher, R. A., & Perez, P. (2004). A Biophysical Toolbox for assessment and management of land and water resources in rural catchments in Northern Thailand. *Ecological Modelling*, *171*(3), 279–300. https://doi.org/10.1016/j.ecolmodel.2003.08.010

Merritt, W. S., Letcher, R. A., & Jakeman, A. J. (2003). A review of erosion and sediment transport models. *Environmental Modelling and Software*, *18*(8–9), 761–799. https://doi.org/10.1016/S1364-8152(03)00078-1

Mihara, H. (1951). Raindrop and Soil Erosion. *National Institute of Agricultural Science Bulletin Series A*, *1*. Tokyo, Japan: National Institute of Agricultural Science.

Miller, R. C., Guertin, D. P., & Heilman, P. (2004). Information technology in watershed management decision making. *Journal of the American Water Resources Association*, *40*(2), 347–357.

Milne, J. R., Tidswell, S., Perrie, A., & Sorensen, P. (2010). *Mangatarere Stream catchment water quality investigation*.

Mitasova, H., Barton, M., Ullah, I., Hofierka, J., & Harmon, R. S. (2013). *GIS-Based Soil Erosion Modeling*. *Treatise on Geomorphology* (Vol. 3). Elsevier Ltd. https://doi.org/10.1016/B978-0-12-374739-6.00052-X

Mitasova, H., Hofierka, J., Zlocha, M., & Iverson, L. R. (1996). Modeling topographic potential for erosion and deposition using GIS. *International Journal of Geographical Information Systems*, *10*(5), 629–641. https://doi.org/10.1080/02693799608902101

Momm, H. G., Bingner, R. L., Wells, R. R., & Wilcox, D. (2012). Agnps GIS-based tool for watershed-scale identification and mapping of cropland potential ephemeral gullies. *Applied Engineering in Agriculture*, *28*(1), 17–29.

Moore, I. D., & Burch, G. J. (1986). Physical basis of the length-slope factor in the Universal Soil Loss Equation. *Soil Science Society of America Journal*, *50*, 1294–1298.

Moore, I. D., Grayson, R. B., & Ladson, A. R. (1991). Digital Terrain Modeling : A Review of Hydrological Geomorphological and Biological Applications. *Hydrological Processes*, *5*, 3–30. https://doi.org/DOI: 10.1002/hyp.3360050103

Morgan, R. P. C. (1974). Estimating regional variations in soil erosion hazard in Peninsular Malaysia. *Malayan Nature Journal*, *28*, 94–106.

Morgan, R. P. C. (2005). *Soil Erosion and Conservation*. National Soil Resources Institute, Cranfield University. https://doi.org/10.1002/9781118351475.ch22

Morris, T. L., Esler, K. J., Barger, N. N., Jacobs, S. M., & Cramer, M. D. (2011). Ecophysiological traits associated with the competitive ability of invasive Australian acacias. *Diversity and Distributions*, *17*(5), 898–910. https://doi.org/10.1111/j.1472-4642.2011.00802.x

Morton, J. F. (1987). *Fruits of Warm Climates*. *Fruits of Warm Climates*. Miami, Florida: Purdue University.

Murphy, S. R. (2010). *Tropical perennial grasses - root depths, growth and water efficiency*. Tamworth, Australia: Industry & Investment NSW.

Nagle, G. N., Fahey, T. J., & Lassoie, J. P. (1999). Management of sedimentation in tropical watersheds. *Environmental Management*, *23*(4), 441–452. https://doi.org/10.1007/s002679900199

Naipal, V., Reick, C., Pongratz, J., & Van Oost, K. (2015). Improving the global applicability of the RUSLE model & adjustment of the topographical and rainfall erosivity factors. *Geoscientific Model Development*, *8*(9), 2893–2913. https://doi.org/10.5194/gmd-8-2893-2015

Nakil, M. (2014). *Analysis of parameters causing water induced soil erosion*. Bombay, India: Indian Institute of Technology.

Nakil, M., & Khire, M. (2016). Effect of slope steepness parameter computations on soil loss estimation: review of methods using GIS. *Geocarto International*, *31*(10), 1078–1093. https://doi.org/10.1080/10106049.2015.1120349

NASA JPL. (2011). ASTER Global Digital Elevation Model v2. NASA JPL. https://doi.org/https://doi.org/10.5067/aster/astgtm.002

NDRRMC. (National Disaster Risk Reduction and Management Council). (2009). *Final Report on Tropical Storm Ondoy (Ketsana) and Typhoon Pepeng (Parma)*. Quezon City, Philippines: NDRRMC.

NDRRMC. (National Disaster Risk Reduction and Management Council). (2012a). *Final Report on the Effects and Emergency Management re Tropical Storm "Sendong" (Washi)*. Quezon City, Philippines: NDRRMC.

NDRRMC. (National Disaster Risk Reduction and Management Council). (2012b). *SitRep No. 38 re Effects of Typhoon "PABLO" (Bopha)*. Quezon City, Philippines: NDRRMC.

NDRRMC. (National Disaster Risk Reduction and Management Council). (2014a). *FINAL REPORT re Effects of Tropical Storm "Seniang" (I.N. Jangmi)*. Quezon City, Philippines: NDRRMC.

NDRRMC. (National Disaster Risk Reduction and Management Council). (2014b). *Updates re the Effects of Typhoon "YOLANDA" (HAIYAN)*. Quezon City, Philippines: NDRRMC.

NDRRMC. (National Disaster Risk Reduction and Management Council). *SitRep No. 14 re Preparedness Measures and Effects of Typhoon "VINTA" as of 8:00 AM*. Quezon City, Philippines: NDRRMC.

Nedkov, S., & Burkhard, B. (2012). Flood regulating ecosystem services - Mapping supply and demand, in the Etropole municipality, Bulgaria. *Ecological Indicators*, *21*, 67–79. https://doi.org/10.1016/j.ecolind.2011.06.022

Néelz, S., Pender, G., & Britain, G. (2009). *Desktop review of 2D hydraulic modelling packages*. *Environment Agency*. https://doi.org/978-1-84911-079-2

NSO. (National Statistics Office). (2010). *2010 Census of Population and Housing: Northern Mindanao*. Quezon City, Philippines: National Statistics Office.

Nontananandh, S., & Changnoi, B. (2012). Internet GIS, based on USLE modeling, for assessment of soil erosion in Songkhram watershed, Northeastern of Thailand. *Kasetsart Journal - Natural Science*, *46*(2), 272–282.

NZ Soils. (2011). Correlation of Soil Classifications. Retrieved April 23, 2018, from http://www.nzsoils.org.nz/Topic-Classifying_Soils/Correlation_of_Soil_Classifications/

Ochoa-Cueva, P., Fries, A., Montesinos, P., Rodríguez-Díaz, J. A., & Boll, J. (2015). Spatial Estimation of Soil Erosion Risk by Land-cover Change in the Andes of Southern Ecuador. *Land Degradation & Development*, *26*(6), 565–573. https://doi.org/10.1002/ldr.2219

Ozsoy, G., Aksoy, E., Dirim, M. S., & Tumsavas, Z. (2012). Determination of soil erosion risk in the mustafakemalpasa river basin, Turkey, using the revised universal soil loss equation, geographic information system, and remote sensing. *Environmental Management*, *50*(4), 679–694. https://doi.org/10.1007/s00267-012-9904-8

Paelmo, R. F., Visco, R. G., Landicho, L. D., Cabahug, R. D., Baliton, R. S., Espaldon, M. L. O., & Lasco, R. D. (2015). Analysis of the farmers' knowledge on the ecosystem services of trees in the Molawin-Dampalit Watershed, Makiling Forest Reserve, Philippines. *Asia Life Sciences*, *24*(1), 169–186.

Palao, L. K. M., Dorado, M. M., Anit, K. P. A., & Lasco, R. D. (2013). Using the Soil and Water Assessment Tool (SWAT) to Assess Material Transfer in the Layawan Watershed, Mindanao, Philippines and Its Implications on Payment for Ecosystem Services. *Journal of Sustainable Development*, *6*(6), 73–88. https://doi.org/10.5539/jsd.v6n6p73

Panagos, P., Karydas, C. G., Gitas, I. Z., & Montanarella, L. (2012). Monthly soil erosion monitoring based on remotely sensed biophysical parameters: a case study in Strymonas river basin towards a functional pan-European service. *International Journal of Digital Earth*, *5*(6), 461–487. https://doi.org/10.1080/17538947.2011.587897

Panagos, P., Meusburger, K., Ballabio, C., Borrelli, P., & Alewell, C. (2014). Soil erodibility in Europe: A high-resolution dataset based on LUCAS. *Science of the Total Environment*, *479–480*(1), 189–200. https://doi.org/10.1016/j.scitotenv.2014.02.010

Panagos, P., Ballabio, C., Borrelli, P., Meusburger, K., Klik, A., Rousseva, S., Tadić, M. P., Michaelides, S., Hrabalíková, M., Olsen, P., Aalto, J., Lakatos, M., Rymszewicz, A., Dumitrescu, A., Beguería, S., & Alewell, C. (2015a). Rainfall erosivity in Europe. *Science of the Total Environment*, *511*, 801–814. https://doi.org/10.1016/j.scitotenv.2015.01.008

Panagos, P., Borrelli, P., & Meusburger, K. (2015b). A New European Slope Length and Steepness Factor (LS-Factor) for Modeling Soil Erosion by Water. *Geosciences*, *5*(2), 117–126. https://doi.org/10.3390/geosciences5020117

Panagos, P., Borrelli, P., Poesen, J., Ballabio, C., Lugato, E., Meusburger, K., Montanarella, L., & Alewell, C. (2015c). The new assessment of soil loss by water erosion in Europe. *Environmental Science & Policy*, *54*, 438–447. https://doi.org/10.1016/j.envsci.2015.08.012

Panagos, P., Borrelli, P., Meusburger, K., Alewell, C., Lugato, E., & Montanarella, L. (2015d). Estimating the soil erosion cover-management factor at the European scale. *Land Use Policy*, 48, 38–50. https://doi.org/10.1016/j.landusepol.2015.05.021

Panagos, P., Borrelli, P., Meusburger, K., Zanden, E. H. Van Der, Poesen, J., & Alewell, C. (2015e). Modelling the effect of support practices (P-factor) on the reduction of soil erosion by water at European scale. *Environmental Science and Policy*, 51, 23–34. https://doi.org/10.1016/j.envsci.2015.03.012

Panagos, P., Borrelli, P., Meusburger, K., Yu, B., Klik, A., Jae Lim, K., Yang, J. E., Ni, J., Miao, C., Chattopadhyay, N., Sadeghi, S. H., Hazbavi, Z., Zabihi, M., Larionov, G. A., Krasnov, S. F., Gorobets, A. V., Levi, Y., Erpul, G., Birkel, C., Hoyos, N., Naipal, V., Oliveira, P. T. S., Bonilla, C. A., Meddi, M., Nel, W., Al Dashti, H., Boni, M., Diodato, N., Van Oost, K., Nearing, M., & Ballabio, C. (2017). Global rainfall erosivity assessment based on high-temporal resolution rainfall records. *Scientific Reports*, *7*(1), 4175. https://doi.org/10.1038/s41598-017-04282-8

Paningbatan, E. P., Ciesiolka, C. A., Coughlan, K. J., & Rose, C. W. (1995). Alley cropping for managing soil erosion of hilly lands in the Philippines. *Soil Technology*, *8*(3), 193–204. https://doi.org/10.1016/0933-3630(95)00019-4

Pappalardo, V., La Rosa, D., Campisano, A., & La Greca, P. (2017). The potential of green infrastructure application in urban runoff control for land use planning: A preliminary evaluation from a southern Italy case study. *Ecosystem Services*, *26*(May), 345–354. https://doi.org/10.1016/j.ecoser.2017.04.015

Paringit, E. C., Sueno, S. A., Quinton, K. R., David, G., Del Rosario, M., & Pavia, M. (2015). Automation of Cagayan de Oro River flood watch system using HEC-HMS and HEC-RAS. In *ACRS 2015 - 36th Asian Conference on Remote Sensing: Fostering Resilient Growth in Asia, Proceedings*. Quezon City, Philippines.

Parker, C., Thorne, C., Bingner, R., Wells, R., & Wilcox, D. (2007). Automated Mapping of Potential For Ephemeral Gully Formation in Agricultural Watersheds. *Joint Federal Interagency Conference*, 1–12.

Pati, R. C., Franco, D. T., Alcantara, A. J., Pacardo, E. P., & Resurreccion, A. N. (2014). Vulnerability to flooding of the towns of Mabitac and Santa Maria, Laguna, Philippines. *Journal of Environmental Science and Management*, *17*(2), 21–22.

Pender, G. (2006). Briefing: Introducing the Flood Risk Management Research Consortium. In *Proceedings of the Institution of Civil Engineers-Water Management* (Vol. 159, pp. 3–8). https://doi.org/10.1680/wama.2006.159.1.3

PSA. (Philippine Statistics Authority). (2018). *CountrySTAT Philippines*. Quezon City, Philippines: Philippine Statistics Authority. Retrieved November 22, 2018, from http://countrystat.psa.gov.ph/

Pimentel, D., Harvey, C., Resosudarmo, P., Sinclair, K., Kurz, D., McNair, M., Crist, S., Shpritz, L., Fitton, L., Saffouri, R., & Blair, R. (1995). Environmental and Economic Costs of Soil Erosion and Conservation Benefits. *Science*, *267*(5201), 1117–1123. https://doi.org/10.1126/science.267.5201.1117

Post, D. A., & Hartcher, M. G. (2006). Evaluating uncertainty in modelled sediment delivery in data-sparse environments : application to the Mae Chaem Catchment , Thailand. In *Proceedings of symposium S7 held during the Seventh IAHS Scientific Assembly* (pp. 80–89). Foz do Iguaçu.

Pribyl, D. W. (2010). A critical review of the conventional SOC to SOM conversion factor. *Geoderma*, *156*(3–4), 75–83. https://doi.org/10.1016/j.geoderma.2010.02.003

Raissouni, A., Issa, L., Lech-Hab, K., & Arrim, A. El. (2016). Water Erosion Risk Mapping and Materials Transfer in the Smir Dam Watershed (Northwestern Morocco). *Journal of Geography, Environment and Earth Science International*, *5*(1), 1–17. https://doi.org/10.9734/JGEESI/2016/20061

Ram, B., Dhyani, B. L., & Kumar, N. (2004). Assessment of erodibility status and refined Iso-Erodent Map of India. *Indian Journal of Soil Conservation*, *32*(2), 171–177.

Ramirez, G. P. (1992). Cultivation, harvesting and storage of sweet potato products. In *Roots, tubers, plantains and bananas in animal feeding* (pp. 203–215). Rome, Italy: FAO.

Reddy, V. R. (2000). Sustainable Watershed Management: Institutional Approach. *Economic and Political Weekly*, *35*(38), 3435–3444.

Reinsch, T., & West, L. (2010). The U.S. national cooperative soil characterization database. In *19th World Congress of Soil Science* (pp. 64–67).

Renard, K., Foster, G., Weesies, G., McCool, D., & Yoder, D. (1997). *Predicting soil erosion by water: a guide to conservation planning with the Revised Universal Soil Loss Equation (RUSLE)*. *Agricultural Handbook No. 703*. https://doi.org/DC0-16-048938-5 65–100.

Renard, K., & Freimund, J. R. (1994). Using monthly precipitation data to estimate R-factor in the revised USLE. *Journal of Hydrology*, *157*(October 1993), 287–306.

Rodda, H. J. E., Stroud, M. J., Shankar, U., & Thorrold, B. S. (2001). A GIS based approach to modelling the effects of land-use change on soil erosion in New Zealand. *Soil Use and Management*, *17*(1), 30–40. https://doi.org/10.1079/SUM200054

Romano, N. (2014). Soil moisture at local scale: Measurements and simulations. *Journal of Hydrology*, *516*, 6–20. https://doi.org/10.1016/j.jhydrol.2014.01.026

Romano, N., Palladino, M., & Chirico, G. B. (2011). Parameterization of a bucket model for soil-vegetation-atmosphere modeling under seasonal climatic regimes. *Hydrology and Earth System Sciences*, *15*(12), 3877–3893. https://doi.org/10.5194/hess-15-3877-2011

Roose, E. J. (1975). *Erosion et ruissellement en Afrique de l'ouest: vingt années de mesures en petites parcelles expérimentales*. Adiopodoumé, Ivory Coast: Institute de Recherche pour le Développment.

Roslee, R., Bidin, K., Musta, B., Tahir, S., Tongkul, F., & Norhisham, M. N. (2017). GIS Application for Comprehensive Spatial Soil Erosion Analysis with MUSLE Model in. *Geological Behavior*, *1*(1), 1–5.

Ross, M., Santiago, J., & Lagmay, A. M. (2015). Integrating and Applying Technology in Response to the Super Typhoon Bopha Disaster. *Procedia Engineering*, *107*, 100–109. https://doi.org/10.1016/j.proeng.2015.06.063

Rozos, D., Skilodimou, H. D., Loupasakis, C., & Bathrellos, G. D. (2013). Application of the revised universal soil loss equation model on landslide prevention. An example from N. Euboea (Evia) Island, Greece. *Environmental Earth Sciences*, *70*(7), 3255–3266.

https://doi.org/10.1007/s12665-013-2390-3

Sadeghi, S. H. R., Gholami, L., Khaledi Darvishan, A., & Saeidi, P. (2014). A review of the application of the MUSLE model worldwide. *Hydrological Sciences Journal*, *59*(2), 365–375. https://doi.org/10.1080/02626667.2013.866239

Saifuddin, M., & Normaniza, O. (2016). Rooting characteristics of some tropical plants for slope protection. *Journal of Tropical Forest Science*, *28*(4), 469–478. Retrieved from http://www.jstor.org/stable/43956813

Santillan, J. R., Makinano, M., & Paringit, E. (2011). Integrated Landsat Image Analysis and Hydrologic Modeling to Detect Impacts of 25-Year Land-Cover Change on Surface Runoff in a Philippine Watershed. *Remote Sensing*, *3*(12), 1067–1087. https://doi.org/10.3390/rs3061067

Santillan, J. R., Ramos, R. V, Recamadas, S., David, G., Paringit, E. C., Espanola, N. C., Mendoza, J. R. T., & Alconis, J. (2013). Use of geospatial technologies and numerical modeling to monitor and forecast flooding along Marikina River, Philippines. In *Proceedings of the 12th SEASC: Geospatial Cooperation Towards a Sustainable Future*.

Saunders, J. F., & Lewis, W. M. (1988). Transport of phosphorus, nitrogen, and carbon by the Apure River, Venezuela. *Biogeochemistry*, *5*, 323–342.

Saxton, K., & Rawls, W. (2006). Soil Water Characteristic Estimates by Texture and Organic Matter for Hydrologic Solutions. *Soil Science Society of America Journal*, *70*, 1569–1578. https://doi.org/10.2136/sssaj2005.0117

Schaap, M. G., Leij, F. J., & Van Genuchten, M. T. (2001). ROSETTA: A computer program for estimating soil hydraulic parameters with hierarchical pedotransfer functions. *Journal of Hydrology*, *251*, 163–176. https://doi.org/10.1016/S0022-1694(01)00466-8

Scharffenberg, W. A. (2013). *HEC-HMS: User's Manual*. Washington, D.C.: Hydrologic Engineering Center.

Schiermeier, Q. (2013). Did climate change cause Typhoon Haiyan? *Nature News*. https://doi.org/10.1038/nature.2013.14139

Schmitt, L. K. (2009). Developing and applying a soil erosion model in a data-poor context to an island in the rural Philippines. *Environment, Development and Sustainability*, *11*(1), 19–42. https://doi.org/10.1007/s10668-007-9096-1

Schwarz, B., Pestre, G., Tellman, B., Sullivan, J., Kuhn, C., Mahtta, R., Pandey, B., & Hammett, L. (2018). Mapping Floods and Assessing Flood Vulnerability for Disaster Decision-Making: A Case Study Remote Sensing Application in Senegal. *Earth Observation Open Science and Innovation*, 293–300. https://doi.org/10.1007/978-3-319-65633-5_16

Shamshad, A., Azhari, M. N., Isa, M. H., Hussin, W. M. A. W., & Parida, B. P. (2008). Development of an appropriate procedure for estimation of RUSLE EI30 index and preparation of erosivity maps for Pulau Penang in Peninsular Malaysia. *Catena*, *72*(3), 423–432. https://doi.org/10.1016/j.catena.2007.08.002

Shen, J., Tong, Z., Zhu, J., Liu, X., & Yan, F. (2016). A new rapid simplified model for urban rainstorm inundation with low data requirements. *Water (Switzerland)*, *8*(11), 1–20. https://doi.org/10.3390/w8110512

Sholagberu, A. T., Ul Mustafa, M. R., Wan Yusof, K., & Ahmad, M. H. (2016). Evaluation of rainfall-runoff erosivity factor for Cameron highlands, Pahang, Malaysia. *Journal of*

Ecological Engineering, *17*(3), 1–8. https://doi.org/10.12911/22998993/63338

Shrestha, B. B., Okazumi, T., Miyamoto, M., & Sawano, H. (2016). Flood damage assessment in the Pampanga river basin of the Philippines. *Journal of Flood Risk Management*, *9*(4), 355–369. https://doi.org/10.1111/jfr3.12174

Sinha, D., & Joshi, V. U. (2012). Application of universal soil loss equation (USLE) to recently reclaimed badlands along the Adula and Mahalungi Rivers, Pravara Basin, Maharashtra. *Journal of the Geological Society of India*, *80*(3), 341–350. https://doi.org/10.1007/s12594-012-0152-6

Smith, D. D., & Whitt, D. M. (1947). Estimating Soil Loss from Field Area of Clay Pan Soils. *Soil Science Society of America Journal*, *12*, 485–490.

Smith, L. C. (1997). Satellite remote sensing of river inundation area, stage, and discharge: A review. *Hydrological Processes*, *11*(10), 1427–1439. https://doi.org/10.1002/(sici)1099-1085(199708)11:10<1427::aid-hyp473>3.0.co;2-s

Sørensen, R., Zinko, U., & Seibert, J. (2006). On the calculation of the topographic wetness index: evaluation of different methods based on field observations. *Hydrology and Earth System Sciences*, *10*(1), 101–112. https://doi.org/10.5194/hess-10-101-2006

Sousa, T. M. I., & Paz, A. R. (2017). How to evaluate the quality of coarse-resolution DEM-derived drainage networks. *Hydrological Processes*, *31*(19), 3379–3395. https://doi.org/10.1002/hyp.11262

Spangenberg, J. H., Görg, C., Truong, D. T., Tekken, V., Bustamante, J. V., & Settele, J. (2014). Provision of ecosystem services is determined by human agency, not ecosystem functions. Four case studies. *International Journal of Biodiversity Science, Ecosystem Services and Management*, *10*(1), 40–53. https://doi.org/10.1080/21513732.2014.884166

Stats NZ. (Statistics New Zealand). (2015). *Estimated long-term soil erosion*. Wellington, New Zealand: Statistics New Zealand. Retrieved February 23, 2018, from http://archive.stats.govt.nz/browse_for_stats/environment/environmental-reporting-series/environmental-indicators/Home/Land/long-term-soil-erosion.aspx

Stewart, B., Woolhiser, D., Wischmeier, W., Caro, J., & Frere M. H. (1975). *Control of water pollution from cropland*. Washington D.C., United States of America: Environmental Protection Agency.

Stürck, J., Poortinga, A., & Verburg, P. H. (2014). Mapping ecosystem services: The supply and demand of flood regulation services in Europe. *Ecological Indicators*, *38*, 198–211. https://doi.org/10.1016/j.ecolind.2013.11.010

Swamy, S. L., Mishra, A., & Puri, S. (2003). Biomass production and root distribution of Gmelina arborea under an agrisilviculture system in subhumid tropics of Central India. *New Forests*, *26*(2), 167–186. https://doi.org/10.1023/A:1024478700645

Tacio, H. D. (1993). Sloping Agricultural Land Technology (SALT): a sustainable agroforestry scheme for the uplands. *Agroforestry Systems*, *22*(2), 145–152. https://doi.org/10.1007/BF00705143

Tamayo, N. C. A., Anticamara, J. A., & Acosta-Michlik, L. (2018). National Estimates of Values of Philippine Reefs' Ecosystem Services. *Ecological Economics*, *146*(November 2017), 633–644. https://doi.org/10.1016/j.ecolecon.2017.12.005

Tang, Z., Li, Y., Gu, Y., Jiang, W., Xue, Y., Hu, Q., LaGrange, T., Bishop, A., Drahota, J., & Li, R. (2016). Assessing Nebraska playa wetland inundation status during 1985–2015 using Landsat data and Google Earth Engine. *Environmental Monitoring and Assessment*, *188*(12). https://doi.org/10.1007/s10661-016-5664-x

Tayefi, V., Lane, S. N., Hardy, R. J., & Yu, D. (2007). A comparison of one- and two-dimensional approaches to modelling flood inundation over complex upland floodplains. *Hydrological Processes*, *21*, 3190–3202. https://doi.org/10.1002/hyp.6523

Tekken, V., Spangenberg, J. H., Burkhard, B., Escalada, M., Stoll-Kleemann, S., Truong, D. T., & Settele, J. (2017). "Things are different now": Farmer perceptions of cultural ecosystem services of traditional rice landscapes in Vietnam and the Philippines. *Ecosystem Services*, *25*(November 2016), 153–166. https://doi.org/10.1016/j.ecoser.2017.04.010

Tempel, P., Batjes, N. H., & van Engelen, V. W. P. (1996). *IGBP-DIS soil data set for Pedotransfer Function Development*. Wageningen, Netherlands: International Soil Reference and Information Centre.

Teng, J., Jakeman, A. J., Vaze, J., Croke, B. F. W., Dutta, D., & Kim, S. (2017). Flood inundation modelling: A review of methods, recent advances and uncertainty analysis. *Environmental Modelling & Software*, *90*, 201–216. https://doi.org/10.1016/j.envsoft.2017.01.006

Ternate, J. R., Celeste, M. I., Pineda, E. F., Tan, F. J., & Uy, F. A. A. (2017). Floodplain Modelling of Malaking-Ilog River in Southern Luzon, Philippines Using LiDAR Digital Elevation Model for the Design of Water-Related Structures. *IOP Conference Series: Materials Science and Engineering*, *216*(1). https://doi.org/10.1088/1757-899X/216/1/012044

Thompson, B. S., Primavera, J. H., & Friess, D. A. (2017). Governance and implementation challenges for mangrove forest Payments for Ecosystem Services (PES): Empirical evidence from the Philippines. *Ecosystem Services*, *23*(July 2016), 146–155. https://doi.org/10.1016/j.ecoser.2016.12.007

Thomson, L. A. J. (2006). *Pterocarpus indicus (narra)*. *Species Profiles for Pacific Island Agroforestry*. IUCN. http://dx.doi.org/10.2305/IUCN.UK.1998.RLTS.T33241A9770599.en

Thomson, A. M., Calvin, K. V., Smith S. J., Kyle, G. P., Volke, A., Patel, P., Delgado-Arias, S., Bond-Lamberty, D., Wise, M. A., Clarke, L. E., & Edmonds, J. A. (2011). RCP4.5: a pathway for stabilization of radiative forcing by 2100. Climatic Change, 109(1), 77-94. https://doi.org/10.1007/s10584-011-0151-4.

Thorne, C. R., Zevenbergen, L. W., Grissinger, E. H., & Murphey, J. B. (1985). *Calculator programe and nomograph for on-site predictions of ephemeral gully erosion*. Washington D.C., United States of America: United States Department of Agriculture Soil Conservation Service.

Tilliger, B., Rodríguez-Labajos, B., Bustamante, J., & Settele, J. (2015). Disentangling Values in the Interrelations between Cultural Ecosystem Services and Landscape Conservation—A Case Study of the Ifugao Rice Terraces in the Philippines. *Land*, *4*(3), 888–913. https://doi.org/10.3390/land4030888

Tolentino, P. L. M., Poortinga, A., Kanamaru, H., Keesstra, S., Maroulis, J., David, C. P. C., & Ritsema, C. J. (2016). Projected impact of climate change on hydrological regimes in the Philippines. *PLoS ONE*, *11*(10), 1–14. https://doi.org/10.1371/journal.pone.0163941

Ty, T. Van, Sunada, K., Ichikawa, Y., & Oishi, S. (2012). Scenario-based Impact Assessment of

Land Use/Cover and Climate Changes on Water Resources and Demand: A Case Study in the Srepok River Basin, Vietnam-Cambodia. *Water Resources Management*, *26*, 1387–1407. https://doi.org/10.1007/s11269-011-9964-1

UP TCAGP. (University of the Philippines Training Center for Applied Geodesy and Photogrammetry) (2015). *Cagayan de Oro River Basin: DREAM Flood Forecasting and Flood Hazard Mapping*. Quezon City, Philippines: UP TCAGP.

Ureta, J. C. P., Lasco, R. D., Sajise, A. J. U., & Calderon, M. M. (2016). A ridge-to-reef ecosystem-based valuation approach to biodiversity conservation in Layawan Watershed, Misamis Occidental, Philippines. *Journal of Environmental Science and Management*, *19*(2), 64–75.

USDA. (2014). *Keys to soil taxonomy*. *USDA National Resources Conservation Service* (Vol. 12). https://doi.org/10.1109/TIP.2005.854494

USDA-ARS. (2002). US Department of Agriculture-Agricultural Research Service. Retrieved from http://www.sedlab.olemiss.edu/rusle

USDA NRSC. (1986). *Urban Hydrology for Small Watersheds (TR-55)*. *Technical Release 55*. https://doi.org/Technical Release 55

Valentin, C., Agus, F., Alamban, R., Boosaner, A., Bricquet, J. P., Chaplot, V., de Guzman, T., de Rouw, A., Janeau, J. L., Orange, D., Phachomphonh, K., Phai, D. D., Podwojewski, P., Ribolzi, O., Silvera, N., Subagyono, K., Thiébaux, J. P., Toan, T. D., & Vadari, T. (2008). Runoff and sediment losses from 27 upland catchments in Southeast Asia: Impact of rapid land use changes and conservation practices. *Agriculture, Ecosystems and Environment*, *128*(4), 225–238. https://doi.org/10.1016/j.agee.2008.06.004

van der Knijff, J. M., Jones, R. J. A., & Montanarella, L. (2000). *Soil Erosion Risk Assessment in Europe*. Europe: European Soil Bureau.

Verheye, W. (2010). Growth and Production of Rubber. In: Verheye, W. (ed.), *Land Use, Land Cover and Soil Sciences*. Encyclopedia of Life Support Systems (EOLSS), UNESCO-EOLSS Publishers, Oxford, UK.

Villarin, J. T., Algo, J. L., Cinco, T. A., Cruz, F. T., de Guzman, R. G., Hilario, F. D., Narisma, G. T., Ortiz, A. M., Siringan, F. P., & Tibig, L. V. (2016). *2016 Philippine Climate Change Assessment (PhilCCA): The Physical Science Basis*. Pasig City, Philippines: The Oscar M. Lopez Center for Climate Change Adaptation.

Voinov, A., & Costanza, R. (1999). Watershed management and the Web. *Journal of Environmental Management*, *56*, 231–245.

Wagner, W., Gawel, J., Furuma, H., De Souza, M. P., Teixeira, D., Rios, L., Ohgaki, S., Zehnder, A. J. B., &Hemond, H. F. (2002). Sustainable watershed management: an international multi-watershed case study. *Ambio*, *31*(1), 2–13. https://doi.org/10.1639/0044-7447(2002)031[0002:swmaim]2.0.co;2

Wheeler, D. M. (2016a). *Characteristics of Soils*. Hamilton, New Zealand: AgResearch Ltd.

Wheeler, D. M. (2016b). *Climate*. Hamilton, New Zealand: AgResearch Ltd.

Williams, R. J., & Renard, K. G. (1983). EPIC—a new method for assessing erosions effect on soil productivity. *Journal of Soil and Water Conservation*, *38*, 381–383.

Wilson, J. P., & Gallant, J. C. (2000). Digital Terrain Analysis. In J. P. Wilson & J. C. Gallant (Eds.), *Terrain Analysis: Principles and Applications* (pp. 1–28).

Wiltgen, N. (2014). Tropical Storm Jangmi (Seniang) Brings Flooding, Landslides to Philippines; 54 Dead, 260,000 Affected By Storm. Retrieved June 5, 2018, from https://weather.com/storms/typhoon/news/tropical-storm-seniang-philippines-jangmi-flooding

Wischmeier, W. H., & Mannering, J. V. (1968). Relation of Soil Properties to its Erodibility. *Soil and Water Management and Conservation*, (15), 131–137. https://doi.org/10.2136/sssaj1969.03615995003300010035x

Wischmeier, W. H., & Smith, D. D. (1978). Predicting rainfall erosion losses. *Agriculture Handbook No. 537*, (537), 285–291. https://doi.org/10.1029/TR039i002p00285

Woodward, D. E. (1999). Method to predict cropland ephemeral gully erosion. *Catena*, *37*(3–4), 393–399. https://doi.org/10.1016/S0341-8162(99)00028-4

Wösten, J. H. M., Lilly, A., Nemes, A., & Le Bas, C. (1999). Development and use of a database of hydraulic properties of European soils. *Geoderma*, *90*(3–4), 169–185. https://doi.org/10.1016/S0016-7061(98)00132-3

Wösten, J. H. M., Pachepsky, Y. A., & Rawls, W. J. (2001). Pedotransfer functions: bridging the gap between available basic soil data and missing soil hydraulic characteristics. *Journal of Hydrology*, *251*, 123–150. https://doi.org/10.1016/S0022-1694(01)00464-4

Wu, S., Li, J., & Huang, G. (2005). An evaluation of grid size uncertainty in empirical soil loss modeling with digital elevation models. *Environmental Modeling and Assessment*, *10*(1), 33–42. https://doi.org/10.1007/s10666-004-6595-4

Yang, T. H., Chen, Y. C., Chang, Y. C., Yang, S. C., & Ho, J. Y. (2015). Comparison of different grid cell ordering approaches in a simplified inundation model. *Water (Switzerland)*, *7*(2), 438–454. https://doi.org/10.3390/w7020438

Yang, X., Chapman, G. A., Gray, J. M., & Young, M. A. (2007). Delineating soil landscape facets from digital elevation models using compound topographic index in a geopgraphic information system. *Australian Journal of Soil Research*, *45*.

Yoon, K. S., Kim, C., & Woo, H. (2009). Application of RUSLE for Erosion Estimation of Construction Sites in Coastal Catchments. *Journal of Coastal Research*, *2*(56), 1696–1700.

Yusuf, A. A., & Francisco, H. (2009). *Climate Change Vulnerability Mapping for Southeast Asia*. Singapore: Economy and Environment Program for Southeast Asia.

Zakerinejad, R., & Maerker, M. (2015). An integrated assessment of soil erosion dynamics with special emphasis on gully erosion in the Mazayjan basin, southwestern Iran. *Natural Hazards*, *79*(1), 25–50. https://doi.org/10.1007/s11069-015-1700-3

Zhang, L., Dawes, W. R., & Walker, G. R. (2001). Response of mean annual evapotranspiration to vegetation changes at catchment scale. *Water Resources Research*, *37*(3), 701–708.

Zhang, S., & Pan, B. (2014). An urban storm-inundation simulation method based on GIS. *Journal of Hydrology*, *517*, 260–268. https://doi.org/10.1016/j.jhydrol.2014.05.044

Zhou, F. J., Chen, M. H., Lin, F. X., Huang, Y. H., & Lu, C. L. (1995). The rainfall erosivity index in Fujian Province. *Journal of Soil and Water Conservation*, *9*(1), 13–18.

Zomer, R. J., Trabucco, A., Bossio, D. A., & Verchot, L. V. (2008). Climate change mitigation: A spatial analysis of global land suitability for clean development mechanism afforestation and reforestation. *Agriculture, Ecosystems and Environment*, *126*(1–2), 67–80. https://doi.org/10.1016/j.agee.2008.01.014